2017

Data Communication Signals of Opportunity for Navigation

Mansfield, Thomas Oliver

Page left intentionally blank.

DATA COMMUNICATION SIGNALS OF OPPORTUNITY FOR NAVIGATION

by

THOMAS OLIVER MANSFIELD

A thesis submitted to Plymouth University
in partial fulfilment for the degree of

DOCTOR OF PHILOSOPHY

Computing and Mathematics Doctoral Training Centre

October 2017

Page left intentionally blank.

i. Acknowledgements

I'd like to thank my supervisors Bogdan Ghita and Adrian Ambroze for the excellent support and advice provided throughout this research. I'd also like to thank my family for allowing me to spend all of my free time staring at a laptop and flying a drone.

Page left intentionally blank.

ii. ***Declaration***

At no time during the registration for the degree of Doctor of Philosophy has the author been registered for any other University award.

Work submitted for this research degree at the Plymouth University has not formed part of any other degree either at Plymouth University or at another establishment.

Relevant scientific seminars and conferences were regularly attended at which work was often presented; external institutions were visited for consultation purposes and several papers prepared for publication.

Journal Content:

Annals of Telecommunications, 72(3), 145-155

Presentations and Conferences Attended:

Tenth International Network Conference (INC) 2014

International Conference on Telecommunications and Remote Sensing (ICTRS) 2015

IEEE European Navigation Conference (ENC) 2016

External Contacts:

UTC Aerospace Systems, Sensors and Integrated Systems, Plymouth.

Word count of main body of thesis:

54,911

Signed: ……..

Date: 5th October 2017

Page left intentionally blank.

iii. Abstract

Candidate: Thomas Oliver Mansfield

Thesis Title: Data Communications in Navigation

Mobile devices with wireless networking capabilities are used in a wide range of environments. Geolocation information increases the value of the data generated by a device and is vital in the development of a wide range of applications from autonomous vehicles to the Internet of things. Systems that generate signals specifically for geolocation have become widely adopted but, due to fundamental constraints, lack coverage and accuracy in complex urban and indoor environments. In addition to this, the reliance on a single signal source is not desirable in many applications that value the integrity of the geolocation estimate. A direction of research aiming to improve geolocation in indoor and urban environments measures signals of opportunity in order to generate a more robust estimate. While this approach improves signal availability, the unpredictable nature of these variable and uncontrolled signals leads to poor geolocation estimates, which are typically not suitable for use in many applications.

This project aims to improve on the accuracy, resilience and integrity of a geolocation estimate obtained from signal of opportunity measurements in indoor and urban environments while reducing hardware requirements. This has been achieved by efficiently coupling signals of opportunity within the radio environment with other system signals, such as those from an inertial measurement unit. Research has been carried out to optimise the coupling of these data sources resulting in techniques to allow the identification and removal of key error drivers from both the radio environment and other system sensors.

This thesis proposes a specifically designed extended Kalman filter to improve on the signal coupling. The filter aims to optimise the accuracy of radio environment measurements while also providing the ability to identify signal error sources in urban and indoor environments, leading to both greater accuracy and resilience of the geo-location estimate. Further, the proposed extended Kalman filter may use the radio environment as a source of geolocation data. The ability of the filter to recognise and mitigate leading radio environment error sources such as multipath and interference allowed the design of filters to obtain detailed and accurate signal strength and time of arrival information.

The thesis also presents a thorough set of simulation and modelling experiments to investigate and optimise the efficiency of the proposed solutions in a range of environments. Validation testing confirmed that in the urban and indoor environments, the average error of geo-location estimates has been reduced from 10 m to 3 m without improvement to the hardware surrounding infrastructure.

The improvements presented in this thesis allow networked devices to improve the value of their data by incorporating the context that comes from increased geolocation accuracy and resilience. In turn, this allows the development of a wide range of new location based applications for mobile devises in indoor and urban environments.

Page left intentionally blank.

CONTENTS

Section Page

TABLES

ILLUSTRATIONS

EQUATIONS

Glossary

CDMA	Code Division Multiple Access
CERN	Conseil Européen pour la Recherche Nucléaire
CRC	Cyclic Redundancy Check
DAB	Digital Audio Broadcasting
DDMTD	Digital Dual-Mixer Time Difference
DGNSS	Differential Global Navigation Satellite System
DoD	Department of Defence
DRM	Digital Radio Modiale
eLORAN	Enhanced LORAN
EKF	Extended Kalman Filter
FAIRs	Facts, Assumptions, Issues and Requirements
FDMA	Frequency Division Multiple Access
FEC	Forward Error Correction
FOC	Full Operating Capability
GLONASS	GLObal Navigation Satellite System
GNSS	Global Navigation Satellite Systems
GPS	Global Positioning System
GSM	Global System for Mobile
ID	Identification
IMU	Inertial Measurement Unit
INRSS	Indian Regional Navigational Satellite System
INS	Inertial Navigation System
IOC	Initial Operating Capability
ITU	International Telecommunications Union
IP	Internet Protocol
JTIDS	Joint Tactical Information Distribution System
LAAS	Local Area Augmentation System
LAN	Local Area Network
LEO	Low Earth Orbit
LF	Low Frequency
LORAN	LOng RAnge Navigation
LOS	Line of Sight
MSEC	Message Security
MW	Medium Wave
NAVSOP	Navigation via Signals of Opportunity
NLOS	Non Line of Sight
NOAA	National Oceanic and Atmospheric Association
NTP	Network Time Protocol
ppm	Parts Per Million
PTP	Precision Time Protocol
QZSS	Quasi-Zenith Satellite System
RF	Radio Frequency
RFC	Request for Comments
RIPS	Radio Interferometric Position System
RSS	Received Signal Strength
RSSI	Received Signal Strength Indicator
SDMA	Space Division Multiple Access
SDR	Software Defined Radio
SLAM	Simultaneous Location and Mapping
SMC	Sequential Monte Carlo
SP	Standard Precision
SPS	Standard Precision Signals
SSID	Service Set Identification
SWAP	Size Weight and Power
Sync-E	Synchronous Ethernet
TDMA	Time Division Multiple Access
TDoA	Time Difference of Arrival
ToA	Time of Arrival

Glossary

TSEC	Transmission Security
UDP	User Datagram Protocol
US	United States
UTC	United Technologies Corporation
WAAS	Wide Area Augmentation System

1. Introduction

1.1 Research Context

The development of autonomous systems has been a topical research area in recent years. Predictions for the common application of unmanned mobile systems and the expansion of the Internet of Things (IoT) [INLOCATION, 2016] will lead to a growing requirement for systems to geographically locate themselves within their environment.

Geolocation systems have become widely adopted in many aspects of modern life [IOANNIDES, 2016]. Satellite navigation systems, such as GPS, and mobile phone mast time comparison technologies provide system designers with a low cost and accurate solution for providing geolocation estimates. While these systems work well in a wide range of environments, they cannot provide a geolocation solution for indoor and dense urban environments [DANA, 2013]. Concerns have also been raised over the security and robustness inherent in relying on a single technology [MARKS, 2013]. To mitigate these challenges, two distinct and parallel areas of research are both currently active.

The first path of research is working towards developing dedicated radio navigation systems with signals designed to provide only a geo-location estimate [KOUHNE, 2014]. This approach as proven highly effective in open environments, producing a range of land and space based systems. The drawback of this approach in urban and indoor environments is the high installation and start-up complexity that will be involved.

A second parallel path of research is concentrating on using signals already present in the urban environment to estimate the user's location [MERRY et. al. 2010] [FARAGHER 2013]. While these signal sources have already deployed and have achieved common use in urban environments, these signals have not been designed for navigation purposes. The ability to obtain usable information from these sources presents a significant research challenge.

This thesis researches the possibility of using a hybrid approach, integrating any available geo-location signals with wireless data communication systems to enhance the accuracy and availability of geo-location estimates in urban and indoor environments,

1.2 Aims and Objectives

This research will investigate the potential benefits of using an integrated hybrid geo-location system. In this context, the aims of the project are:

- Describe an integration method that allows the coupling of typical system sensors to provide robust geo-location estimations.
- Allow indoor and urban geolocation in low size, weight and power mobile systems.

To achieve these key aims, the following objectives have also been identified:

- Identify the shortcomings of the current state of the art for indoor and urban geo-location.
- Identify sources of geo-location data.
- Create filters to obtain robust information from raw data sources.
- Research algorithms to efficiently combine data sources

Existing studies acknowledge that current navigation systems are unable to adequately meet the needs of these systems. Two particular shortcomings of current technology have been identified; 1. Minimising the impact of the key error drivers associated with low size, weight and power equipment. 2. Navigating in dense urban and indoor environments.

The traditional approach is fusing sensor data sets to provide information that neither data set could have provided alone. This approach is commonly used to couple Inertial Navigation System (INS) and Global Navigation Satellite Systems (GNSS) to provide higher resolution and more robust navigation estimates. In recent years, work has been carried out to combine optical camera data sets with INS systems, again to improve the accuracy and robustness of the navigation estimate. One of the main advantages of this approach is that the data sets obtained are from sensors that were never designed to provide navigation data, but are available to the system designer to fuse into the navigation solution.

1.3 Contributions to Knowledge

The work carried out in this thesis has advanced current state of the art. Novel contributions to knowledge have been provided in the following areas:

- Sources of geo-location data
    - Interferometric data sources
    - The combination of several narrow-band radio channels to provide sudo wide-band data.

- Raw data filtering
    - Leading edge detection in high multipath environments with frequency hopping transmitters.
    - Kalman filtering to identify leading edges in received signals.
    - Kalman filtering for leading edge detection.

- System integration algorithms
    - Algorithms to allow the integration of typical indoor and urban signals of opportunity in to system level geo-location estimators.

1.4 Thesis Structure

Chapter 2 of this thesis consists of a literature review which analyses the state of the art in navigation systems, identifying their encompassing strengths and limitations. This analysis reveals the environmental requirements for future navigation technologies by identifying the application areas that current technology cannot meet. The results of an industry interview, carried out to supplement and confirm the literature review findings, are also presented. Chapter 3 of this thesis presents the high level application assumptions and proposed architecture to frame the project research. The creation and application of a novel high level sinusoidal Kalman filter is presented. Chapter 4 presents the findings of research carried out to allow the use of time of arrival ranging estimates in high multipath environments. Chapter 5 details research carried out to improve the resolution of existing signal strength analysis and optimises the resulting data for use in the top level architecture. Chapter 6 details work carried out allows seamless transition from existing technologies to the novel technologies developed during this research project. The research findings are benchmarked and validated in section 7. Chapter 8 presents a summary of the project conclusions and proposes further development opportunities.

Page left intentionally blank.

2. Radio Signal Analysis and Sensor Fusion Techniques

This chapter of the thesis will review current techniques and approaches to geolocation. The review will begin by discussing techniques that utilise radio signal analysis to determine a user's geolocation. The review will then discuss non-radio based techniques before examining approaches used to combine and fuse the two fields. This chapter also presents findings from an industry interview, where a leading company in the field was used to verify the conclusions of the technique review.

The first objective of this thesis is to identify the shortcomings of the current state of the art for indoor and urban geolocation and navigation systems. This chapter details the techniques applied in currently deployed systems as well as reviewing those currently being applied in academic research. This chapter will highlight the shortcoming of these techniques and discuss current research to resolve these issues.

2.1 Radio Geolocation Techniques

Radio geolocation systems have become extremely common in everyday life. A huge range of devices from cars to mobile phones utilise geolocation systems to provide a wide range of services. The Navstar Global Positioning System (GPS) is perhaps one of the most widely recognised radio navigation systems in the world. Commonly available in a range of devices, GPS and other radio navigation services are vital to the correct operation of a vast number of services throughout the world from aircraft safety to banking security [VOLPE, 2001] [IOANNIDES, 2016].

A range of radio signal analysis techniques can be applied to estimate geolocation and many current and emerging geolocation techniques utilise radio signals to derive a-user's geolocation. This chapter will present the range of techniques used, along with examples of the application that are discussed in order to provide details of the achieved performance. Reflecting the nature of the current technology applications, the research areas intended to be covered by this section are very broad and wide ranging. An overview of the most common radio geolocation techniques has been summarised in Figure 1.

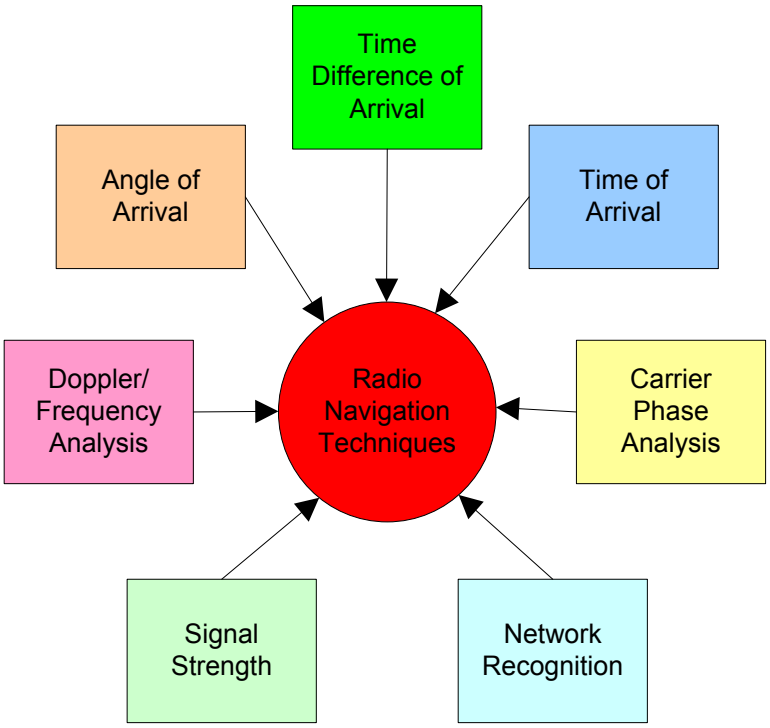

Figure 1 - RF Navigation Information Source Summary

Each of these techniques are discussed throughout this section.

2.1.1 Time Difference of Arrival (TDoA)

Time difference of arrival (TDoA) system measure the difference in time taken for a signal to travel from a range of transmitters to a receiving node. Difference in time taken is assumed proportional to the distance between the nodes allowing a location to be calculated. This technique is perhaps the most commonly applied and mature geolocation technique available with applications common in many everyday systems. While general algorithms for quantifying the navigational performance of the system are available [FISHER 2005], two key application areas of this technique, radio and satellite systems, will be discussed to provide further detail of the techniques strengths and shortcomings.

2.1.1.1 Beacon TDoA Systems

Early electronic navigation systems involved building a system of radio transmitters in locations where external navigation services were required. These systems started as far back as world war two with aircraft positioning beacons. The systems described in this section developed from these early systems and became the first widely adopted electronic global navigation systems.

The LOng RAnge Navigation (LORAN) system was introduced by the United States (US) Coast Guard to provide position and timing information to ships and aircraft in many locations around the world [COAST GUARD, 1994]. A system of radio transmitters to transmit a synchronised pulse that could be used by a user to locate themselves with a typical error of 400m in the X and Y planes. A network of transmitters has been developed by the US coast guard around the world's busiest shipping lanes in North America, Europe and the Middle East. A Russian system compatible with LORAN, Chayka, has made available around northern Europe and the Baltic. User devices are interoperable with both the US and Russian systems and have led to the use of the term LORAN-C to describe the combined network [COAST GUARD 2012].

Based on a 100 kHz carrier signal, a series of increasing analogue signal pulses are generated by each transmitter every 30 microseconds allowing users within range of several transmitters to compare the pulse patterns and derive their location in two axes.

The LORAN-C transmitters were switched off in January 2010 following 52 years of serviceto be replaced by the enhanced LORAN (eLORAN) system.

eLORAN is a system that, like LORAN, provides positioning, navigation and timing information to users throughout the world [LORAN 2007]. eLORAN has been designed to improve and replace the existing LORAN system with a number of upgrades. The main improvement in eLORAN is the addition of a data channel in the transmitted pulse signal. This data channel contains signal integrity information that allows signal corrections to be made to account for multipath propagation, allowing improved accuracy and improved estimate error predictions to be made. The accuracy provided by the eLORAN system is less than 20 meters 99% of the time. While remaining independent of global navigation satellite systems, eLORAN and GPS share a synchronised time source, allowing users to mix the signals when both systems are operational and in range.

[S. BASKER, et. al. 2007] describes the physical system that provides signals in the low frequency range of 90-110 kHz. Coverage is provided around the US, parts of Europe and the Middle East via a system of transmitters up to 500 miles apart. Due to the physical location constraints of the radio transmitters, the successful operation of the system relies on the cooperation of a worldwide network of countries, presenting a challenge for system reliability in regions of political instability.

Table 1 – Beacon System Summary

Technology	LORAN	eLORAN
Centre Frequencies	90 – 110 kHz (LF)	90 – 110 kHz (LF)
Multiplexing Method	NA	NA
Signal Authentication	None	None

Technology	LORAN	eLORAN
Error Detection or Correction	None	Signal integrity data message
Target Accuracy	<0.25 miles (≈400 m)	< 20 m
Operational Status	Retired	Fully Operational

2.1.1.2 GNSS Systems

This section of the review will summarise the current and planned satellite navigation systems and look at ways to mitigate any remaining issues with this technique.

Although terrestrial systems have achieved good coverage around many of the world's busiest air and water ways, it is not possible to receive good quality signals in very remote or physically complex locations. The additional issue of international ownership and operation of the transmitters presents many users, such as the military, with undesirable robustness concerns. These problems provided the key requirements for a global positioning system that can be controlled by a single global owner. The solution for these issues was identified in the form of a space based system.

Global Navigation Satellite System (GNSS) is a generic term for all satellite systems primarily used for navigation. The most commonly used GNSS systems available today are the US Department of Defence (DoD) Global Positioning System (GPS) and the Russian Military GLObal NAvigation Satellite System (GLONASS). Although these systems have been continually upgraded since their introduction in the 1980s, they have so far remained largely unchanged. This section will review the main components and key operating principles of both the GPS and GLONASS systems allowing the capabilities and shortcomings of each of these widely used systems to be discussed.

GPS has been developed by and is controlled by the United States DoD. [DANA 2013]. The system consists of three segments; The space segment, the ground segment and the user segment. [BONNOR 2012]

The space segment of the GPS system currently consists of 24 satellites at an altitude of approximately 20,000 km from the earth's surface. Each satellite orbits the earth every 12 hours. The satellites are arranged around 6 orbital planes, each spaced 60º apart. This constellation provides a user with between five and eight visible satellites almost anywhere on earth. The only areas with coverage of less than 5 satellites are extremely high and low latitudes around the poles [DANA 2013]. Each satellite in the space segment transmits information on 2 separate channels.

The channels are known as the L1 (civilian) and L2 channels (military). The L1 channel is transmitted at 1575.42MHz and the L2 channel is transmitted at 1227.6MHz. The main difference between the information transmitted on each channel is the robustness of the data and the encryption methods used. [BONNOR 2012]. Both the L1 and L2 signals are transmitted to achieve a minimum reception power level of -160dBw and -166dBw at the earth's surface respectively [NAVSTAR 1995]. Using Eq 1, the reception power on the earth's surface can be as low as $1x10^{-13}$ mW.

$$P_W = 10^{(\frac{P_{dBW}}{10})} \quad \text{Eq 1}$$

The L1 carrier for the standard precision signals (SPS) are Bipolar-Phase Shift Key (BPSK) modulated by the navigation data Modulo-2 added to the C/A code.[NAVSTAR 1995]. The signals from all satellites use are centred on the same L1 and L2 carriers and use Code Division Multiple Access (CDMA) to allow the user segment to differentiate between satellites using each satellites individual PRN code [NOVATEL 2013]. The L1 channel has a Coarse/Acquisition (C/A) code applied to provide CDMA coding. The CDMA code is different for each satellite and allows the user to determine the source of each received signal. This C/A code is a 1.023MHz Pseudo Random Noise (PRN) code sequence that is applied to the ranging signal [NAVSTAR 1995]. Error detection in the GPS messages are in the form of a CRC check and parity bit at the end of each 276 bit message[NAVSTAR 1995]. The second ranging signal on the L2 channel is used to provide the precise positioning service (PPS). The ranging data provided by the L2 signal is encrypted by a classified encryption algorithm. It is possible, though not confirmed by any publicly released US interface control document, to include forward error correction (FEC) and signal authentication to provide a more robust and reliable service.[NAVSTAR 1995]

The ground segment for the GPS is used for system maintenance and long term error removal. The ground segment comprises of the master control station, monitor stations and ground antennas. The master control station is the central node for the worldwide GPS ground segment and is based in a US Air Force base in Colorado, USA. The master control station uses a worldwide network of monitor stations and ground antennas to continually monitor the performance of the space segment. [NAVSTAR 1995]. The data gained from tracking the space segment satellites is used to calculate the required corrections to the satellite clocks which are updated via a data link on a regular basis. [DANA 2013].

Finally, the user segment is the part of the GPS system that most civilian users would recognise. Four satellites are required to be in view from the user segment to provide full 3 dimensional data to the user. Three satellites are required to provide the X, Y and Z positional information and the 4th satellite is used to provide accurate timing information.[DANA 2013]. Early GPS user devices were used for ship navigation and, as they did not require altitude positioning, could work with only 3 visible satellites providing X, Y and time information. [BONNOR 2012].

GPS officially met its initial operating capability in 1993, the positional performance has met and exceeded expected performance levels of horizontal accuracy of 3 meters or better and vertical accuracy of 5 meters or better 95% of the time. [US DoD 2008]

GLONASS has been developed in parallel to the US GPS systems by the Russian military. Like GPS, the system consists of space, ground and user segments [BONNOR 2012]. The GLONASS space segment is designed to consist of 24 satellites but, despite being commissioned in the early 1980s no more than 18 satellites have ever been simultaneously serviceable. The system is not believed to have ever reached its positional requirements of less than 20 m in altitude and less than 10 m in coordinate position 95% of the time. [NOVATEL 2013].

The full constellation would use three orbital planes 68.4º apart. This provides a slightly lower level of coverage than GPS at high latitudes around the poles but positions the satellites at a higher angle in the sky at other latitudes increasing reliability in complex terrain [BONNOR 2012]. The satellites orbit at a nominal altitude on 19,140km above the earth's surface, slightly lower than that of GPS [NOVATEL 2013]. The space segment transmits ranging information using a frequency divisional multiple access (FDMA) system with 10 channels to allow the user to differentiate between satellites.[NOVATEL 2013].

Like GPS, the ground segment consists of a network of tracking stations and a central control system. This system is spread across Russia and allows a twice daily update of navigation and timing data to each satellite[NOVATEL 2013]. GLONASS has a wide range of military and civilian user segments that track and receive satellite signals. As the satellites use FDMA, the user segment must be able to track and process at least 4 signal frequencies simultaneously[NOVATEL 2013]. Again, like GPS, each satellite in the GLONASS space segment transmits on two, L1 and L2 channels. An SA code is added to the L1 channel to degrade its performance for civilian use. [NOVATEL 2013].

Each satellite visible to the user transmits the same code on both channels, but on a different carrier frequency. The frequency allocation is set by the ground segment and is separated above and below 1602 MHz by multiples of 0.5625 MHz, allowing a 562.5 kHz guard band between each satellite [NOVATEL 2013]. The messages transmitted by each of the satellites consists of the position, velocity and acceleration of the satellite, synchronisation bits, satellite health, timing information and almanac data of all other GLONASS satellites[NOVATEL 2013]. The message is transmitted at 50 bits per second and contains a contains a hamming code for error correction every 30 seconds [SCIENTIFIC INFO CENTRE 1998]. The expected positional accuracy of the GLONASS system is less than 20 m in altitude and less than 10 m in coordinate position 95% of the time [SCIENTIFIC INFO CENTRE 1998].

Both GPS and GLONASS have similar system architectures with space, ground and user segments. Although there are differences in the methods used to provide ranging information and the satellites constellation in the sky, a similar range of shortcomings are found in both systems. The shortcomings fall into two distinct categories of technical and political susceptibility. One particular technical challenge of both GPS and GLONASS systems stem from the weak signals present on the earth's surface. These tiny signals can be easily jammed or obstructed with low power devices. Due to the low power required intentional or unintentional jamming is easily implemented and difficult to mitigate. Further, common obstructions such as building materials, vehicles and vegetation and completely obstruct the user segments ability to receive a signal. While both GPS and GLONASS could provide excellent global coverage, signal obstruction leads to a coverage problem in many applications. In urban, indoor wooded and mountainous regions, GNSS coverage is poor. While the higher GLONASS constellation improves performance, it is not enough to mitigate the issue successfully in many applications. A second technical challenge is the presence of multipath at the user segment. Both existing GNSS systems rely on TDoA signal analysis. The frequencies used by moth systems are susceptible to multipath in a range of environments, including those found in indoor and urban areas. This multipath reduces the accuracy of the estimated location and is not commonly detected by the user segment. Non-technical shortcomings come from the fact that there are a finite number of GNSS systems that are controlled by single political sources. Further, both GPS and GLONASS have integral systems designed to degrade the provide location estimate. The ability for the service to be degraded or removed by a single source at any time is not desirable in many applications. As seen in the GLONASS system, unintentional system degradation may occur due to other political challenges such as an unwillingness or inability to maintain the expensive space segment over a period of several decades.

Motivated partly by a desire to overcome these shortcomings, there is currently a move from these 1st generation GNSS systems (GNSS-1) to a second generation called GNSS-2. This second generation will consist of upgraded GPS and GLONASS systems as well as new European (Galileo), Chinese (Compass), Japanese (QZSS) and Indian (INRSS) systems [BONNOR 2012]

2.1.1.3 GNSS-2 Systems

The second generation of GNSS systems is currently under development. The next decade will see GPS and GLONASS modernized and upgraded as well as many other parallel systems come on-line as several countries aim to operate their own GNSS systems. An overview of these planned systems will be described in this section, providing an overview of the next 10 to 20 years of GNSS architecture.

The second generation of GPS systems shall be backwards compatible with the current generation of GPS allowing the first generation of user segments to remain operational. It will however contain two new carrier signals. The new carrier signals are known as L2C and L5. L2C will be a signal designed for civilian use, but carried in the current military only L2 carrier. The ability to monitor three signals at different frequencies will allow improved accuracy as environmental effects on the signals can be more accurately compensated by the user. The L5 signal is broadcast in the aviation safety frequency band, at 1176MHz, so should be free from interference throughout the world. The addition of a third carrier adds redundancy, allows further correction for environmental effects and jamming resistance and could allow sub 1-meter accuracy to civilian users [NATIONAL COORDINATION OFFICE 2013].

The upgraded GLONASS system, known as GLONASS-CDMA is based on the existing GLONASS system and still contains the FDMA L1 and L2 signals. The network has recently begun transmitting an L3 signal that is CDMA multiplexed and centred around 1207.14MHz [GMV 2013]. The CDMA signal aims to provide better accuracy, multipath resistance and greater interoperability with GPS and Galileo systems [GMV 2013]

Galileo is the European Union GNSS system that is currently in an initial operational state. When fully operational, Galileo navigation signals will be transmitted in 4 separate frequency bands centred at 1176.45MHz, 1207.14MHz, 1278.75MHz and 1575.42MHz. The lower frequency band coincides with the improved GPS L5 signal and the upper band coincides with the existing GPS L1 signal [GALILEO 2010]. The signals are CDMA encoded and provide a ground receive level of between -157 and -155dBW [GALILEO 2010]. The transmitted signals also include forward error correction (FEC) via a convolutional coding scheme and include a cyclic redundancy check (CRC) for error detection and correction [GALILEO 2010]. The accuracy of the civilian Galileo signal is expected to be comparable with existing GNSS systems [GALILEO 2010].

Compass is the Chinese GNSS system that started development in 2000 and aims to be fully serviceable, providing worldwide coverage in 2020 [CHINA SAT NAV OFFICE 2011]. The system space segment consists of 14 satellites, including 5 geostationary (high altitude) satellites, 5 in inclined geosynchronous (medium-high) satellite and 4 satellites in medium earth orbit. All satellites provide a minimum user power level of -163dBW at the earth surface [CHINA SAT NAV OFFICE 2011]. The system comprises of a single CDMA multiplexed channel at 1561.098 MHz [CHINA SAT NAV OFFICE 2011]. Little reliable information has been released about the data structure or any error detection or correction capability within the ranging message.

India and Japan are both creating their own satellite navigation systems that will provide coverage of their local regions using typical GNSS techniques. There are currently no plans for either system becoming a global navigation system.

While these systems have attempted to address some of the shortcomings observed in the first generation of GNSS systems, the improvements have only been evolutionary and challenges still exist. The first improvement is the increase in signals strengths. Although signal strengths in GNSS2 systems are 3 to 4 times stronger than those found in the first generation of the systems, with a reception signal strength approximately $4x10^{-13}$ mW, they still remain incredibly weak when compared to terrestrial transmissions. While an increase in the number of frequencies are available, signal jamming and obstruction still remains a significant risk. While an increase in the number of satellites also allows improved line of sight in many applications, urban and indoor environments with limited or no direct view of the sky will still not receive coverage from second generation systems. The advent of second generation GNSS systems has also seen a broadening of systems available, reducing the political dependency on only 2 national governments. The provision of GNSS still however remains in the control of a small number of political entities still limiting the robustness of the system for many users.

While the second generation of GNSS systems has been developed to mitigate the technical and political shortcomings of the system, the fundamental nature of many of the issues means that any improvements expected will be relatively minor. While these shortcomings exist, GNSS has become vital to many aspects of modern life and provides an indication as to the potential use of improved geo-location services in urban and indoor environments. Key technical information and an indication of the performance achieved by GNSS systems can be seen in Table 2.

Table 2 – GNSS Summary

Technology	GPS	GLONASS	Improved GPS	GLONASS CDMA	Galileo	Compass
Centre Frequencies (MHz)	1227.6 1575.42	1562 to 1642	1176.0 1227.6 1575.42	1562 to 1642 and 1207.1	1176.45 1207.14 1278.75 1575.42	1561.098
Multiplexing Method	CDMA	FDMA	CDMA	FDMA and CDMA	CDMA	CDMA
Signal Authentication	None in civilian signals	None in civilian signals	None in civilian signals	None in civilian signals	Unknown	Unknown
Error Detection or Correction	CRC and Parity Check	Hamming Code	CRC and Parity Check	Hamming Code	FEC via convolutional coding and CRC	Unknown
Target Accuracy	< 5 m	< 10 m	< 1 m	< 5 m	< 1 m	Currently < 20 m

Technology	GPS	GLONASS	Improved GPS	GLONASS CDMA	Galileo	Compass
Operational Status	FOC	IOC	IOC Planned 2015	IOC	IOC Planned 2015	FOC Planned 2020

2.1.1.4 Augmented GNSS

Despite the shortcomings highlighted in the previous chapters, GNSS systems have revolutionised navigation based services all over the world. GNSS services have even begun to be used in safety systems, requiring greater robustness. This has led to a significant area of research, looking into ways of mitigating GNSS shortcomings. Due to the inability of users to influence the ground or space segments of the system, this research has concentrated on implementing system improvements to the user segment in an attempt to improve accuracy, reliability and robustness in hostile environments.

Some of the key systems that have been developed to augment GNSS are summarised in the following section, along with a review of their additional infrastructure, requirements and inputs.

Differential GNSS (DGNSS) techniques use the basic principle that if a user can receive a GNSS signal at a receiver with a fixed and known location, the offset added to the GNSS signal can be corrected. [Dana 2013].

Two main approaches have been developed to implement this principle. The first is a Wide Area Augmentation System (WAAS). A WAAS uses a wide range of reference stations spread over a large national or continental area to each receive GNSS signals and apply corrections that are possible to their own accurately known positions. These corrections are then broadcast via a second set of satellites to provide users with further information to correct their GNSS data [PULLEN Et. al. 2002]

A second augmentation system uses a similar principle of correcting GNSS signals using receivers at known locations, but only provide corrections in the local area, typically less than 50m, around the receiver. These systems are known as Local Area Augmentation Systems (LAASs). These local systems can produce centimetre accuracy of relative receivers, even with an SA code enabled GPS signal by comparing the signal received at each terminal via a data link. [PULLEN Et. al. 2002]

A selection of competing communication satellite systems exists, providing two way communications between satellites and user terminals. To allow low power user terminals, the satellites orbit in a low earth orbit, just 780km above the surface of the earth[RABINOWITZ Et. al. 2013]

The Iridium satellite constellation consists of 66 Low Earth Orbit (LEO) satellites in six orbital planes orbiting the earth in 100 minutes. This allows each satellite to be visible to a user for approximately 10 minutes. Each satellite footprint is overlapped, providing global coverage. At least 2 satellites can be seen by most users at any given time. Towards the poles, a larger number of satellites can be seen at any one time.[IRIDIUM 2013].

One of the commercial satellite communication systems, Iridium, also provides a uni-directional ring alert channel at 126.27MHz. This ring alert channel provides a powerful signal on a TDMA architecture that allows the user to receive incoming call notification, even indoor with the user device antenna stowed. The carrier for this signal is tightly controlled, with 1.5ppm frequency stability.[VEENEMAN 2013]

This paging channel could provide a very useful reference signal for navigation in indoor and other areas with poor GNSS signal coverage. No practical application using the Iridium ring alert channel for navigation can be found.

2.1.2 Time of Arrival (ToA)

GNSS and other TDoA systems are not the only methods for providing gei-location estimates from radio signals. As well as recording the time difference of arrival from a selection of transmitting nodes, a user can accurately find ranging information from one or more known locations if they can calculate the absolute time taken for the data to travel from the transmitter to receiver. If the receivers distance from three or more locations can be found they can locate themselves in three dimensions to a level of accuracy that is relational to the accuracy of the time measurements, assuming the time travelled to be related directly to the distance at the speed of light, ignoring the effects of multipath.

ToA information can be provided by a range of data communication systems. If the network can provide either round trip timing or single hop duration information, it is possible to calculate the relative position from the changes in the required transfer time taken, assuming a direct and single propagation path from one node to another. A review of common network data communication timing systems that could be applied in this scenario is reviewed in the following section.

While the absolute time synchronisation of a network is key to its ability to provide range information, the jitter in the time signals is important to calculate the relative motion of a node. It is assumed in this review that the jitter if the system is relative to its accuracy or that the effects of jitter can be removed by averaging the data over a sufficiently long period.

The most mature ToA application is the JTIDS system. The Joint Tactical Information Distribution System (JTIDS) is a military network designed to share data and voice information between aircraft and other large military units. Commonly known as JTIDS, the official NATO name of the complete data link system is ‘Link 16’. The network runs on a TDMA infrastructure to synchronise transmissions. Each node of the network is allocated a number of timeslots to transmit its data. [3SDL 2009].

A relative navigation system has been integrated into the JTIDS system using the tight time control in the network to provide relative distance information for each node. The difference in the time of arrival (ToA) of each message and the start of the allocated timeslot are compared. This provides a ranging calculation to be made from the sender to receiver. As the transmitted data contains information about the transmitting nodes own locations and its confidence in those locations, a navigation position can be calculated for the receiving node. [FRIED 1978]

The accuracy of the system is hard to define as it depends on how many nodes are in the network and their own positional confidence. However, an accuracy of around 0.25 miles is typical in many situations [FRIED 1978}

2.1.3 Angle of Arrival (AoA)

IN addition to timing based systems, positional information can also be derived from calculating the relative bearing of the received signal to a node. If the relative bearing can be found from several known locations, an intersect can be derived that will provide the receivers location. Several of the key techniques of achieving angle of arrival data are discussed in the following sections.

2.1.3.1 Sectored Antennas

Several commercially available antennas arrays are used by a wide range of communication systems. These sectored antennas are used for two primary reasons;

Sectored antennas allow a higher gain antenna to be developed with a limited power source or receive sensitivity. The fact that the antenna field of view is lower than that of an omnidirectional antenna allows the equivalent of high gain antenna amplification without the limited azimuth field of view.

Sectored antennas allow traffic management in congested wireless networks. The sectors in the antenna can be used to add capacity to a mobile phone cell by allowing multiple channels to operate within each cell. This increases the user capacity within a cell.

A schematic of the benefits discussed can be seen in Figure 2.

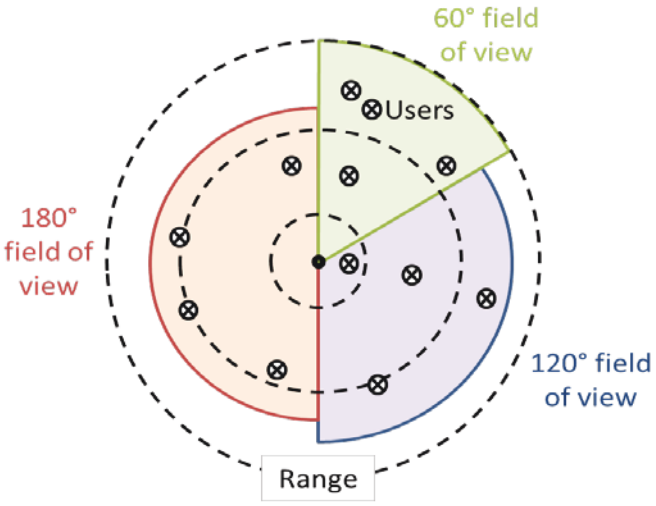

Figure 2 - Sectored Antenna Schematic

In this example, the capacity of the cell has been limited to four users. It can be seen that the highest density of users occurs in the sector with the narrowest field of view. In addition, if we assume that the transmission power and receiver sensitivity of each transmitter is constant, the greatest range is achieved by the antenna with the narrowest field of view.

The number of sectors in a sectored array can vary but rarely exceeds 10. This is considered the main limitation in their use in positional systems each sector is > 36 °. At a range of more than a few meters this leads to a very poor positional accuracy.

2.1.3.2 Rotating Antennas

Another class of antennas that provides similar functionality but with increased accuracy is rotational antennas. These systems contain a single antenna that is rotated at relatively low speed. The antenna commonly has a very high gain and small azimuth beam profile. The position of the antenna is continuously monitored and compared with received signal strength to calculate the range of the RF source with a typical accuracy of < 1 °. This provides a slightly more mechanically complex solution that does not bring all of the additional user capacity benefits if a sectored antenna but does provide a far more accurate solution to estimating the angle of arrival of a signal with physical antenna design.

2.1.3.3 Carrier Phase

Another method of calculating the angle of arrival is via carrier phase analysis. Carrier phase analysis was initially developed to allow solid state, steerable radar antennas in several military applications.

This method requires the receiver to have multiple, omnidirectional antennas. Upon receiving a user's transmitted signal, the phase of the signal received at each of the antennas is compared.

The difference in received phase at each of the known antenna locations allows the relative direction of the signal source to be identified. This technique has been used to derive received angles of a few degrees [Roxin et. al. 2007].

This method is used to calculate the direction of a client in the IEEE802.11ac protocol. The same carrier phase technique is also used to generate and steer the transmitted signal, increasing the range for a specified power and antenna gain and allowing an increase in capacity via Space Division Multiple Access (SDMA) technique

While cost effective low power hardware has been produced to enable the implementation of the 802.11ac protocol, transferring the technique to other transmission hardware would be require considerable technical effort.

2.1.4 Frequency of Arrival (FoA)

2.1.4.1 Doppler Shift Geolocation

A series of data gathering [Lee et. al. 2007] and data analysis [Gai, et. al. 2007] techniques have been discussed for their use in using Doppler shift effect to be used for geolocation.

This technique utilises the frequency shift obtained by a transmitter and receiver moving in relation to each other. If a component of the motion moves the transmitter and receiver apart, a frequency shift is seen at the receiver. This frequency shift directly relates to the speed at which the nodes are moving apart. If multiple receivers are used an estimation of the transmitter location can be derived. Alternatively, if the receiver is on a movable platform, such as an aircraft, techniques can be used to determine the location of the transmitter by moving around and generating Doppler shifts.

This technique does though have several drawbacks. On its own it cannot determine the range between the transmitter and the receiver but could feed into higher level algorithms to allow this. More importantly however, the method for accurately gaining the frequency of the received signal is problematic. If the nodes are not fast moving or are only moving at an oblique angle to one another the frequency shifts are very small. The hardware required to accurately record these small shifts can be expensive, bulky and unsuitable for many deployable applications. Another problem with using the often small frequency shift estimation technique is the fact that the technique cannot easily cope with frequency modulated transmissions and suffers from the frequency shift multipath effects.

2.1.4.2 Interferometry

Interferometric geolocation is a location method that uses the beat frequency between two transmitters as the source of a signal for carrier phase analysis. This method has been discussed by [MAROTI ET. AL. 2005] as a novel way of obtaining carrier phase information using rugged commercial hardware. This technique has then been successfully applied to tracking wireless nodes in open indoor environments, such as sports stadia [Kusy et. al. 2007].

Interferometry requires two wireless nodes transmitting simultaneously at slightly offset frequencies. The receiving nodes receive a signal that is centred between the two transmitting frequencies. The two transmitting nodes cause constructive and deconstructive interference that results in a beat frequency with a relatively low frequency, equalling the separation in transmission frequencies. Due to this deconstructive and constructive interface moving as the phase relationship varies, the apparent received signal strength varies with time. This can easily be measured by the Received Signal Strength Indicator (RSSI) functionality in the 802.11 mac sub-layer. This also allows relatively low rate sampling, easily achieved with cheap Commercial Off The Shelf (COTS) hardware, to be used to collect the raw phase analysis data for off line analysis without crossing the Nyquist frequency.

This technique has been successfully applied by the Radio Interferometric Position System (RIPS) [Maroti et. al.2005]. RIPS commonly used 3 fixed nodes to calculate the position of a 4th node. A typical RIPS system architecture can be seen in Figure 3.

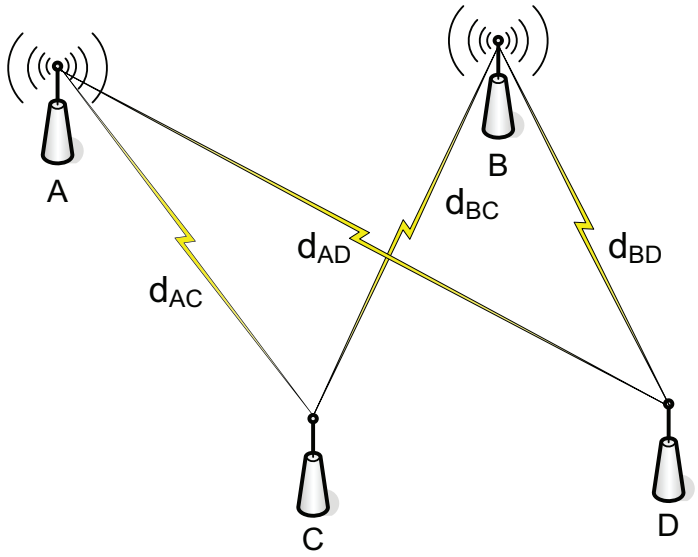

Figure 3 - Typical RIPS Architecture [Maroti et. al. 2005]

The phase offset between the two receiving nodes (C and D) provides the equation shown in Eq 2.

$$Phase\ offset = 2\pi \frac{d_{AD-}d_{BD+}d_{BC-}d_{AC}}{\lambda_{mean\ carrier}} (mod\ 2\pi) \qquad \text{Eq 2}$$

If the relative locations of three of the nodes A, C and D are known the location of B can be calculated in three dimensions by comparing the received phase shift. The phase shift is determined by the RSSI value.

This technique is vulnerable to multipath techniques corrupting the results. If the process is repeated using a pair of radios at a drastically different frequency, the number of possible locations caused by multipath is drastically reduced, this is known as stochastic interferometry. [DIL HAVINGA 2011]

One variable that that is not considered in the RIPS system is the effect of Doppler shift. If any of the nodes are moving the received phase will be altered by the Doppler shift leading to an error in the calculated position. A correction for Doppler shift has been proven [Szilvasi Et. al. 2012].. As a node moves the received frequency will shift in relation to its speed. Analysis of the resulting frequency at multiple points in the network will allow the user to determine the speed and direction of the node. If the original location was known, the new location of the node can be calculated from the monitored motion, although this will be subject to drift over time as measurement inaccuracies sum together.

This Doppler caused frequency shift technique has been achieved on the same COTS hardware that was used to calculate the received phase shift in the previously discussed RIPS system [Szilvasi Et. al. 2012].

The system has been proven to work well in open environments with few RF propagation variations. In ideal conditions the system has produced location errors as low as 3 cm at a range of greater than 160 m using low SWAP radio hardware. Experimentation results with the RIPS system do however indicate that the system suffers significant degradation when used in areas that contain multipath [Maroti et. al.2005]. This is caused by the four signal paths, showm in Figure 3, may suffer difficult to predict apparent phase corruption, degrading the accuracy of the resulting location. This currently limits the potential applications for the RIPS technology due to the fact that it is unsuitable for use in dense urban environments where multipath is common.

2.1.5 Signal Strength

A common area of research in using radio signals for localisation is to use the received signal strength of a variety of networks. This technique has been applied using a variety of networks to provide the signal, from GSM to Wi-Fi [CHEN KOBAYASHI 2002].

The most basic principle is to use a mobile RF receiver and a single RF transmitter. If the received signal strength falls, it can be assumed that the receiver is moving away from the transmitter. If the signal strengthens, it is assumed that the receiver is moving closer to the transmitter. Due to the complex nature of RF signal propagation the accuracy of this technique severely limits its accuracy in such a simple application.

The accuracy of the system does however improve if multiple transmission sources are used [DERENICK et. al. 2013]. This scenario allows a range of calculations to be made to infer the range from each transmitter. As many ranges are calculated, the aggregated combination of information sources can significantly improve the reliability and accuracy of the system, even in indoor or urban environments.

The drawback of many of the systems used by both Derenick et. al. and Kobayashi is that the location of the transmitters must be known in advance, so the technique is not suitable for areas where the locations are not known prior to arrival or in situations where the transmitters are mobile.

Work has been carried out [MERRY et. al. 2010] to develop a solution to this limitation that uses a mathematical algorithm, known as Simultaneous Localisation And Mapping (SLAM) to deduce where the local transmitters are while simultaneously calculating the receivers position. This has also been applied to allow the receiver to learn not only where it is in relation to the transmitters, but also to allow a map of the physical environment to be built.

The signal strength map obtained from the signal strength mapping process provides some features that are highly beneficial to a geo-location system. These unique benefits come from the fact that the complex multipath environment, rather than hampering the mapping process, actually enhances it. The more complex and difficult the multipath and general RF environment, the more features there are to map. This property could be of vital significance to many likely system users.

2.1.6 Signal Fingerprinting

Traditional SLAM techniques based solely on signal strength [MERRY et. al. 2010] struggle when calculating transmitter positions over multiple cells. The issue is based on the fact that in most RF networks, cells are distributed in clusters.

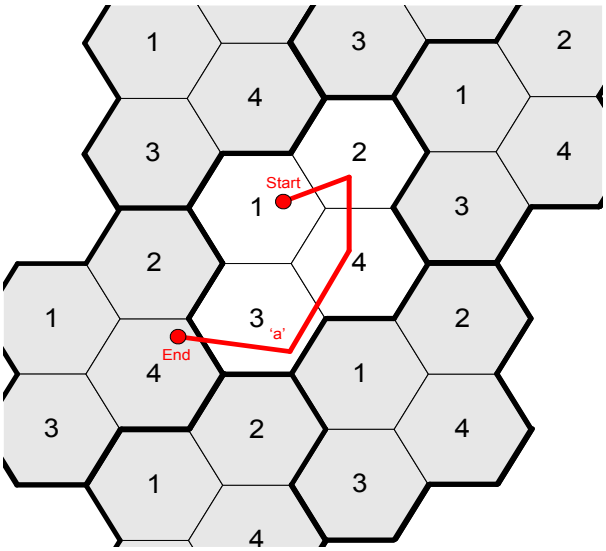

Figure 4 - Typical RF Cell Structure with Example Mobile Receiver Path

When the receiver travels from one cell cluster to another, it has no way of knowing whether the received signal is from the original cell of from a new cell. This problem can be seen in Figure 4 where the mobile receiver node path is denoted by the red line. The receiver starts in cell 1 and can receive signals from all cells in the centre cluster.

As the receiver moves from the start to point ‘a’, the signals from transmitters with the cell ID of “1”, “2”, “4” then “3” will dominate with the strongest received signals. This allows the receiver to estimate its position relative to these cell transmitters. As the receiver moves from point ‘a’ to the end, it has no way of knowing whether it is moving towards the cell “4” it’s already passed or moving away to another cell outside the cluster with the same cell ID. This behaviour is a significant problem for many SLAM systems.

To overcome this, other information identifying the cell can be taken from the transmission. This other information comes from the RF transmission features that are likely to be unique to the transmitter used. This includes signal rise times, signal noise, frequency non-linearities, jitter and clock inaccuracies. This technique has been well described for system security [Daniels et. al 2005] where it is used to detect unknown and spoof nodes in a wireless network.

If this technique were applied in a navigation environment, as the user moves from point ‘a’ to the end, it can verify whether the signal transmitted from cell ‘4’ is the same as the already passed cell or if it’s an entirely new cell on its journey solely by looking at the ‘fingerprint’ of the transmitter and not solely its centre frequency.

2.1.7 Combined Radio Sources

So far in this section, we have concentrated on using only physical layer properties for geolocation. While this has several important benefits, such as being able to use encrypted data as a source of information, extra information sources may be available from higher level data analysis.

Common civilian wireless data communication networks such as WiMAX, GSM, DAB, DVB and 3G all contain cell ID information, transmission time stamps, centre frequency and other useful data. If this data can be decoded by the receiver, it is possible for them to calculate their bearing, speed, location or even all three. Using the Cell ID is a common method for rough geolocation [Bshara et. al. 2009] and can be developed further by combining other cell ID sources. One specific application of this is the centre frequency transmission information used in the GSM protocol. If the transmitted centre frequency is known it can be compared to the received frequency. The offset is likely to be caused by Doppler shift directly relates to the speed and bearing of the receiver. Combined with the cell ID data that can often be compared to a central registry of all cell IDs in the local area would allow the user to determine its location down to a single possible point on earth.

The possibilities of research in this area are considerable and are limited only by the number of wireless systems present in the area. Due to this fact and that navigation by any of these systems is easily prevented by the user encrypting their data or changing their protocol, it is considered that is area of research is outside of the scope of this project as it is unlikely to be able to be applied to a hostile environment that requires the use of encrypted data.

2.1.7.1 NAVSOP® – A Commercial Signals of Opportunity System

The current leading commercial RF based navigation system is the BAE Systems navigation via signals of opportunity (NAVSOP®) [BAE 2013]. This commercial system is based largely on the work carried by BAE Systems and the Australian Centre for Field Robotics [Merry et. al. 2010]. This work used many of the techniques discussed so far in this literature review, such as time of arrival, time difference on arrival, cell ID, signal strength, fingerprinting and carrier phase technique and applied them to simulations of real world systems and transmitter configurations.

The work used common civilian networks as the transmitter network for the receiver to navigate from. The location of the transmitters was known to the receiver prior to the start of navigation. The simulation attempted to recreate the transmitter locations and urban complexity of central Sydney, Australia.

The paper details and compares the experimental results of using medium wave (MW) radio signals, GSM signals, Digital Audio Broadcasting (DAB) signals and 3G signals. It was seen that many of the tested data sources have their own strengths and weaknesses. Perhaps the most significant finding was the relatively good results found when carrier phase analysis was applied to MW radio transmissions this is combined with the beneficial range propertied of MW transmissions that allow the technique to be applied hundreds of kilometres from the transmitter locations. These results were hampered by the fact that there are very few transmitters in the test area and the fact that MW radio transmissions are due to be discontinued around the world in favour of more power and bandwidth efficient DAB radio signals.

3G data transmission was also a good source of information due both to the fact that dense urban environments contain a large number of transmitters and the fact that the data sent across the network contains cell ID, centre frequency and timing information, allowing high level data analysis to be carried out to provide an estimate of range from known transmitter locations. This technique is again hampered by changing technologies as the widely adopted CDMA technique limits the number of transmitters that can be located to the number of separate operator networks available.

As no one technology yielded the best results the paper also described the effects of combining received signals to use the strengths of one signal source in an area where another signal source may have been weak. Good results were gained from combining MW, DAB and 3G data to provide sub 1m accuracy even in a wide range of very harsh urban environments. [FARAGHER 2010].

2.1.8 Radio Geolocation Summary

Table 3 – Radio Geolocation Technique Comparaison

Technology	Time Difference of Arrival	Time of Arrival			Angle of Arrival		Frequency of Arrival		Signal Strength	Signal Fingerprinting	Higher Level Data Analysis
		NTP	PTP	Sync-E	Sectored Antennas	Carrier Phase	Doppler Shift	Interferometry			
System Maturity	Very High	Very High	Medium	Low	Very High	High	Medium	Low	Medium	Low	Low
Accuracy	< 1 m	< 230 Km	< 23 m	< 0.23 m	< 1 °	< 1 °	< 5 m	< 1 m	< 10 m	< 10 m	< 10 m
Implementation Difficulty	Very High	Low	High	High	Very Low	Medium	Medium	Medium	Low	Medium	Medium
Resistance to RF Effects (Multipath etc)	Low	Low	Low	Low	Medium	Medium	Medium	High	High	High	High
Suitability for inclusion	Low	Low	High	Medium	Medium	High	High	High	Medium	High	Medium

A considerable range of technologies and techniques are available that show the potential to address some the shortcomings of current navigation techniques. This chapter has covered the key active areas of research and technology development aiming to allow navigation using wireless communication networks. The key research projects that have applied these technologies to mitigate the issues presented by the current established navigation systems have also been discussed.

A summary and comparison of all of the key technologies that could enable data communication networks to be used for navigation can be found in Table 3. Each technology has its own strengths and weaknesses. It is considered likely that the project to develop a navigation system based on these technologies will use a combination of techniques as, unsurprisingly, no single technology has been demonstrated to sufficiently fulfil the project requirements.

TDoA technologies were the first to be discussed in this chapter. They have been found to already by of a very mature nature and this is not an area that has received much novel research, except of course for recent advancements in providing small, localised and portable systems. These systems have the same drawbacks as larger TDoA networks, such as eLORAn and GNSS systems and have little potential to provide the solution to this project for the reasons discussed in previous sections.

It is worth noting however, that a useful navigation entropy formula has been developed for TDoA networks [Fisher 2005]. It may be desirable to expand on this entropy formula for evaluating and comparing other wireless navigation techniques later in this project.

Deriving ranging information from ToA techniques, such as those developed by the CERN White Rabbit system, does provide some interesting capabilities. The key variable in this area is the transition to a wireless physical layer that, while the technologies were developed with this in mind, makes a significantly more complicated scenario [HE et. al. 2013]. The RF effects of the physical layer will certainly make the ranging calculations more inaccurate, but the very accurate measurements made by the White Rabbit system do allow a large level of degradation possible while still obtaining useful results. As discussed previously, it is unlikely that this technology will be able to provide the solution on its own, but it could provide an additional source of information to aid the final system.

Similarly, several angle of arrival techniques provide a useful potential addition to a final system. Carrier phase analysis in particular, as demonstrated by the 802.11ac protocol, provide a widely used COTS implementation of a complex system. This system is likely to be already in use in several potential applications for a RF based geo-location system and, like ToA ranging information, could provide data to aid the complete system.

Perhaps one of the key pieces of research in recent years has been that of the interferometry systems discussed in the frequency of arrival chapters. This technique seems to perfectly suit several of the key applications for this project. The complex RF environment that this project aims to provide a navigational solution for will be a good source of interfering signals. It seems likely that the constructive and deconstructive interference found in a complex RF environment with many different, competing systems will provide the raw data required by interferometric systems. This is one of the systems covered by this review that, as the RF environment gets more complicated and causes problems for many RF geo-location techniques, this system will have more sources of information. These sources of information can be used in a stochastic manor to mitigate the remaining detrimental RF effects.

A similar property can be found with the signal strength approach. Again, in this scenario as the RF environment gets more and more complicated and congested the systems has more to use as it's map source and is able to achieve a higher level of accuracy.

Signal fingerprinting also could provide some useful features to the system; however the proposed implementation of this in a system that consists of existing COTs hardware seems to cause significant issues.

Higher level data analysis has been largely omitted from this project as although very good performance has been found and the scope of systems suitable for integration into the system is considerable, the fact that the source of the data is unlikely to be reliable is a major issue. This assumption is made as the system will be using data that is likely to be encrypted, generated by rapidly developing protocols or commercial in nature. These dependencies are unlikely to create an elegant solution to the problem posed.

Great potential can be seen in the field of collaborative navigation. It has been demonstrated that systems with physically separated nodes can use information in a more efficient way than single nodes. The exact methods and algorithms used to enable this need to be discussed further.

This section of the literature review has provided a summary of a wide range of information sources. It is considered likely that further work will needed to be carried out to investigate and simulate the performance of interferometry and signal strength mapping, as these techniques appear to be strongest in the hostile environments typical to the environments this system is likely to encounter.

It also seems likely that these systems will not provide the answer alone and will need to be combined with several other techniques, such as ToA, AoA and cooperative navigation techniques. The methods for combining these technologies, other established technologies such as inertial sensors and the benefits of collaborating between multiple nodes will be discussed in the following mathematical modelling section.

These theoretical results are only likely to provide relatively poor positional estimations, expected to be at least 1 order of magnitude wore than indicated, due to the complications of the RF environment and the temporary nature of many data communication systems. This section has highlighted some of the possible mitigation steps that can be taken to improve the system level positional estimate by either filtering the raw RF data or combining and coupling many navigational systems.

The navigational filters discussed both have their individual merits depending on the application. Many application specific filters that extend the discussed operation have been developed and should be research further as the project develops to allow the resulting navigation system to be as efficient in complementing other systems as possible. The Kalman filter in particular has also been used not only to combine navigational sensors but also to mitigate some of the error sources in RF transmissions, particularly when ToA or TDoA systems are used [THOMAS et. al. 2002] [FAULKNER 2001].

It is possible that, depending on the operational scenario, that RF navigation may only provide a few nodes in a network with the ability to reduce the error of a few coupled sensors and will not be able to provide a robust navigational system on its own. It has been shown however that via a navigational filter, this occasionally accurate source of navigational information may be able to greatly increase the positional estimate of a node. This in turn, via cooperative navigation and SLAM techniques, could allow an entire swarm of systems to gain a good navigational estimation with relatively low grade, lightweight and low-power sensors if the information is combined successfully.

As the project develops it should be noted that, if the system is co-located with other navigational aids, the resulting RF navigation technique does not need to provide an accurate position all of the time on all of the system nodes to be able to provide a very useful system improvement.

This idea should be considered further as we look at the available networks, application and environments intended to be used on the system.

2.2 Non-Radio Geolocation Systems

This thesis has reviewed the key radio geolocation techniques that are currently in use throughout the world. In addition, these geolocation techniques, a number of non-radio approaches have been developed to determine a user's geolocation. An overview of the key techniques and technologies are provided in thesis section along with a summary of their key strengths and shortcomings.

2.2.1 Inertial Navigation System Overview

Although RF navigation is the major focus of this literature review, not all modern navigation sources need external RF aids. An alternative form of navigation allowing a user to locate their position is by using an Inertial Measurement Unit (IMU) to provide information about changes in velocity or angular rate. This information can be used to calculate a user's relative position via the method of dead reckoning.

IMU hardware varies significantly from very large, highly accurate aerospace and space navigation systems to extremely lightweight but error-prone gyros and accelerometers that can be found in small mobile devices such as smartphones. These low grade sensors have drift rates typically in the region of 0.5 to 1 °/second and 100 mg for gyros and accelerometers respectively. Clearly, with these large biases, inertial and other dead-reckoning systems will rapidly accumulate. In combination with other error drivers such as noise, scale factor and misalignment, errors will quickly accumulate in an unpredictable manner over time, causing the users calculated position to 'drift' with respect to their actual position. To compensate this, many systems use some form of external input to limit the accumulated drift. Methods to do this can be found summarised in this section.

2.2.1.1 Coupled INS

A coupled IMU and GNSS applies the input from both systems into a Kalman filter. The Kalman filter provides a navigation solution that uses the IMU to provide attitude information and the GNSS system to provide location information. IMU features such as gravity may be used to correct attitude drift. GNSS information may also be used to correct heading drift. [FAULKNER 2001]

2.2.1.2 Tightly Coupled INS

A tightly coupled system integrates the IMU and GNSS more closely in the Kalman filter. In this scenario, the GNSS information can be used to continually calibrate the IMU, providing the best accelerometer and gyro outputs possible based on good quality delta position updates from the GNSS system. In this way, if the GNSS system loses signal, the IMU is well positioned to continue to provide high quality navigation information until the GNSS signal returns. The re acquisition of the GNSS signal may also be enhanced by the improved navigation data provided by the IMU during the signal outage.[FAULKNER 2001]

2.2.1.3 Ultra Tightly coupled INS

Closer coupling allows the GNSS system to provide information, even in areas of very poor GNSS signal or during jamming events. The Kalman filter is again developed to receive data from the GNSS carrier signal, as well as the usual GNSS packet data.[FAULKNER 2001].

During periods of poor GNSS signal reception, the data contained within the GNSS signal is often unobtainable. It is still possible however to conduct phase shift analysis on the carrier signal from one or more satellites. This is particularly useful in the FDMA GLONASS signals and multi-frequency GNSS-2 systems. To achieve this, the Kalman filter must calibrate the IMU during periods of good GNSS signal, as in the tightly coupled scheme. When the GNSS signal level falls, the IMU is used as the primary source of navigation, but the bias errors from the gyros and accelerometers can still often be corrected by looking at phase shifts in the weak satellite carrier frequencies. Even if only 1 satellite signal is received, it is still possible to make corrections to several IMU parameters. This method allows for longer periods of high quality IMU data between high quality GNSS updates being received.[FAULKNER 2001]

2.2.2 External Information Sources

While INS based systems utilise internally generated sensor signals, external signals other than radio signals are also available to systems. Several mature approaches have been developed to utilise a range of inputs. These approaches are summarised in the following sections.

2.2.2.1 Visual Odometery

Visual odometery is the technique of utilising an optical sensor to measure and monitor the environment surrounding a mobile device in order to determine its geolocation. This area of research has been active for a significant number of years but has not achieved widespread adoption in developed systems [SCARAMUZZA 2011]. The strengths of the technique are the ability for it to operate passively, without a requirement for any transmissions from the mobile device. This passive operation makes the system difficult to jam or interfere with in any way. There are however a number of significant drawbacks that limit the practical applications of the technique. The first is the robustness of the system in a range of lighting and environmental conditions. The technique does not perform well in areas of poor lighting or lack of contract. The second key shortcoming of visual odometery is the processing power required to analyse the video stream. Despite work carried out to optimise the process [SIRTKAYA 2013], the processing power and associated power consumption required to analyse image data in real time systems is a key concern in many target applications. Finally, the difficulty in comparing visual maps remains a significant limitation on the accuracy and robustness of the technique. Developing algorithms that enable the ability to recognise objects from different angles, in varying lighting conditions and with different sensors remains a significant challenge that is yet to be resolved in a mature manner.

2.2.2.2 Terrain Referencing

The terrain referencing technique builds on many of the principles of visual odometery with the addition of a transmitted range finder to survey a mobile platform's surroundings. The data obtained from this sensor is used to compare observed terrain profiles with a database of recoded terrain profiles. One of the most common systems in use is the proprietary UTC Aerospace Systems TERPROM system.

In areas where no other navigation data is available, the TERPROM system can maintain an accuracy of 15-30 meters by combining an IMU and monitoring the terrain surrounding the aircraft. The terrain profile, recorded by a radar altimeter is compared with a database of terrain profiles in the surrounding area. To reduce processing time and increase accuracy, the search in the database is constrained by the inertial data provided by the IMU. [GOODRICH 2013]

The system is used solely in aircraft applications due to the requirement to quickly map comparatively large areas of terrain to provide an accurate positional fix. [GOODRICH 2013].

2.2.3 Non-Radio Geolocation System Conclusions

Table 4 – Non-Radio Geolocation System Comparison

Technology	Radio Navigation Systems	GNSS	Augmented GNSS	JTIDS Relative Navigation	Inertial Navigation System	Visual Odometery	Terrain Referencing Navigation
Global Coverage	No	Yes	No	Yes (If required)	Yes	No	Yes
Accuracy	< 20 m	< 10 m	< 1 m	< 400 m	Unlimited drift	< 1 m	< 30 m
Resistance to Interference and Jamming	Low	Very Low	Low	High	Very High	Very High	Very High
Typical Applications	Shipping Aircraft	Shipping Aircraft Rail Personal Devices	Aircraft Rail	Large military devices	Shipping Aircraft	Robot Localisation	Aircraft

Radio navigation systems have provided an accurate and robust navigation system for military and civilian users for several decades. The most popular system, LORAN, was retired in 2010. This system used a worldwide chain of terrestrial transmitters to allow users to locate their position with a comparatively high level of accuracy is most of the worlds most congested air and water ways.

This network was less well suited to military users due to the facts that large parts of the globe had no coverage and that the control of the transmitters was governed by local governments around the world. During times of conflict, the coverage and operation of the system could not be guaranteed by a single nation.

The desire for centralised control of a global navigation solution is one of the major contributing factors to the development of the world's GNSS systems. Providing coverage almost everywhere in the world these systems have become a vital source for military and civilian navigation systems. Even stand-alone IMU devices almost always use GNSS systems to correct drift errors in practical applications.

The planned upgrades to a GNSS-2 network as well as several new GNSS systems indicate that GNSS is expected to dominate navigation for the next few decades.

One of the main reasons for the emergence of several parallel GNSS systems is perhaps the main drawback of relying on GNSS systems – political control. As seen with radio navigation systems, political control of the network is a very important issue for military users. The difficulties LORAN and eLORAN have experienced with worldwide cooperation needed to ensure system reliability have been replaced by the problem of GNSS networks being controlled from a single source.

The only currently fully operational GNSS system is the US DoD GPS system. While GPS currently provides a civilian C/A channel without the addition of an SA code to artificially degrade the signal, the GPS performance standard [US DoD 2008] still permits its re-introduction if desired by the US DoD. This prevents the adoption of GPS as a core reliable source of navigation information in many safety critical applications. While this risk is being mitigated by several countries that plan to launch their own GNSS systems, the patchy history of the Russian GLONASS system demonstrates the high cost, engineering difficulty and political commitment required to keep the system fully operational.

GNSS systems are also vulnerable to a range of threats due to the nature of the space segment signals. The signals are very weak at the earth's surface, with a maximum received signal strength of -155dBW, and require a line of sight between the space and user segments. This makes the system vulnerable to disruption in complex urban and mountainous environments where a line of sight with at least 4 satellites cannot be guaranteed. The weak received signals also make them susceptible to natural disruption from atmospheric effects and malicious disruption from low powered jamming and spoofing systems.

Addressing these shortcomings is the major focus of GNSS-2 systems. While these effects can be partially mitigated with additional satellites, channels and increased power levels, this second generation of GNSS systems will still be too vulnerable to disruption for many safety and military applications.

Another method for securing and verifying the GNSS data has been to use DGPS and INS systems. DGPS systems attempt to increase the accuracy of the GNSS signals in a range of local and wide area systems. These systems allow the accurate operation of relative navigation devises, even during times of degraded GNSS data. They are however still vulnerable to natural and malicious disruptions. Novel methods of augmenting GNSS via powerful communications satellites could yield considerable reliability improvements, however the concerns of system control could still dominate.

The addition of an IMU to make an inertial navigation system (INS) allows the user to provide some confidence estimations to the received GNSS data. It also allows a user to bridge areas of local GNSS signal disruption. This system, even with ultra-tight coupling, does not however produce a completely reliable system as some form of GNSS input is required to correct for IMU drift.

While terrain reference navigation offers one possible mitigation path for correcting IMU drift without using an external source, the required terrain information and limited availability of reference data limits it's uses to only a very niche range of aerospace applications.

The ability to robustly verify and correct for GNSS errors is greatly in demand. The following chapters of this literature review shall discuss novel methods and current research papers aimed at producing this solution.

2.3 Data Fusion

The previous sections indicate that neither radio or non-radio techniques can be applied to provide the level of geo-location accuracy on its own. It is very likely that a system that can provide the levels of accuracy and resilience required by many system users will use a combination of RF sources and navigation techniques as well as other navigation devices, such as inertial navigation equipment. The resulting system may also consist of several cooperating nodes, physically distributed in an area.

This section of the literature review aims to summarise the mathematical algorithms that will allow the various RF and other raw data sources to be integrated together to provide a navigational solution. The benefits of cooperative navigation in a range of scenarios will also be discussed.

2.3.1 Navigation filters

Many current navigation systems use data from a range of sources. Section 2.2.1 of this document has already discussed the combination of GNSS signals and an IMU to create a coupled system. The coupling of these sensors is carried out in a navigation filter. A summary of the most common navigation filters can be found in the following sections.

2.3.1.1 Recursive Filters

Recursive averages are commonly used in navigation systems to produce a low noise and low latency location estimate from a noisy measurement input [FAULKNER 2001]. In order to provide an efficiently filtered output, the measurement system that populated the recursive filter must provide not only a measurement value, but also a dynamic confidence indicator.

When using a simple threshold detection algorithm to detect the leading edge of a received signal, the only information that can be provided to the navigation filter is the time when a received value is greater than the selected threshold [FARAGHER et. al. 2010]. If this information is available for each FHSS channel, a simple un-weighted recursive filter shown in (5) can be constructed to update the users filtered location based on the its previous position and the latest sensor data where, as commonly used in filter notation, $\hat{x}$ represents the filter output, $\bar{x}$ represents the previous state and $\tilde{x}$ represents the latest sensor value. The measurement confidence is represented by α.

$$\hat{x} = \alpha\bar{x} + (1-\alpha)\tilde{x} \qquad \text{Eq 3}$$

The filter represented in (5) may be tuned by adjusting the value of α by a predetermined value.

A value of α < 0.5 reduces the noise of the filter output at the expense of a higher latency if the receivers true location changes. A value of α > 0.5 generates a more responsive, lower latency filter output but the filter output noise will be adversely affected. Both of these options are unsuitable for many system applications.

2.3.1.2 Kalman Filtering

One of the key set of equations used in navigational data fusion was created in 1960 and is known as the Kalman filter [KALMAN 1960]. The Kalman filter is a generic filter that is commonly used to smooth noisy data signals. It achieves this by combining a recursive filter with an additional estimation stage. The Kalman filter is also commonly used to combine several data sources during the measurement stages, using each measurement to update the state estimation. A schematic representation can be seen in Figure 5.

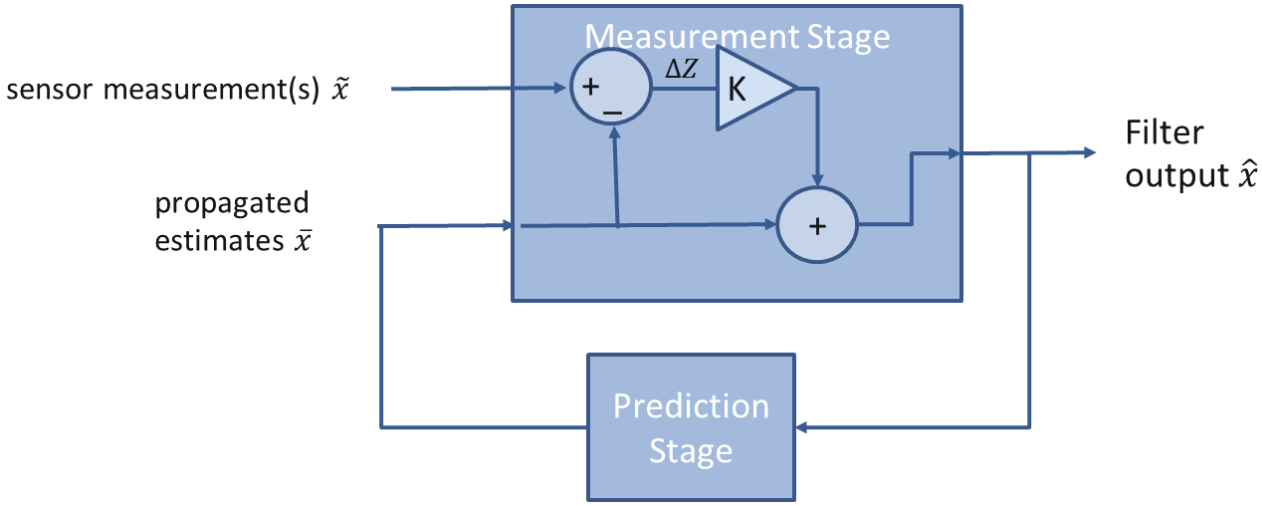

Figure 5 - Kalman Filter Overview

The initial concept of the Kalman filter was to provide this functionality in a computationally efficient manner. The Kalman filter typically consists of using vector algebra to combine multiple data streams, using that assumption that they are Gaussian distributed to ease the calculations. A common description of the Kalman filter is a method of combining Gaussian distributed data streams to provide a single Gausian distributed estimation of the users location. In addition to this the Kalman filter assumes additional knowledge in the following areas:

The current state of the system. The filter uses previous knowledge of the users location, velocity and bearing in the computation of the new state.

Time. The Kalman filter relies on discrete steps in its computation and the time between each step to be known.

Control inputs. Knowledge of the system's ability to react to control inputs in included in the new state prediction

The sensor noise (R Matrix). For each sensor, the nominal noise in each state must be estimated prior to system operation. The noise from all sensors must be Gaussian.

The transformation accuracy (H Matrix). The accuracy of the sensor to record the transfer of position from one time sample to another.

The core requirements for the filter to operate are the R matrix and H Matrix of each sensor. The R Matrix is the noise distribution of the sensor. This allows the filter to estimate the width (3σ value) of the data. The R Matrix value may be updated at each calculation step if the sensor is known to have differing noise characteristics at a known state, as is commonly the case with inertial sensors that get noisier as rate or acceleration increases.

The H Matrix represents the translational measurement accuracy of the sensor. This defines the ability of the sensor to accurately measure the transition from the last calculated state. The sensor provides the relative estimate of its position confined by the known accuracy of it in its pervious state.

The fact that the Kalman filter takes sensor data in these basic R and H matrix formats allows the filter to be applied in a computationally efficient manner to a wide range of sensors, as anything from an IMU to a visual odometry system can produce estimated in a R and H matrix form and be at least loosely coupled together [Ebcin, Veth 2007]. The ability for systems to gain tighter coupling is also possible in the Kalman filter. This has been an active area of research since the creation of the Kalman filter in the 1960s and is commonly achieved via two main methods.

Firstly, if a sensor performance if known to vary depending on the state of a system, the Kalman filter can be provided with a lookup table that alters the H matrix depending on the system state. This technique is known as an extended Kalman filter [Simon 2006]. An example of why this may be required is if the IMU and visual odometery system is considered on an aerial platform in an outdoor environment. If the camera providing visual odometer is facing down, it is assumed that it will provide good odometery information, so the H matrix defines a very small measurement accuracy. If the aerial platform is then inverted so that the camera is no longer pointing down, the H matrix of the sensor will be radically different. As the camera is likely to unable to track any motion the H matrix constraints need to be altered. The visual odometery system itself may have no knowledge of the platform attitude so the Kalman filter that has been monitoring the system state must now use a different H matrix for the data. This attitude specific data can be found in a pre-loaded lookup table that produces an H matrix value that varies with platform attitude.

A second method for tighter coupling in a Kalman filter is also available. If we again consider the coupling of a visual odometery system and an IMU, there is a possibility that when the visual odometery system is in a state that provides a very accurate translational estimate, the other sensors in the system may have their errors removed [FAULKNER 2001]. IMU systems typically have bias errors that are stable when the IMU is powered up, but include an unknown turn on bias. This method could allow the IMU in the system to have its turn-on biases removed by the visual odometery system when the camera is looking down via a Kalman filter comparison during operation. This can be achieved within the Kalman filter by comparing data that has a high integrity H matrix with the other sensors in the system. Even if this high integrity H matrix is only available for a comparatively short time, the ability to measure the offsets in the other sensors may allow the Kalman filter to provide an improved positional estimate for a prolonged period.

The main constraint in the use of Kalman filters, particularly in navigation systems is the difficulty in calibrating, testing and verifying the system. Navigation system calibration techniques do not allow the successful calibration of non-linear systems [TEDALDI et. al. 2014]. Specialised calibration techniques are required when using Kalamn filter systems. These techniques are complex and difficult to verity and test in a full range of use case environments.

Extensive research has been carried out to utilise Kalman filters to allow robotic systems to observe and map their environment [F. Kong et.al, 2006]. Common approaches utilise a sensing system, such as a laser range finder, to record features within the environment around the mobile system. The mobile system runs an extension to the Kalman filter. This additional stage allows the Kalman filter estimation step to progress only when a feature that will enhance the geo-location estimate is observed as shown in Figure 6.

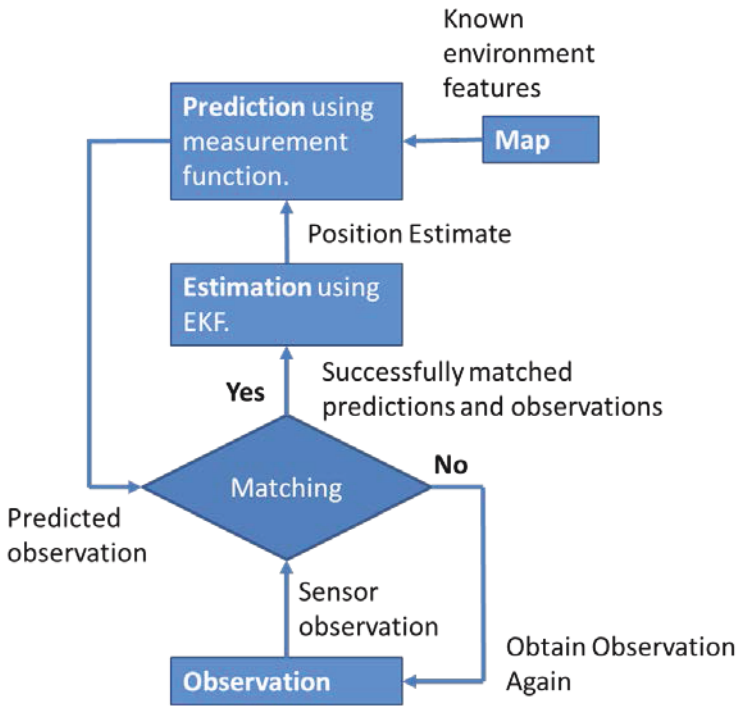

Figure 6 - Extended Kalman filter with Feature Recognition

Kalman filters have also been used in radio signals of opportunity navigation [FARAGHER et. al., 2014]. In this application, the Kalman filter is run as the centre of a smartphone system that combines several sensors to produce a location estimate. The Kalman filter in this application runs a similar extension to that shown in Figure 6 however the recognised features are sensor characteristics and fingerprints rather than physical features. This allows the Kalman filter to form the basis of a SLAM mapping system that has the ability of combining a range of sensor inputs.

The drawback of these systems is that extended Kalman filters scale poorly when they are used to map an input, requiring rapidly increasing processing power as the mapped environment grows. Whether mapping with feature recognition or sensor fingerprints, the maintenance of the mapped environment requires considerable processing power. In almost all research papers reviewed the results were calculated by post processing collected data. Very few research examples exist where the mobile system has been capable of mapping the environment in real-time.

2.3.1.3 Particle Filters

Particle filters, occasionally known as Sequential Monte Carlo (SMC) filters, have several uses in navigation [GUSTAFSSON 2002] and signal processing application [DJURIC et. al. 2003]. The applications that are commonly addressed by particle filters are those that need the type of functionality provided by a Kalman filter but don not have Gaussian distributed sensor systems feeding the filter.

Like Kalman filters, a particle filter requires information about the measurement error of each sensor, but not specifically the sensor noise and transformation accuracy. The particle filter also maintains state, so that the sensor coupling techniques similar to those discussed in section 2.3.1.2 are still possible to implement.

Where the particle filter differs from the Kalman filter is in the method of estimating position from the system sensors. The Kalman filter sums the Gaussian distribution of the inputs to reduce the computational effort to produce a Gaussian distributed positional estimation. The Particle filter does not require its sensor data to have a Gaussian distribution. Instead the particle filter carries out a recursive Monte Carlo calculation of its position with each piece of received sensor infuriation. This produces a particle cloud that can be used to estimate the platforms position, with the platform likely to be at the densest part of the particle cloud.

This recursive Monte Carlo approach to positional calculation can be very computationally intensive and is the main drawback of the technique when compared to the Kalman filter. This often leads to a trade off when deciding how has to run the particle filter in many implementations. A high frequency filter produces many particles that provide a good navigation solution, but is computationally intensive. Reducing the number of particles reduces the computational load, but also the positional accuracy.

Work has been carried out to try to improve particle filters with extra system information [Lin Chang 2008] leading to application specific examples that can begin to provide Kalman filter type of efficiency without the need for Gaussian distributed senor inputs.

2.3.2 Radio Filters for Multipath Mitigation

Extended Kalman filtering has been used successfully to help mitigate the effects of multipath in a range of RF applications [Thomas et. al. 2002] and even calculate the position of the transmitting node from the spread of multipath signals in a known physical environment. [Popescu Rose UNKNOWN].

The application of a Kalman filter has been used to address the problem in many RF navigation systems and TDoA systems in particular, that while the distance between line of sight transmitters and receivers can be accurately measured, in many environments the measurement is dominated by the multipath environment and the received signal does not follow a line of sight path.

The multipath effects are removed by feeding the symbol receive times as a noisy data source (H and R matrices) into a biased Kalman filter. From this the Kalman filter can estimate the true time of arrival of the signal. This Kalman filter aims to remove several time of arrival errors including non-line of sight errors, quantisation errors and noise. A bias is added to the Kalman filter as non-line of sight errors are always positive and the filter is biased to the low end of the Gaussian distributed data. This filter was shown to reduce the mean location errors of a time of arrival system using a 3G mobile phone signal in an urban environment by an order of magnitude.

The same biased Kalman filter technique could be applied to virtually any RF based time of arrival system.

2.3.3 Cooperative Navigation Techniques

A key to almost all of the discussed navigation systems in this thesis is the requirement to have at least one part of the system at a known location. The signals transmitted or received from this known location then allow the user to calculate their position. A different approach is required in systems where no local nodes know their exact location.

Cooperative navigation is a very active area of research in alternative navigation techniques. The basic concept utilises the fact that if a group of independent nodes each calculate their own position, the confidence of their estimation and the circular error probability estimation of each node can be reduced.

In its simplest form the technique can be used to remove some of the physical payload from autonomous systems, using separate navigation only nodes to calculate their position and share it with the rest of the local nodes. [Wilcox et. al. 2006]. This concept also allows a single nominated navigation node to break away from a semi stealthy configuration, update its position via an external source and inform the other local nodes.

A more advanced corporative navigation system allows mathematical analysis to be carried out between the nodes. The aim of which is to use the nodes that have a good positional confidence to provide relative range data to aid nodes that have poor positional confidence, this allows the network to limit drift and maintain a higher level of accuracy at each node than can be achieved alone.

[Wilcox et. al. 2006] has shown that underwater systems can generate relative positional information between each node, meaning that only one node on the extent of the network need to acquire a firm GNSS fix and can allow the other nodes in the system to remain submerged. Other research [Sand et. al. 2013] has shown that some nodes in a cooperative system may also be able to carry different equipment sensing equipment and share their navigational estimates with each other. These estimates may allow the network to obtain a very accurate positional estimate even if no single node knows its exact location or contains the equipment to determine its position alone.

This research has combined visual odometry, RF and inertial navigation, SLAM algorithms and extended Kalman filtering to realise very good positional accuracy across a connected system of separate nodes. Although the system uses relatively simple and inaccurate RF ranging techniques it is a good example of how many systems can operate together in an application specific navigation filter to achieve very good navigational performance.

2.3.4 Simultaneous Localisation and Mapping

Simultaneous Localisation and Mapping (SLAM) has become a very large field of research in autonomous system navigation. Already briefly described in section 2.3.3, SLAM allows a user with no predetermined information about their location to determine both the position of markers of interest around them, such as visual markers [Lategahn et. al. 2011] or RF antennas [Anwar et. al. 2013].

The main advantage of SLAM algorithms in particular is the ability to calibrate a range of sensors in an unknown environment. This is achieved by a systems travelling around an unknown environment and recording its surroundings. The system then tries to return to a position it has already sampled. When the system returns to that position, it can perform loop closure and update the recently built map. This action makes it possible to remove many of the previously unknown sensor biases and errors, updating the navigation filter appropriately.

This method has been successfully applied to RF navigation via radio waypoints, radio and visual integration [Anwar et. al. 2013] and via the signal strength techniques [MERRY et. al. 2010]. The conclusions from this work is that SLAM algorithms tend to work best in very complex RF environments where there are many ‘contours’ in the received signal properties.

A novel area of improvement that may need to be carried out during the course of this degree is the application of SLAM techniques to available military networks and complex hostile environments in particular.

2.3.5 Sensor Fusion Summary

We have shown that there are many techniques that could in theory provide very good positional estimates from data communication systems. These theoretical results are only likely to provide relatively poor positional estimations, expected to be at least 1 order of magnitude wore than indicated, due to the complications of the RF environment and the temporary nature of many data communication systems. This section has highlighted some of the possible mitigation steps that can be taken to improve the system level positional estimate by either filtering the raw RF data or combining and coupling many navigational systems.

The navigational filters discussed both have their individual merits depending on the application. Many application specific filters that extend the discussed operation have been developed and should be research further as the project develops to allow the resulting navigation system to be as efficient in complementing other systems as possible. The Kalman filter in particular has also been used not only combine navigational sensors but also to mitigate some of the error sources in RF transmissions, particularly when ToA or TDoA systems are used. It is possible that, depending on the operational scenario, that RF navigation may only provide a few nodes in a network with the ability to reduce the error of a few coupled sensors and will not be able to provide a robust navigational system on its own. It has been shown however that via a navigational filter, this occasionally accurate source of navigational information may be able to greatly increase the positional estimate of a node. This in turn, via cooperative navigation and SLAM techniques, could allow an entire swarm of systems to gain a good navigational estimation with relatively low grade, lightweight and low-power sensors if the information is combined successfully.

As the project develops it should be noted that, if the system is co-located with other navigational aids, the resulting RF navigation technique does not need to provide an accurate position all of the time on all of the system nodes to be able to provide a very useful system improvement. This idea should be considered further as we look at the available networks, application and environments intended to be used on the system.

2.4 Radio Data Communication Techniques

The motivation for this project is to provide navigation via data communication networks in hostile RF environments. Hostile RF environments are commonly found in battlefield and disaster scenarios. These environments are likely to contain a rich resource of military networks. This section of the literary review aims to summarise the key components of common military networks that may be used for navigational purposes, using the techniques previously discussed.

2.4.1 Ruggedisation Principles

Key to the success of many military data links is security. Security in military data links related to a number of key areas:

- Encryption – The ability to allow only authorised users to understand the messages transmitted in the network.
- Anti-Jamming – The ability to keep the data link working reliably in hostile environments.
- Covert Operation – The ability to transmit data without unauthorised users knowing a transmission has taken place.

2.4.2 Message Security

Message security (MSEC) is often used to provide message encryption. This is a field of research that is by no means unique to military networks, with considerable attention given to message encryption within civilian data communications, such as the RSA algorithm [R.L Rivest, 1977]. Little public information is available about the encryption methods used in military networks, the RSA algorithm was however developed by the USAs Office of Naval Research at the same time as several NATO data links were being developed by the same office. The closed nature of military networks also allows the possibility of 'shared secret' encryption algorithms to be used more commonly than in civilian networks.

2.4.3 Transmission Security

In addition to message security, transmission security (TSEC) may allow the anti-jamming and covert operation aspects of military security to be implemented. Typical TSEC techniques are described in the following section.

2.4.3.1 Frequency Hopping

Frequency Hopping is a technique of making a signal difficult to jam by jumping between carrier frequencies during transmission. An overview of channel selection over time can be seen in Figure 7.

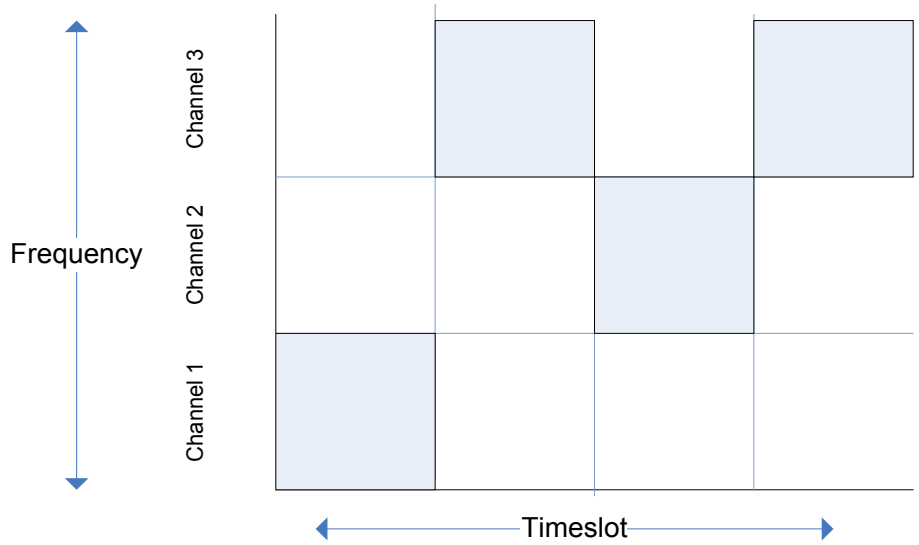

Figure 7 - Frequency Hopping

The frequency selected for each timeslot is calculated by a shared secret algorithm. This allows the transmitting and receiving node to be in synchronisation. This provides anti-jam resistance when it is considered that the frequency channels used may be over a wide range of frequencies. The only way for the system to be completely jammed is if all channels are jammed simultaneously. Jamming this many channels would require a high power jamming signal. Such a high power signal would be comparatively easy to detect and disable in many hostile environments. Several frequency hopping systems also maintain a record of the link quality for each channel used and can prevent the use of jammed channels on the fly [3sdl, 2009].

2.4.3.2 Carrier Frequency Jitter

To prevent attempts being made to receive, decode or spoof signals of the above systems, many also use a variable jitter on the carrier frequency [3sdl, 2009]. This system adds a pseudo random jitter on the carrier frequency to provide a further layer of security. As the length of each bit varies in a seemingly random manner, it prevents an unauthorised user from collecting messages and attempting to decode them either in real-time or during post processing. The jitter algorithm is derived from a shared secret algorithm between authorised nodes.

2.4.3.3 Spread Spectrum Techniques

Direct sequence spread spectrum (DSSS) is a TSEC technique that 'hides' a narrow bandwidth signal in a wide bandwidth transmission. This allows anti-jamming in a similar way to frequency hopping, in that it prevents the use of low power, narrow bandwidth jamming equipment. In addition the technique makes detecting the transmission harder, preventing unauthorised users knowing a transmission is taking place. To achieve spread spectrum transmission, the signal to be transmitted is combined with a pseudo noise (PN) code. This code is again most likely to be a shared secret algorithm. Again, little information is available about the codes used, but may be similar to the 4 phase Barker sequence, developed at a similar time to many NATO spread spectrum technologies. [R Turyn,1974].

Frequency hopping spread spectrum (FHSS) is commonly used in military (link 16) [3sdl, 2009] and civilian (802.22) networks. FHSS switches between a range of low bandwidth channels in a pseudo-random manner to provide many of the benefits of DSSS networks. FHSS does not require a pseudo noise code to modulate the data, but instead used a shared secret algorithm to choose the order of the channel hoping. The hopping rate can be up to 111 channels per second making it prohibitively difficult to follow the transmission to jam them.

2.4.3.4 Satellite Communications

NATO currently uses the Paradigm Skynet 5A satellite communications system [Paradigm, 2014] for the majority of its satellite communications. The system was launceh in 2007 and is designed to provide a robust satellite data-link in hostile battlefield environments.

The Skynet system uses a TCP/IP system to provide interoperability and message security to allow nodes to collect over a global, fibre-optic back-haul network with an RF satellite final hop to remote nodes.

The RF satellite link component provides a range of X-band (8 GHz to 12 GHz) data links offering a range of bandwidths from 20 MHz to 40 MHz. Each satellite can provide a wide range data link as well as an unspecified number of directional data links. The satellites operate in a global constellation, using geostationary orbits. The high altitude of the satellites is countered by their high power 160 W RF transponders that are able to provide steerable beams for high bandwidth directional data links providing 56 dBW signal strength. The system is likely to use a wide range of transmission security techniques to provide battle hardness.

2.4.4 Robust Network Conclusions

This section has provided an overview of the most commonly used radio security and encryption techniques. These techniques are likely to be applied in any developmental or future data link systems and provide a valid summary of the challenges presented by current military networks when viewed from a navigation point of view.

Key themes appear from this section, firstly that fact that many military networks seem to lag civilian networks in terms of transmission sophistication and data rates. While this may aid the ability to use the networks for navigation with low accuracy hardware bue to lower clock rates and a reliance on TDMA network topologies, the addition of some security aspects make the task more challenging.

The ability to deal with spread spectrum and frequency hopping should be considered. This may help to make the battlefield RF environment appear less congested, any proposed system may need to take into account any timing errors introduced by the system. These techniques, along with carrier frequency jitter, may also mean that only authorised or 'friendly' data links can be used in the battle field environment, reducing the ability to use a Signals of Opportunity' approach to navigation.

2.5 Industry Interview

2.5.1 Industry Interview Aims

To provide further evidence and to support the literature review, an industry interview has been carried out to assess whether any shortcomings identified in the literature review are affecting technology development and deployment within industry. The key aims of the industry interview are to:

- Identify if the current state of the art is limiting technology development
- Identify the key reasons for any limitations
- Identify key criteria that, if satisfied, would allow an assessment of the success of any contribution of knowledge obtained by this this research.

An industry interview event was held at the Sensors and Integrated Systems division of UTC Aerospace Systems. UTC Aerospace Systems are a global technology company, the Sensors and Integrated Systems division, where the interview took place, specialise in carrying out research and developing algorithms to combine sensors and systems in novel ways. These applied algorithms provide navigation solutions in both aerospace and automotive environments. The industry interview event was attended by 8 directors and other senior representatives from the sites business development, engineering and technology departments. The aim of the interview was to confirm that, as found by the literature review, current navigation solutions have significant limitations that are not being addressed by current research.

The industry interview was carried out in a structured style with panel questioning. The detailed method, results and analysis of the event can be found in Appendix A- Industry Interview Findings.

2.5.2 Key Findings from the Industry Interview

The industry interview provided a source of information that is complementary to the academic literature review. Several of the technical shortcomings of GNSS technology has been confirmed, with the additional information that the reliance on only a small number of national systems is considered a significant risk to those that don't control a GNSS system.

The second main theme that came from the industry interview was that bringing together many data sources in an efficient manner is a key aspiration and is seen as the next step in technology. Two main areas of data fusion were mentioned. The first was the accuracy improvement that is expected from collaborative navigation of several mobile systems. The second was the ability to overcome system shortcomings by combining data from a range of unconnected sensors. The ability for each of the sensors to be passive was also highlighted as a key area of development.

These shortcomings have not been directly addressed by any the techniques emerging from academia, reviewed in the project literature review. The view of the industry interview will be used throughout this project to shape and guide the direction of the research to allow it to provide a useful and useable advance in technology. The concerns of the industry interview will be reviewed in the project conclusions.

2.6 Literature Review Conclusions

2.6.1 The Limitations of the State of the Art

The literature review, including an industry interview, has been carried out to detail the current state of the art and to highlight where opportunities for further development may lie in the use of data communication systems for navigation.

Radio navigation systems have a long history of providing navigational data to mobile devices stretching more than 80 years. Without further analysis, following this long history, it may seem that the opportunities for further development are limited. Early systems relied on the installation and operation of dedicated navigation radio beacon to provide systems with the information required to calculate their location. These systems provided only a localised position estimate and many areas were never included in the transmission network. Today, these systems still operate in specific areas, but wider rollout to dense urban environments around the world is unlikely to happen. Global coverage is achieved with GNSS systems. The first generation of these systems have been very widely adopted by civilian systems and the navigation and timing information provided by the available GNSS systems is a common part of everyday life for many.

The 2nd generation of GNSS systems are currently being rolled out by a limited number of nations and promise to improve the reliability and coverage of the signal. This will undoubtedly increase the widespread adoption of GNSS services by a wide range of products even further. May applications will still not be served by this new generation of GNSS system, in particular systems that rely on operation in areas with poor visibility of the skies or those that do not wish to rely on a very small number of governments for their continued ability to operate correctly. The inability for even 2nd generation GNSS systems to operate in dense urban environments due to the continuation of weak reception signal at ground level, mean those applications cannot rely on it in locations that are most in need of navigational aids, where dense populations of users and service providers are in close contact. This application area is one that is fuelling considerable research and is considered to be one of the significant contributors enabling the future success of the internet of things and urban advertising technologies. The second significant and continued shortcoming of GNSS systems is the limited selection of third parties that are able to provide the signals for the system. The signal provider can easily stop, encrypt, add offsets or errors to the system that are difficult to detect. This is a major concern for many important and safety critical applications, limiting the adoption of GNSS even in areas of good reception. This particular concern was emphasised by the panel at the industry interview. Creating a system that does not rely on such a limited set of service providers was highlighted as being a significant development that could be very appealing to industry.

To mitigate these shortcomings promising work has been carried out to combine GNSS signals with other systems. DGNSS effectively combines GNSS with fixed position radio navigation towers. In areas of good coverage by both GNSS and fixed radio navigation towers, the system works very well. The coverage of these systems is however very limited and their widespread adoption is very unlikely. The combination of GNSS and other sensors, such as INS also shows good promise. The resilience of the receiver to poor GNSS signal is greatly improved and short time periods without sufficient GNSS signal can be coped with well. Longer periods without GNSS signal however result in comparatively rapid system accuracy degradation as INS errors integrate together. To allow sufficient time periods without GNSS signal the sophistication, and so size and cost, of the INS device required makes the technique impractical in real world applications.

TRN shows excellent robustness and reliability as a navigation technique. The key to the benefits of the system are that the system relies on prior knowledge of environmental features that cannot be controlled by any small number of 3rd part operators. Clearly the terrain of an environment is outside of the control of the system that is navigating within it, but the wide availability of terrain maps from a large number of sources mean that reliance on it is acceptable to many systems.

This is an important concept that should be considered throughout the research required for this project; although the reliance on a 3rd party for the navigation system is not desirable, if the 3rd party infrastructure is not controlled by only a few providers, it does allow reliable systems to be built upon it. The drawbacks of TRN is that it only works well on a large scale as mapping information below a certain scale is either unavailable or too transient to be used reliably, making it a poor choice for indoor and urban navigation where common systems are on a smaller scale.

While the altimeters and topological maps required for TRN are unlikely to work at the small scale of indoor navigation, RF receivers and a rich seam of radio level navigation data is likely to be available. The wide range of detectable RF effects that are at their most adverse in indoor and urban environments are likely to provide a robust resource of radio topology. With a highly accurate radio receiver, indoor areas may be mapped with a very wide range effects including signal strength, angle of arrival, time of flight and frequency shifts. Varying effects across the frequency range add further information to the data that can be collected. The availability of such a wide range of information seems to be an area that provides a very significant opportunity. The progress made by research into signals of opportunity has begun to show promise, but much further research could be carried to find the limits of what navigation information can be gained, particularly in indoor and urban environments. To allow the extraction of information from this area, two areas will need to be researched by this project. The first is to identify what effects should be monitored in the RF and which RF signals these effects should be monitored. There are a very wide range of RF transmission effects in most indoor and urban environments. Those deemed to be obtainable and of use in generating navigation estimates have been initially characterised and tested in signal of opportunity research papers. Detailed testing with a range of RF effects in urban environments is less well documented. In addition to this, the literature review has highlighted the common application of spread spectrum techniques that require the receiver to monitor a very wide range of frequencies. Again, much research has been published about how the different propagation of this wide range of frequencies can be analysed to increase transmission reliability and data rates. Significantly less research exists that has been carried out to analyse whether this data contains additional information about the receivers local environment.

Once the selected RF effects to be monitored have been identified, filtering techniques will be required to extract the required information. Much work has been carried out to filter radio signals in indoor and high multipath networks to obtain the communication data contained within it. Less research exists to analyse and filter the received signals to determine to what degree multipath has affected it. This data could be of use in determining the character of the received signal, potentially revealing information about the receiver's surroundings.

The efficient combination of sensors ranging from visual odometery to INS and GNSS systems is a well-documented field of research. Very mature papers, such as the development of the Kalman filter, date back more than 50 years. Development has led to specific interfaces for each type of sensor data into a range of navigation filters. The developed filters allow very efficient use of even small data sets, providing the end user with robust and reliable navigation solutions. While this is a generally well-documented area, the integration of signals of opportunity systems is not mature. Work has been carried out to loosely couple signals of opportunity data, but ultra-close coupling between raw RF sensors and other data streams in a generic system has not been documented.

This review of the current state of the art has completed the initial aim of the project; to identify the shortcomings of the current state of the art for indoor and urban geo-location. Further to this, a number of research opportunities have also been identified.

2.6.2 Research Opportunities

Recent studies demonstrate the potential of coupling data streams to produce information that neither system could produce in isolation. This is well demonstrated with the ultra-tight coupling of GNSS and INS systems. It is anticipated that typical systems that will need to navigate around urban and indoor environments will contain a wide range of sensors as is particularly demonstrated with recent developments with smart phones that contain a wide range of inertial, optical and radio sensors. The review of current research has led me to identify an opportunity that a range of radio sensors, typical to many systems to provide data communications connectivity, may be used to provide an improved geolocation estimate. This improvement could be achieved by efficiently analysing the existing sensor data streams without the addition of any extra hardware. This elegant approach will provide the system designer with additional information with no trade-off for power, space or weight.

To achieve this output, further research is required throughout a series of radio sensor layer stacks. The first is in researching the correlation of specific RF effects with geo-location change. This research is required to the raw data that will build up through the system. There are a wide range of RF effects that may be monitored by radio receivers, further research into what geo-location data can be gained from the effects is to be carried out. The raw data is suitable for use in typical systems as it is likely to be from a range of sources, providing multi-spectral reliability and removing the reliance on a single RF data provider which limits the application of many current systems.

A second area of research is required. This area needs to build upon current data processing filtering techniques and find ways of analysing the data required with common data communications hardware. The limitations provided by the hardware are commonly around timing accuracy and frequency ranges. It is likely that the ability to accurately detect the required RF effects will need to be investigated as they may vary from those commonly required to receive data communications.

Novel filtering techniques will be required to overcome hardware limitations, enabling the geo-location information to be received.

In addition to the identification and sampling of the raw RF information, higher level navigation filtering schemes will need to be designed to allow the efficient integration of the new information at a higher level. Using filtering schemes such as Kalman filters should allow the information obtained from the RF environment to be used efficiently. Further, the design of efficient integration modules into a Kalman filter could allow improvement back into the RF reception and filtering through a scheme of close coupling.

The development of each of the three layers, to enable a higher level geo-location estimate to be achieved, will be described in the following chapters of this thesis, as detailed in Figure 8.

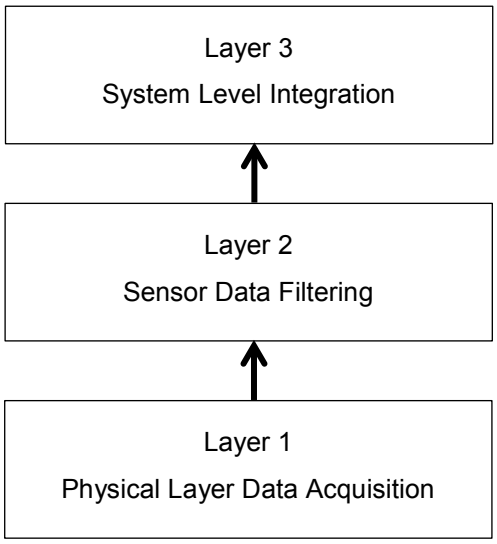

Figure 8 - The Three Principle Stages of Location Estimation

It is clear from the review of the current state of the art that opportunities exist to build upon sensor fusion techniques applied to inertial and optical navigation in the area of radio signals of opportunity. A hypothesis has been formed that raw RF data can be sampled and filtered with common data communications hardware and efficiently integrated into a higher level system, even if strict hardware limits are assumed. This approach shows the potential to allow many of the shortcomings of current applications to be overcome, providing a wideband navigation solution in indoor and urban environments that does not rely on any single radio signal provider.

This page is intentionally blank.

3. Architectural Design

The literature review has highlighted a shortage of practical applications around the integration and combination of radio signals of opportunity to provide a robust and reliable geo-location solution in indoor and urban environments. The literature review has also highlighted the potential of developing a closely coupled system approach to fusing existing sensor data if techniques applied in other areas of navigation can be adapted and optimised for a signals of opportunity application. This project will research further possible solutions that can be used to optimise an integrated navigation solution, suitable for use in low size, weight and power applications where existing applications only provided limited capabilities. Further research in these areas has the potential to further academic understanding as well as industrial capability in geo-location techniques.

This section will detail the key aims of the high level design architecture, detail the initial design constraints that will guide the architecture design before presenting the proposed design architecture. This section will conclude with analysis of the design architecture, highlighting the key error drivers.

3.1 Design Aims

This project will investigate the design of an architecture that allows for the scalable integration and coupling of radio signal of opportunity sources. This architecture is required in order to increase the accuracy and robustness of geo-location estimates in indoor and urban environments. The key aims of the system architecture are:

i. To minimise system complexity.
ii. To optimise the filtering of sensor data by tightly coupling data streams.
iii. To make use of existing hardware, preventing the addition of sensors specifically for indoor or urban geo-location.

The work carried out to design a system that allows these aims to be achieved is discussed in the remainder of this section.

3.2 Architecture Development

This section outlines an architecture that combines signals of opportunity in order to improve geolocation estimates. The research first proposes a generalised architecture that will allow the design aims to be met, describing the key principles that will allow a benefit from the integration of signals of opportunity to be achieved. Once the generalised architecture has been defined, consideration is given to a common signal of opportunity Kalman filter. The adoption of common data sources into the proposed filter will then be discussed further.

Key to the development of a system architecture is the concept that coupling measurement data streams leads enables the potential to gain further information from each data stream. While the approach of closely coupling data sources is well documented in certain applications, described in the literature review in 2.2.1.1, an approach that is applicable radio signals of opportunity will required further research. One significant difference between existing data coupling techniques and coupling signals of opportunity is the fact that the input data sources may not be reliable, known or stable. An architecture is required that can recognise and compensate for changes in signal availability and integrity in a reliable and robust manner. A second significant research challenge is that the designed architecture must be able to cope with a wide range of potential data sources.

Research into combining signals of opportunity provides the potential to couple complementary data streams whenever they may be available, leading to further iterations of information gathering. The iterative benefits that can be achieved by stages of closer interactions are made possible due the wide range of complementary sensor measurements made by a typical system, depicted in Figure 9.

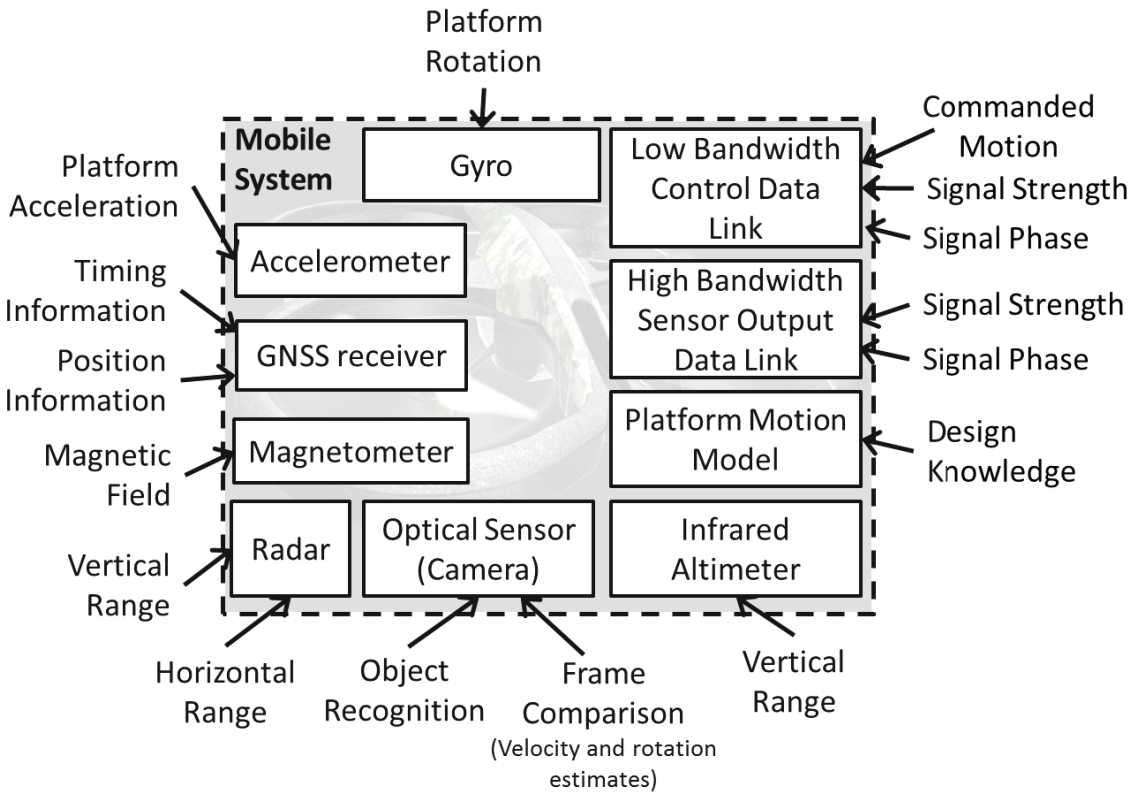

Figure 9 – Typical Opportunistic Inputs

Research has been carried out to combine this wide range of measurement data streams in specific applications. The development of a more generic system integration architecture has been limited due to poor scalability and system complexity.

This limiting factor needs to be addressed to allow a closely coupled approach to be developed for use in generic systems where detailed knowledge of the properties of each data stream are not needed. The ability to minimise system complexity and provide a scalable solution that utilises a wide range of sources is one of the significant drivers this design approach and is investigated further in this thesis. Dead reckoning using the output of an inertial measurement unit can be used to maintain the user's location, allowing the development of a scalable system. As described in the literature review, section 2.2.1, inertial sensing systems are common in almost all mobile platforms with low size and power gyro and accelerometer chips are mass produced and low cost. Further, inertial sensing systems are commonly deployed in existing mobile systems for a wide range of applications from screen orientation checks to camera stabilisation.

Specific benefit comes from coupling an IMU with radio signal based ranging estimates. As described section 2.1 of the literature review ,these estimates are commonly achieved via time-based and signal strength methods. Time based ranging estimates may be efficiently used in conjunction with other geo-location data to provide an improved geo-location estimate as shown in Figure 10.

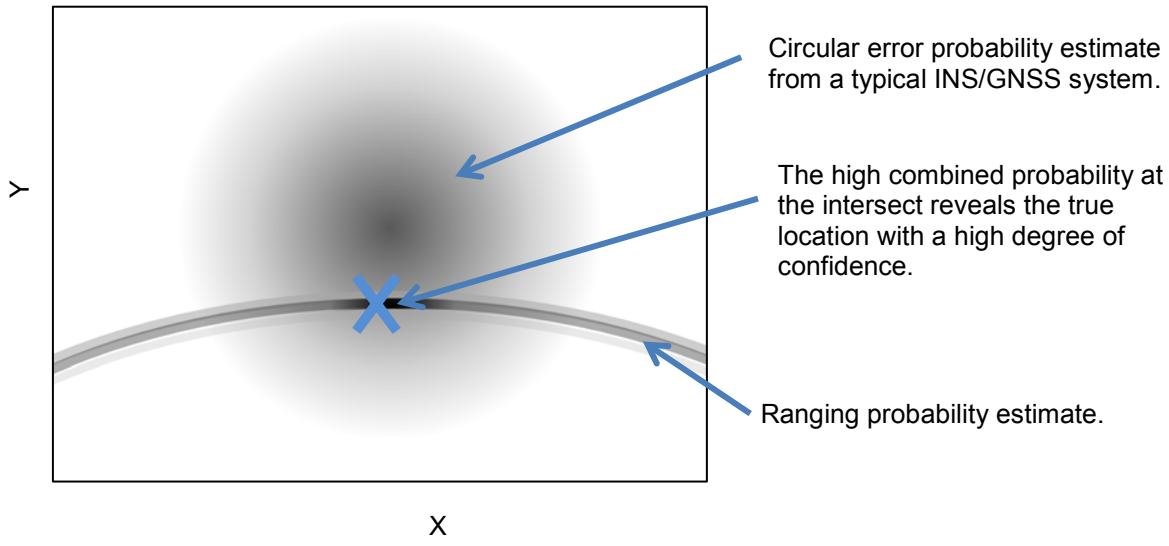

Figure 10 – Geo-location example optimised with the addition of a ranging estimation.

The example in Figure 10 shows that the IMU dead reckoning approach provides a circular error probability that has diverged from the true location. The provision of a ranging system allows a multiplication of the INS and ranging probability distributions to provide an improved geolocation estimate. The provision of two or more ranging systems further enhances the capability of providing an accurate geolocation estimate by calculating the intersect of the two ranging estimates Signal strength topology estimates provided an update in a similar manner when observable signal strength contours are recorded, as shown in Figure 11.

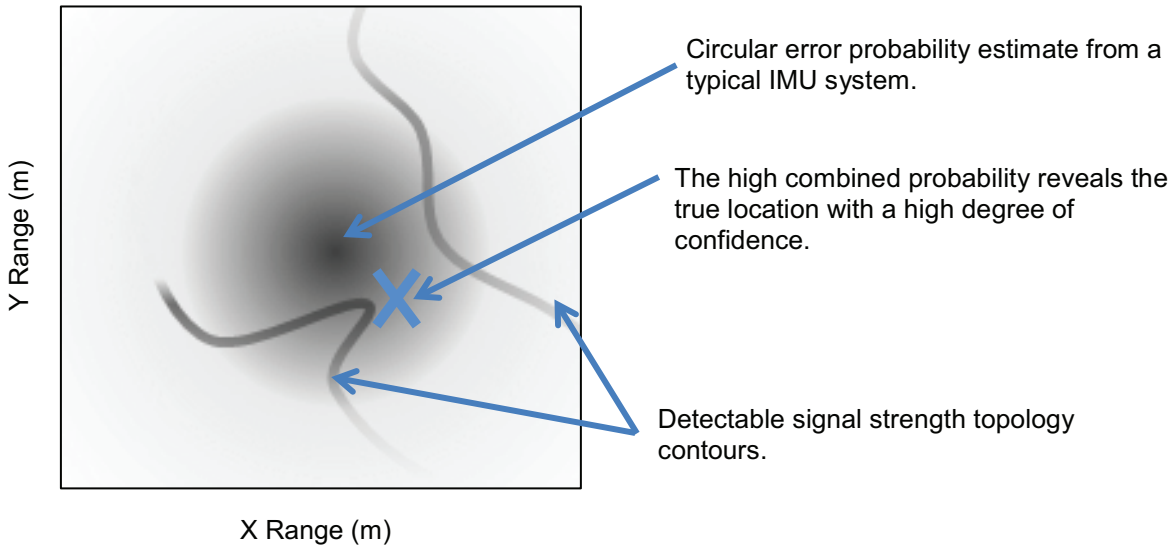

Figure 11 – Geo-location example optimised with the addition of RF topology estimation.

A key reason that many existing research approaches do not use the inertial measurement units (IMU) as a core part of the geo-location estimates is that, as described in the literature review, low cost IMUs have comparatively poor performance over long periods. This limitation was overcome in outdoor geo-location solutions by closely coupling the IMU to the GNSS receiver, effectively calibrating the IMU on-the-fly. This approach removes the dominant long-term errors by comparing the IMU dead reckoning estimate with the known motion from the GNSS receiver. This mission specific calibration allows greatly improved performance from the IMU after the GNSS is lost. This thesis will investigate the close coupling of signals of opportunity data with an IMU, using the signals of opportunity to continually identify and remove errors from the IMU in real-time. Placing the IMU at the centre of the system allows the system to scale well with the application of a large number of signal of opportunity inputs, where each is combined and analysed to estimate the exiting IMU errors. Also inherent in this design approach is the robustness and resilience to short term transients in the quality and availability of external sources of radio data that are common in indoor and urban environments.

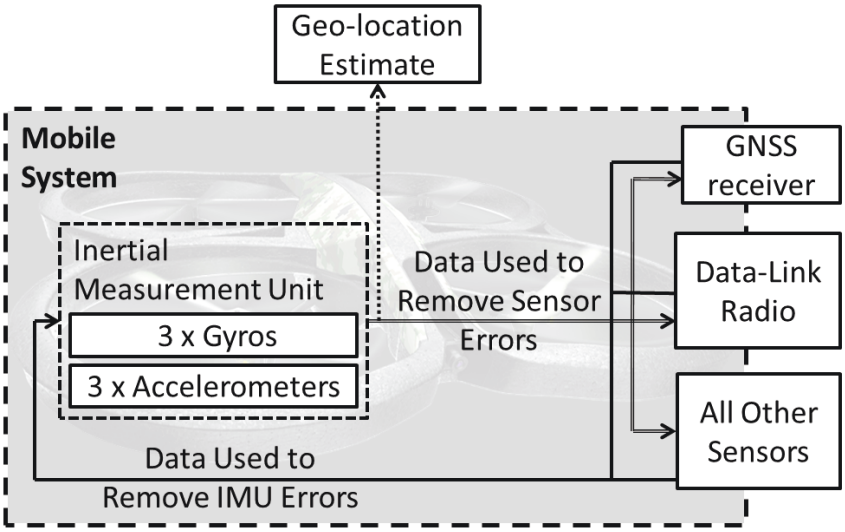

Figure 12 - Architecture Overview

By providing a central integration step in the system, the architecture shown in Figure 12 allows the first key design aim, to minimise system complexity and power usage, to be met. This design aim has been met while still allowing the combination of a wide range of varied sensor inputs. To be able to efficiently implement the proposed architecture, a filter must be designed to allow the required data analysis and allow a geo-location estimate to be produced. The location of the required filter in the system and an overview of the required interfaces is shown in Figure 13.

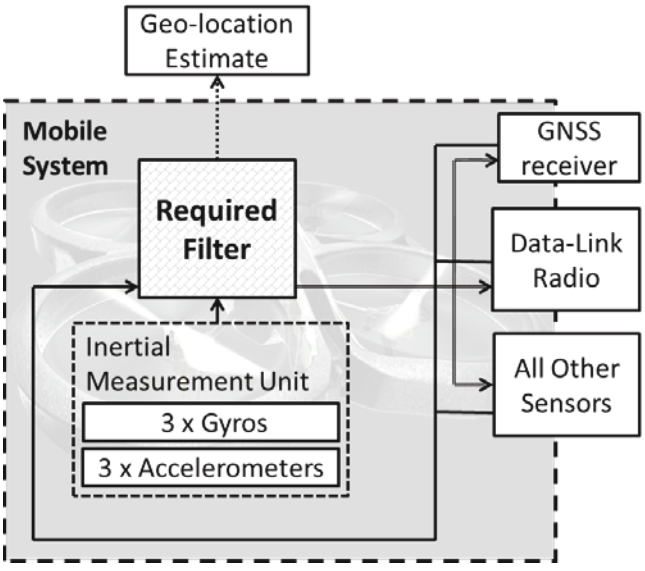

Figure 13 - Required Filter Interfaces

To enable the second design aim, allowing the filtering of sensor data to be optimised by a process of tightly coupling data streams to be achieved, the filter is required to integrate closely with the IMU calibrating rate and accelerations on the fly. To enable the final design aim, minimising hardware requirements, the filter must be able to cope with a wide range of sensor inputs from a wide range of sensors that are unlikely to have been designed for geolocation. To enable this, the filter is also required to obtain information from a diverse range of senor inputs, using its own geolocation estimate to remove errors, filter the inputs and derive an improved geo-location estimate.

Literature review section 2.3.1.2 revealed that Kalman filters can be efficiently used to optimise the coupling of IMU errors with other data streams. While many Kalman filters provide a generic approach to allowing the combination of data sources and feature recognition, few have been optimised for combining signals of opportunity data in hardware constrained systems. Specifically, research has not provided an ability to monitor the user's surroundings and generate a geo-location estimate in hardware constrained applications. This thesis will continue onto researching an approach to generating a Kalman filter based signals of navigation solution that can use feature recognition to provide a geo-location estimate. This thesis will carry out research that will enable a geolocation estimate to be maintained that will scale well to allow long term accuracy with minimal hardware requirements. As discussed previously in this chapter, an opportunity exists to allow the efficient coupling of a wide range of radio sources with a central IMU. Using an IMU as a central point within the system will allow a dead reckoning integration approach to be taken with an extended Kalman filter used to minimise the integration of error. To allow this approach to be successful, the development of an extended Kalman filter that will integrate a varied and unknown set of signals of opportunity geolocation data is required.

One key principle that makes the proposed Kalman filter based solution unique is the fact that the data central to the position estimate is generated by the IMU hardware. The benefit of this is that the geolocation estimate can be obtained simply by integrating the recorded acceleration and rate messages. The drawback of this approach is that accumulated error increases rapidly in low power IMUs. To mitigate accumulated drift errors, the IMU will be calibrated on the fly by removing the errors calculated by a Kalman filter that will be optimised to track and monitor any available physical layer radio data. To carry out the IMU calibration operation, only the covariance of the estimate is maintained by the Kalman filter. When the covariance is below a set threshold, the errors generated by the IMU can be estimated accurately and removed, calibrating the IMU on the fly. It is anticipated that, following further developments to obtain accurate geo-location data from the radio environments, this operation can maintain an accurate position estimate while limiting the hardware requirements of the host system.

The developed Kalman filter will also be truly generic, applicable to any source or selection of sources depending on the radio sensors present. Further, as an improvement to many existing radio geo-location techniques, using a Kalman filter to maintain the latest measurements, estimates and covariance's provides significant robustness against temporary and transient multipath effects, common in indoor and urban environments, while still using the IMU data to provide a low latency geo-location estimate.

While radio signals of opportunity come from a varied set of sensors and a variety of parameters can be observed, the presence of sinusoidal patterns in the received data are common. Radio transmissions frequently utilise a sinusoidal carrier frequency. Being able record and predict this carrier frequency value can be carried out with phase analysis. This technique is called carrier phase analysis and is discussed in section 2.1.3.3 of the literature review. Tracking this characteristic of the signal with a Kalman filter in an urban or indoor environment would be very desirable. Comparing the recorded signal phase to the estimated value would allow sub-meter geo-location accuracy. The comparison between the predicted and measured step would also allow the user to identify a wide range of signal characteristics that are of interest to mobile systems. These characteristics include the ability to identify signal distortion due to multipath reflection, interfering signals and propagation through obstacles. While this approach is extremely desirable when considered in a theoretical sense, the practical implementation of such a system is considered impossible due to the required accuracy of system clocks, with a required clock stability and resolution significantly higher than 2 times greater than the carrier frequency to prevent distortion due to the Nyquest effect. A second limiting factor is the availability of this information from the sensors themselves. Raw carrier frequency data is not commonly output from commercially available sensors.

While it is possible to obtain this information from sensors that monitor lower frequency signals, a requirement to use this data would severely limit the number of data streams available to the Kalman filter in the described architecture, preventing the benefits that come from combining a wide range of data sources.

While requiring carrier phase analysis would prevent the coupling of a wide range of sensors, it is possible that many of the benefits of the technique could be realised if interferometric phase analysis was carried out. Interferometery, described in section 2.1.4.2 of the literature review, allows the low frequency beat between two interfering signals to be monitored. Urban and indoor environments frequently contain congested radio environments, making signal interference common. This is particularly true in the lightly licences and unlicensed radio bands that are commonly available to mobile systems. Monitoring changes in the interferometric radio environment will still allow the radio features of multipath, congestion and NLOS that are desirable when calculating geo-location to be monitored.

The significant benefit of this approach is that that low frequency interferometric phase analysis does not require highly accurate clocks. Further, observations are possible in measurements that are made available by all radio sensors such as signal strength.

To allow the efficient analysis of these sinusoidal interferometric features, this thesis will research coupling a central IMU and a sinusoidal Kalman filter to maximise the effectiveness of sampling radio signals of opportunity.

This thesis has carried out research to investigate whether a sinusoidal Kalman filter can be applied to the radio receiver data stream in an attempt to maintain a phase estimate of the received interferometric signals. The resulting phase estimate will be used to closely couple the IMU and the radio environment in 2 ways. Firstly, the radio environment can be used as an external input to the IMU, removing dead reckoning errors. The second and most innovative aspect of the design is that the resulting, improved IMU estimates can be used to allow the recorded radio signal and the filter estimate to be compared and analysed. The ability to carry out this analysis improves the robustness of the system in complex radio environments, allowing multipath and other signal distortion effects to be observed and accounted for. Further, these previously unrecognisable features may be used by the filter and the higher level system to obtain additional information about the user's environment and their likely geolocation. An example of this approach is shown in Figure 14.

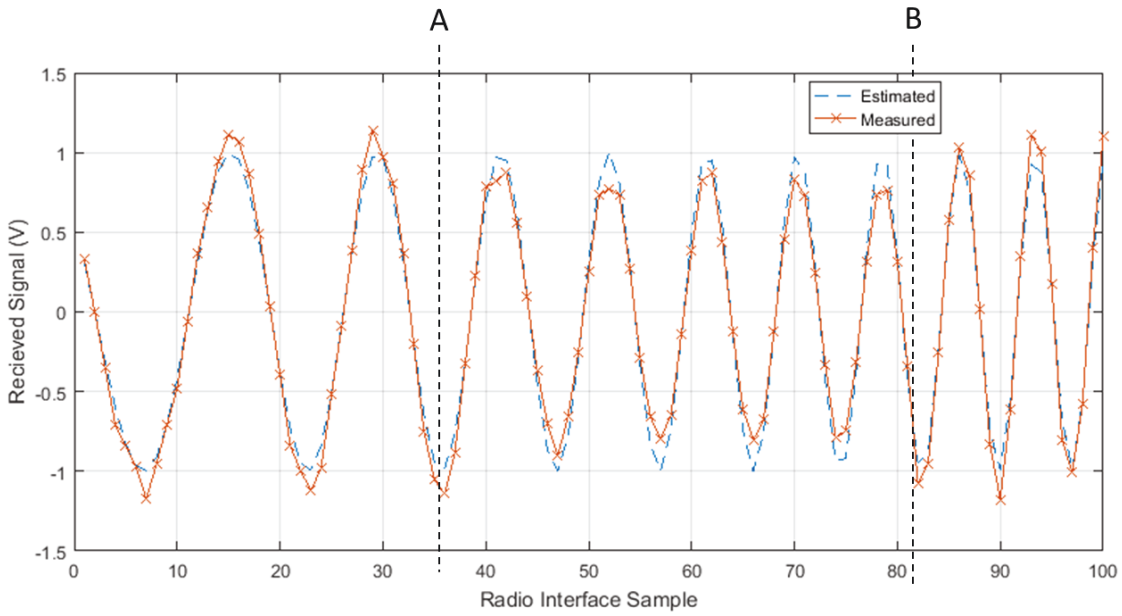

Figure 14 - Example of Additional Radio Channel Information

Figure 14 shows an example of the measured signal from a radio interface in a mobile device. In this example, the device is accelerating towards the signal transmission in an indoor environment.

The frequency change over the logging period may be predicted as inertial acceleration data is available to the filter. The improved ability to estimate the signal phase has allowed an additional feature to be recognised. The signal strength from 'A' to 'B' is lower than expected, producing further information about the user's environment such the potential presence of multipath or a physical obstruction.

This data allows the filter to make intelligent decisions about the data and alter its weightings appropriately, producing a more accurate and robust geolocation estimate.

The optimised Kalman filter has been created in two stages, one to predict the phase at the next step and a second to record data and combine it with the estimation. The filter has been designed to update a ranging estimate at each filter iteration. Matrices have been created to maintain state within the Kalman filter as well as pass information into and out of the Kalman filter. The implementation of these matrices are described in Eq 4 to Eq 9.

The Φ matrix maintains the translation matrix for a sinusoidal system.

$$\Phi = \begin{bmatrix} \cos(\omega\tau) & \frac{\sin(\omega\tau)}{\omega} \\ -\omega\sin(\omega\tau) & \cos(\omega\tau) \end{bmatrix} \quad \text{Eq 4}$$

The P matrix maintains the initial state covariance. As the location of the first reading is unknown, the following P matrix is typically applied.

$$P = \begin{bmatrix} 1e^{6} & 0 \\ 0 & 1e^{6} \end{bmatrix} \quad \text{Eq 5}$$

The measurement noise is represented in the Q matrix.

$$Q = \begin{bmatrix} 1e^{-4} & 1e^{-4} \\ 1e^{-4} & 1e^{-4} \end{bmatrix} \quad \text{Eq 6}$$

The system noise is represented in the R matrix.

$$R = [1e^{-4}] \quad \text{Eq 7}$$

And the measurement matrices are represented by the H and I matrices.

$$H = [1\ 0] \quad \text{Eq 8}$$

$$I = \begin{bmatrix} 1 & 0 \\ 0 & 1 \end{bmatrix} \quad \text{Eq 9}$$

The estimation step is completed by carrying out the Riccatti equations as described below. The estimation step is carried out for each filter iteration:

$$M = \Phi * P * \Phi' + Q \quad \text{Eq 10}$$

$$H_{mtrinv} = (H * M * H' + R)^{-1} \quad \text{Eq 11}$$

$$K = M * H' * H_{mtrinv} \quad \text{Eq 12}$$

$$K_h = K * H \quad \text{Eq 13}$$

$$P = I - K_h * M \quad \text{Eq 14}$$

Following the estimation for the current filter step, the measurement can be made and combined into the estimated location using the maintained Kalman gain, K. Again the measurement stage, shown in Eq 15 to Eq 18, is run at each iteration of the Kalman filter.

$$x_{hold=}x_h \quad \text{Eq 15}$$

$$r = \frac{\mathrm{Xs} - \mathrm{Xh} * \cos(\omega\tau) - \sin(\omega\tau) * x_{dh}}{\omega} \quad \text{Eq 16}$$

$$x_h = \frac{\cos(\omega\tau) * x_h + x_{dh} * \sin(\omega\tau)}{\omega + K_{(1,1)} * r} \quad \text{Eq 17}$$

$$x_{dh} = -\omega \sin(\omega\tau) * x_{hold} + x_{dh} * \cos(\omega\tau) + K_{(2,1)} * r \quad \text{Eq 18}$$

This initial Kalman filter provides the coupling from an RF source to the resulting range estimate as shown in Figure 15.

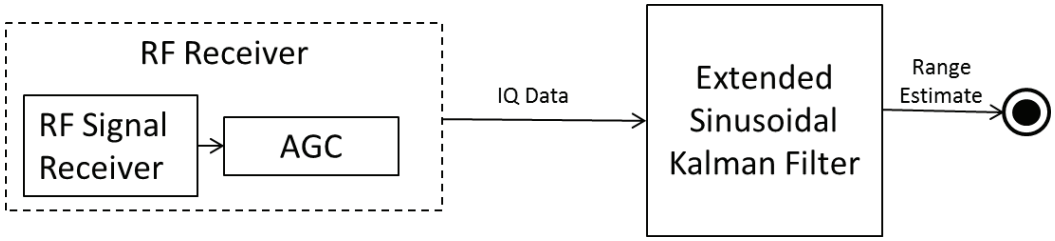

Figure 15 – Basic system configuration.

This implementation provides a ranging estimation from an RF source that is resilient to the signal interference common in indoor and urban environments. The use of a sinusoidal Kalman filter also allows the system to have low latency, resulting in a minimised risk of drift due to phase cycle slip. The lack of estimate drift over long time periods makes the resulting ranging estimate an ideal signal to be coupled to higher level IMU based navigation systems as anticipated. The implementation of the Kalman filter and a coupled IMU is seen in Figure 16.

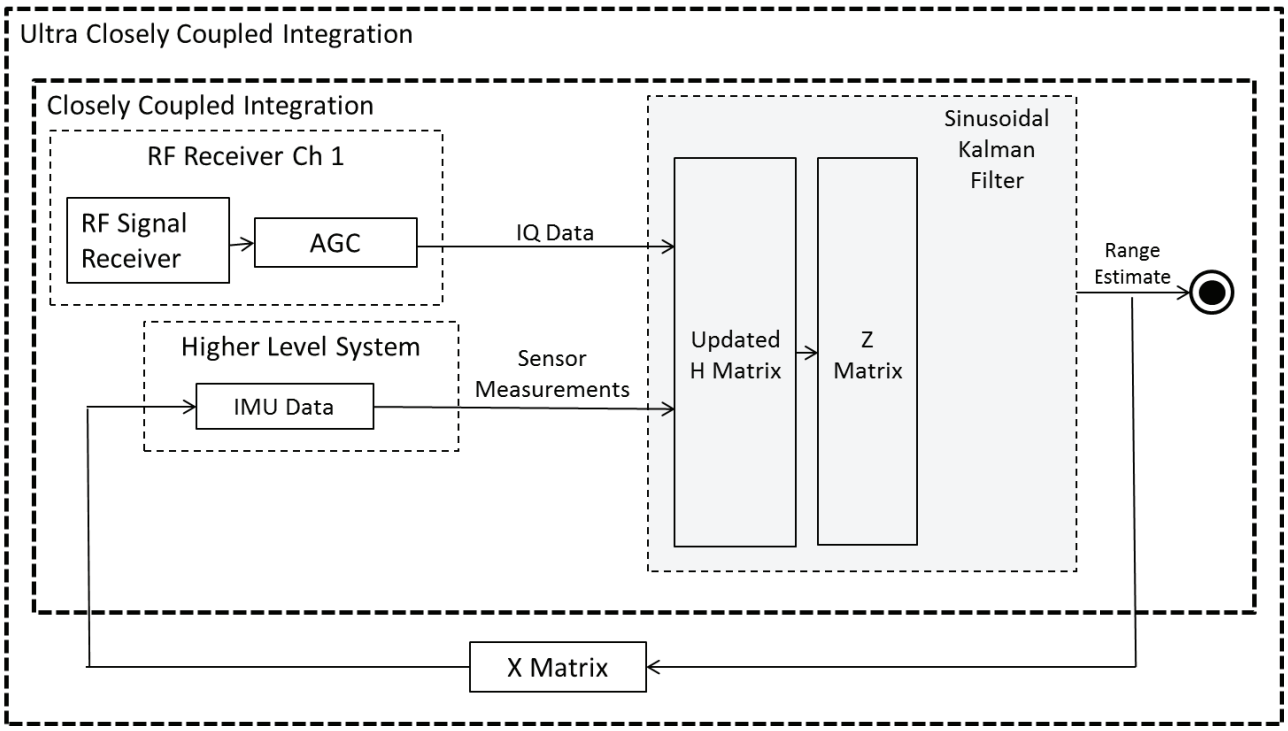

Figure 16 - Kalman Filter Coupled with an IMU.

Further to this, the use of a sinusoidal Kalman filter offers the opportunity for the proposed technique to become the core of a more complete navigation system, with any other available navigation systems coupling directly to enhance the accuracy of each subsystem. Prior knowledge such as the content of any control messages can be decoded and added into the Kalman filter with bespoke input matrices.

This research will continue to present a series of methods for efficiently integrating other navigation sensors into a closely coupled system. Figure 17 shows the three stages of system architecture required for coupled and closely coupled navigation system integration as well as control data link data decoding. The complete system has the sinusoidal Kalman filter at its core, maximising the information that can be obtained from the raw RF data.

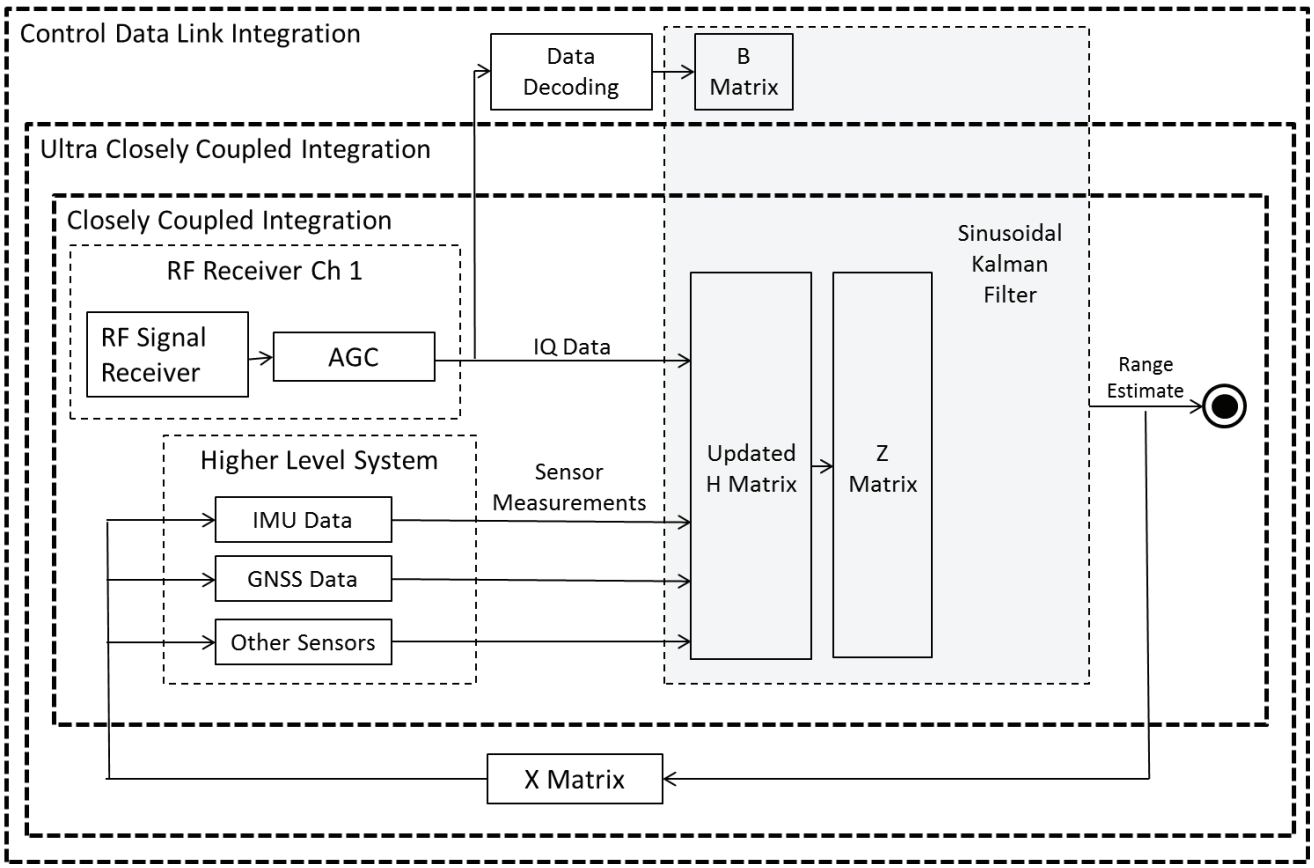

Figure 17 – Three stage system integration with additional higher level navigation sensors. The figure describes the architecture required for closely coupled integration, ultra-closely coupled integration and a method for utilising encoded data in a control data link.

The method for integrating the proposed sinusoidal Kalman filter based system consists of three stages. Stage 1 will be the initial close coupling of additional navigation sensors into the sinusoidal Kalman filter, improving the robustness of the RF phase estimation. Stage 2 is the addition of a feedback loop. This allows the ultra-close coupling of the system, improving the performance of surrounding navigation sensors. Stage 3 is the addition of control link data from systems where the motion of the system is controlled via a RF data link.

Stage 1 of the system is an open loop closely coupled system where the sinusoidal Kalman filter measurements come from all available navigation sensors. Methods exist for closely coupling navigation sensors to provide an improved geo-location estimate, described in sections 2.2.1.1 to 2.2.1.3. This thesis proposes a novel application of a sinusoidal Kalman filter to maintain an estimation of phase allows the additional data to be used to further improve the robustness of the system to multipath and other urban and indoor RF effects. The system requires an update to the Kalman filter H matrix and the addition of an F and Z matrix. The updated H matrix relates to the measurements received from each sensor. The F matrix converts the measured sensor reading into a phase estimate based on the calculated range from the transmitter. An example of an updated H and F matrix for a typical data stream with RF and GNSS data can be seen in Eq 19 and Eq 20.

$$\mathrm{H} = \begin{bmatrix} 1 & 0 \\ 1 & 0 \end{bmatrix} \quad \text{Eq 19}$$

$$\mathrm{F} = [1 \quad \sqrt{x^2 + y^2} * \sin(\omega\tau)] \quad \text{Eq 20}$$

Upon each time separation iteration of the Kalman filter, the H matrix is multiplied by the corresponding F and then Z matrix.

$$\mathrm{Z} = [\mathrm{a}\ \mathrm{b}] \quad \text{Eq 21}$$

The Z matrix is updated at each iteration, depending upon what fresh measurement data is available from the system. When a raw RF data measurement is available, a = 1 and b = 0, if a GNSS measurement is available, a=0 and b=1.

This implementation allows the Kalman filter to be updated with all available data. The covariance of the H matrix is maintained by Kalman filter, providing additional robustness to multipath effects. Erroneous RF signals are identified by a lowering in the covariance values in the Kalman filters P matrix and will have limited effect on the maintained phase estimate.

Following the integration of the additional navigation sensors an additional stage of ultra-close coupling is possible using conventional methods of using an X matrix to convert the range update back into a known position estimate for each sensor. The advantage of this technique for the proposed system is that further robustness to indoor and urban RF effects is provided, allowing a highly robust phase estimate to be maintained by the Kalman filter due to accurately maintained measurement covariance's in the P matrix.

The system architecture described so far is applicable to any signals of opportunity source, where the location of the transmitter is either known in advance or can be calculated using simultaneous localisation and mapping techniques. The system uses only the RF carrier signal, so can be used without knowledge of any of the data on the link. Even encrypted data links can be used to provide a ranging estimate.

The movement of many robotic systems is controlled by an RF data-link. This data-link is likely to provide an ideal RF data source from a known transmitter location and could be utilised in many systems. In systems that use the control datalink as the RF input to the system, the data contained within the data-link can be decoded, providing the commanded system motion. This commanded motion can be, via a control matrix (B), used to update the prediction estimate made by the Kalman filter. The B matrix is multiplied with the Φ matrix, allowing the prediction part of the Kalman filter to account for the motion expected by the system. The B Matrix must have a prior knowledge of the system dynamics that will apply following any commanded motion input. Once again, the addition of an improved prediction estimate within the Kalman filter will provide additional robustness to measurement uncertainty. The ability for the system to command data in this way is a unique benefit that comes from using signal of opportunity inputs into a sinusoidal Kalman filter architecture.

3.3 Filter Data Sources

This section of the thesis aims to identify the inputs and to the designed filter. The existing technology selected, along with rational for its selection will be discussed. The output from this discussion will be a base set filter inputs that will allow the initial filter architecture to be analysed, simulated and verified.

The literature review has shown that radio signals of opportunity are available in almost all indoor and urban environments. A sample of specific signal characteristics that are likely to be of use during the research have been identified by the literature review and will be assumed as inputs during this investigation. A summary of each, along with a brief rationale for their inclusion, is presented in this section.

The fist data stream that may be available to the filter is signal strength analysis. Signal strength readings may be performed efficiently on most radio reception hardware and is commonly available on commercial receivers. While this technique applies to a wide range of radio equipment and frequencies, a mature source of signal strength topology can be obtained from WiFi signals. The worldwide adoption and common implementation of WiFi means that a reasonable assumption can be made that multiple WiFi transmitters will be available in an urban or indoor location. Simulations throughout this research will add to the common modelling method detailed in Eq 22 [ALSINDI, 2004] with the addition of measurement noise and quantization.

$$h(t) = \sum_{k=0}^{L_p - 1} \alpha_k \delta(t - \tau_k) \qquad \text{Eq 22}$$

Where L_p is the number of multipath components, α is the complex attenuation and $\boldsymbol{\tau}$ is the propagation delay.

The resulting measured RSSI over on open environment without indoor or urban effects is described in Figure 18 can be seen in Figure 19.

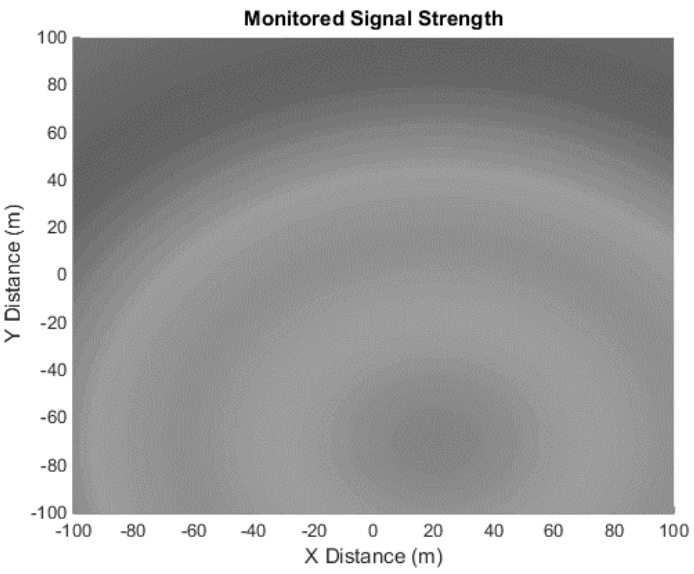

Figure 18 – Simple Signal Degradation Model in an Open Environment

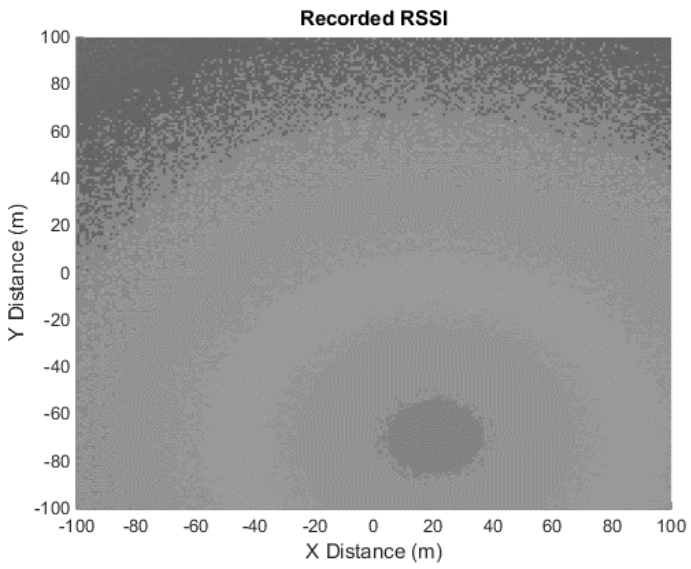

Figure 19 - Simple Signal Degradation with Hardware Measurement Uncertainty

The quantised recorded WiFi RSSI can be used as a filter input. The same approach can be taken for any other available radio inputs, such and command links, allowing the quantised signal strength value to be used by the filter.

A second data stream available to the filter is a carrier phase analysis. While this technique is possible in any frequency range, specialist hardware is required to carry out the technique at frequencies of more than approximately 100 MHz. This hardware is not commonly available in mobile devices. Even lower frequency carrier phase analysis requires an accurate and stable time source to allow accurate sampling of the carrier signal. Two proposed sources of low frequency, high carrier frequency stability, radio signals have been identified. The first is the short wave digital Digital Radio Mondiale (DRM) signal. The DRM radio service is a shortwave radio service that uses a modulated carrier wave frequency of 5-6 MHz, providing a wavelength of approximately 50 m. Due to the commercial nature of the DRM service, transmitter location is optimised in urban environments to allow good population coverage. The second source of low frequency and high stability carrier phase data is in the unlicensed 27 MHz band. This band is commonly used to enable low bandwidth links to robotic sensors due to its worldwide unlicensed status. These data links are common in automated and robotic systems to provide a control link and to allow the system to report system test results to a local ground station.

Many small autonomous systems still rely on a local low-bandwidth data link to communicate command and report system statuses. This link commonly uses the unlicensed 27 MHz band. Where this project requires the analysis of time of flight data, a two way, low bandwidth 27 MHz amplitude modulated data-link will be assumed.

A stable clock source is still required to sample the 27 MHz data souce. Hardware clocks are available with very high levels of accuracy although they require expensive, large and high power hardware which is not available to many small autonomous systems and so are not to be considered in this thesis. External clock sources may also be available over data communication protocols such as the PTP. It should however be noted that the transmission of these protocols over wireless networks in urban environments are themselves likely to be adversely affected by propagation effects. This is likely to make them unusable in many applications, although the propagation effects may result in a signal that contains a stable but considerable latency with low jitter which may still be of use in the proposed application.

A viable alternative that may be able to provide a source of clock data, even in the environments proposed in this project, are available from GNSS services. To provide a 3D location estimate, a GNSS receiver needs a clear line of sight view of at least 4 satellites. Although there are many urban areas where there are less than 4 satellites in direct line of sight, many densely populated areas are likely to still allow visibility of 1 or more satellites due to the good constellation spread of existing the multiple GNSS satellite networks. This external time source may also be provided in indoor environments by a GPS time repeater system with acceptable latency and jitter. This thesis has investigated a method to remove the reliance on GNSS services, any required additional clocks will assume GNSS levels of accuracy with considerations made as to the propagation effects of the GNSS signal in urban environments, even if only 1 clear signal is required.

3.4 Architecture Analysis

This section uses the inputs common to indoor an urban environments that have been identified in section 3.3 to allow an analysis of the designed filter to be discussed. The aim of this section is to identify the key system error drivers allowing further investigation and the identification of mitigation techniques. The available inputs and data sources that may be used to mitigate the identified error drivers are summarised in Figure 20.

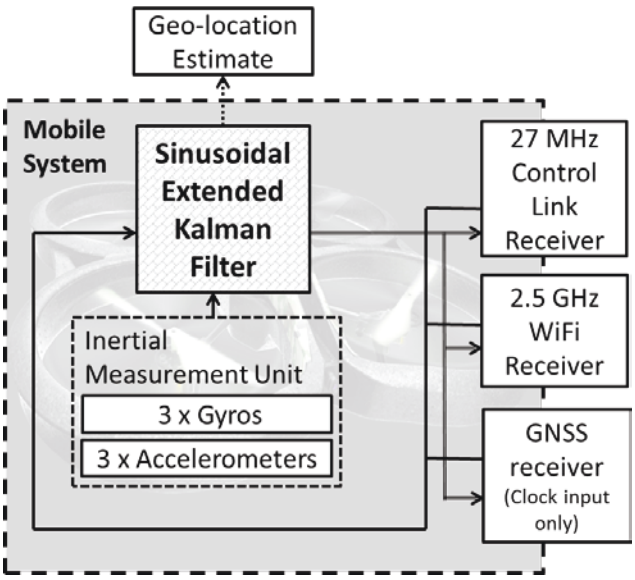

Figure 20 - System to be Analysed

The components considered by this analysis are commercial grade MEMS IMU that will be combined with typical urban WiFi signals and a low bandwidth control link, controlling the motion of the mobile device. As discussed in section 3.3, the WiFi signal element analysed is the is the received signal strength (RSSI), as received from common WiFi hardware. The control link channel allows for the monitoring of both signal strength and time or arrival data.

The simplified IMU has been modelled with the following functionality. As this is an initial prediction of significant error sources, only IMU biases are considered at this time. Other common IMU errors such as scale factor and misalignment will be considered in more detailed system analysis later in the thesis.

IMU parameter values, shown in Table 5, allow for an angular random walk and velocity random walk parameter to be calculated and estimated after 40 seconds of operation.

Table 5 - Simplified IMU Parameters.

Gyro Bias (°/hr)	250
Acc Bias (mg)	100

A typical distribution of dead reckoning location estimates resulting from class if IMU has been shown in Figure 21.

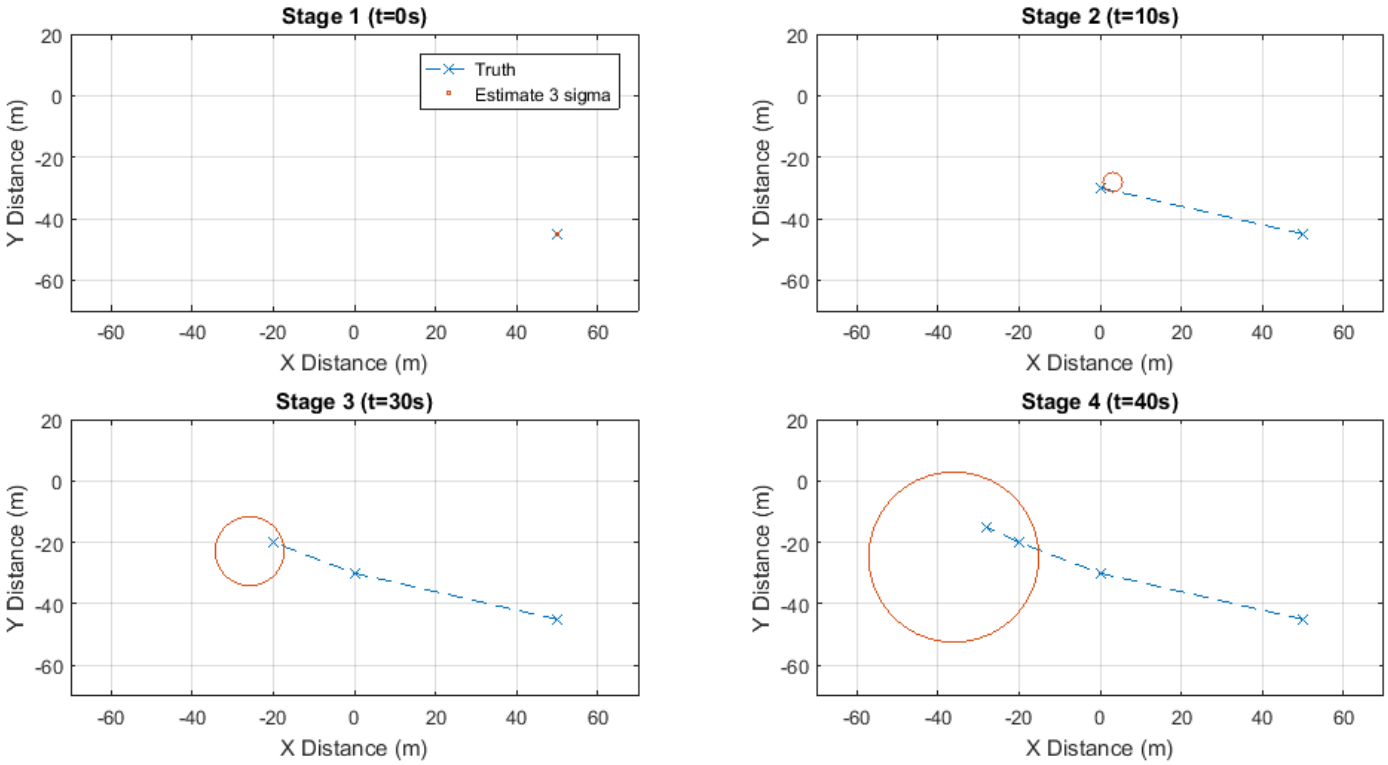

Figure 21 – Time Lapse Performance of Typical IMU Error Growth

As discussed in 2.2.1, generic example of IMU based systems shown in Figure 21 demonstrates the integration of errors resulting in a geolocation estimate that decays in certainty over time. The error will continue to grow indefinitely in the absence of an external correction from another geo-location source. Higher grades of IMU with improved bias and noise parameters will reduce the drift rate but will not limit the final geolocation error.

The first available external source that can be considered can be obtained from analysing the ToA of signals on a radio data communications link. The time of arrival from two or more transmitters can be recoded to provide an estimate of the receiver's location. While this can work well in open environments, as described in section 2.1.2 of the literature review, multipath effects prevent it's correct operation in urban and indoor environments. The effects of multipath produce signals that look acceptable to the receiver, but contain an error in their apparent receive time. This leads to a location estimate that provides a last known location only where the error around the uncertainty cannot be known. The performance typical to this technique can be seen in Figure 22.

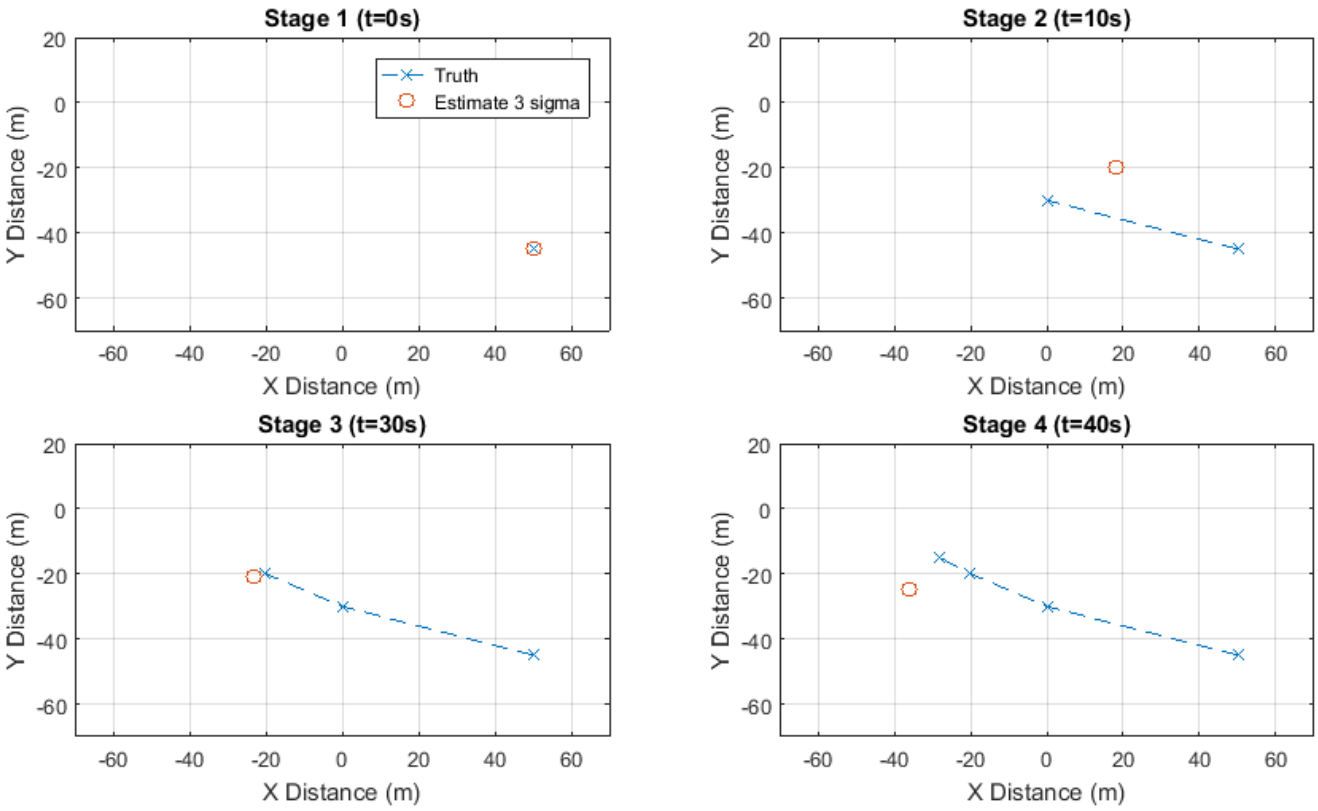

Figure 22 - Time Lapse Performance of Typical ToA Estimate

It is possible to combine the IMU and ToA estimates to limit the IMU dead reckoning error. Combining the ToA result with that of the IMU with a simple probability density multiplication will result in the IMU error growth being limited by the maximum error due to multipath. While this provides a benefit, the maximum uncertainty discussed in section 2.1.2 of the literature review remains in at levels of more than 20 m which this thesis aims to improve upon.

A third common source of information is signal strength analysis. The degradation of signal over area, along the motion of a user is shown in a simplified example in Figure 23.

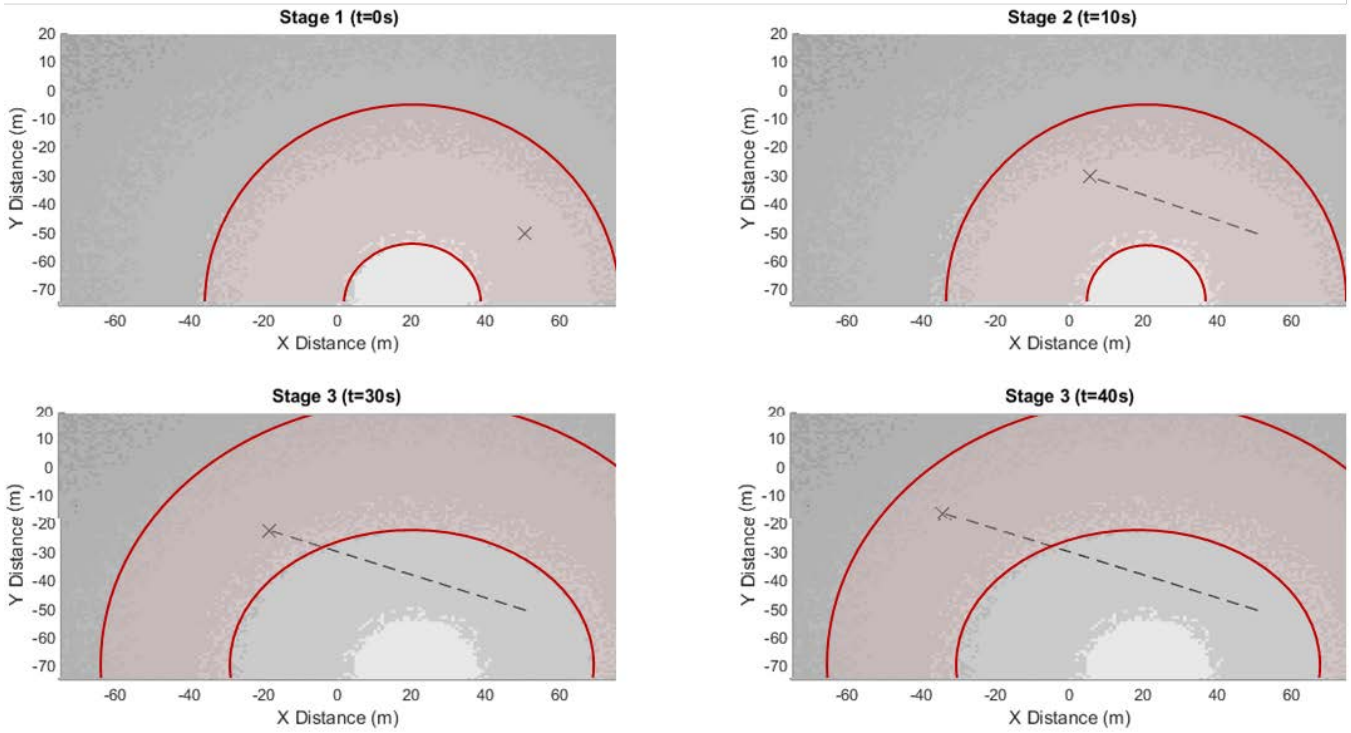

Figure 23 - Time Lapse Performance of Typical Signal Strength Estimation

Figure 23 shows geolocation information available from a quantized signal strength measurement. While the geo-location estimate available from a single radio source is very course, it has two key features that may be used by the system. The first is that there are specific areas with a high contrast in signal strength at the boundaries of each signal strength quantization step. At points where these boundaries are traversed, a more accurate reference of location may be made. The second key feature is the stability of the measurement. As with ToA estimates, signal strength estimates are significantly affected my multipath in urban and indoor environments. This may become a positive feature when using signal strength measurements for geolocation as the number of signal strength boundaries increases, even in a quantized environment. The second key feature of this information source is that signal strength environments changes little over time in most scenarios providing a relatively stable data source.

The combination of these three data sources will now be considered. Again, a simple probability multiplication approach may be taken, providing an improved geolocation estimate than any single data source could provide a more robust estimate. This approach could be achieved by using an recursive filter as described in literature review section 2.3.1.1. An example of this approach can be seen in Figure 24.

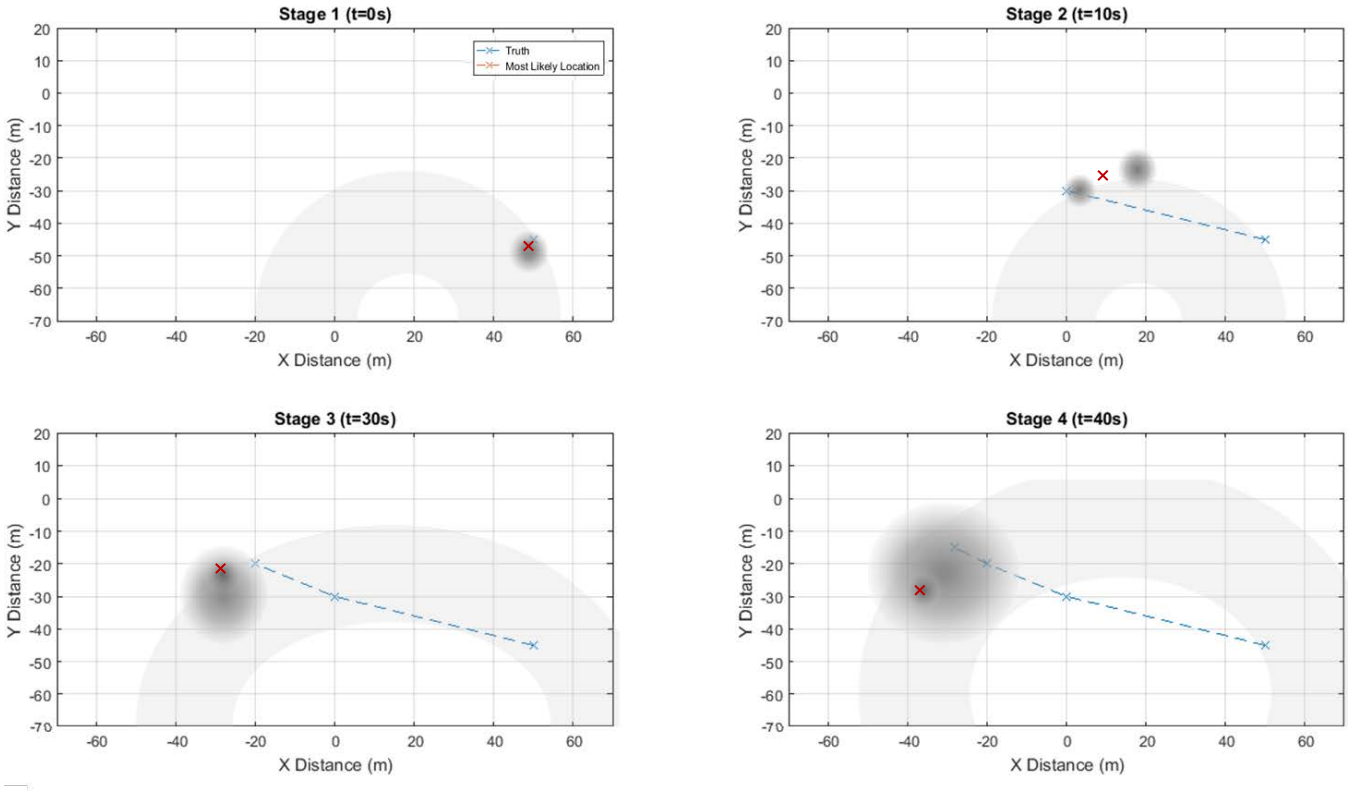

Figure 24 - Probability Density Approach for Sensor Combination

While this approach provides a more robust geolocation estimate than any of the information sources may provide on their own, the error sources associated with each information source are not known. The lack of this information allows the geolocation estimate to become corrupted with erroneous measurements. Further, as the IMU error continues to grow with time, its usefulness to the geo-location reduces and the probability distribution from this source effectively carries less weighting with time.

The application of the extended filter proposed by this thesis is predicted to counter these shortcomings, further improving the geolocation estimate. The correction of IMU errors on the fly prevents the growth of its associated 3σ geolocation estimate. This updated IMU estimate allows the proposed extended Kalman filter to recognise and omit erroneous ToA estimates, while increasing the weighing of ones that occur within the expected results. Further, the extended Kalman filter is able to utilise its improved geolocation estimate to extract further information form the radio environment. ToA and signal strength measurements that have varied due to multipath and other propagation effects will have their respective quality rating lowered, providing further mitigation against effects common in indoor and urban radio environments. An example of the anticipated extended Kalman filter output with the inputs discussed throughout this section can be seen in Figure 25.

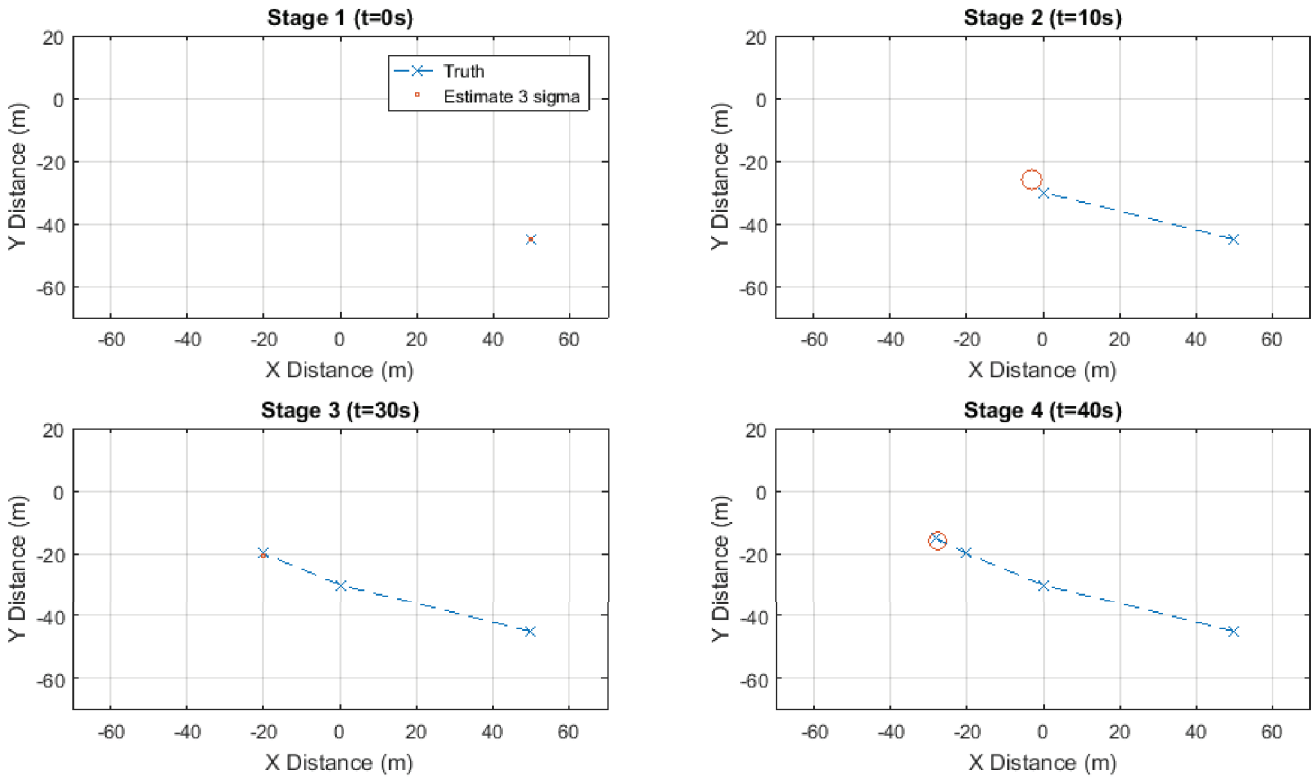

Figure 25 - Time Lapse Performance of Typical Combined Estimate

3.5 Anticipated Error Drivers

The presented extended Kalman filter has been designed to be robust against common errors found in IMUs and the radio environment. The design may however allow for particular susceptibilities and error drivers. The reasons for these anticipated susceptibilities will be discussed in this section.

The first significant error driver discussed is associated with the ToA measurement data. The design of the filter weights radio readings by comparing them against the filter estimate. Erroneous radio readings will be recognised and weighted accordingly, preventing degradation to the filter's geolocation estimate. The filter does however assume that that erroneous estimates will be normally distributed over time. It is possible that this is not the case and areas of similar radio interference may exist. Prolonged periods in these areas will present the filter with a steady and constant geo-location measurement with an unknown error. Over time and in areas of constant signal strength the filters K matrix value (Eq 12) for the radio input will increase. In parallel to this, the IMU K matrix values will decrease as the IMU based dead reckoning estimate diverges from the users true location. This behaviour will in time cause the users location to tend towards the erroneous ToA estimate of location. While changes to Q matrix values (Eq 6) may be possible to mitigate the short term effects of this behaviour at the expense of system latency, the behaviour cannot be prevented from happening.

A second significant error driver is the lack of fidelity in signal strength. Again, the filter measures the signal strength on its radio interface and compares the received signal against a world model estimate. This technique has been selected as indoor and urban environments have high levels of signal strength contrast in small areas. Errors from this measurement will grow in areas of low contrast or when the mobile device is static or slow moving. While still constrained to the signal strength topology, system errors will grow larger over time in the absence of signal strength contours.

A final effect likely to be witnessed in the system is related to the start-up time of the filter. The measurement noise matrix, Q, can be tuned to set the starting sensitivity of the filter to measurement uncertainty on each of the sensors. The measurement noise matrix determines the weighting given to each of the sensor readings. While the weightings or each measurement are compensated by the K value in operation, the early performance of the filter relies on pre-set Q matrix values. While the system designer may be able to tune the Q matrix values in known environments, filter start-up in unknown environments will provide less accurate results for a period. While this will not affect the final solution accuracy, errors at the start of the filer operation may be a limiting factor in some use-case scenarios.

Despite these error drivers, a significant improvement over existing data source combination filters is expected in most scenarios when the proposed extended Kalman filter is utilised. To further research this improvement a model of the anticipated radio environment is to be generated, allows the performance of the filter to be analysed in the range of environment. This simulation will the benchmarked practical test.

3.6 System Modelling

Throughout this thesis the performance of proposed techniques will be analysed with modelling and simulation. This modelling and simulation environments have been developed using standard radio propagation and hardware simulation techniques. Details of this implementation are contained throughout this section.

Default values for each of the parameters discussed throughout this section can be seen in Appendix B2 – Example Simulation Parameter Settings.

3.6.1 Simulation Environments

A simulation environment has been created in Mathworks® Matlab® 2014b. This simulation environment has been generated to allow the proposed techniques to be demonstrated, analysed and discussed. The aim of the simulation environment is to create representative physical layer effects in defined environments that are typical of those found in urban or indoor areas.

There are two main inputs into the simulation. The first is physical factors such as walls and floors. Physical factors that can be set by the user are the size and location of the surfaces, along with the material properties of the surfaces. The second main inputs into the model are the location, power and frequency of radio transmitters. The main user inputs used to set the physical environment, the radio environment an run the simulation are detailed in the Unified Modelling Language (UML) use case diagram shown in Figure 26.

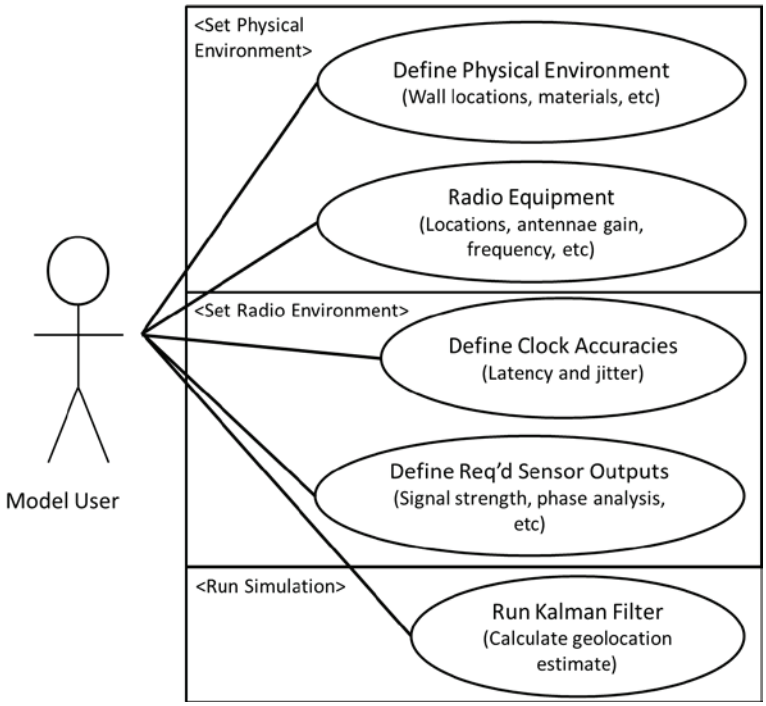

Figure 26 - Use Case Diagram of the System Model

A simplified top level flow diagram of the simulation environment can be seen in Figure 27. This flow diagram shows the signal transformation steps that are carried out on each of the transmitted signals. The content of each of the blocks identified is described further throughout this section of the thesis. In addition to the descriptions provided, example parameter values and a rationale for their selection can be found in Appendix B2 – Example Simulation Parameter Settings.

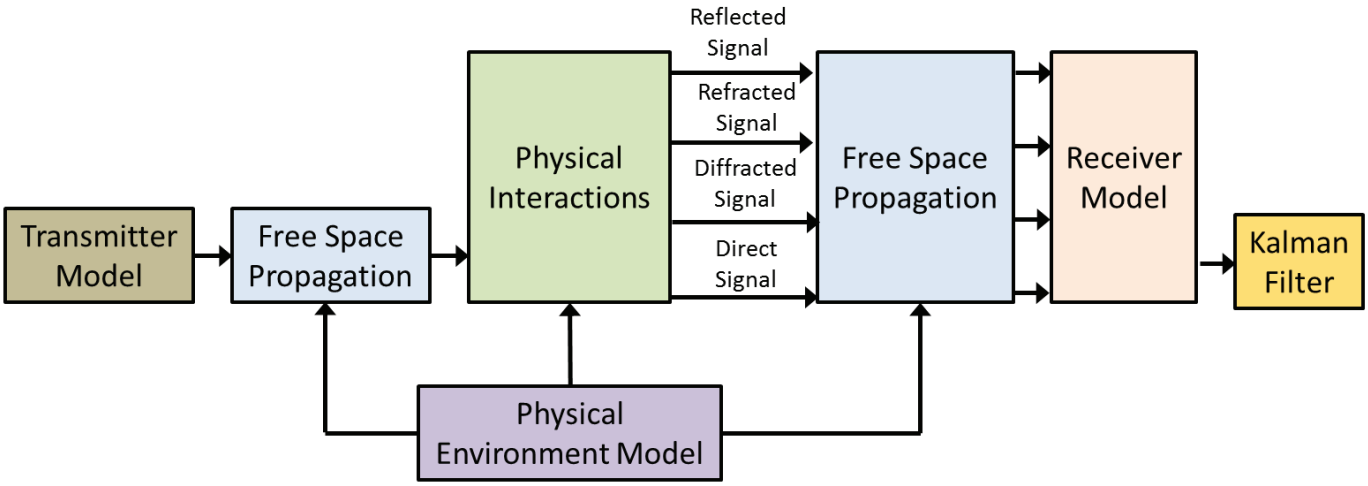

Figure 27 – Simplified Flow Diagram of the Model Interactions

3.6.1.1 Transmitter Model

Each generated signal is created using the transmitted signal model. Further detail on the content of the model can be seen in Figure 28.

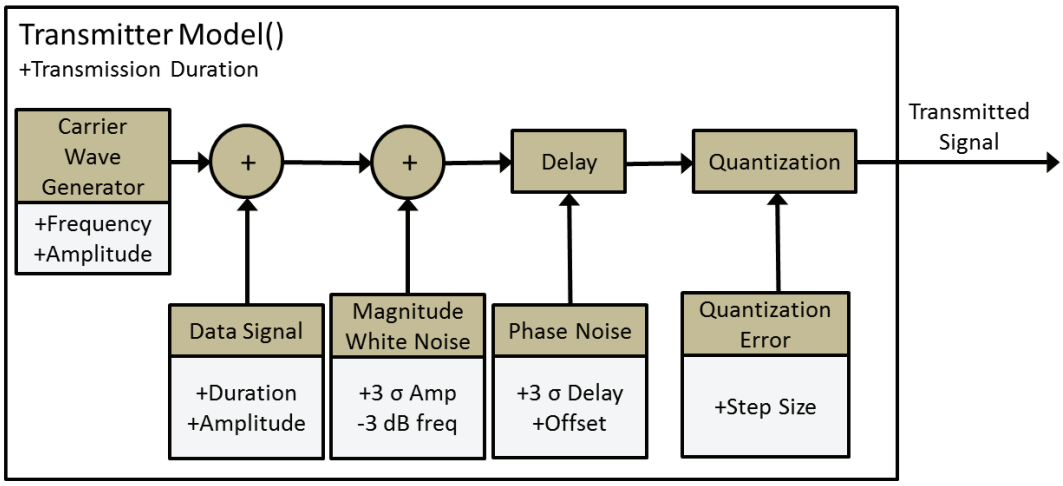

Figure 28 – Flow Diagram of the Transmitter Model

The transmitter model allows a simulated amplitude modulated signal to be generated for a continuous time period that is set by the simulation user. The model first generates a sinusoidal carrier signal with a user controllable frequency and amplitude. This signal is then combined with a user defined data set.

This data set if transmitted added to the signal in a recurring loop for the duration of the simulation. The simulation user can set the transmitted signal amplitude and duration to simulate real user inputs into a control channel. Following the generation of a sine wave that includes amplitude modulated data, magnitude noise is added to the signal. The noise added is Gaussian white noise, tuneable with a 3 σ amplitude value and a -3 dB value for a 2nd order low pass filter which can be set by the user. To generate a noise effect that may be representation of a real system, the -3 dB value of the low pass filter should be set to a value at least ten times greater than the carrier wave frequency. Following the addition of magnitude noise, a phase noise is added with a dynamical tuneable delay function. The delay function allows the user to tune the average delay offset, the amplitude of the jitter and the low pass filter of the jitter noise. The noise generated by this function is a normally distributed delay around the offset value. To prevent an advance being set by this function, the minimum value of the output is set to zero. Finally, the signal is modified with a quantization error where the output value is rounded according to the user defined step size.

The output of this model is a data set, saved to the Matlab workspace, that represents the output of a signal generator for a period of time. This output is then transformed by the free space and physical interaction blocks.

3.6.1.2 Free Space Propagation Model

The simulation environment utilises common signal propagation techniques for free space propagation losses.

The first equation used to estimate the free space losses is the simplified Friis transmission formula shown in Eq 27 [K. LAASONEN, 2003], where *d* represents the distance between the transmitter and the receiver and λ represents the wavelength. In addition to this, the simulation also uses the standard multipath simulation model [ALSINDI, 2004] shown in Eq 24 where L_p is the number of multipath components, α is the complex attenuation and τ is the propagation delay.

$$L = 20\log_{10}\left(\frac{4\pi d}{\lambda}\right) \qquad \text{Eq 23}$$

$$h(t) = \sum_{k=0}^{L_p-1} \alpha_k \delta(t-\tau_k) \qquad \text{Eq 24}$$

Where the free space propagation block as more than one signal input, for instance following the physical interaction model where diffracted, refracted, reflected and direct signal paths are present, the free space model is applied to each of the signal inputs.

3.6.1.3 Physical Environment Model

The physical environment model allows the user to set the physical location of the transmitter and receivers as well as creating objects, wall and floors. At run time the free space distances of each radio path are calculated for use in the free space model. The details of the angle of any physical interactions are also calculated and passed to the physical interaction model.

3.6.1.4 Physical Interaction Model

The physical interaction model has been generated to estimate the interactions of radio signals with simple, known objects. An overview of the classes within the model can be seen in Figure 29. Each of the classes are instantiated with user-configured attributes. Each of the classes calculate the losses for their specific signal sub-path and attenuate the signal accordingly.

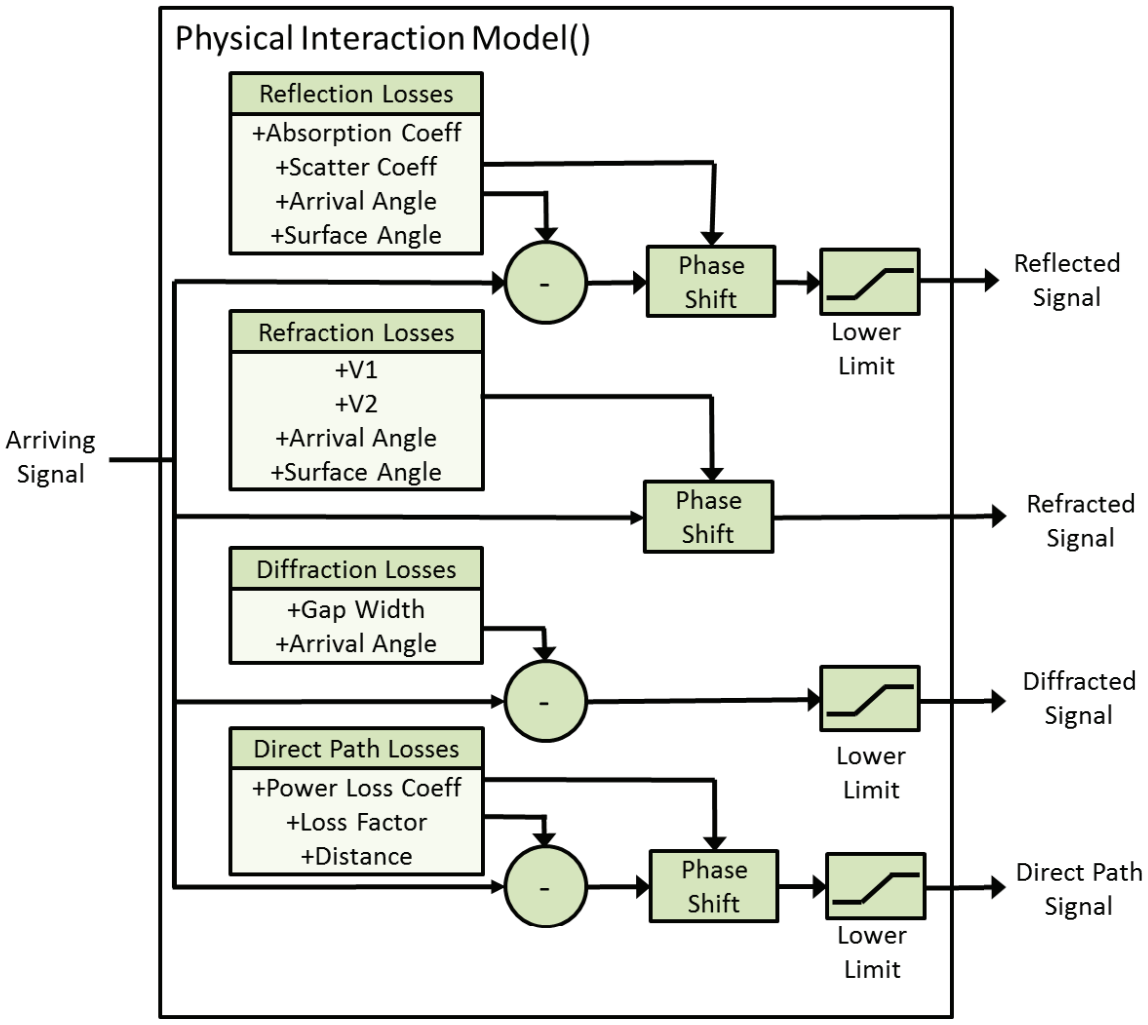

Figure 29 - Physical Interaction Model Schematic

For each of the main propagation path loss methods, the losses for the arriving signal are calculated based on information from the environmental model. Each path loss effect is represented by the generation of a signal sub-path that contains information about the affected signal. These signal sub-paths will be analysed for further free space losses by the free space loss model before their combined effects are considered in the receiver model as shown in Figure 27. To generate the correct signal sub-path the attenuation and, if applicable, phase shift is calculated and then subtracted from the received signal. A lower limit is applied to ensure that negative signals cannot be present. The calculations carried out by each of the modelled loss mechanism use industry standard simplified equations. A description of each can be found in the following paragraphs.

The direct path signal attenuation is calculated to estimate the signal that passes through the simulated object on a straight line from the transmitter to the receiver. This block affects the gain and, due to the change in propagation velocity in different materials, a phase shift. The losses incurred by passing through an object are modelled using the International Telecommunications Union (ITU) model for indoor attenuation shown in Eq 29 [ITU, 2017].

$$L = 20\log_{10} f + N\log_{10} d + P_f - 28 \qquad \text{Eq 25}$$

Where f is the transmission frequency, d is the distance, N is the power loss coefficient and Pf is the object loss factor.

The diffraction losses model allows the effects the signal passing through a gap between objects or though other narrow gaps to be simulates. The parameters required by the the class are the gap width and the angle to the receiver. These parameters are provided by the physical environment model. The diffraction loss model uses refraction principles to calculate the content of the signal sub-path. The diffraction affects only the amplitude of the signal.

The Refraction Model allows the effects of the radio signal moving from one medium to another, such as when the signal passes through a wall or other obstacle, to be simulated. The model uses the Snell formula, shown in Eq 30, to calculate the change in phase of the resulting sub-signal.

$$\frac{\sin\theta_1}{\sin\theta_2} = \frac{v_1}{v_2} \qquad \text{Eq 26}$$

The Reflection model uses two empirical coefficients to estimate the effects on signal strength. The coefficients relate to the main causes of signal degradation during reflection events; absorption, scatter. The effects on phase shift are calculated from the change in angle that comes with knowing the angle of the arriving signal to the angle of the object. This information is provided by the environmental model.

Each of the identified sub-signals are passed out of the physical interaction model for subsequent processing within the simulation environment.

3.6.1.5 Receiver Model

The operation of the receiver model used in the simulation is shown in Figure 30.

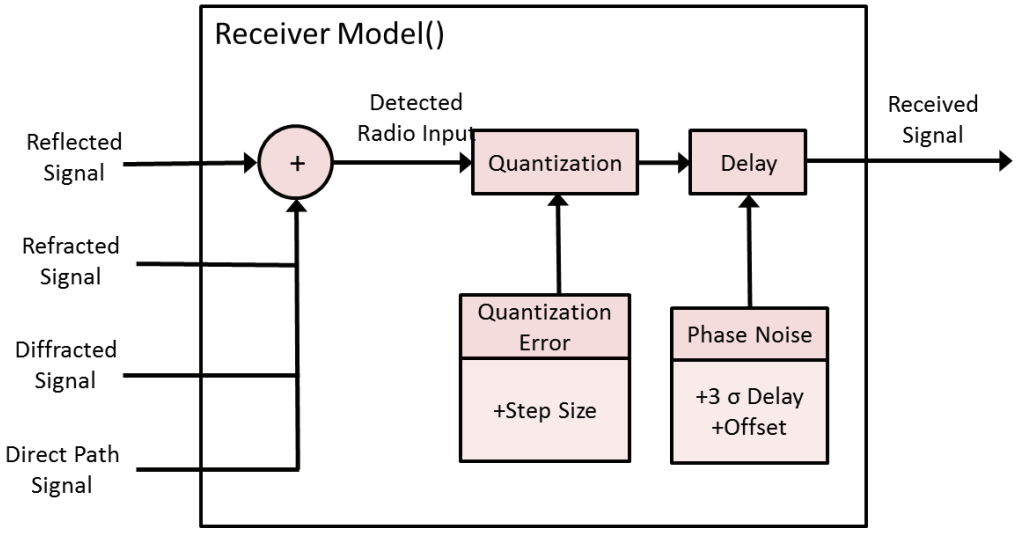

Figure 30 – Flow Diagram of the Receiver Model

The receiver model transforms the radio environment input detected at the location of the receiver and transforms it into the signal that will be available to the Kalman filter. This model allows the key effects of the receiving hardware on the signal to be considered in the simulation. The model processed all data in the input file. The first effect considered in the model is the quantization error. The user may define the quantization step size. The input signal values are rounded according to this input. The second effect considered in the reciever model is the delay and jitter. A user selectable nominal delay is set along with normally distributed jitters around the offset value. A check is placed into the mode code that prevents advances in the data transmission from being possible by setting the minimum delay to 0.

3.6.1.6 Kalman Filter Model

The Kalman filter model uses the radio input from the simulated environment and uses it as a user configured radio input as detailed in section 3.2.

Further detail and examples of key sections of the model's Matlab® code can be found in Appendix B – Simulation Environment.

3.6.2 Model Application

The full system model is validated against hardware test as a complete system in later chapters of this thesis. Full details of the test are provided in section 7. The simulation is used at stages throughout this thesis to aid discussion and to help illustrate the effects of the key error drivers discussed throughout the research. The simulation model used throughout this research has been set to simulate the performance of the proposed system with typical low size weight and power system components in a simulated urban environment.

The simulated performance of the proposed system over time in an urban test environment is demonstrated in Figure 31 to Figure 34. The performance of the proposed Kalman filter architecture is compared to both the performance obtained from a probability density estimate [WENDLANDT et. al 2005] obtained from the same senor inputs and the true motion of the simulated robotic platform.

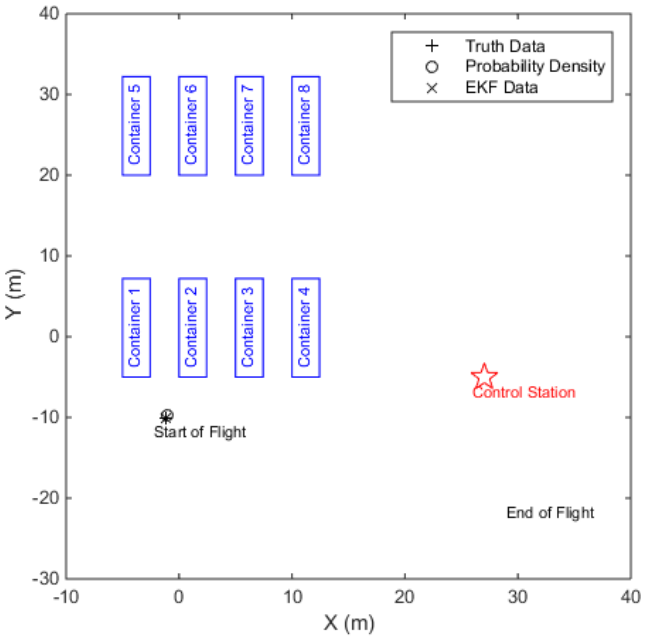

Figure 31 - Urban environment simulation 1, t = 0.

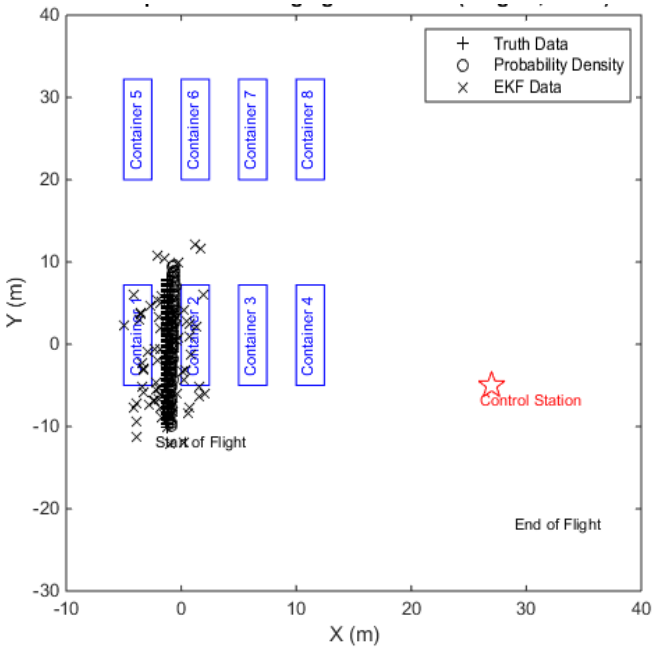

Figure 32 - Urban environment simulation 2, t = 10.

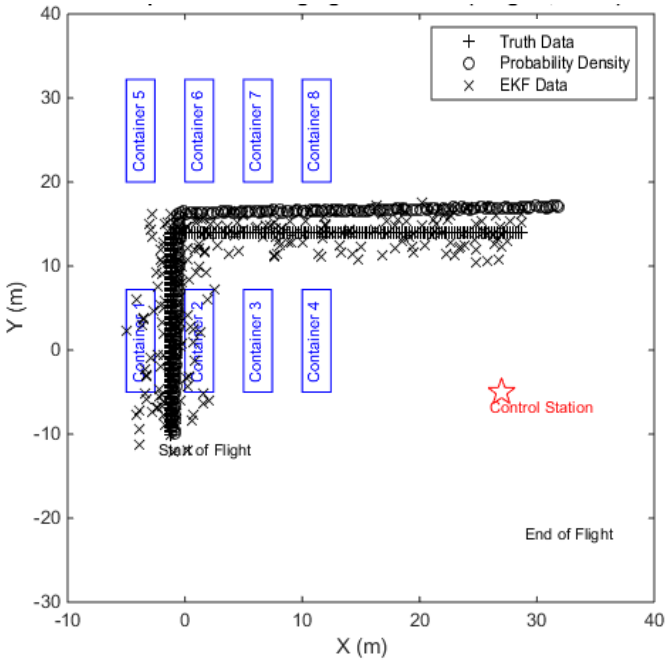

Figure 33 - Urban environment simulation 1, t = 30.

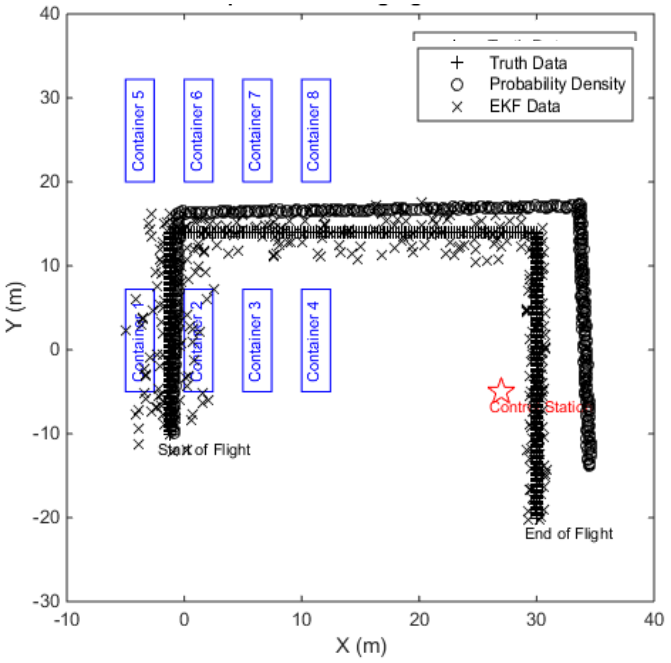

Figure 34 - Urban environment simulation 1, t = 50.

The simulation results show that the geolocation estimate obtained from the extended Kalman filter matches the truth data better than using a probability density approach in the range of environments tested. The simulation results for the Kalman filter based system and that from a probability density method have been tabulated and compared in Table 6.

Table 6 - Designed Architecture Performance Summary

Simulation	Simulation Stage	Time from Start (s)	Max Probability Density Position Error (m)	Max Kalman Filter Position Error (m)	Improvement [Degradation] (m)
1 – Typical Urban Environment	1	0	N/A	N/A	N/A
	2	1 to 10	1	7	[-6]
	3	11 to 30	5	4	1
	4	31 to 50	8	2	6

The simulation has demonstrated the expected performance of the designed architecture over time in an urban environment. The performance shown demonstrates the key features discussed in the architecture analysis and key error drivers discussed in sections 3.4 and 3.5. The architecture analysis predicted an improvement in performance from the proposed Kalman filter based system compared to that obtained from a probability density estimate. The data shows that the final position estimate error has seen an 75 % improvement, reducing from an error of 8 meters to just 2 meters. The simulation is also likely to have demonstrated the effects of the previously discussed key error drivers, particularly early in the simulation where the proposed Kalman filter method showed degraded performance when compared with other techniques. As anticipated, the error drivers shown are likely to be from the identified sources; the presence of unidentified multipath, poor signal strength resolution and a poorly optimised measurement error model in the Q matrix.

The first error drivers to be confirmed are the linked to the radio environment effects of multipath and poor signal strength resolution. As shown in Table 6, the performance of the Kalman filter position estimate was worse in simulation stages 2 and 3 than was obtained at stage 4 of the simulation. The degraded performance at stages 2 and 3 of the simulation may be correlated to 2 main effects. The first is the presence of structures and so multipath effects. The second is the change in performance of the filter over time. The analysis of the extended Kalman filter performance and identification of key error drivers predicted that this error is likely to be correlated to the radio environment with less correlation to the time from the start of the simulation. To confirm this prediction, the simulation is to be re-run with the mobile device moving at 25 % of the speed in the original simulation, detailed in Table 6. The output of the filter is expected to correlate well with that of simulation 1 at the corresponding simulation coordinates. The performance of the filter in a slower moving mobile device can be seen in Figure 35 to Figure 38.

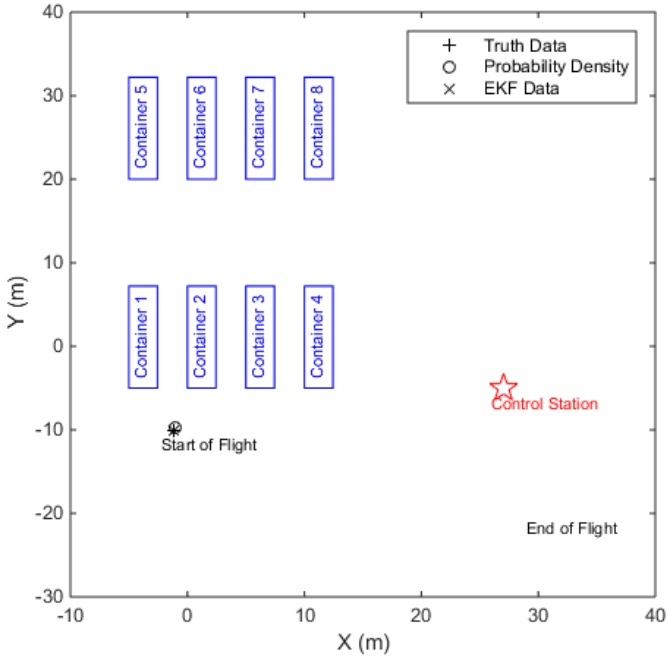

Figure 35 - Urban environment simulation 2, t = 0

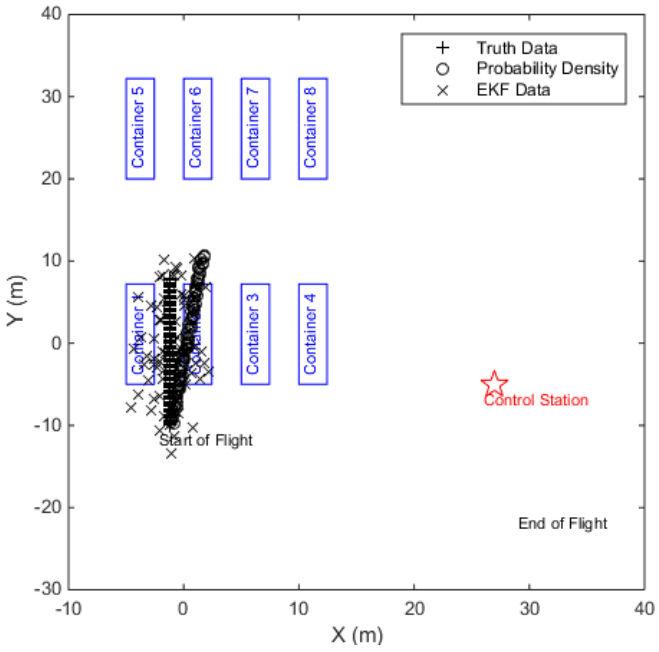

Figure 36 - Urban environment simulation 2, t = 40.

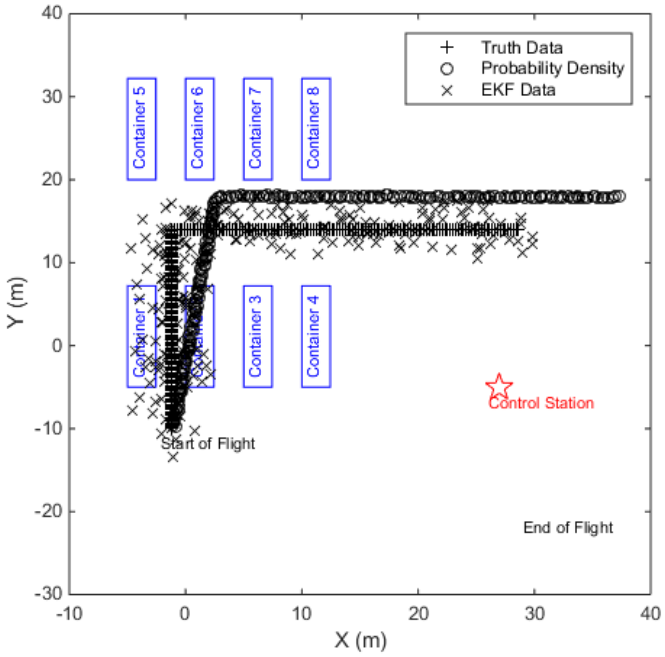

Figure 37 - Urban environment simulation 2, t = 120.

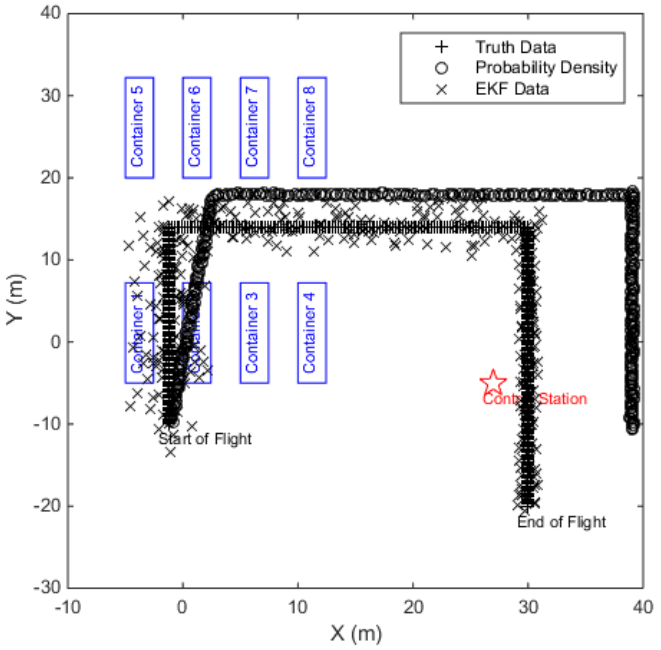

Figure 38 - Urban environment simulation 2, t = 200.

Tabulated simulation 2 results with a comparison against simulation 1 is presented in Table 7.

Table 7 - Error Driver Confirmation Test 1 Results

Simulation	Simulation Stage	Time from Start (s)	Max EKF Simulation 1 Position Error (m)	Max EKF Simulation 2 Position Error (m)	Improvement [Degradation] (m)
2 – Slow Movement in an Urban Environment Simulation	1	0	N/A	N/A	N/A
	2	1 to 40	7	6	1
	3	41 to 120	4	5	[-1]
	4	121 to 200	2	2	0

Moving through the environment at a significantly lower velocity has had no noticeable effect on the accuracy of the filter. This indicates that, as predicted, the leading extended Kalman filter system error drivers are caused by fixed environmental effects rather than by changes to the filter state over time. The confirmation that the performance of the filter over time does not change significantly also allows the improvement in performance from simulation stage 2 and 3 to that seen in at simulation stage 4 to be analysed. The significant improvement in performance between stage 4 and the others is likely to be because of the comparative lack of multipath in the later stages of the simulation. This provides further indications that as anticipated, the leading error drivers in the system are caused by the multipath effects common to urban environments.

Simulation 2 has also confirmed that unlike the extended Kalman filter technique developed as part of this thesis, existing probability density solutions do degrade over time as expected.

The presented simulation model has confirmed the key features discussed in the analysis of the design architecture. Specifically, the simulation has validated the assessment findings that the use of the filter design can provide an improved geolocation estimate over existing techniques in urban signal of opportunity environments. Further, the simulation as provided some evidence that that likely error drivers identified in the design analysis are present and have a significant effect on the resulting geolocation estimate. The following sections of this thesis will carry out further research into the identified leading error drivers. Methods for mitigating these error drivers will be presented, leading to filter design updates to build in resilience to their prescience in the radio environment.

3.7 Architecture Summary

This chapter proposed a system architecture that combines radio signals of opportunity to provide a geo-location estimate. One key benefit of utilising data sources from existing sensors is that a system designer may provide a geolocation estimate to a mobile device without the need to add additional hardware. A further benefit is that the large number of different input sources across many spectra has the potential to provide an inherent robustness to the resulting geolocation estimate. The drawback of this approach in existing topologies is that the system does not scale well with the addition of a large number of data sources, leading to high system complexity and increased power requirements. An approach has been proposed that maintains a dead-reckoning geolocation estimate based on inertial measurement updates to reduce system complexity and power requirements. The proposed method reduces the accumulated errors associated with inertial dead-reckoning techniques by using an extended sinusoidal Kalman filter that allows existing sensor data to be integrated into the geolocation estimate with a simplified interface that can be integrated with any available radio signals of opportunity. The proposed extended Kalman filter utilises any available data at the point at which it is available from the sensor. The Kalman filter utilises this data, comparing it to the position estimate that has been generated from all previous location estimates from a range of sensors.

The proposed filter allows the design of a system that meets the two of the key design aim specified in section 3.1:

i. To minimise system complexity and power usage.

The architecture is capable of producing a scalable architecture that can integrate a large number of sensor inputs with low system complexity, processing load and minimal additional power requirements.

ii. To optimise the filtering of sensor data by tight coupling data streams.

The extended Kalman filter also allows the tight coupling of filtered data streams. The proposed filter design also allows the final design aim to be achieved, allowing a geolocation estimate optimised for use in urban indoor environments.

The optimisation for these environments has been achieved by selecting signals of opportunity inputs. Signal of opportunity inputs have been selected as they are common in the target environments, provide a range of multi spectral inputs and are commonly controlled by a distributed range of operators.

Analysis of the filter performance has been discussed with signal strength and ToA signal of opportunity estimates. Error drivers in these typical environments have been identified and discussed in section 3.5. The error drivers in the radio environment have been identified as incorrect but consistent ToA measurements caused by multipath effects and a lack of resolution in the signal strength environments. Further, short term errors at start-up due to the use of signal noise estimates that are not optimised for the specific radio environment were have been discussed.

The operation of the proposed architecture design has been simulated in an urban environment to confirm that the performance improvements expected over existing methods are present. The simulation has also provided evidence that the anticipated error drivers are the dominant error drivers on the geolocation estimate.

The simulation identified a 75 % reduction in geolocation error over existing signal of opportunity geolocation techniques in the simulated environment. The following sections of this thesis will investigate these error drivers further and will provide techniques to allow mitigation against them. The operation of the mitigation techniques will be analysed before the simulation is re-run with any mitigation techniques included. The final simulation model will then be benchmarked with practical test in an urban environment. Section 4 of this thesis will investigate method to mitigate the susceptibility of the filter to prolonged and constant ToA errors. Section 5 will research techniques to mitigate the lack of signal strength contrast while section 6 will investigate methods to optimise the filter start-up time in unknown environments.

4. Improved ToA Data Development

The previous chapter proposed an architecture that significantly improves the performance of existing geolocation techniques in indoor and urban environments, while analysis of the architecture identified key error drivers. This chapter will research methods of using the identified strengths of the architecture to mitigate the identified error drivers.

To improve the system accuracy of the filter design proposed on section 3, an approach will be researched that allows the extended Kalman filter to mitigate the identified error drivers. The first error driver to be addressed is the ability for non-normally distributed ToA errors to introduce an undesirably high confidence value in the associated filter matrix. These high confidence values may cause the filter to converge in either an erroneous geolocation estimate or increased geolocation estimate uncertainty over time. As discussed in section 3.5, in areas of stable multipath effects, the mobile device may receive a stable but offset ToA estimate. The repeated reception of a seemingly valid ToA estimate for a long period causes the associated filter gain K value, defined in Eq 12, to grow. This causes the filter to converge on an erroneous geolocation estimate.

4.1 Mitigation Technique Design Aims

The design of a technique to provide mitigation in this scenario requires the consideration of several key design requirements. The key aims of the mitigation technique are:

- To allow the identification of multipath effects in ToA systems.
- To allow an estimate of the magnitude of any multipath effects, allowing the filter to take appropriate action in assigning a filter confidence value.
- To allow the technique to be applied to data links that utilise message security. This will require the use of physical layer properties in the radio channel.

The work carried out to design a mitigation technique that allow these design aims to be met is detailed in the following sections.

4.2 Mitigation Development

The filtering of multipath effects is required to provide resilience to its affects. This will require the development of a signal fingerprinting technique to analyse the radio environment to identify signs of multipath. Research into potential techniques is described in the following sections of this thesis.

4.2.1 ToA Detection Filter Design

Although multipath signals may be the largest received signal, a direct path signal, however low the signal to noise ratio, will travel the shortest distance and be received by the user first. This is however not the case, due to the potential presence of deconstructive interference from the multipath signals. It is likely that, in high multipath environments, the first symbols of a message will be destroyed by deconstructive multipath, resulting in the inability to detect the direct path signal at the physical layer. A simulated example of this can be seen in Figure 39.

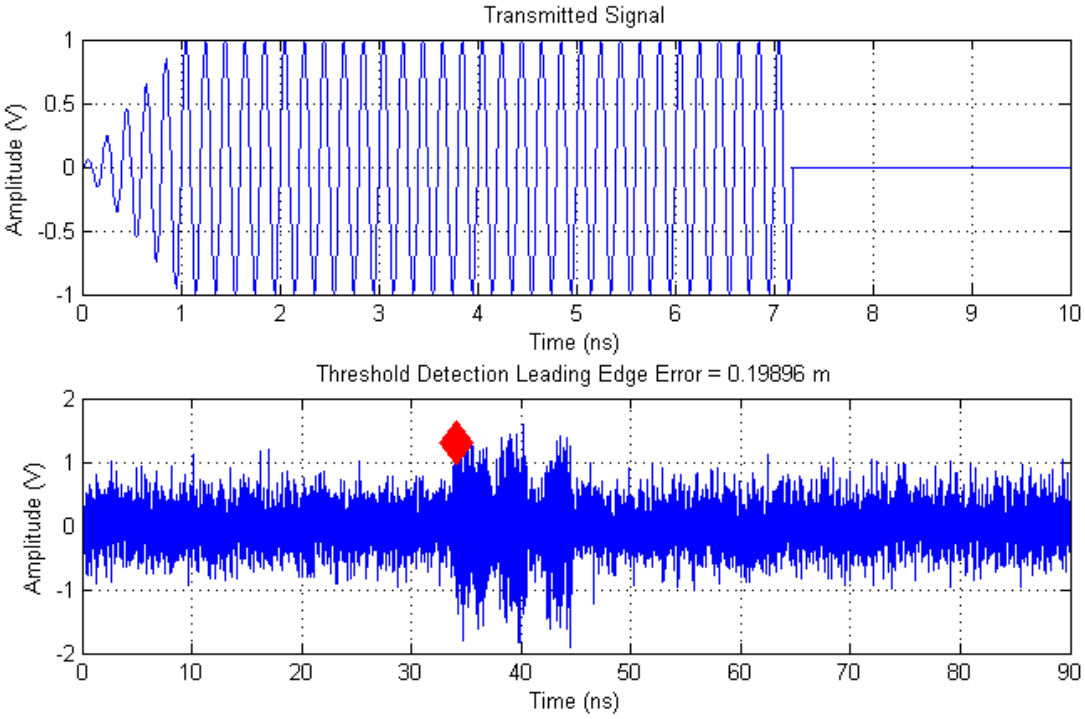

Figure 39 – A simulation of Typical Multipath Effects on a Transmitted Message

The red diamond in the figure demonstrates where the detecting start of a received message has been identified. The receiver has no way of knowing if this is accurate, as deconstructive interference, seen throughout the message, may have obfuscated the start of the message too. It is however possible to record the raw RF at the receiver at a high data rate with little computational load. This may provide opportunities to still obtain fingerprinting information from the RF environment around the receiver if a suitable higher level filtering scheme can be developed.

The drawback of this method is that recording and mapping the environment around the receiver is a very complex task with high rate measurements required. This is likely to provide a significant computational load on the recording system, requiring hardware that is unlikely to be found in mobile and portable devices. Work will need to be carried out at a higher level to reduce this requirement with efficient filtering and location state estimation.

Search-back algorithms improve on the ToA accuracy by analysing the received packet and performing a search-back to determine physical layer properties of the message to determine the time of arrival more robustly. These algorithms require prior knowledge of the multipath environment, which cannot be provided in many applications.

The UWB signal processing uses a signal as an input and includes the following stages. If $h(t)$ represents the received signal in the time domain, it is first passed through a rectified moving average filter as shown in Eq 27.

$$y(t) = \frac{1}{n} \sum_{i=t-n+1}^{t} abs(h([t])) \qquad \text{Eq 27}$$

The averaged signal $y[t]$ is then passed through two filters of sizes n_1 and n_2 which return the maximum value from a sliding window, as shown in Eq 28 and Eq 29.

$$\max\_n_1[t] = \max(y_{t-n_1} \ldots y_t) \qquad \text{Eq 28}$$

$$\max\_n_2[t] = \max(y_{t-n_2} \ldots y_t) \qquad \text{Eq 29}$$

A binary indicator of whether a leading edge has been detected can be obtained from Eq 30.

$$r[t] = (\max\_n_1[t] * 2 > \max\_n_2[t]) \qquad \text{Eq 30}$$
$$\& \ (\max\_n_2[t] > thresh)$$

When using this technique, the threshold detection level, *thresh*, will be set to 3σ of inter-message in-channel received signal noise. This value has been picked to limit false alarms as far as practical during the testing while allowing a rapid response to abnormal events.

These UWB signal-processing techniques utilise the wide frequency range of the received signals to provide an improved ToA estimate. The analysis of the full frequency range available allows the user to determine frequency specific multipath variations and make an improved estimation of the true ToA reading. Further research into these UWB signal-processing techniques has been carried out to allow the extended Kalman filter described in section 3 to detect the leading edge of a signal obtained from a wide bandwidth transmission. It has been selected for further development due to the fact that the running filters applied to the raw data may provide additional data to the user following further analysis. A comparison of edge detection seen by employing UWB signal processing techniques to each narrow bandwidth channel as opposed to simple threshold detection is shown in Figure 40.

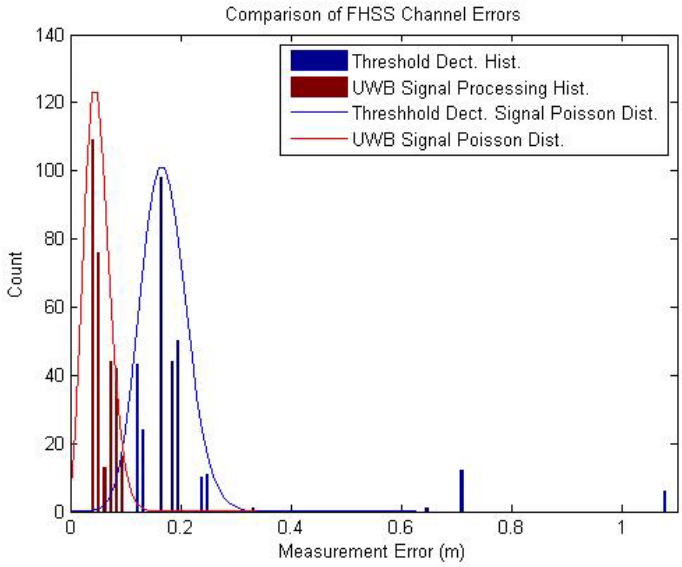

Figure 40 - Comparison of threshold based and UWB signal processing leading edge detection methods.

Analysis shows that the Poisson distribution of the UWB signal has a variance λ value of 17 for the threshold detection algorithm and an improved λ value of 5 for the UWB threshold detection. The received estimates across the range of networks not only have less average error but also a greater distribution density than can be obtained from simple threshold detection alone. As well as a significant improvement in the Poisson distribution, the UWB based edge detection algorithm removes the erroneous outliers seen at ≈ 0.7 m and ≈ 1.1 m error in the threshold detection algorithm.

4.2.2 ToA Detection Filter Analysis

A simulated radio frequency (RF) environment has been modelled in Matlab and Simulink, using the basic architecture described in Appendix D - System Test Plan, to evaluate the effectiveness and performance of the proposed data source. The simulation uses the standard multipath simulation model, Eq 31, where L_p is the number of multipath components, α is the complex attenuation and τ is the propagation delay.

$$h(t) = \sum_{k=0}^{L_p-1} \alpha_k \delta(t - \tau_k) \qquad \text{Eq 31}$$

The simulation assumes that an idealised transmitter generates a single frequency modulated pulse; for validation, the FHSS network parameters included 100 20 kHz channels evenly spaced from 3 GHz to 5 GHz. Modelled propagation and receiver distortions are applied to produce a received signal for analysis. The resulting signal includes simulated effects of multipath with the use of separate propagation channels. The simulations evaluated throughout this stage of the project will consider a LoS propagation path of 10 m with several multipath reflection paths with an apparent time path from the transmitter to the receiver consistent with 10.1 m to 11.2 m propagation distances.

This simulated environment has been used to ascertain the performance of a simple threshold detection algorithm in a Monte Carlo based simulation of a wide range of FHSS channels in a fixed geometry. An example of a typical single transmitted message and the received signal patterns in a high multipath environment can be seen in Figure 41.

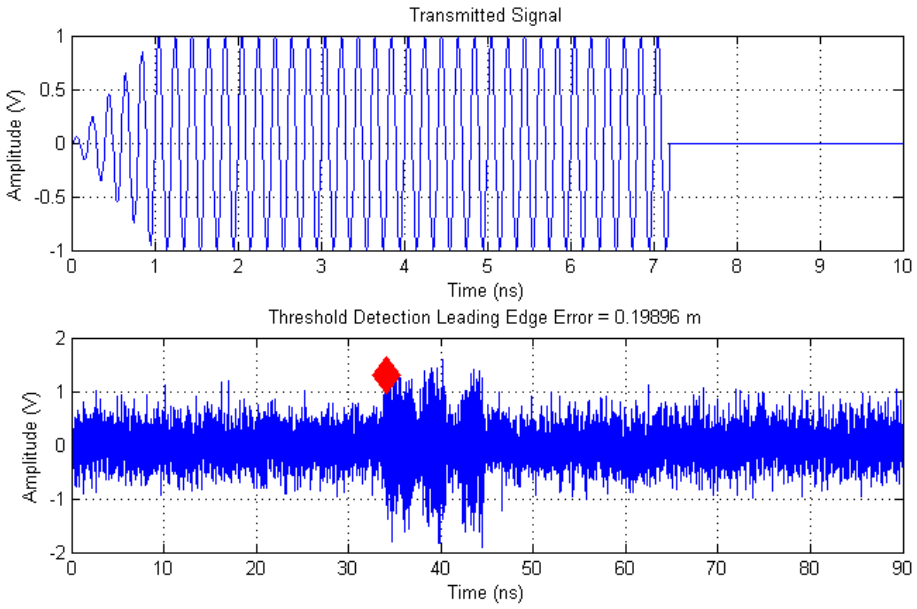

Figure 41 - Transmitted (top) and received (bottom) pulse with the location of the detected leading edge of the pulse marked by the red symbol.

This threshold detection algorithm simulation assumes a static receiver and transmitter across a range of FHSS channels to benchmark the simulation. The results in Figure 41, show the properties that are expected in multipath environments. These properties include the loss of definition in the leading edge, constructive and deconstructive interference. These effects cause varying and seemingly unpredictable changes to the signal strength through the receipt of the message. This behaviour accounts for the high multipath uncertainty seen in commonly applied techniques that use leading edged detection to estimate either a ToA and range estimate.

The mechanisms that cause these errors are shown in more detail in Figure 42Figure 41, a magnification of the area of interest in Figure 41, and will be discussed in further detail.

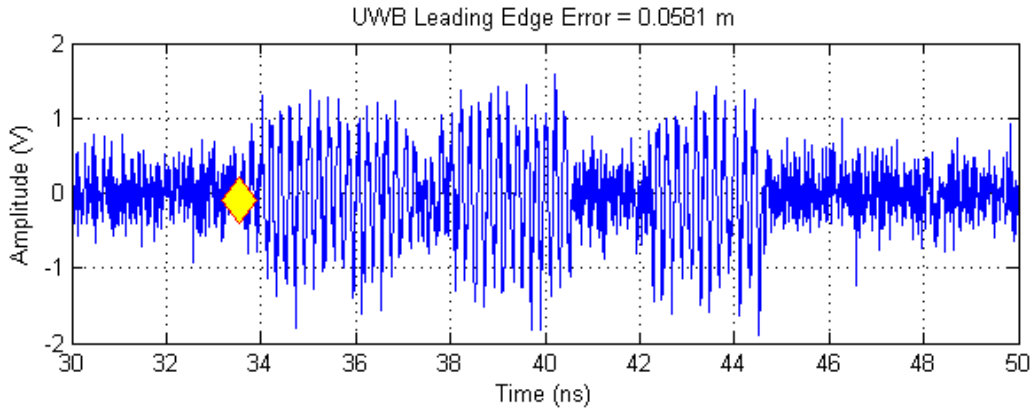

Figure 42 - UWB leading edge detection of pulse in a noisy multipath environment (Area of interest).

Areas of constructive and deconstructive multipath effects can be seen throughout the [34ns:42ns] interval, where a non-multipath signal would be expected to produce a stable series of 1 V peaks. The UWB algorithms discussed in section 2.3.2 of the literature review produce a significant improvement over threshold detection when providing ToA estimation in high multipath FHSS networks when only a single narrow bandwidth channel can be analysed at a time.

While the application of this UWB edge detection technique will provide an improvement in ranging estimates in many applications, additional data available in the developed extended sinusoidal Kalman filter again allows a closely coupled architecture to be built building further robustness into the error driver mitigation technique. The structure of the closely coupled Kalman filter and UWB leading edge detection estimates will now be discussed.

4.2.3 Closely Coupled ToA Detection Filter Design

The equation described in Eq 30 utilises a pre-set value for the threshold limit *thresh*. The availability of an estimated signal arrival time allows the pre-set threshold value of 3σ of the in-channel noise, set to prevent false alarms in non-coupled operation to be reduced to provide a more agile response with the same chance of a false alarm being triggered. The value at which the *thresh* can be set is based on a chi-squared probability density function approach where the confidence of the measured trigger and be foud depending in the sinusoidal Kalman filter confidence in its estimation step, determined by the value of the K matrix (Eq 12). The equation to determine the applicable value of *thesh* that will provide 3 σ false laram protection as a function of K detailed in Eq 32.

$$thresh_{3\sigma\_equivalent} = \sum_{i=1}^{v} \frac{(x_i - u_i)^2}{(1/K_{[1]})_i^2} \qquad \text{Eq 32}$$

A summary of the previously designed architecture is shown in Figure 43. Modification is required to the greyed boxes to couple the UWB leading edge detection equations into the design.

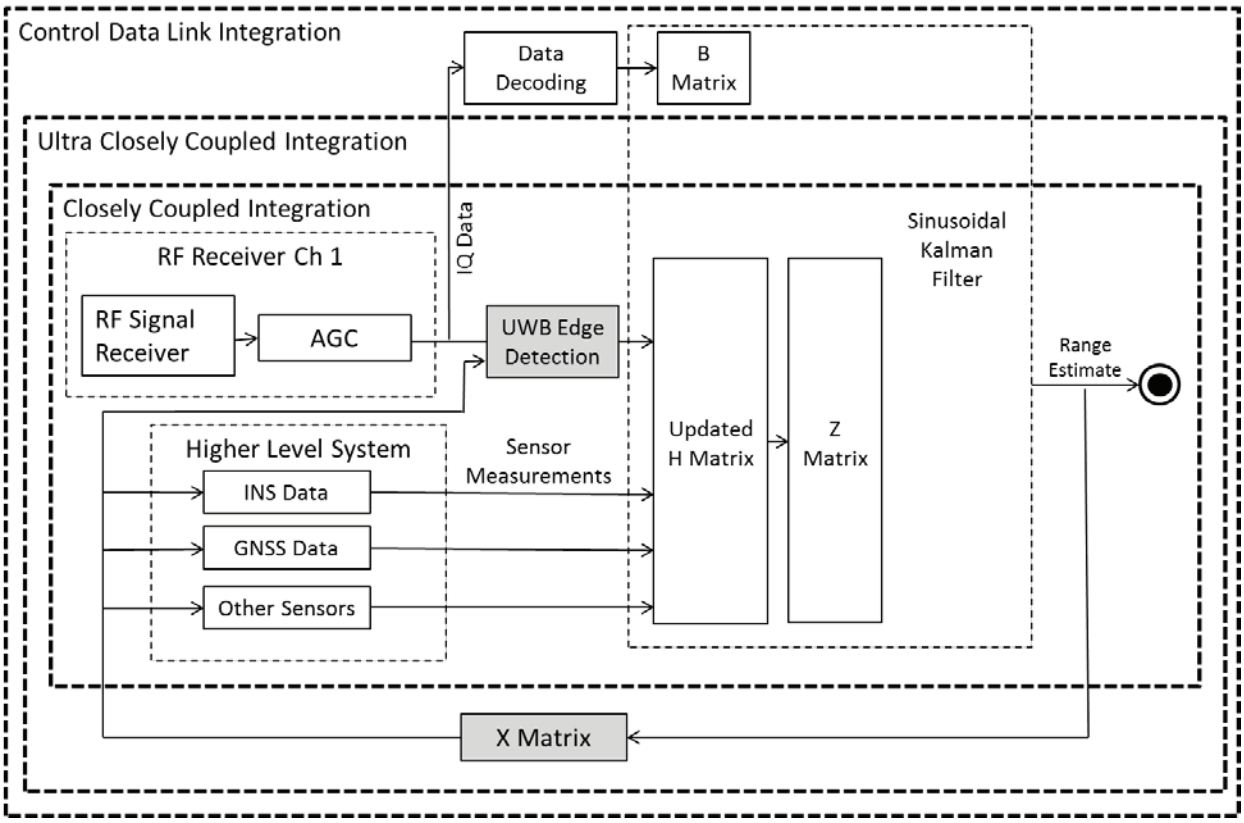

Figure 43 – Required System Modifications

The first system modification required is the addition of the UWB Edge Detection analysis step to the raw I and Q data from the radio receiver. The addition of this process simply requires the addition of the analysis described in Eq 27 to Eq 30 in the typical manner.

The second system modification required is to simply allow the X matrix to contain the threshold values required by Eq 30 for the current Kalman filter prediction step with the addition of the Eq 32 as a matrix entry.

4.2.4 Closely Coupled ToA Detection Filter Analysis

This thesis will next consider the effects of this improved leading edge detection performance when both non-coupled and closely coupled approaches are applied to the addition of the UWB edge detection algorithms. The analysis of both methods will stages will allow the improvement associated with closely coupling the systems to be discussed and the benefits of the sinusoidal Kalman filter architecture to be shown.

The analysis will use the simulation environment discussed earlier in this chapter in a multipath environment. The first scenario considered is a static system that sweeps through 100 FHSS channels over a 5-second period.

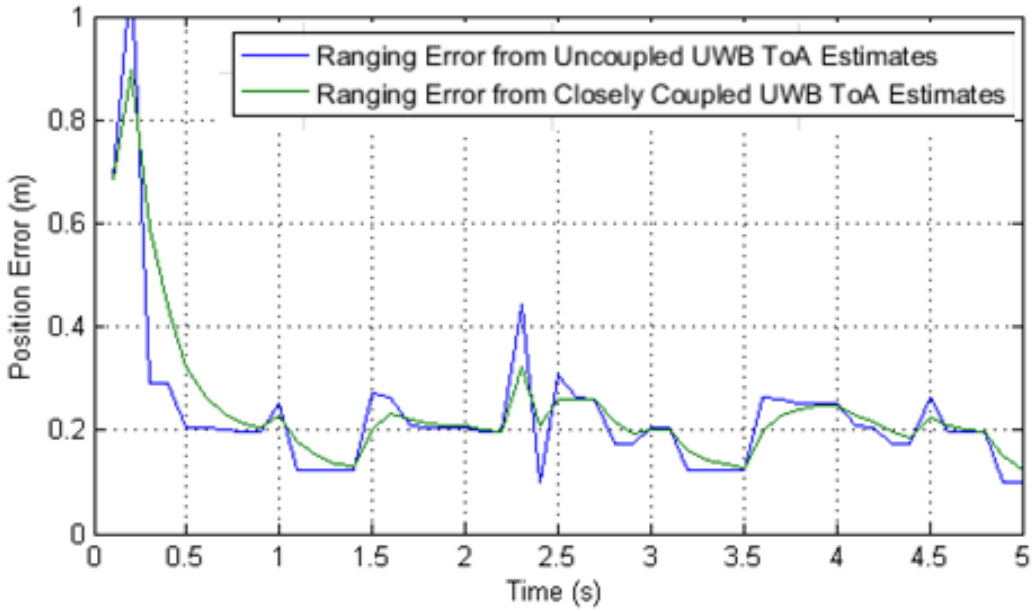

Figure 44 - The raw and filtered output from the threshold detection algorithm with a pre-selected static confidence interval.

A plot showing the ranging error from the UWB technique in coupled and uncoupled scenarios is shown in Figure 44. Table 8 provides a quantified measure of the improvements achieved.

Table 8 - Threshold Detection Performance Improvements

	Ranging Error from Uncoupled UWB ToA Estimates	Ranging Error from Closely Coupled UWB ToA Estimates	Improvement Provided by the System Coupling
Max Error (m)	3.2	0.9	72 %
Mean Error (m)	0.24	0.23	4 %

The results presented in table Table 10 summarise the improvements obtained to 2 parameter that are key to geo-location systems. The first is the maximum error received during the simulation which may be important to agile systems that cannot carryout extensive averaging or filtering of data. The addition of closely coupled data from the sinusoidal Kalman filter has led to a 72 % reduction of error, clearly showing measurement integrity benefits from using data made available by the designed architecture. While the maximum error is important for some agile systems, the majority of higher-level systems are likely to be able to mitigate these temporary errors with filtering schemes. The majority of users will be concerned with the mean error of the system over a period of several seconds. In this aspect of the ranging error performance, there has been significantly less benefit from closely coupling the signals. This low level of benefit is likely to stem from the fact that over a range of frequencies, multipath errors do not accumulate and a true range to the transmitter can be obtained.

While the mean error improvement over the full simulation time is modest in the closely coupled technique, this only considers a static test where the receiving node is not moving, which is unlikely to be typical of a system requiring geolocation estimates. A more likely scenario is that the receiving node is moving in its environment during the sweep across the UWB channels.

The effect of receiver motion on the ranging estimate will be estimated in an rerun of the initial simulation with the addition of receiving node motion. The simulation has been re-run starting with a stationary period for 1.2 seconds before applying a 1 m range change between the transmitting and receiving nodes. To simplify the simulation the motion applied to the receiving was a step change to minimise the Doppler effects associated with a change in velocity of the receiving node and, to remove noise from the results, a the performance of single channel will be considered.

The results of the simulation are shown in Figure 45, with a change in receiver location occurring 1.2 seconds into the simulation.

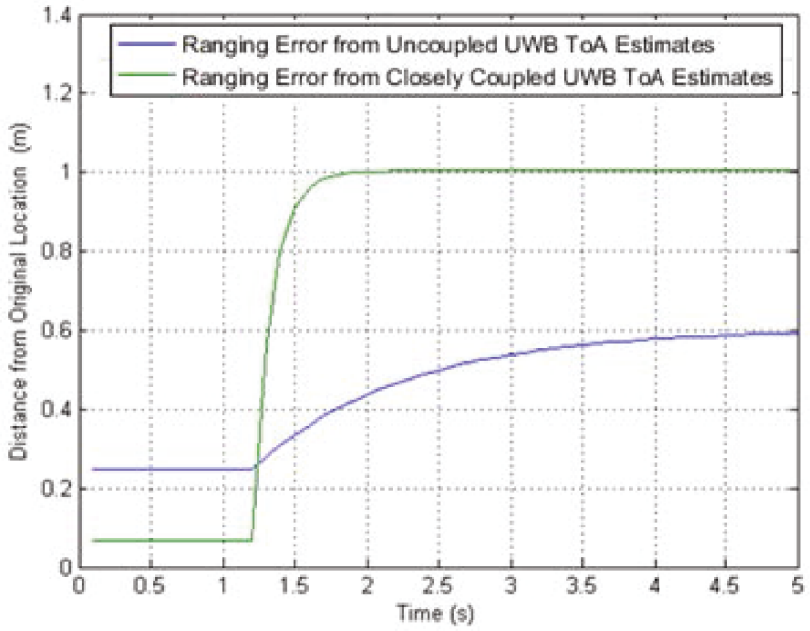

Figure 45 - The response of the filters to a step response of the receiving node.

The performance of the techniques and percentage improvement from the closely coupled system is detailed in Table 9.

Table 9 - Threshold Detection Performance Improvements

	Ranging Error from Uncoupled UWB ToA Estimates	**Ranging Error from Closely Coupled UWB ToA Estimates**	**Improvement Provided by the System Coupling**
Time taken to record 90 % final range estimate (s)	3.7	0.6	**83 %**

The addition of coupled data from the sinusoidal Kalman filter provides a significant improvement to the bandwidth of the geolocation data, reducing the time required for the UWB measurement to achieve 90 % of it's final ranging estimate by 83 %. The ability for the technique to adapt to changing ranging estimates is vital to many agile and mobile users of a geo-location system.

4.3 Analysis of the ToA Filter as an Error Driver Mitigation Technique

This section will summarise the improvements obtained by adding the researched error mitigation techniques into a higher-level system. The system level simulation environment described in 3.6.2 has been repeated with the addition of the researched ToA system. The improvements will be highlighted and discussed

The system level simulation has been repeated with the addition of the filtered leading edge detection technique. In the simulation, the developed error mitigation technique has been applied to the data command link as designed in Figure 43. The effect of improving the accuracy and robustness of ToA estimates in a multipath environment in the closely coupled system will increase the accuracy of the geo-location estimate, providing a smaller error distribution around the true location without adding latency to un-anticipated changes in location. The error mitigation technique has been designed to produce a reduction of errors in range measurement, most clearly detectable as a reduction of error in the first stages of the simulation where ranging errors at this stage were the dominant error symptom in the first set of simulations. A summary visualisation of the simulation output is shown in Figure 46.

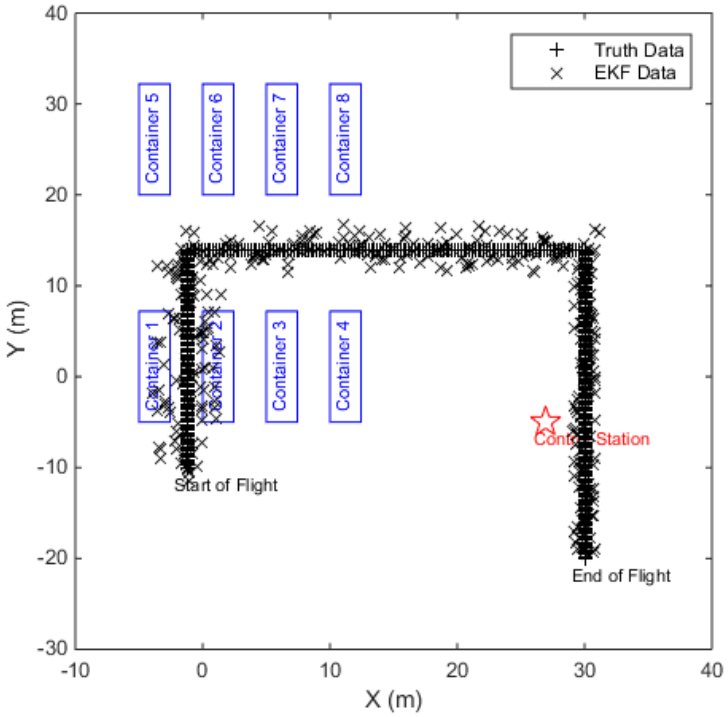

Figure 46 - Simulated Performance with the Addition of Leading Edge Detection Improvements.

The simulation results, shown graphically in Figure 46 are summarised and compared to previous simulation results in Table 10.

Table 10 - Summary Effects of Improved Leading Edge Detection

Simulation Stage	Time from Start (s)	Max EKF Simulation 2 Position Error (m)	Max EKF with Addition of Improved Leading Edge Detection Filter Position Error (m)	Improvement [Degradation] (m)
1	0	N/A	N/A	N/A
2	0 to 10	6	4	2
3	10 to 30	5	4	1

Simulation Stage	Time from Start (s)	Max EKF Simulation 2 Position Error (m)	Max EKF with Addition of Improved Leading Edge Detection Filter Position Error (m)	Improvement [Degradation] (m)
4	30 to 50	2	2	0

Research has been carried out to design a ToA error mitigation technique in multipath environments. The motivation for this research has been to improve the performance of ranging estimates in areas with significant multipath effects, producing a valuable information source for the sinusoidal Kalman filter. Table 10 provides an example, showing the magnitude of improvement that the researched mitigation technique brings. This improvement is shown most clearly in the location accuracy improvement in areas that ace close to densely positioned buildings. These are areas where multipath effects are greatest and the sinusoidal Kalman filter is now able to identify and mitigate erroneous ToA estimates. Further, the availability of stable ranging data in a multipath environment allows the sinusoidal Kalman filter to effectively identify inertial measurement unit drifts earlier in the simulation. The identification of these errors allows increased accuracy and robustness throughout the simulation, including areas of low multipath, demonstrating the benefits of a closely coupled system.

The simulation has demonstrated that the researched technique to mitigate against erroneous ToA measurements has significantly improved the uniqueness of the geo-location estimate. The simulation has demonstrated that poor integrity message receptions have not degraded the performance providing confirmation that the filter is working correctly.

4.4 Closely Coupled ToA Detection Filter Conclusions

This chapter has discussed the research carried out into the ToA detection methods in multipath environments. The key aims of the mitigation technique were to allow the identification of multipath effects in ToA systems, allow an estimate of the magnitude of any multipath effects and to allow the technique to be applied to data links that utilise message security.

The designed ToA filtering technique meets each of these aims, allowing the physical layer signal to be analysed to detect both the presence and magnitude of mitigation techniques. This information has been integrated into the higher-level sinusoidal Kalman filter via the expansion and modification of existing signal measurement matrices. This integration provides a closely coupled system that provides a more accurate position estimate that, in turn, allows improved performance of the ToA filtering technique. The benefits of this error mitigation technique has been demonstrated in a system level simulation. The results of this simulation has allowed the performance improvements obtained to be discussed and analysed.

The following chapters will detail the research and design of techniques that will mitigate the remaining sinusoidal Kalman filter system level error drivers.

Page left intentionally blank.

5. Improved Received Signal Strength Contour Development

A sinusoidal Kalman filter based geolocation architecture was researched and designed in chapter 3 of this thesis. The design suffered from errors induced by a small number of key error drivers. Chapter 4 identified mitigation techniques for the most significant error driver, ToA estimate errors in multipath environments. The second key error driver that is limiting the performance of the sinusoidal Kalman filter based geolocation architecture is the ambiguity of RSSI measurements. The primary cause of this ambiguity is the measurement quantization, preventing the generation of detailed RSSI fingerprints. While measurement accuracy could be improved by using higher-grade hardware, this is not be desirable in many applications. Research may show that it's possible to manipulate and filter the environment to provide a higher fidelity RSSI signal measurement without addition hardware requirements. This section will present the research carried and discuss the design of techniques to provide an improved RSSI measurement into the sinusoidal Kalman filter architecture.

5.1 The Signal Strength Environment.

The signal to noise ratio recorded by the receiving sensor is vital for successful data communications between nodes. The received signal strength at any given location is determined by geographical features including the distance from the transmitter, obstructions and multipath effects. These characteristics may each be of use when determining the location of a receiver. Due to the fact that signal strength is such a key parameter to the primary function of data communications hardware, it is easily available in standard hardware implementations and so can be used as a data source for higher level applications.

To allow the performance of signal strength measurements to be discussed and analysed, modelling has been carried out as part of this project to determine the likely accuracy of a system within a typical dense urban environment. The accuracy of any available geolocation data from signal strength indicators will be determined by the quantity of signal strength contours, the stability of signal strength over a period of time in a typical urban environments and the uniqueness of each signal strength region. Signal strength modelling has been carried out with standard multipath simulation models, described in Appendix B – Simulation Environment.

Utilising signal strength maps from systems such as Wi-Fi and Bluetooth is a common method of determining a user's location. As highlighted in the literature review section 2.1.5, generating Wi-Fi signal strength maps is an active areas of current research. This research typically aims to generate signal strength maps with corresponding SSID tags. These maps are used to construct world models of many urban and indoor locations. A limitation on commonly researched signal strength mapping techniques is that the generated map, even in complex indoor locations, have few contours. Due to the significant quantization effects on the measurement of RSSI, much of the simulated environment receives the same signal strength measurement leading to few topological boundaries. An example of RSSI measurement quantization in a simplified radio environment is shown in Figure 47.

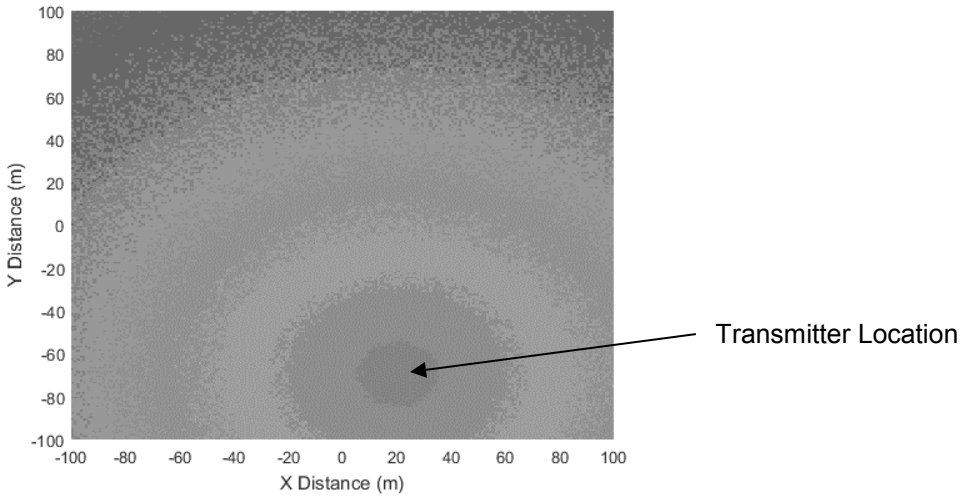

Figure 47 - Example of a Quantized Signal Strength Map

To obtain knowledge of where the user may be, the receiver must move a considerable distance through the mapped environment, crossing at least one contours, to allow a matching system to build up knowledge of the user's location. The additional knowledge and computing to allow the user to be tracked over a large difference means that considerable computing power is required, often running particle filter systems. Another limitation of current research is the ability to deal with poor environmental stability. Changes in the radio signal environment can be cased by a wide range of physical changes. These changes are particularly common in indoor and urban environments where changes in the environment such as doors opening, large vehicles passing and large number of mobile transmission devices will cause significant changes to the RSSI map.

Poor environmental stability combined with the requirement to monitor the environment for long periods means that current research techniques do not provide a reliable, robust or accurate data source for the sinusoidal Kalman filter architecture. Two possible mitigation paths are available; either the stability of the radio environment could be improved or the frequency of contour changes could be increased. Either of these improvements would allow an improvement to the quality of the information obtained.

The first mitigation path, to improve the stability of the environment is not considered applicable to the research carried out in this thesis. Improving the quality of radio environment is only possible by controlling the surrounding radio environment. While this may be possible in a small number of controlled environments, and is another active area of research, it is not possible in the generic urban and indoor environments that this thesis aims to address.

The second mitigation path, to increase the number of contours and minimise the reliance on long-term radio environment stability may be possible in a wide range of environments. One common method of overcoming quantization effects in all systems, not just radio environments is to add noise to the signal of interest. The addition of noise with a 1σ value that is larger than the equivalent least significant bit of the RSSI indicator will significantly mitigate the effects of quantization. A model summarising the required location of additional generated noise is shown in Figure 48.

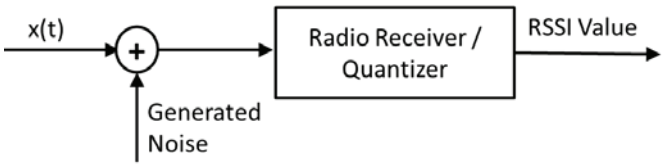

Figure 48 - Addition of Generated Noise to Overcome Quantization

While it is not considered possible to control urban and indoor environments while meeting the aims of this thesis to produce a global approach to urban and indoor navigation, it may be possible to add noise into the radio environment, using the addition of noise to improve the resolution of the RSSI values from the hardware. The ability for the system to generate noise while still meeting the design aims of using existing hardware is likely to be possible due to the un-licenced nature of the signals of interest in urban and indoor environments. The mobile system is likely to contain WiFi hardware, utilising a frequencies that have been identified as the target frequency for this technique in the sinusoidal Kalman filter architecture.

Interferometric geolocation is an area of research that utilises signal interference to determine greater geolocation accuracy. This technique is discussed in literature review section 2.1.4.2. Interferometric methods rely on the beat frequency between two similar carrier frequencies to generate RSSI readings that beat at the separation frequency. This technique can be applied to introduce noise into the signal environment is the mobile node transmits at a low power level onto the same frequency channel as the signal being monitored. This beating in RSSI level effectively adds noise into the samples signal environment due to a process of constructive and deconstructive interference. The addition of this noise will reduce the quantization effects and provide further fidelity in the RSSI signal from the hardware. An example of the resulting RSSI environment in a simplified example is shown in Figure 49.

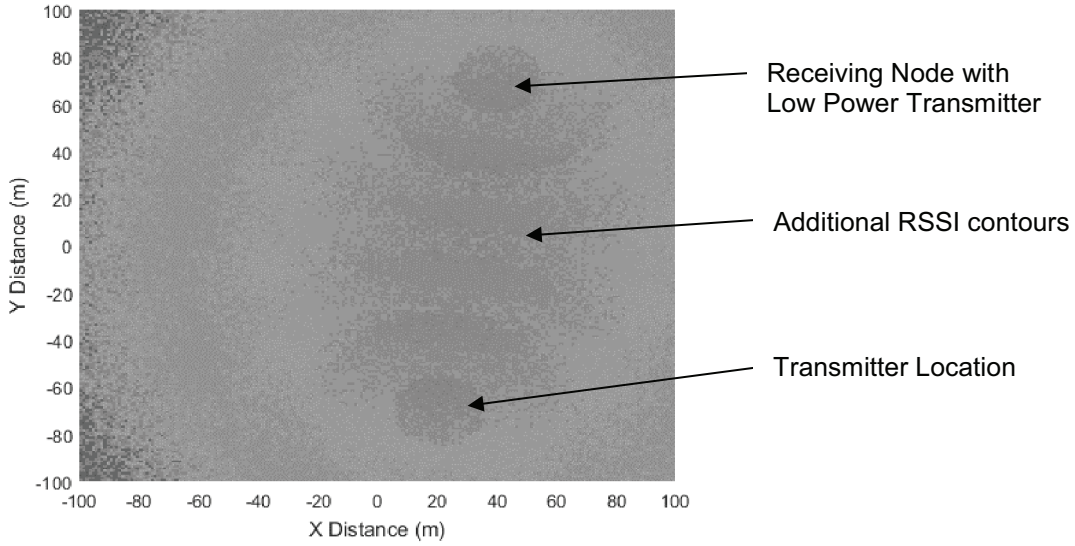

Figure 49 - Example of a Quantized Signal Strength Map with 2nd Low Power Transmitter

The example demonstrates an example environment at a point in time. The additional RSSI contours will produce and interferometric beat signal that will allow the filtered average RSSI values to better represent the monitored signal strength over time. This increased resolution significantly reduces the distance required to be traversed by the user to determine their likely location within the mapped area. One significant benefit of this is that any movement of the user will be detected sooner, allowing the sinusoidal Kalman filter to be able distinguish between biases and real motion in a timelier and less computationally intensive manner. The combination of signal strength decay areas has also lead to a greater range of areas where the signal strength is unique although there is still considerable ambiguity in any single point RSS level. The reduction in sampling time required to recognise changes in signal strength improves the resilience of the system in areas of radio environment change with time.

The following chapter will research the design required to select and control the transmitted signal frequency in relation to the surrounding signal environment. The integration of this technique into the sinusoidal Kalman filter architecture will also be designed.

5.2 Interferometric Signal Strength Filter Design

The interferometric technique discussed in the previous section will be used to inject noise into the radio signal strength environment. This section will design the filters that are required to select a transmission frequency and integrate the RSSI beat frequencies into the sinusoidal Kalman filter architecture.

This analyses the relative carrier phase for the signal strength at the measured location and uses multiple transmitters to generate a low frequency and long wavelength beat signal. The first step is to select the transmission frequency and power of the mobile node. Typical low size weight and power (SWAP) hardware polls the RSSI no faster than twice a second due to power conservation. These settings are typically written into the device firmware and are not easily changed. Ideally, this provides a requirement for the transmission signal to be matched to the received signal to an accuracy of greater than 1 Hz for the full beat to be observed. This equates to an error less than 0.1 parts per million (ppm) and isn't considered practical in hardware. While this type of full interferometry isn't possible, the use of interferometer to generate noise does not require the beats to be monitored at any particular update rate. This allows the selection of the beat frequency to be arbitrarily set by hardware errors, typically in the region of 25 ppm, meaning that the user must simply select the same transmission frequency as that received. It is desirable that the beat frequency of the received signal varied between a SNR of 0 and twice that of the received signal to provide an optimised RSSI range. To achieve this, the transmitted signal should match that of the received signal in the location that the mobile node is receiving the signal. Again, this principle dictates that the transmitted signal strength should simply match the received signal strength as no further optimisation is possible. These features provide a relatively simple to implement approach to determining the transmitted signal characteristic, summarised for frequency (f) and amplitude (A) in Eq 33 and Eq 34.

$$f_{Tx} \approx f_{Rx} \qquad \text{Eq 33}$$

$$A_{Tx} \approx A_{Rx} \qquad \text{Eq 34}$$

As the errors in the hardware are used to provide the required separations in frequency and amplitude, the two competing signals may be considered approximately equal and require no specific additional hardware requirements.

To integrate the signals into the extended Kalman filter architecture, a tailored SLAM technique has been designed. This design uses a modified fingerprint extended Kalman filter (FEKF) to analyse received signal strength indicator (RSSI) 'fingerprints' in an area to produce a real time map of the RF environment. The accuracy achieved by the SLAM technique increases as the signal strength topology becomes increasingly complex as typical in high multipath environments. The fingerprint extended Kalman filter defines a fingerprint to be a vector of N received signal strength (RSS) measurements from N distinct radio transmitters. The Kalman filter Z matrix is populated with the fingerprint data, shown in Eq 35.

$$z_t = w = [RSS_1, RSS_2 ... RSS_n]^T \qquad \textbf{Eq 35}$$

The predicted value matrix, h, values are drawn from any populated values in the signal strength map, M.

$$h_t = [M_1(x,y), M_2(x,y), ...M_N(x,y)]^T \quad \textbf{Eq 36}$$

The measurement noise matrix, R, is populated form the variance of the noisy RSS measurements, R, and the variance of the predicted measurements, V , as shown in Eq 37.

$$R = [\sigma_{R_1}^2 + \sigma_{V_1}^2, \sigma_{R_2}^2 + \sigma_{V_2}^2, ...\sigma_{R_N}^2 + \sigma_{V_N}^2]I \quad \textbf{Eq 37}$$

The measurement matrix, H, is populated from the loop-up coordinates shown in Eq 38.

$$H(i,1) = J_{i,x}(x,y)$$

$$H(i,2) = J_{i,y}(x,y) \quad \textbf{Eq 38}$$

The advantage of the map is that, as the number of contours in the SLAM map increases, the accuracy of the estimated location and the reliance to unrealistically large geo-location jumps increases.

The accuracy of the SLAM algorithm is increased as the resolution of the maintained RF map increases. The technique described in this investigation uses the inputs from the interferometric signal in a multipath environments as the source of the data for the FEKF SLAM technique.

$$RSS_N = RSS_{BeatSignal} \quad \text{Eq 39}$$

The interferometric RSS_N values are used as the input to the Kalman filter *w* matrix. In high multipath environments, the phase offset will have many contours due to the varying level of multipath in each of the contributing signals. In multipath environments, the RSSI of the beat signal has many times more contours in that in of a set of separate channel RF transmitters these contours can be monitored at a low frequency, allowing low SWAP hardware to maintain a high resolution topology map of the environment. The remainder of the FEKF matrices are dynamic and will maintain their state efficiently in a range of conditions. No further modifications will be required when transitioning from single channel to interferometric signal strength analysis.

The following section of this thesis will apply the designed interferometric noise injection system into the extended Kalman filter architecture simulation to demonstrate the achieved improvement in performance.

5.3 Predicted Performance with Additional WiFi Contouring

A interferometric noise injection system and a method for integrating the data obtained into the top level sinusoidal Kalman filter architecture has been designed. This research has been carried to mitigate a leading error driver identified in the analysis of the top level system. The simulation that was used to demonstrate the error driver has been repeated with the addition of both ToA edge detection filter and an the designed interferometric radio technique, producing an increased number of signal strength contours. The performance obtained from the system is demonstrated in Figure 50.

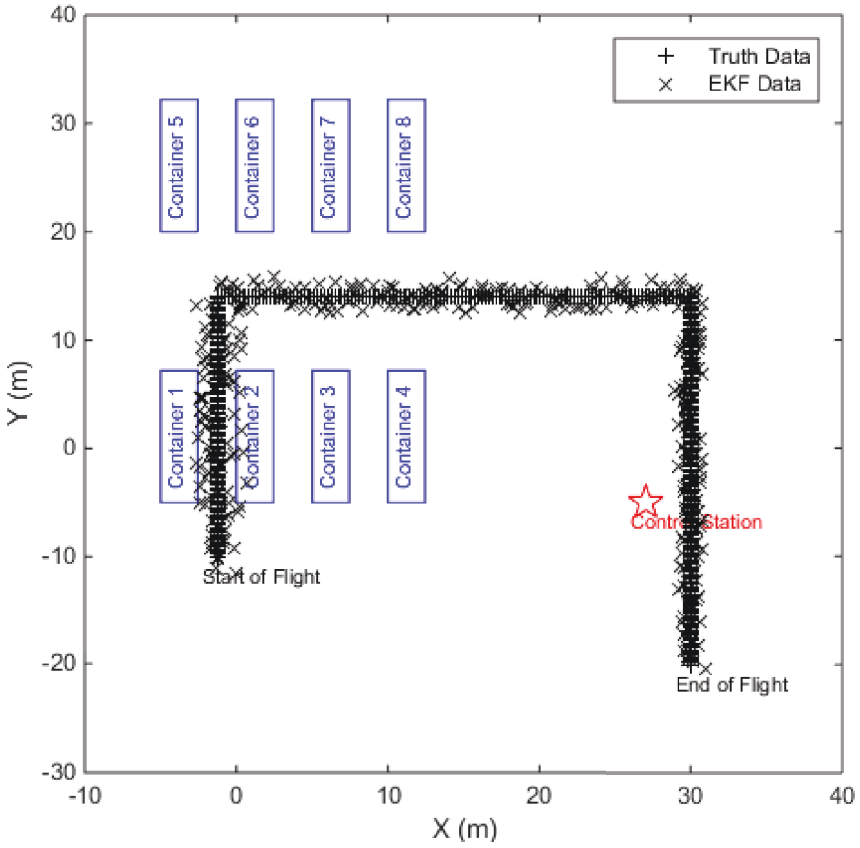

Figure 50 - Simulated Performance with Contour Improvements.

The simulation results, shown graphically in Figure 50 are summarised and compared to previous results in Table 11.

Table 11 - Summary Effects of Improved Signal Strength Detection

Simulation Stage	Time from Start (s)	Max Position Error (m) with Improved Leading Edge Detection Filter	Max Position Error (m) with Improved Leading Edge Detection Filter and Signal Strength Contouring	Improvement [Degradation] (m)
1	0	N/A	N/A	N/A

Simulation Stage	Time from Start (s)	Max Position Error (m) with Improved Leading Edge Detection Filter	Max Position Error (m) with Improved Leading Edge Detection Filter and Signal Strength Contouring	Improvement [Degradation] (m)
2	0 to 10	4	3	1
3	10 to 30	4	3	1
4	30 to 50	2	2	0

The error driver mitigation makes the most significant improvement in the initial stages of the simulation where multipath effects are the most significant. Again, as expected, there is no recordable improvement in areas with less multipath effects.

The simulation also shows that significant error exits in areas due to the ambiguous nature of the signal strength contours. No data is available from the IMU and signal strength sources that is able to provide a single centre point to the possible geo-location estimates. To improve this system, the addition of a known distance from a reference point would greatly improve the position estimate by allowing the removal of many false geo-location estimates.

The simulations summarised in Figure 50 and Table 11 has confirmed that the error drivers identified in section 3.5 have been correctly identified and can be mitigated. Perhaps more significantly, the simulation has indicated that it is possible to provide a geolocation estimate with an error of less than 3 m in urban and indoor locations. While this level of accuracy is an improvement over other geolocation systems available in indoor and urban environments GNSS navigation systems are able to provide improved geolocation accuracy in more open environments. Improvements to the system could benefit from using the improved accuracy of GNSS systems in open environments, transitioning to the proposed system when the user moves to an indoor or urban environment when the GNSS signals become too weak to use. The ability for the system to transition from one system to another efficiently will be developed in the following section of this thesis.

5.4 Signal Strength Filtering Conclusions

This section of the thesis has discussed research carried out to improve the accuracy and robustness of signal strength measurements. Two possible approached have been identified. The first, stabilising the radio environment over time, would only be possible in areas where the radio environment is designed and controlled by the system operator. This is not practical in many urban and urban environments. The second identified method required the ability to obtain more accurate signal strength readings from hardware that provides a quantized output. This has been achieved by using transmission hardware in the mobile node to inject interferometric noise onto the radio environment at the frequency and amplitude of the received signal. The addition of this noise allows the effects of quantization to be reduced, providing additional information to the higher level sinusoidal Kalman filter.

This section of the thesis continued to research a dynamic and efficient fingerprint Kalman filtering scheme, designed for use on portable hardware such as smart phones, to provide a mechanism for using signal strength data to generate a real-time SLAM map.

Sections 4 and 5 have carried out research into methods to mitigate the major error drivers identified during the design of the sinusoidal Kalman filter. The sections have successfully design filters and algorithms that allow the error drivers to be mitigated while still addressing the key design aims of this thesis; filtering existing data, coupling systems and minimising hardware requirements. The designs presented have been discussed and analysed, with simulations carried out to demonstrate their operation. This thesis will continue to identify techniques for integrating the sinusoidal Kalman filter into system level applications, considering handover from traditional geolocation techniques and optimising the speed and accuracy in hand-over and start-up situations.

Page left intentionally blank.

6. Sinusoidal Kalman Filter Start-Up

This thesis has discussed research that aims to provide geolocation estimates in indoor and urban environments. This research has resulted in the design of a sinusoidal Kalman filter architecture. This architecture has been analysed, demonstrated and discussed. This discussion has led to the identification and mitigation of key error drivers allowing the design to achieve it's key design aims in urban and indoor environments.

In open environments, greater geolocation accuracy is likely to be provided by GNSS systems, resulting in the continuous use of this system whenever it is available. Users in urban environments may frequently transition from areas of good GNSS reception to areas of limited or no GNSS reception. These transitions can occur at any time and, in many applications, are difficult to predict. This chapter will research improvements to the algorithms for transitioning between GNSS and the previously researched indoor and urban geolocation estimate methods. This research again uses the principle of closely coupling sensors, optimising the use of decaying GNSS signals to provide a fast start-up to the Kalman filter while optimising the information that can be obtained from a low signal to noise ratio GNSS signal.

6.1 Existing Start-Up Limitation

In operational scenarios, handover is likely to take place as the system transitions from an outdoor environment where its location is known from a service such as GNSS into an area with weak or no GNSS signals. If the previously researched sinusoidal Kalman filter is started without a known staring location, the filters covariance must be initialised with large values. The time taken for the covariance's to decrease can be considerable, approximately 10 seconds as shown in Figure 51, due to the low Q matrix values provided by the proposed filtering techniques. As the penetration of GNSS signals into a building may only be for less than 1 to 2 m, in target applications, where the user may be walking, the receiver may move from an outdoor location with good GNSS signal to an indoor location out of the range of GNSS signals in less than approximately 2 seconds. Tuning the Kalman filter to allow a 2 second maximum time limit at start-up will have adverse effects on the accuracy of the system. To allow this target start-up time to be achieved, a handover scheme should be developed to seamlessly transition from areas of good GNSS reception to areas of limited or no GNSS reception.

Demonstrations of the sinusoidal Kalman filter, discussed in section 5.3, highlighted a trade-off within the Kalman filter implementation between system accuracy and start-up time. The simulated indoor environment in section 5.3 demonstrates that the noise of the measured input is competitively high, resulting in a large values in the associated Q matrix. Lower noise in the measured radio values will reduce the required Q matrix values and will improve the geo-location performance of the system. The only trade-off for geolocation performance improvement is to increase the sampling time, leading to a longer start-up time of the system. This problem will be particularly severe in scenarios where the user transitions slowly from open areas with little signals of opportunity data, where GNSS is likely to be available, to areas with a greater number of signals to monitor. This trade off can be seen when the Kalman filter K matrix value that corresponds to the IMU vectors is plotted over time when a GNSS location fix unexpended becomes unavailable 2 seconds from the start of the log. A simulation of this performance is show in Figure 51.

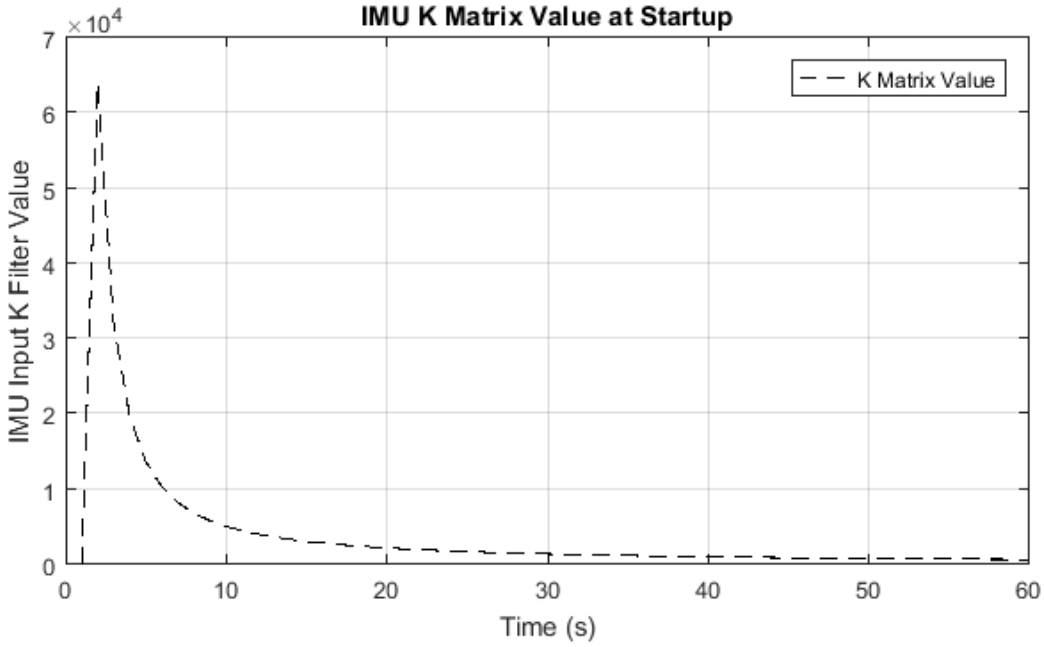

Figure 51 - Kalman Filter Reaction To Loss of GNSSS

While the filter recovers comparatively quickly from the start up errors, resulting in long term degradation, an uncertainty occurs in the filter as it starts up. The scenario of the user transitioning from current geo-location systems such as GNSS to the proposed techniques is commonly encountered in typical urban environments. To allow the trade-off to be overcome and to provide an accurate geo-location estimate in a timely manner, novel techniques have been researched further. The specific areas of research have been to build upon the techniques described in the literature review, section 2.1, and are discussed in the following sections of this thesis.

6.2 Carrier Phase Analysis with Secondary Clock Source

The phase of a carrier signal from a known transmitter source may be used as a source of physical layer data. This approach has been detailed in literature review section 2.1.3.3 and has been applied to mature systems. Typically , approaches use hardware clocks to provide the sampling time control for the carrier phase analysis. The accuracy required in the hardware clocks, where a 3σ error of less than 0.25 of a clock cycle is assumed to be required, produces a requirements for additional hardware that may not always be available in the target system, highlighting a shortcoming of current techniques. If this shortcoming of current implementations could be overcome, carrier phase analysis of a signal of opportunity would be possible and would provide an additional data source that is accurate in transition areas.

Additionally, literature review sections 2.2.1.2 and 2.2.1.3 show that when that when GNSS signals are limited to fewer than four satellites or they become weak and the SNR reduces to a level that the signal data cannot be accurately detected, the tightly tolerance clock timing information can still be monitored allowing Doppler effects to be monitored in ultra-closely coupled applications.

This thesis has carried out research that aims to combine these approaches. The research carried out carrier phase analysis on signal of opportunity using low accuracy GNSS signals, where even a 2D location fix would not normally be possible due to only one or two satellites being in view, to provide an external clock signal source. This approach allows carrier phase analysis to be carried out without the additional hardware requirements of existing methods. In order to succeed, the technique required a low frequency signal from a known transmitter and a high frequency clock signal, which are combined for carrier phase analysis as shown in Figure 52.

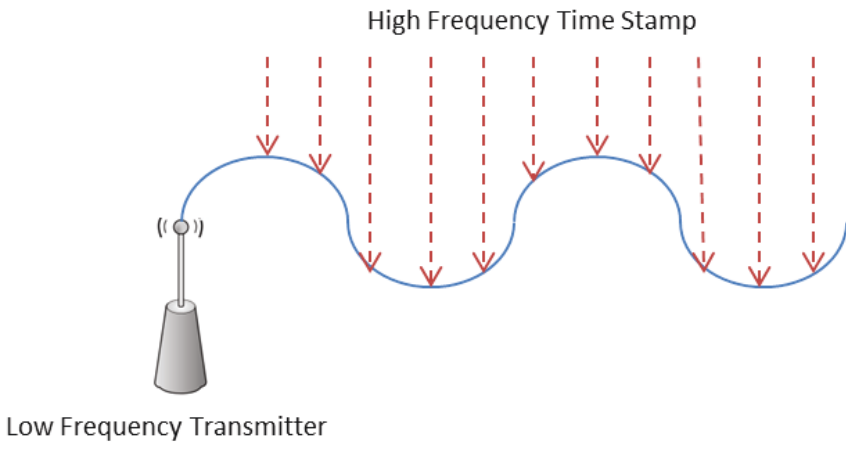

Figure 52 – Example of Carrier Phase Analysis without a Hardware Clock

The required data sources can be found in urban environments, allowing an accurate location estimate may be achieved, but several key challenges in indoor and urban environments need to be addressed. Most significantly, the signal path of both the low frequency signal under analysis and the clock signal will be affected by multipath refection's and NLOS issues [FARAGHER et. al. 2010].

6.2.1 Carrier Phase Performance Analysis

This section will develop an understanding of the researched carrier phase technique's potential. The accuracy of the technique and the key limitations of the data sources will be analysed.

The application of the technique requires two data sources, the amplitude of the carrier phase value and the external timing data. Error sources are present for each of these data sources. In indoor and urban environments, the key error driver for carrier phase analysis is multipath interference, where the received signal my amplified or attenuated when combined with signal reflections. Transmission errors will also be present in the transmitted signal, these transmission effects are dominated by jitter in the transmitting signal. Other platform specific error drivers include the accuracy of the sampling hardware and local attenuation effects. These groups of errors have mutually exclusive sources, as such a root sum of the squares (RSS) approach has been taken to the calculation of errors. The resulting equation for carrier phase accuracy is shown in Eq 40.

$$X_m = \sqrt{(X_t - E_{Multipath})^2 + (X_t - E_{Jitter})^2 + (X_t - E_{Meausurment})^2} \quad \text{Eq 40}$$

Where X_m is the measured phase amplitude and X_t is the transmitted phase amplitude.

In addition to these error sources, there are also timing errors associated with the eternal clock source. These errors are dominated by the path length effects of multipath, which may be considered insolation. Effects such as amplitude errors will not significantly the time received and transmission jitter is considered negligible due to the intended GNSS uses of the signal. A summary of the clock signal error is provided in Eq 41.

$$C_m = C_t - E_{Multipath} \quad \text{Eq 41}$$

The susceptibility of this effect to multipath and the low SNR nature of GNSS signals mean that the technique will not provide significant information for the sinusoidal Kalman filter in indoor or dense urban environments. The reduction of information required in the GNSS signal does however mean that it can be used in areas of poor GNSS coverage, effectively extending the range of the GNSS signal and providing additional data to the sinusoidal Kalman filter in the low multipath areas to improve it accuracy and robsutness.

The performance of the technique with anticipated error sources, combined in the method discussed in this chapter has been demonstrated in a simulation. The aim of the simulation is to demonstrate the anticipated performance of the technique with normally distributed values for the error terms described in Eq 40 and Eq 41. The simulation has conducted a Monte Carlo error estimates with scaled and normally distributed error inputs. The anticipated ranging accuracies predicted by the model are shown in Figure 53.

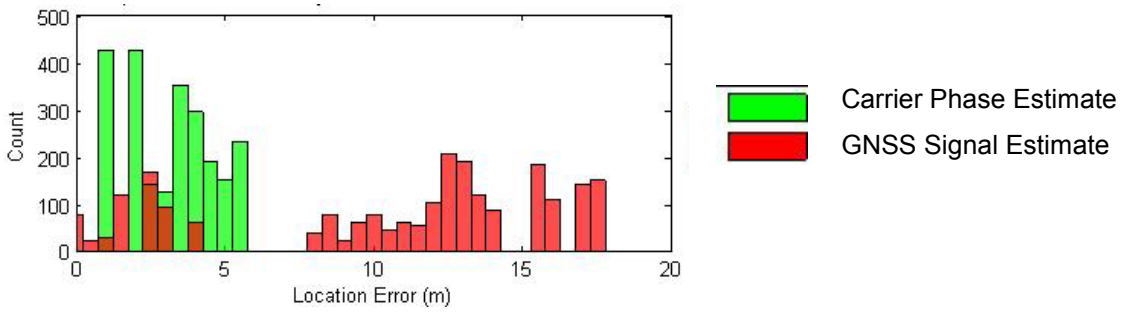

Figure 53 –Phase Analysis and GNSS Ranging Estimates in an Urban Environment.

The performance observed in Figure 53 is summarised in Table 12.

Table 12 - Summary of Ranging Estimates in an Urban Environment

Technique	Max Error (m)	Mean Error (μ) (m)	3 Sigma Error (μ + 3σ) (m)
Carrier Phase Estimate	5.5	3.2	6.0
GNSS Estimate	17.5	13.1	20.0

As expected, the Monte Carlo simulation has demonstrated that even with the discussed urban environment error sources, the carrier phase estimate provides a significant improvement over using a low SNR GNSS signal. The estimation error has reduced to 30 % of that provided by GNSS alone.

This initial simulation has demonstrated that improved accuracy levels may be achieved in urban environments without the requirement for accurate clock hardware on the receiving node. This additional information can be used by the previously discussed sinusoidal Kalman filter in areas of low GNSS SNR or where less than three GNSS transmitters are visible. While this performance improvement is not available in many of the sinusoidal Kalman filters intended environment, it does provide an improved data source when handing over from open environments with good GNSS signal coverage to areas of non-GNSS geolocation estimation.

6.3 Carrier Phase Analysis during Filter Start-Up

This thesis has researched a technique that allows an improved geolocation estimate in areas that the number of available satellites or the SNR of the GNSS signal degrades. This thesis has also researched This this has also researched a sinusoidal Kalman filter architecture that allows geolocation estimates to be generated in urban and indoor environments. This section investigates methods for combining the techniques to provide imported handover from GNSS to the sinusoidal Kalman filter and analyses it's expected performance.

The start-up of the system with and without handover technique was represented in Figure 49. The representation has been carried out a second time to identify the response of the Kalman filter is a new input is added that provides ranging updates with mean (μ) and variance (σ) values defined in the carrier phase estimate row of Table 18. The timestamping can be used to carry out carrier phase analysis, resulting in an additional Kalman filter data source and allowing the filter to respond more gracefully to the loss of GNSS. The results of the simulation can be seen in Figure **54**

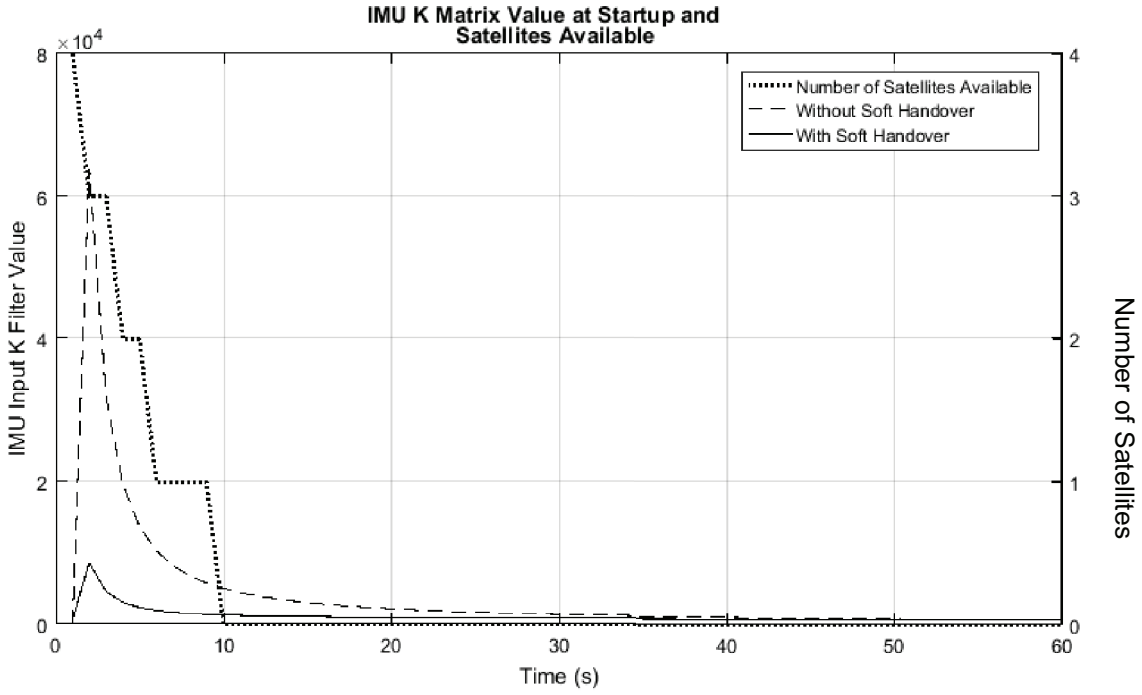

Figure 54 **- Kalman Filter Reaction To Loss of GNSSS with Soft Handover**

The demonstration shows that, as expected, the Kalman filter responds in a more controlled manner in the event of GNSS degradation. The researched technique will allow a smoother handover when GNSS signals are lost, allowing the geolocation estimates obtained from the filter development to be obtained within approximately 10 seconds after the transition of the system into a GNSS denied urban or indoor area.

The performance improvement associated with the improved filter performance is again demonstrated by adding the technique to the simulation described in Appendix B – Simulation Environment. Re running this simulation will allow the improvement in performance at the start of the simulation be demonstrated and discussed. The performance obtained from the system is demonstrated in Figure 50.

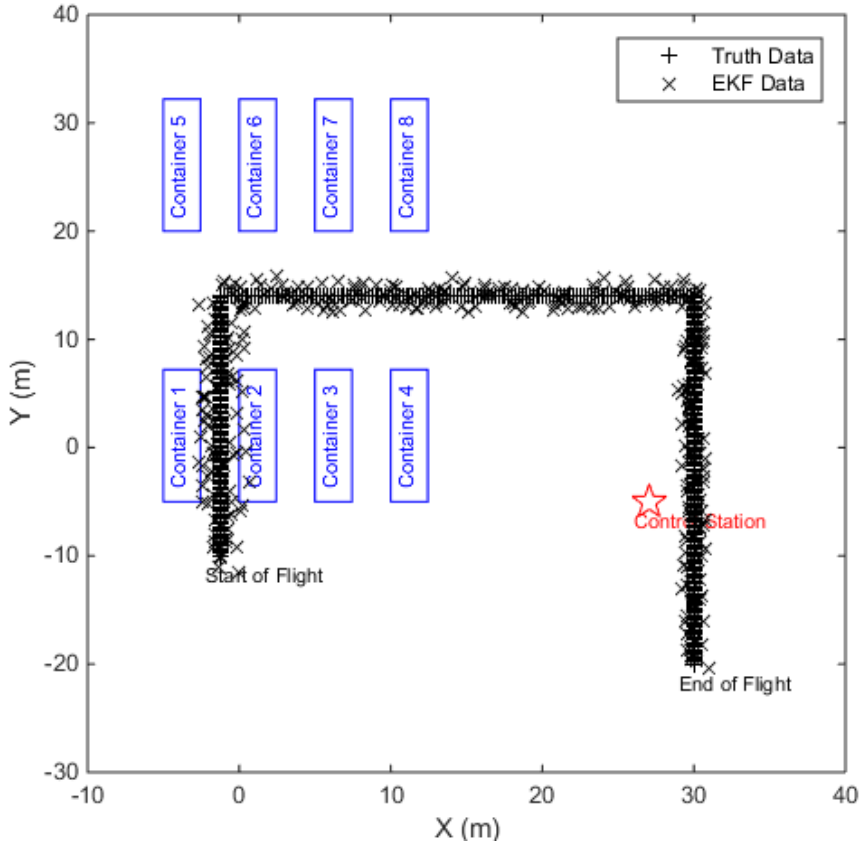

Figure 55 - Simulated Performance with GNSS Hand Over.

The simulation results, shown graphically in Figure 50 are summarised and compared to previous results in Table 13.

Table 13 - Summary Effects of GNSS Hand Over

Simulation Stage	Time from Start (s)	Max Position Error (m) with Improved Leading Edge Detection Filter and Signal Strength Contouring	Max Position Error (m) following the addition of GNSS Handover	Improvement [Degradation] (m)
2	0 to 10	3.2	2.5	0.7
3	10 to 30	4	3	0
4	30 to 50	2	2	0

A few meters into the urban environment past the start point, there is no discernible GNSS signal data to use as a carrier phase clock. As discussed during the research into the start up data source, there are no long-term improvements from the addition of this data source. There are however two significant areas of interest shown in this demonstration. The first is that there is a small improvement in the geolocation estimate in the first few seconds of operation. This improvement is available in an area that had comparatively large errors in previous demonstrations. The second important note is that, despite the addition of a data source that will perform poorly in many indoor environments, the sinusoidal Kalman filter has not shown a degradation to it's performance in these areas, where other information sources are emphasised by the filter implementation.

This thesis has discussed research into an integrated system architecture that allows improved geolocation estimates in indoor and urban environments. The discussion describing the design, architecture and error driver mitigation within the filter has been articulated and demonstrated with the use of a simulation environment described in Appendix B – Simulation Environment. This thesis will now evaluate the appropriateness of this simulation environment and will benchmark several of the simulations with test data to verify the validity of the discussed designs.

7. Validation and Benchmarking

During the course of this research simulations of radio environment detection and IMU errors have been a key part of explaining and analysing the performance of the key system components. To further demonstrate the system improvements and validate the simulations carried out, the performance of the model has been benchmarked through a set of hardware test scenarios

The validation carried out as part of this thesis has been carried out in two stages. The first stage is to validate the simulations carried out during the design and analysis stages of the research. This testing will create a hardware scenario that replicates the simulated environment and allows a comparison to be made against the simulation environments. The comparison will concentrate on proving that the design works in a way that has been discussed and that key error drivers have been appropriately mitigated. The second stage of the validation approach is to prove that the designed architecture is able to provide improved geolocation estimates in a wide range of urban and indoor environments. This testing will involve moving a representation module node around real life urban and indoor environments to ensure that the geolocation estimates obtained are accurate and robust, as indicated by the design knowledge and analysis presented in this thesis.

7.1 Simulation Validation

During the design of the geolocation architecture presented by this thesis, we considered the target application to be a low cost mobile device, with low SWAP hardware that is typical in current and future mobile devices. In addition to this, the target environment was the dense urban and indoor environment that is typical to areas of high population density.

To allow the performance of the designed architecture in these applications and environments, low SWAP hardware and a dense urban environment have been selected to validate the research.

The simulations carried out in earlier sections of this thesis have demonstrated the performance of the proposed system in a high multipath environment. The modelled environment was based on an available test facility near the research location. The test environments can be seen in Figure 56.

This test environment was selected for a number of reasons. Firstly, the physical environment is located in a rural area with no near-by electronic devices that transmit in the region of interest. This was confirmed by a survey of the area with radio receiving equipment before and after each test. The absence of 3rd party signals allowed improved control and monitoring of the systems response to inputs. Secondly, the environment contained a series of uniform, empty shipping containers in a set configuration.

This again allowed control over the test environment and also allowed experiments to be carried out empirically estimate key property parameters such as the reflection qualities of the surfaces. The final key feature of the initial test environment is the ability of the tests to be exposed to each of the key object interaction components that make up path losses in urban and indoor environments; reflection, refraction, diffraction and absorption. Tests have been designed, see Appendix D - System Test Plan, which allow a comparison to be made between the real and simulated environments for each these key attributes.

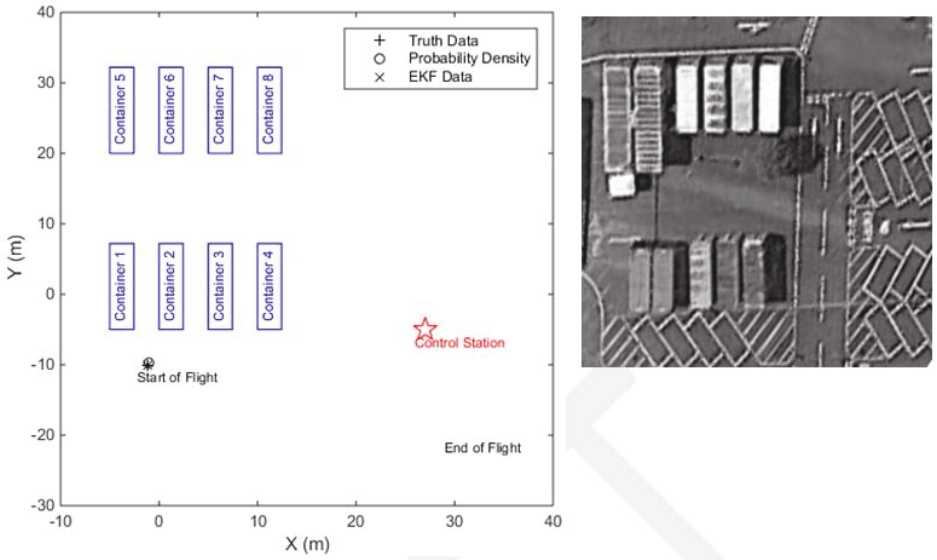

Figure 56 – Simulated Urban Environment and Test Location

In addition to selecting a representative environment, low SWAP hardware typical to mobile devices has been selected to test. These devices have been selected to represent applications that, currently, do not have a mature and robust geolocation source. All testing has been carried out with a low power drone, modified to be controlled with a 27 MHz amplitude modulated transmitter. The flying drone contains a micro electro-mechanical system (MEMS) IMU with three accelerometers and three gyros. The Single RF channel has been recoded using a low power software defined radio (SDR) receiver attached to the drone. The test apparatus can be seen in the photographs below. A smart phone GPS receiver has been added to the drone to provide comparative GNSS geo-location data. The hardware used in the test can be seen in Figure 57, Figure 58 and Figure 59.

Figure 57 – Drone System

Figure 58 – SDR Receiver

Figure 59 – 27 MHz Transmitter

In addition to the hardware shown, the SDR receiver data was logged using open source software called SDR# [AIRSPY, 2016]. The tool was used to log the raw I and Q channels from the SDR hardware. The logged values were recorded to a timestamped file. The key settings used in the SDR# software for collecting the data during the trail can be seen in Table 14. Further information about the software configuration used and an example of the data collected can be found in Appendix C – Test Environment Details.

Table 14 - Key SDR# Data Logger Configuration Settings

Key Parameter in the Logging Software	Selected Setting	Notes and Rationale for Selection
Centre Frequency	27 MHz	Selected to match the centre frequency of the transmitter used to control the vehicle from the base station.
Data source	RTL-SDR USB	The USB SDR radio shown in Figure 58 was used to capture the data.
Radio Modulation	Amplitude Modulated	Selected to match the modulation of the transmitter used to control the vehicle from the base station.
Filter	20 kHz, 2nd order.	This setting was determined from the simulation environment. The 2 kHz 2nd order filter has been selected to maintain a low ripple in the region of interest which may not exist with high order or lower bandwidth filters. The high frequency noise selected will not significantly affect the designed filter which has a significantly lower bandwidth.
Use AGC	Off	With the AGC on the logged signal amplitude will remain roughly constant over the logging period. The signal amplitude is one of the parameters of interest to the Kalman filter so should not be corrected by the logging software. In this case, the lowest gain is automatically used by the logging software to limit saturation at close range.
Data format	32 bit IEEE float	The highest precision data format used. Note: The data files collected during the trail were very large. It may be possible to select other data types.
Record Baseband	Checked	The baseband data file is processed by the filter to determine location.

The test hardware and the test environments were configured to represent the simulations carried out to demonstrate the anticipated performance of the designed geolocation architecture. The key aspects selected to match the simulated environment were the locations of the transmitters and receivers, the power, frequency and antenna properties of the transmitting and receiving nodes as well as the size, shape and material of the objects within the environment.

The drone was configured to record a multi-GNSS signals so that the performance of existing drone navigation techniques can be used for comparison. The multi GNSS receivers available to the drone system allow the reception of both civilian GPS and civilian GLONASS signals. A constellation of eight satellites were available to the drone throughout the test.

The software used to capture the GNSS data was GPSLogger for Andriod [MENDHAK 2017]. The default settings were used to collect timestamped GNSS data in a KML format. An example of the collected data can be seen in Appendix C – Test Environment Details.

To allow the collection of data for use in the sinusoidal Kalman filter implementation, the drone logged sensor data from all available MEMS accelerometers and gyros. The received signal strength and phase readings of the 27 MHz command link were also logged. The de-coded control inputs from the command link were also time stamped and logged. The logged data was post processed by the designed system architecture.

To simplify the control inputs required during the simulation the drone's altimeter was set to maintain an altitude of 1.5 m above the ground at all times. This altitude was selected to minimise ground reflection effects in any received radio signals. Prior to starting the tests, all equipment was allowed to thermally stabilise.

The flight path from the start point to the finish point, shown in Figure 56, has been flown at a constant velocity along the path represented in the design simulation tests.

Summarised results of the initial test flight compared with the results of the architecture simulation have been presented in Table 15.

Table 15 – Summarised Hardware Test Error

Simulation Stage	Time from Start (s)	Max Hardware Test Position Error (m)	Max Simulated EKF Position Error (m) (Table 13)	Difference (m)
1	0	N/A	N/A	N/A
2	0 to 10	3	5	2
3	10 to 30	3	4	1
4	30 to 50	2	4	2

The summary of results in Table 15 show good similarity with those obtained from hardware test. The results obtained from the initial test flight shows that better than expected geo location accuracy has been obtained. The practical testing showed that, while the multipath effects were enough to prevent GNSS working accurately, the signal of opportunity data received was of a higher quality and considerably less corrupted by multipath than simulated. This is likely to be because the simulation carried out simulated worst-case multipath effects from idealised signal to object interactions. In contrast, initial practical testing has inferred that additional noise and signal absorption may have led to a cleaner and more ordered radio environment.

The initial simulation test carried out was in a simplified test environment with a controlled number of significant error sources. While this approach allows the operation of the system to be compared to the simulation environment, it prevents a detailed analysis of the contribution of individual error drivers and an analysis of the performance of the filter in each error driver environment to be made.

Further to the initial hardware test to verify the simulation, additional hardware testing has been carried out in a rage of scenarios. The tests have been designed to exercise the error drivers described in section 3.5. The tests have been designed using a design of experiments approach to gradually build up the contribution of non-normally distributed ToA errors, signal strength variation due to multipath effects and varying start conditions. The method used to derive the test profiles and the error drivers exercised are described in Appendix D - System Test Plan.

The ability of the designed system to cope with the presence of the error drivers in both simulated and hardware test environments is summarised in Table 16.

Table 16 – Summarised Hardware Test Plan Results

Test (As defined in Appendix D - System Test Plan)	Test Description	Validated Error Driver	Mean Simulation Position Error (m)	Mean Hardware Test Position Error (m)	Difference Between Simulation and Test Result (m)
Test 1	Static Test	Baseline Test	3	4	1
Test 2	Open Space	Baseline Test	4	4	0
Test 3	Reflected Multipath	ToA Errors	4	5	1
Test 4	Multipath and Obstruction	Signal Strength Errors and Unknown Start-Up Environment	5	8	3

Test (As defined in Appendix D - System Test Plan)	Test Description	Validated Error Driver	Mean Simulation Position Error (m)	Mean Hardware Test Position Error (m)	Difference Between Simulation and Test Result (m)
Test 5	Corridor Effect	ToA Errors and Unknown Start-Up Environment	6	9	3

The testing carried out and the results obtained have been summarised in Table 16. The baseline tests, 1 and 2, measuring the performance of the system in areas of little environmental interaction have shown good similarity between the simulation and the hardware tests. As the same data processing and filtering tools have been used to analyse both sets of data, these tests demonstrate that the signal transmission simulations do accurately reflect the tested hardware. These tests validate the signal transmission error models used in all subsequent tests. These tests also validate the attempts to maintain an altitude in order to reduce ground reflection effects as far as practicable possible.

Test 3 simulates a controlled addition of multipath effects. This test applies the multipath effects in a controlled manner from a single source. Again, throughout the test good similarity between the simulated results and those from practical testing has been observed. This test provides confidence that both the applied multipath effects are simulated correctly and that the designed filter architecture I successfully mitigating the effects of the error driver.

Test 4 allows the gross geo-location errors caused by both signal strength variations and filter start-up in multipath environments. Again practical test showed god similarity with the simulated environment further validating the simulated environments. Further the test analysis confirms for the first time in this thesis that, in built environment's, the location estimate obtained is better than could be expected from existing systems such as GNSS where, as discussed throughout literature review section 2.1.1.2, errors of greater than 10 m are common.

Test 5 shows the performance of the filter in more complex multipath environments. Again, good similarity has been observed between the simulation results and the results obtained form practical test. This test also demonstrates that the proposed filter architecture has mitigated complex environmental errors and continues to provide an improved geolocation estimate over existing geolocation techniques such as GNSS.

This testing has validated the geo-location estimates obtained in the simulation environment's carried out in the research, analysis and discussion of the designed filter architecture. Good similarity between the simulation predictions and practical testing has been observed when the techniques have been applied to all of the controlled environments. This testing has shown that encouraging results have been obtained with the researched architecture and, as designed, key error drivers have been mitigated. Further testing is required to validate the effectiveness of the designed architecture in a range of urban environments. The performance of the system when compared against simulated predictions has been analysed further in a series of testing in more complex environments in the following sections of this thesis.

7.2 Design Validation

A simulation model has been used to discuss and demonstrate the operation of the designed filter architecture. Testing has been carried out to validate the model and it has been confirmed that the designed filter architecture operates as expected in a controlled test environment. This section will validate the performance of the filter in a range of urban environments.

The aim of the testing is to comparatively benchmark the accuracy if the designed filter system verses the most commonly applied existing technique, [FARAGHER 2010], in terms of accuracy and robustness. A series of tests will be carried out in a range of dense urban environments. These environments have been selected to provide a range of topological environments, with varying radio environments. The test locations are all in the Plymouth University campus, UK (Approx. 50.3745° N, 4.1406° W). A summary of the five test locations, labelled A to E, are shown in Figure 60.

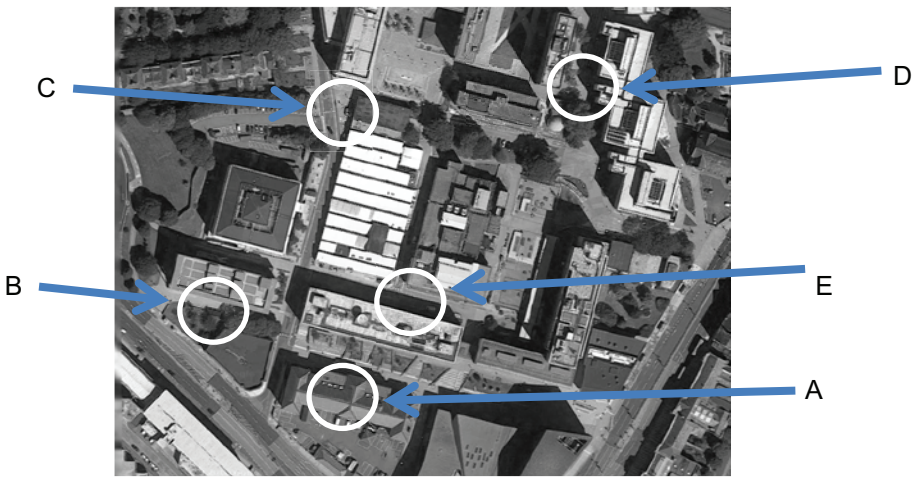

Figure 60 - Urban Environment Test Points

Reception points A to E were selected to allow performance analysis in areas of high and low multipath by selecting areas of comparatively high and low building density. To validate and benchmark the filter performance, the proposed method has been tested with the same hardware used to validate the model in section 7 at each test location. At each test location, 30 second flight was carried out with the mobile drone hardware. A controlled flight path was executed. An overview of the validation flight can be found in Appendix D - System Test Plan.

The method that has been benchmarked against, [FARAGHER 2010], has been carried out using the 'Medium Wave' techniques described in the paper. Details of the data collected and the hardware used can be found in Table 17.

Table 17 - FARAGHER 2010 Key Parameters

Signal Logged	Hardware Used and Key Settings	Notes
MW	**Hardware used:** SDR RTL Dongle Frequency: 693 MHz Modulation: Amplitude	The test location for the trail was in Plymouth city centre. Throughout the trial, three MW transmissions were expected to be seen, although as discussed in [FARAGHER 2010], this cannot be verified from the collected data.

The geolocation estimate obtained throughout the flight has been obtained at each of the five map locations. The average error from the true location throughout the flight was calculated and recorded. A summary of the geolocation accuracies obtained at each of the test stages is shown in Table 18.

Table 18 - Tabulated Range Estimate Averages

Test Location	Building Density	Average Error (m)		Proposed Method Improvement (%)
		[FARAGHER 2010] Method	Proposed Method	
A	Low	6.7	5.8	13
B	Medium	17.3	15.3	12
C	Low	4.7	3.9	17
D	High	33.2	10.8	67
E	Low	2.0	0.7	65

An improvement in geolocation estimate has been obtained at all test locations. As expected, due to the Kalman filter receiving additional information in areas of increased signal distortion, the greatest improvements in geolocation accuracy have been made in areas of relatively high multipath, with the method designed in this thesis producing an average error improvement during the flight of up to 67 % over the exiting methods developed for use in the same environment. The test area that showed the most significant improvement over exiting methods was test location D. This test location was the most densely urban city centre location tested. To gain a further understanding of how the designed filter performed during the trial and to further validate the discussed filter function, this thesis will further analyse the performance of the filter during this test stage.

As previously described, the test stage was in an area with buildings surrounding the trial. A clear view of the sky above the trial was present, although sight was limited by tall buildings on all sides allowing a GPS receiver at the test location to receive data from a constellation of five satellites. As was carried out at each of the test locations, the flight profile consisted of the four main steps. The flight profile carried out at test location D is shown in context with its surroundings in Figure 61.

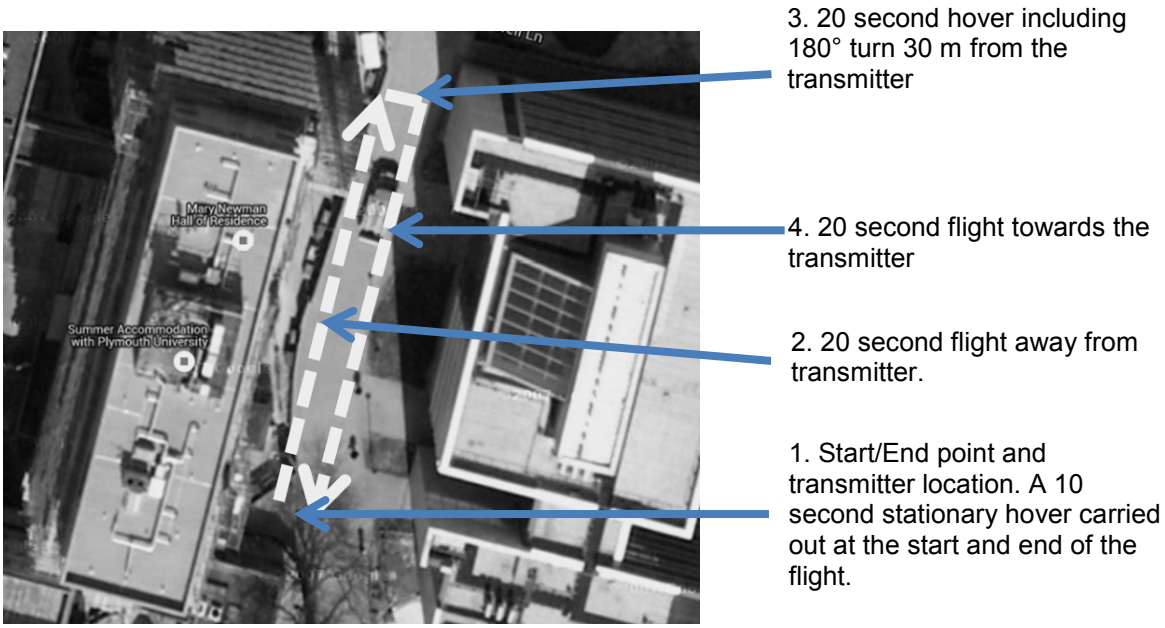

Figure 61 – Test Point D Trial Flight Map

The flight profile and environment was selected to test the system in a high multipath 'corridor' environment with sources of signal path interference on both sides of the trail area. This environment has been highlighted by literature review section 2.1.2 to be the most challenging for existing urban and indoor navigation geo-location systems. The selected flight profile, described in Appendix D - System Test Plan, environment exercises all of the suspected system error drivers with the proposed approach and have been chosen to stress the system. Analysis has been carried out on each of the data sources influence on the geolocation estimate throughout the trial. By design, the applied flight profile exercised the y, or ranging, axis throughout the test. To allow a comparison of performance of each of the data sources, the range accuracy from the control transmitter location will be analysed and discussed further.

All flight data was collected in separate files to allow post processing of the data and further analysis of the contribution of each data source. Post processing has been carried out on the data recorded by each of the trial sensors. Raw IMU and GPS data has been collected.

This section will analyse the performance of the designed filtering scheme in a practical test. Prior to this the thesis will discuss the raw adat collected, validating that the test environment has produced the errors anticipated in an urban environment. The raw data sources available to the designed filter throughout the trial have been plotted against the elapsed trial time in Figure 62.

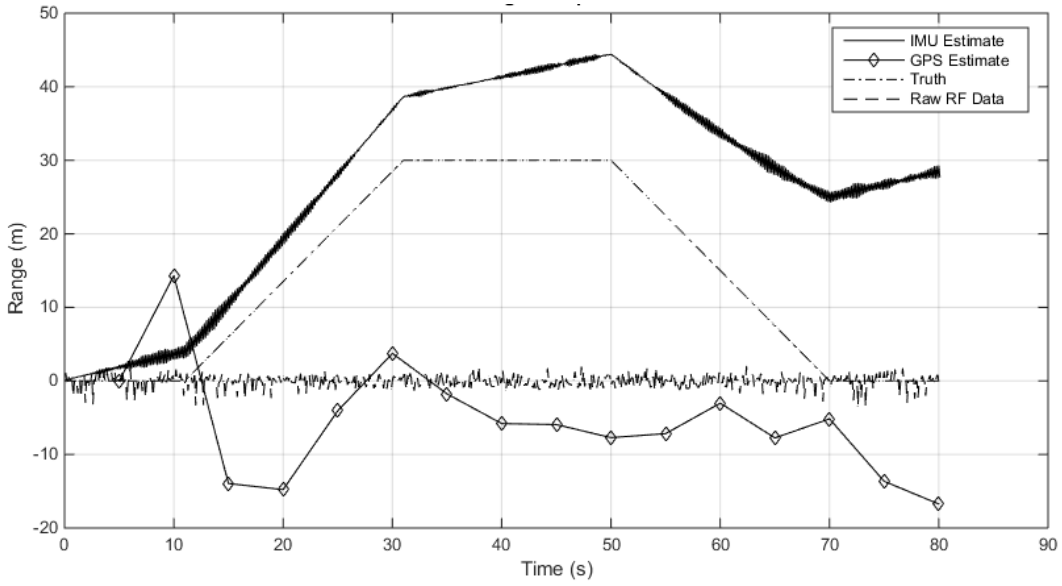

Figure 62 – Ranging estimate from the raw data sources.

The data summarised in Figure 62 shows the ranging data available from the inertial systems, GPS receiver and the raw radio data. Figure 62 also shows the true range of the mobile receiver from the transmitting system throughout the trial. A summary of the key measurement points are shown in Table 19.

Table 19 - Key Test Measurements

Time from the Start of the Test (s)	Accumulated Error (m)	
	GPS	Inertial Measurement
20	27	5
40	34	11
60	15	17
80	18	29

The data presented in Figure 62 and Table 19 shows the challenges faced by many systems navigating in an urban environment. The first challenge is the poor fidelity of the GPS location provided in a dense urban environment; it is hard to determine any component of the flight during the trial by analysing the GPS estimate data in Figure 62 alone. The poor performance of the GPS is typical when receiving signals in urban environments with low size, weight, and power receivers. The inertial data presented by the INS system shows that the stages of the flight can be determined; however the significant drift of up to 29 meters at the end of an 80 second flight presents the second challenge of error integration. The inertial drift will continue to accumulate for the entirety for the mission without the aid of an external data source. Whilst this project aims to use the RF signal present in the systems control datalink to provide an external source of navigation data, it is hard to see how this data source could provide information when the time domain RF amplitude data is plotted. Due to the limited flight range and the fact that the datalink contains an automated gain control loop, the amplitude of the raw RF data does not appear to provide any useful ranging information. The raw data obtained from the flight appears to show that accurate, low drift navigation for a drone system, using only the existing hardware will be a very challenging task. These challenges were discussed throughout the literature review. The raw data collected from the trail has validated this discussion. The raw data has also shown that the test environment has produced the anticipated errors that the filtering techniques in this thesis have been designed to mitigate. The filtering techniques proposed by this project shall now be applied in stages to show that the discussed error drivers are successfully mitigated and that the contribution of each mitigation technique can be used to build an accurate drift free navigation solution.

The first mitigation technique will be to setup the Kalman filter to analyse the raw RF carrier signal. As discussed in section 3.2 of this thesis, the phase of this low noise sinusoid is analysed and shifts in the maintained phase estimate have been be used to estimate a change in range from the transmitter to the recording receiver mounted on the drone. Analysing the data's phase shift with a sinusoidal Kalman filter provides the ranging estimate shown in Figure 63.

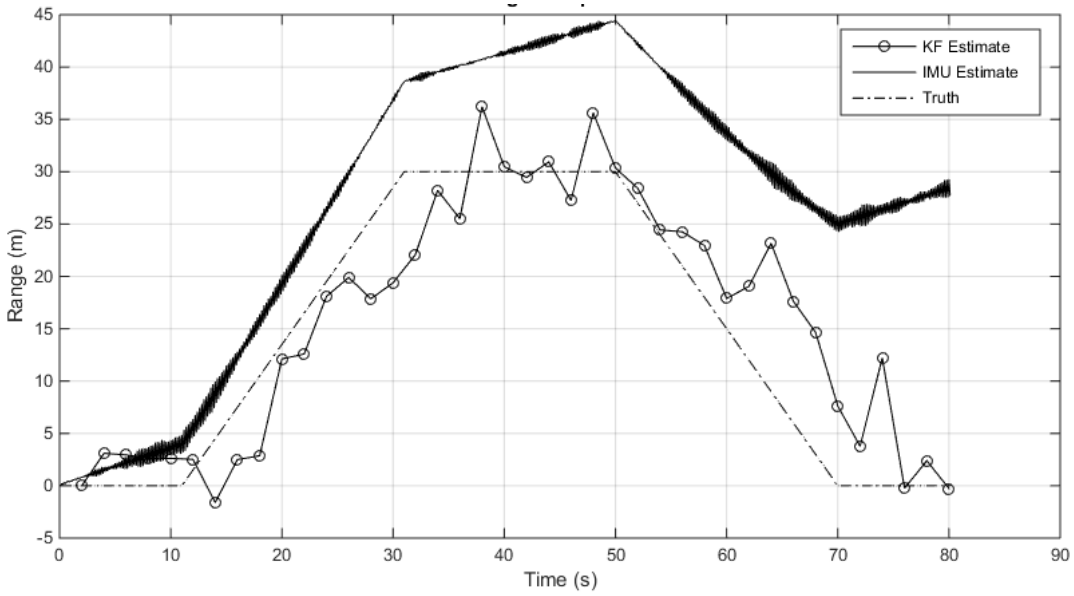

Figure 63 – Ranging estimate from the RF post sinusoidal Kalman filter processing.

Figure 63 again shows the truth and raw inertial data shown in Figure 62. In addition, the output of the sinusoidal Kalman filter following analysis of the raw RF data is also presented. A summary of the key results are detailed in Table 20.

Table 20 - Key Test Measurements after Initial RF Analysis

Time from the Start of the Test (s)	Initial Kalman Filter (KF) Range Estimate Error (m)
20	1
40	12
60	3
80	1

It can be seen that by comparing the estimates from the low noise sinusoidal Kalman filter a low drift range estimate can be seen throughout the 80 second flight. This low drift ranging estimate was able to track the range changes with low latency throughout the flight, resulting in a good localisation estimate throughout the flight. As predicted, errors in the recordings throughout the flight don't integrate together and the estimate accurately follows the true location at the stationary points in the data. The limitation of the processed RF data is that there that range estimation errors of up to 12 m are present for periods of several seconds. This are likely to have been caused by other lower level error drivers such as ground multipath effects in the RF data caused by the test being carried out at low altitude in a dense urban environment. The observed performance is significantly better than existing navigation systems, reducing ranging errors to less than 1 m at the end of the 80 second test. This improvement provides evidence that the using the sinusoidal Kalman filter at the core of the system provides a significant benefit when analysing sensor of opportunity data streams.

The next analysis proposed by this thesis is designed to remove these short term errors by closely coupling the RF data with that of a low noise, but high drift INS system as described in section 3.4. This technique has been carried out and is presented in Figure 64.

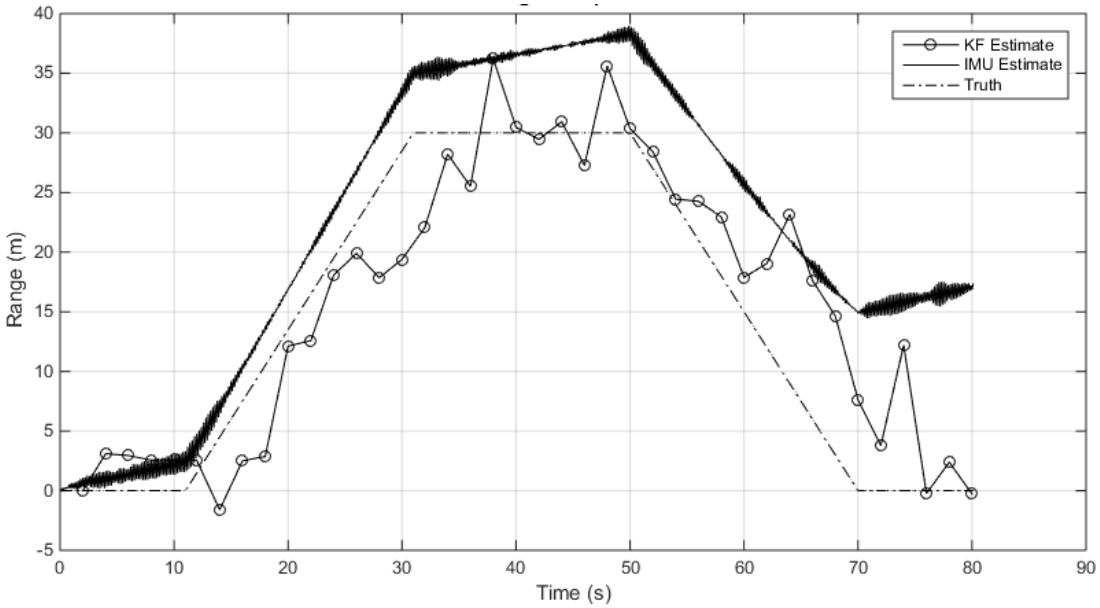

Figure 64 – Ranging estimate from the processed RF and ultra-closely coupled IMU data

Figure 64 displays both the output of the closely coupled Kalman filer estimate and the inertial measurement error obtained after the calibration improvements obtained from closely coupling the IMU to the Kalman filter have been estimated.

Table 21 - Key Test Measurements after Initial RF Analysis

Time from the Start of the Test (s)	Kalman Filter Performance			Inertial Sensor Performance		
	Initial Kalman Filter (KF) Range Estimate Error (m)	Closely Coupled Kalman Filter (KF) Range Estimate Error (m)	Kalman Filter Range Improvement (%)	Uncoupled IMU Range Estimate Error (m)	Coupled IMU Range Estimate Error (m)	Inertial Range Improvement (%)
20	1	1	0	5	2	60
40	12	1	92	11	6	45
60	3	3	0	17	10	41
80	1	1	0	29	17	41

Table 21 shows that ultra-closely coupling the Kalman filter and IMU system has improved the Kalman filter estimate. This improvement has occurred as the IMU error drift, also summarised in Table 21 has reduced throughout the test. The integrated inertial error at the end of the flight has reduced by 41 %. The magnitude of the IMU error reduces significantly during the stationary periods in the flight profile. During these stationary periods, the Kalman filter covariance experiences a period of convergence on the present system errors, allowing them to be estimated and accurately compensated.

In many systems the RF signal recorded by the mobile equipment is not controlled by the system operator. This limitation is commonly found in signal of opportunity systems where 3rd party RF networks are used as the data source. In these scenarios, no further navigation data is available from the techniques proposed in this project. The results presented in Figure 64 would show the performance of the system with commonly available inertial, and data link RF signals of opportunity. When this performance is compared with the GPS ranging estimate shown in Figure 62 and Table 19, a drastic performance improvement has been achieved with the ranging error reduced from 18 m to 1 m at the end of the test. Even if the GPS data were to be combined with the INS data also shown in Figure 62, no accurate ranging estimate during the flight would have been provided; The GPS signal obtained in an urban environment was of such poor quality that the INS estimate could not have been improved by coupling it with the GPS signal with existing techniques. Coupling the INS data to the output of the proposed system has reduced the maximum error observed throughout the test from 12 m to 3 m, a 75 % improvement in max error.

Further to this already considerable improvement in performance over existing INS coupling systems, the drone system under test is controlled by a frequency modulated transmitte. This transmitter is operated by the system designer and the data contained within the transmitted message, allowing the drone to manoeuvre as commanded, is also available to the system. This data may also be integrated into the Kalman filter, providing an additional signal of opportunity soured of information using the methods developed and described in section 3.3 of this thesis. This data is used to identify the stop, forward, backwards, turn left and turn right commands in the control data link. This is decoded by the on-board RF receiver. Another aspect that is available to the system designer in most applications is a basic kinematic model representation of the drone. The following information about the kinematic model is known and is captured in Table 22.

Table 22 - Kinematic Model Parameters

Typical Maximum Velocity	5 m/s
Typical turn rate	90 °/s.

The resulting ranging estimate from using the encoded command data and with knowledge of the basic kinematic data is presented in Figure 65.

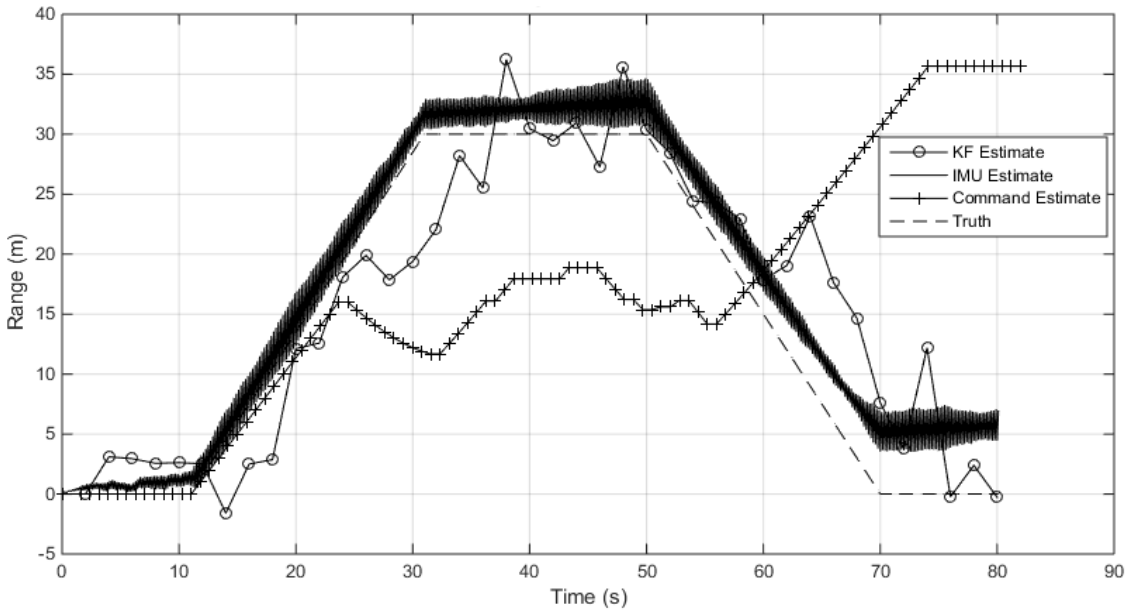

Figure 65 – Ranging including data obtained from the encoded data.

Figure 65 displays both the closely couples IMU dead reckoning estimate and the ranging estimate obtained from generating a dead reckoning estimate by integrating the commanded movements with the know system dynamics. The resulting Kalman filter estimate, generated by coupling these inputs is also shown.

Table 23 - Summary ranging estimate including encoded data

Time from the Start of the Test (s)	Kalman Filter Performance		
	Kalman Filter (KF) Range Estimate Error (m) excluding encoded data	Closely Coupled Kalman Filter (KF) Range Estimate Error (m) including encoded data	Kalman Filter Range Improvement (%)
20	1	0.5	50
40	1	0.5	50
60	3	3	0
80	1	0.5	50

The addition of the encoded data into the Kalman filter reveals further detail about the system behaviour. The first thing to note is the fact that the assumed kinematic model described in Table 27 appears to be incorrect. The system appears to have not correctly measured the 180° yaw command at the turning point half way through the trial. Despite this, the Kalman filters estimated range remains accurate. The benefit of adding the decoded command data is seen in the first 10 seconds of the trial where the covariance matrix is converging. The addition of the stop command information has allowed the Kalman filter to better remove the IMU biases. This has reduced the integrated IMU drift at the end of the trial from 1 m to 0.5 m. This will again further increase the systems resilience to multipath and other urban and indoor RF effects.

7.3 Validation and Benchmarking Conclusions

This chapter has described a range of practical validation and demonstration testing. Initial testing was carried out in a controlled environment that represented the simulated environment used in the analysis of the designed filtering techniques. The testing was carried out with hardware typical to both low cost mobile systems and with error characteristics simulated in previous performance analysis. This initial testing validated a range of key principles discussed in the design of the filtering system. The first key principle is that current GNSS and inertial navigation systems have considerable shortcomings in urban environments. The data provided by the test system validated the findings of the literature review, including that from industry interview, producing considerable errors in the test system. The performance of the proposed system was demonstrated in the controlled environment. Very good similarity in filter performance was seen when comparing the function of the filter in simulated and real test environments. Geolocation error differences between simulation and practical test results of less than 2 m were recorded thought the test.

This initial demonstration provided confidence that the filter would operate as discussed in a wide range of urban environments. To confirm this, a series of tests were carried out in a range of controlled test environments, introducing environmental complexity in stages. Again, good similarity was observed between the simulated results and those obtained from practical test.

Building on this, hardware tests were then carried out in a range of urban environments, providing the opportunity to record the system performance in a range of real-world environments. The results of this testing allowed a performance comparison between the designed filter and that of the current leading technique [BAE, 2013]. As expected, the designed filtering scheme outperformed the exiting technique with geolocation errors reduced in all tested environments by up to 67 %.

Further analysis of the filter performance in a range of configurations has been carried out by post-processing the data collected at one of the urban environment test points. The controlled addition of data streams into the Kalman filter allowed the performance improvement associated with each data set to be demonstrated. The resulting performance of the filter was again to be a significant improvement over exiting techniques, with ranging errors of less than 1 m observed in the urban environment when all available data streams were used by the filter architecture.

The following chapters of this thesis will review the achievements, limitations and further work opportunities provided by this research.

8. Summary and Further Work

This section reviews and summarises the research carried out in the previous sections of this thesis. The key purpose of this section is to review and ensure the main aims of the research have been achieved. The research has been carried out to satisfy the following key aims:

- Develop algorithms to efficiently couple data sources
- Identify sources of geo-location data.
- Develop filters to obtain a robust data source.

8.1 Achievements

The literature review highlighted several current capabilities that are capable of combing signal of opportunity data into generic filtering systems, such as a Kalman filter. Existing systems are however limited by their implementation where the geo-location estimate is abstracted away from the raw measurement data. This leads to a system that does not allow the close coupling of sensors without the significant processing required to convert the geo-location to an estimated radio signal. To alleviate this limitation of current systems, the thesis proposed in chapter 3.2 a filtering scheme that differs significantly from the current state of the art and provides the novel ability to closely couple signals of opportunity data streams with IMU data via a sinusoidal Kalman filter implementation. The use of an IMU in such a closely coupled scenario minimises the processor loading required by the current state of the art as the filter needs to only estimate and predict the comparatively simple IMU error sources, not the more complex radio signals commonly required. The proposed technique has been modelled and simulated to provide a viable demonstration of the systems proof of concept.

Due to the significant and novel conceptual difference in this area, it is considered that the first key aim has been satisfied. Further, the new application of a sinusoidal Kalman filter in the area of signal of opportunity geo-location has allowed further improvements to the acquisition of information from available sensor data in indoor and urban environments.

The use of ToA measurements is required to mitigate the ambiguity of signal strength measurements. ToA measurements are commonly used in closely coupled navigation systems, but are poorly suited to high multipath environments where multipath can cause prolonged and undetected error bursts. This problem was resolved by using the benefits of a closely coupled sinusoidal Kalman filter, allowing the raw RF measurement to be monitored and combined with other information to provide a ToA filter. This filter allows signals badly affected by the surrounding environment to be identified and discarded. The reception of a signal that passes the filter threshold removes location ambiguity and allows the higher level Kalman filter to further identify and remove IMU error sources. The development of this novel filtering technique has allowed the third key aim of this research to have been achieved.

This thesis has developed a technique that allows the application of a sinusoidal Kalman filter to a system containing several data inputs of opportunity. This addition of this filter allows the the system to respond efficiently to the signal strength environment around the radio receiver have also been developed. Using only the RSSI value in a simulated WiFi environment, commonly provided by COTS hardware, the system could significantly reduce the accumulated IMU errors and provide a significant improvement to the geo-location estimate, reducing errors down to between 1 m and 2 m . Research in this area led to the novel application of monitoring interfering signals to increase the resolution of the available topology. This technique further improved the accuracy of the resulting geo-location estimate while simultaneously providing additional robustness to the system in typically challenging transmitter dense indoor and urban environments. The combined use of ToA measurements and enhanced signal strength monitoring has been demonstrated to show that they can provide a suitable geo-location estimate in an indoor location. The identification and simulation of these data sources is considered to have satisfied the second key aim of this project.

Further to the initial aims set out for this project to achieve, a trade-off between filter accuracy and start-up time was identified during system simulation. The identification of this trade-off required further research to identify techniques that could allow the seamless transition from GNSS positioning to an indoor geo-location system.

The identification of a trade-off between system start-up time and system accuracy led to further work to assess the suitability of applying techniques in a novel manner to overcome the proposed problems. The research showed that there is a viable method to transition from GNSS systems as they degrade when the user transitions into dense urban or indoor environments. The ability to improve the robustness of carrier phase analysis in multipath environments to a suitable level has been simulated to provide a proof of concept. The research in this area is considered to have satisfied the identified aim and will allow the developed Kalman filter system to be trialled and utilised in real-world applications.

The research carried out as part of this thesis has developed a multi-input system that can utilise any available radio data sources to improve the dead reckoning estimate from an inertial measurement unit. While each of the key inputs of the system may have considerable error limits associated with them, the architectural design of the system is designed to prevent the accumulation of error in the final geo-location estimate.

While the architecture minimises the the effect of error source, there are two potential environments that would still drive errors into the resulting geo-location estimate. The first error driver is caused by the accumulation of error in the IMU outputs in certain environments. IMU error is a significant error driver in dead-reckoning solutions causing large errors to accumulate over time. The proposed architecture improves on existing techniques by using time separated external measurements to calculate and remove IMU integration errors, allowing the IMU to be re-calibrated and future errors minimised. This approach does however rely on the presence of external signals. In areas where there are no external signals and where the IMU calibration may alter rapidly, such as in significant thermal changes, the system is still likely to quickly integrate error. The only available option to mitigate this is to increase the accuracy of the IMU in changing environments, which may add cost and additional hardware into the mobile device. It is considered that, in most urban environments, signal availability will be sufficient for the system to function as required.

The second scenario that may drive errors into the system is in scenarios where multipath symmetry provides false leading edge detection. Multipath symmetry is particularly common in physical environments such as corridors and narrow city streets. The effect of this phenomenon on hardware is difficult to model as, even slight variations in the two propagation paths will create destructive interference and remove the possibility of a false leading edged detection with the filters described in this thesis. It is considered unlikely that this effect will occur with enough regularity to alter the performance of the Kalman filter. Partly due to the complexity of simulating this error driver, hardware testing in the environment described has been carried out and the results analysed.

The performance of the developed geolocation system has been demonstrated in section 7 of this thesis. While a limited comparison has been made between the researched system performance and the benchmark of [BAE 2013], this section of the thesis compares the achieved performance with the researched technique against that of all identified leading technology estimates in urban and indoor environments.

As described in section 2.2 of this thesis, mature systems exist that closely couple INS and GNSS data to enable an improved geo-location estimate. GNSS does not provide a suitable external coupling partner for INS systems in these systems. Research has also been carried out, summarised in section 2.1.7 of this thesis, into using signals of opportunity to provide a ranging estimate. These systems are adversely affected by multipath in urban environments or require prior knowledge of 3rd party data-links to provide a ranging estimate.

This investigation has resulted in novel techniques for using a single RF data source to maintain a ranging estimate by comparing the predicted output of a sinusoidal Kalman filter with a noisy recoded RF signal. This comparison allows a low latency ranging estimate to be produced that provides resilience to the adverse effects of multipath. Testing has shown that in a typical urban environment this ranging estimate can be coupled to the output of an INS to produce a high fidelity and robust ranging estimate. Further, an addition to the basic technique allows for closer coupling of the signals of opportunity system and the existing INS system can be made if the contents of the data-link message can be decoded by the target system.

Table 24 - Estimated geo-location accuracy comparison in a dense urban environment.

Technique	Typical Error (3σ) (m)	Notes
Proposed Technique (Test Results)	12	Error of 12 m (3σ) achieved with hardware test when no prior knowledge of a 3rd party system required.
WiFi SLAM[7]	10	Prior knowledge of 3rd party infrastructure required.
Phase Estimation[14]	30	Single multipath source discussed. A lower level of accuracy is anticipated in urban and indoor environments.
GNSS[1]	40	Not available indoors.
INS [3]	100	Accuracy related to operational time due to integration of error.
ToA Estimation[11]	300	Quoted performance may further degrade in the environments considered in this thesis.

This project has presented a significant improvement on the resilience and robustness of signals of opportunity systems and allows them to provide a reliable external source of information for ranging systems without the need for any additional system hardware. This will enable system designers to gain more information from their mobile robotic and IoT data, enabling the next generation of advanced urban information networks. Further analysis of the limitations, conclusions of the research carried out as part of this thesis are discussed in the following sections.

8.2 Limitations

This thesis has presented research that allows an improved geolocation estimate to be obtained in urban and indoor locations. While this research has demonstrated improved geolocation accuracy in a range of environments, some limitations remain in the research findings. The key limitations identified are the requirement of prior system knowledge to maximise the geolocation accuracy and the difficulty in specifying location estimate accuracies in a range of environments.

The first identified limitation is in the data required to achieve imporved geolocation estimate accuracy. A significant improvement in geolocation accuracy is possible if prior knowledge of the systems physical features and communication protocols are known. This information allows the user to obtain range estimate errors of less than 1 m. There are unfortunately very few practical applications that have this information available to them during use. Small, low cost mobile and IoT devises are by their nature easily moved and transported in a variety of ways. The characteristics of these movements are controlled by 3rd parties and are both unknown to and difficult to measure by the geolocation system. In recognition of this limitation, the final system performance described in Table 24 is limited to that achieved in a geolocation system that does not have access to the encoded data or prior motion knowledge.

The second limitation identified following this research is the difficulty system designers will have in estimating the systems accuracy in a wide range of environments. While the proposed system will provide an more accurate and robust geolocation estimate in a range of environments, the magnitude of the error is determined by the availability of identifiable features in the surrounding radio environment. This limitation in performance robustness may be unacceptable in a range of applications where maximum geolocation errors must be assured to provide safety or security protection. This limitation is fundamental in signal of opportunity systems and must be mitigated at the higher system integration level.

8.3 Conclusions

A literature review and industry interview revealed that the current state of the art does not allow for robust or accurate geolocation in indoor or urban locations. Prior works have demonstrated success in optimising the data extracted from GNSS systems in areas of poor reception by closely coupling GNSS and IMU data with Kalman filtering implementations. While this technique has increased the reach of GNSS systems in urban environments, it can never provide a geo-location estimate in dense urban and indoor environments. The approach of closely coupling IMU and radio inputs may however show equal promise when the GNSS signals are replaced with radio signals of opportunity. This approach could, if developed successfully, provide the robust and accurate geo-location estimate in indoor and urban environments that is required by current academic and industrial applications.

To provide further knowledge as to the opportunities and limitation of a closely coupled approach, the project set out with the following key aims:

- Describe an integration method that allows the coupling of typical system sensors to provide robust geo-location estimations.
- Allow indoor and urban geolocation in low size, weight and power mobile systems.

These key aims have been achieved by the conducted research.

The design architecture was founded on the principle of cross correlating differing information sources to gain a robust and reliable set of information. The principle allowed only small amount of strategic information to be required, fundamentally building in resilience to many of the effects found in indoor and urban environments. This approach allows many of the key concerns highlighted by the industry interview to be addressed, allowing a multi spectral interface with no single third party control.

This initial architecture offers the ability to build a geo-location estimate from small amounts of data. Extracting the data from a noisy radio environment with COTS hardware still presents a significant challenge. The radio hardware alone is unlikely to be able to filter and separate out useable geo-location data with such significant limitations. To maximise the ability of useful information to be gained, the radio reception equipment needs external assistance. Existing art in other fields of navigation have shown that closely coupling sensors improves the robustness of data extraction in an efficient manner. A novel Kalman filter, suited to radio navigation with the addition of a sinusoidal plant, has been researched for use in such scenarios. IMUs are commonly found in small mobile devices, leading to work to research the possibilities of efficiently coupling the sinusoidal Kalman filter to an IMU. The Kalman filter also allowed the efficient coupling of other available data sources, such as control link data and data from more traditional navigation sources, such as GNSS, if available.

Research showed that this implementation allowed navigation data to be obtained from the radio environments. The results were significantly improved in areas where large observable shifts in the radio environment were visible. Simulation also showed that while the system performed well in specific areas there were too few contours in typical urban and indoor areas. The research investigated potential ways of increasing the number of areas where the system performed well be generating specific channels of interference in the areas of interest. The generation of the interfering signals used only common hardware and no additional processing complexity. Simulation showed that this approach significantly increased the performance of the system in typical environments.

Further simulation demonstrated that the proposed system could provide a localised geo-location estimate, but could not locate a user within a wider field of reference. At this point, a system designer could integrate the system with prior signal mapping data or with a SLAM implementation to gain a wider geo-location context. Both of these approaches have drawbacks in real world implementations. Prior mapping data needs to be collected and maintained, a task that is not trivial in dynamic and changeable indoor and urban environments. SLAM generation requires a prolonged training period to generate a wider map and even when complete, may not provide an absolute geo-location estimate. The research looked for alternative methods to provide information of the users location with reference to a known landmark.

ToA estimation has been used to provide geo-location estimates in more open environments and makes up a significant amount of the prior art in radio localisation. Commonly adopted techniques are not however well suited to high multipath indoor and urban environments. Research has been carried out devise a filtering method that is capable of removing reflected or corrupted ToA estimates, allowing the system to identify and use reliable ToA estimates as they occur within the sampled environment. The performance of the proposed technique has been verified via simulation. As predicted these information snippets can be utilised within the high level system architecture to allow further identification of system errors while simultaneously allowing the user to gain a unique location estimate on a larger scale.

Further simulation of the system within a range of environments confirmed the effects of a trade-off within the Kalman filter between geo-location accuracy and start-up time. As the proposed Kalman filter was configured to allow an optimised geo-location estimate, poor start-up performance would be achieved. Common use case scenarios in indoor and urban environments will see the system start-up in a hand-over scenario from existing navigation solutions. Research was carried to see if signals of opportunity data can also be used to provide a seamless handover from GNSS systems to the proposed Kalman filter system. This research has identified that as well as operating in indoor and dense urban environments, signals of opportunity data can also be used in less dense urban environments to hand over from GNSS systems as their performance degrades and they can no longer provide an accurate estimate. The results of this research showed, via simulation, that the trade-off identified within the Kalman filter would not cause a loss of performance in operation.

The research carried out relied heavily of common simulation techniques to construct radio environments and evaluate the performance of the proposed techniques. These simulations have been benchmarked with hardware testing of a small mobile system in a dense urban environment. The benchmarking exercise showed that the proposed techniques performed will in a real world environment. The practical challenges of sampling low cost sensors in COTS hardware were achieved. The resulting geolocation estimates were significantly more accurate than GNSS could provide and, as predicted, were more accurate than existing geo-location estimates.

8.4 Further Opportunities

This thesis has carried out research into improve the accuracy and robustness of geolocation estimates in environments that cause in increase in estimation errors with existing techniques. The research has proposed a sinusoidal Kalman filter based system that incorporates mitigation techniques to handle key error drivers. Initial validation and benchmarking testing has been carried out to prove the anticipated geolocation benefits can be obtained. A number of promising areas of further research have been identified but are considered outside of the scope of this thesis.

8.4.1 Map Integration

An opportunity exists to allow the designed architecture to be closely coupled with a prior knowledge of mapping information. The filter architecture researched by this thesis has been designed to contain a common, expandable and adaptable data input interface. The proposed uses for the designed filter is in urban and indoor environments. Map information for these environments is often available and could provide an additional source of information in many environments. To optimise the application of this data, a particle filter approach may be taken to the resulting Kalman filter estimates, eliminating locations that the user cannot exist in and redistributing the remaining error likelihoods. Examples of this approach are typical for GPS and are explained in section 2.3.1.3 of the literature review. The efficient integration of this data into a coupled system will also provide an improvement in the ability of the filter to maintain a geolocation estimate in areas of low SNR GNSS signals providing improved start-up performance as well as lower long accumulation of errors in certain environments.

8.4.2 SLAM Map Development

Developing further from the integration of mapping information. An opportunity exists to utilise the information in the filter architecture developed as part of this thesis to generate maps using SLAM techniques discussed in section 2.3.4 of the literature review. The information that may be used to improve these techniques comes form the users ability to monitor the Kalman filters confidence values associated with each of the inputs. Further research into both the effects of physical features on the radio environment and the effects of this on the Kalman filter confidence in-puits for specific data sources will provide the user information about the physical environment surrounding the receiver. This information could then be used in existing SLAM techniques to generate maps. Further, these techniques are likely to allow forms of remote sensing, allowing SLAM maps of the surrounding area to be quickly and efficiently generated. Additional research could also explore the possibility of closely coupling the data, further in proving the range of radio environment techniques that can be monitored by the architecture researched by this thesis.

8.4.3 GNSS Anti-Jam and Anti-Spoofing

A final promising area for the application of this research as well as further investigation has been identified is using the additional physical layer information obtained from the designed system for increasing the robustness and security of GNSS signals. Specific threats against GNSS signals are spoofing and jamming [VOLPE 2001]. These threats are commonly mitigated by monitoring the signal to noise ratio as well as the angle of arrival of the incoming signals [BORIO et. al. 2014].

The filter architecture detailed in this thesis maintains an estimate of the expected GNSS physical layer phase and amplitude. Unanticipated and prolonged changes to these properties are able to be detected quickly and clearly, even in indoor and urban environments. Future work could research a quantified trigger based on the information provded by the filter to trigger when spoofing or jamming events take place. Building on the work carried out in this thesis to determine GNSS attacks could bring significant benefits to many GNSS applications.

9. Appendix A- Industry Interview Findings

Industry Interview Method

The industry interview event was broken into three sections. Each section followed the same format where I, as the event host, asked the panel an open ended question. The panel were then left, undisturbed by the host, to discuss what was meant by the question and discuss answers. The host recorded each answer on a 'Post-It®' note and attached it to the wall. The 3 questions were designed to be very open ended at the start and more specific at the end. The structure of the even was designed to allow the expert team share their views without being influenced any pre-conceived project ideas held by the host.

The following three questions were asked in the event:

- What do you value in navigation products?
- Why do customers need GNSS denied navigation?
- What scenarios require GNSS denied navigation?

Answers for all of the questions were colour coded so that they could be associated with each question and collected for further analysis. In all 63 answers were received from the panel.

Following the collection of the answers results were analysed to provide a simple weighted reference to help for the project scope. This analysis was carried in three stages. The first stage was to group the answers. The groups do not need to be in any specific order, the aim is to simply put together the answers that appear to be related. The second stage is to provide titles to these groups. Again the titles are not specified, but should describe the contents of the group in a few words, the resulting groupings were:

- Shortcomings of Current Technology
- Low Level Technical Requirements
- Business Requirements
- Environments the product could be used in
- Potential Applications
- System Level Requirements

The third stage of the analysis was to carry out a Facts, Assumptions, Issues and Requirements (FAIRs) review on the data to provide a concise list of priorities. The analysis involves listing the answers provided in each group and comparing their relevance to any key performance parameters that have been provided by the panel's answers. The resulting table can be seen in Table 25.

Industry Interview Results

Table 25 – Industry Interview Analysis

	Shortcomings of Current technology					Low Level Tech Requirements											System Level Requirements						Environments	Business Requirements	Potential Applications	Can be Integrated into UTAS System	Payload Sesitive Application
	Political Control	Signal Masking	Jamming	Spoofing	No infastructure control	Reliable	Secure	Accurate	Wide Coverage	Adaptable	Manufaturable	Robust	Available	Covert	Autonomous	Portable	Rapid	Modular	Collaboarative	Simple to use	Simple to Integarte	Redundency	Mulit spectral interface					
Covert					1									2					1				2			2		
Accurate	1	1	1	1	2	1	1	2		1			1				2		2			1	2			2		
Reliable	2	2	2	2	2	2	2	1	1	1	1	2	2	2	1			2	2	2	2	2	2	1		1	1	
Usable	1	2	2	2	1	2	1	1	1	2	1	2	2	1	2	2	2	1	2	2	1	1	1	2	1	1	2	2
Secure	2	2	2	2	2	1	2						1	2	1				2				1			1		
Autonouous						1			1	1				1	2	1			1	2	1		1			1		
Score	6	7	7	7	8	7	6	4	3	5	2	4	6	8	6	3	4	3	10	6	4	4	9	3	1	8	3	2
Priority	5	4	4	4	3	4	5	7	8	6	9	7	5	3	5	8	7	8	1	5	7	7	2	8	10	3	8	9

The importance to the success of the project of each of the provided answers can be seen in the Priority row. Any decision points in the project, such as devising a project scope, devising the required contents of the literature review or providing a course of action when confronted with multiple paths shall reference the Impact Matrix to ensure the project continues along it desired route

Industry Interview Analysis

The industry interview revealed that there are indeed shortcomings of current industry products, preventing the development of navigation technology in indoor and urban environments. Key unaddressed areas have been highlighted in Table 25. Each of the high priority areas are discussed further in the following sections.

Collaborative Navigation

The industry interview revealed a desire for advancement of 'collaborative' navigation. When collaborative navigation was discussed with the industry panel, the conversation was predominantly around current hardware limitations of single devices. There is recognition within industry that there is a $\sqrt{n}$ improvement in inertial navigation accuracy is n sensors can communicate and share their geo-location estimates. The collective improvement was of particular interest as all of the generated data can be generated by the system operator, with no 3rd party external operator.

Multi-Spectral Interface

The dependence on a single data source is perceived to lead to a lack of robustness in the navigational output. Anecdotal evidence was provided by the panel about the use of a visual odometer system that failed to provide any useful data in adverse weather conditions such as fog. The ability to combine sensors to provide a robust system was cited as a clear aspiration.

Covert

Several use cases were presented by the industrial panel that required the system to be passive and not transmit any detectable energy. Military reconnaissance applications for uraban and indoor navigation systems are anticipated to be based around reconnaissance and intelligence applications. These tasks must be carried out without 3rd party detection to maximise the effectiveness of the data collected.

No 3rd Party Infrastructure Control

Following questioning in the shortcomings of current GNSS systems, in addition to the limited reception in urban and indoor environments, the panel were keen to highlight the 3rd party control that is required by many nations. Few nations control their own GNSS systems, most have tp rely on the American GPS or Russian GLONASS systems. If a nation such as the UK wanted to use a national asset that relied on GPS in a military operation it would in effect need the permission of the United States to use this. This dependency was seen as one of the major reasons for developing reliable alternative navigation systems.

Page left intentionally blank

10. Appendix B – Simulation Environment

10.1 Appendix B1 – Overview and Key Code Description

This appendix provides further information about the simulation environment used throughout this thesis. Key functions of the simulation environment are described with code snippets provided. As described in section 3.6, the user first configures the physical environment before adding transmitter locations and defining their transition power and frequency.

The simulation environment is first configured to provide the physical environment properties. A two dimensional map is defined. Obstacle size, location is added to the map. The default setting used throughout this thesis are a map size of 100 m^2 and a mesh size of 1 m^2.

The user determines the attenuation coefficient, refractive index and reflective propagation constant for each of the materials within the simulation. Example values of all the required parameters can be seen in Appendix B2 – Example Simulation Parameter Settings.

The first stage of the simulation setup uses the following function code to add the transmitter location and receiver locations and properties.

```
%User set the object locations

Reciever_location = [90 -90]; %(X Y coordinates)


Transmitter_1_location = [0 20];

Transmitter_2_location = [70 40];

Transmitter_3_location = [-20 70];


Obs_1_location = [-0 -100];

Obs_2_location = [-80 -100];

Obs_3_location = [-80 20];


Obs_x_size = 10;

Obs_y_size = 5;
```

Once the mapped environment has been configured, the user can select the sensor data that will be made available to the Kalman filter. This data is typically selected to represent that available from commercial sensors to represent data likely to be available in a practical implementation. The simulation model builds the simulated environment Finally, the model runs the Kalman filter discussed in section 3.2 with the following function.

```
function [ArrayT, ArrayXH] = Run_Kalman_Filter(TsRf, RawRfData, IMUTime, IMURange, PlotsRequired)
%RUN_KALMAN_FILTER Summary of this function goes here
%
%   Draft 1A. Updated 29th Oct 15.

ORDER=2;
W=TsRf*7; %Source signal
TS=TsRf;
XH=0.;
XDH=0.;
SIGNOISE=0.01;
IDNP=eye(ORDER);

PHI=  [cos(W*TS) sin(W*TS)/W ;...
   -W*sin(W*TS)  cos(W*TS)];

P = [99999999      0;...
       0      999999999];

Q=zeros(ORDER)+0.0001;

RMAT=SIGNOISE^2;

HMAT=[1 0]; %How does the prediction model update with relation to the measured input.
```

```
HT=HMAT';

PHIT=PHI';

count=0;

[r, ~] = size(RawRfData);

SimTime = r*TsRf;

ImuStep = 1;

x = 1;


FMAT = [x sin(W*(x/3e8))];

ZMAT = [1 0];


ArrayT = zeros(1,((SimTime-2)/TsRf)+1);

ArrayX = zeros(1,((SimTime-2)/TsRf)+1);

ArrayXH = zeros(1,((SimTime-2)/TsRf)+1);


for T=1:TsRf:SimTime-1

   count=count+1;


   PHIP=PHI*P;

   PHIPPHIT=PHIP*PHIT;

   M=PHIPPHIT+Q;

   HM=HMAT*M;

   HMHT=HM*HT;

   HMHTR=HMHT+RMAT;

   HMHTRINV=inv(HMHTR);

   MHT=M*HT;

   K=MHT*HMHTRINV; %#ok

   KH=K*HMAT;

   IKH=IDNP-KH;
```

```
P=IKH*M;

x = RawRfData(count); %This is the input (z) matrix (A column vector of the input data sources.).
FMAT = [x sin(W*(x/3e8))];
XS = FMAT*ZMAT';

if rem(T/IMUTime(ImuStep),1) == 0; %If new IMU data is available...
   ImuStep = ImuStep+1;

   x = sin(W*(IMURange(ImuStep)/3e8)); %Provides the amplitude

   FMAT = [x sin(W*(x/3e8))];
   ZMAT = [0 1]; %Change Z Mat to use IMU data.

   XS = FMAT*ZMAT';

   ZMAT = [1 0]; %Change it back for the next RF input.

end

XHOLD=XH;
RES=XS(1)-XH*cos(W*TS)-sin(W*TS)*XDH/W;
XH=cos(W*TS)*XH+XDH*sin(W*TS)/W+K(1,1)*RES;
XDH=-W*sin(W*TS)*XHOLD+XDH*cos(W*TS)+K(2,1)*RES;

ArrayT(count)=T;
ArrayX(count)=XS(1);
ArrayXH(count)=XH(1);
```

end

To allow further analysis of the radio environment, an intuitive mapping function was developed. This intuitive mapping function allowed the user to visualise the main signal sub-paths on a coloured map. An example of the output can be seen in Figure 66 with the code shown below.

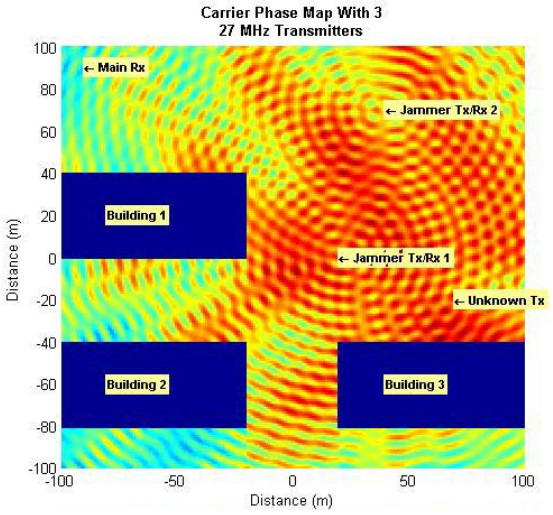

Figure 66 - Example of the Mapping Interface

```
%Make the Z map to colour

Z = T1W + T2W + T3W + R1W + R2W + R2WA + R3W + R3WA;

% Colour the obsticles as a solid colour (The lowest value of the matrix)

Z(Obs_1_location(1):Obs_1_location(1)+O1row,Obs_1_location(2):Obs_1_location(2)+O1col) = min(Z(:));

Z(Obs_2_location(1):Obs_2_location(1)+O2row,Obs_2_location(2):Obs_2_location(2)+O2col) = min(Z(:));

Z(Obs_3_location(1):Obs_3_location(1)+O2row,Obs_3_location(2):Obs_3_location(2)+O2col) = min(Z(:));

figure;

surface(X,Y,Z,'EdgeColor','none'); xlim([-100 100]); ylim([-100 100]); xlabel('Distance (m)'); strY(1) = {'Distance (m)'};  ylabel(strY);

text(Transmitter_1_location(2),Transmitter_1_location(1),'\leftarrow Tx 1','FontWeight','bold','FontSize',8,'BackgroundColor',[1 1 .6]);

text(Transmitter_2_location(2),Transmitter_2_location(1),'\leftarrow Tx 2','FontWeight','bold','FontSize',8,'BackgroundColor',[1 1 .6]);
```

```
    text(Transmitter_3_location(2),Transmitter_3_location(1),'\leftarrow Tx
3','FontWeight','bold','FontSize',8,'BackgroundColor',[1 1 .6]);

    strT(1) = {'Simulated RIPS RSS Map with 3'};

    strT(2) = {'27 MHz Transmitters'};

    text(Reciever_location(2),Reciever_location(1),'\leftarrow Main
Rx','FontWeight','bold','FontSize',8,'BackgroundColor',[1 1 .6]);

text(Obs_1_location(2)-180,Obs_1_location(1)-180,'Building
1','FontWeight','bold','FontSize',8,'BackgroundColor',[1 1 .6]);

text(Obs_2_location(2)-180,Obs_2_location(1)-180,'Building
2','FontWeight','bold','FontSize',8,'BackgroundColor',[1 1 .6]);

text(Obs_3_location(2)-180,Obs_3_location(1)-180,'Building
3','FontWeight','bold','FontSize',8,'BackgroundColor',[1 1 .6]);

title(strT,'FontWeight','bold'); colorbar('location','southoutside',  'XTickLabel',{''})
```

This annex has provided an overview of the key functions that make up the simulation model. Additional Kalman filter function have been added to the model as described in sections 4 and 5.

10.2 Appendix B2 – Example Simulation Parameter Settings

The simulation environment designed in section 3.6 of this document may be run with the values contained in Table 26.

Table 26 - Simulation Environment Default Parameters

Model	Simulation Block	Parameter	Value	Rationale for the Value Used
Transmitter Model	Carrier Wave Generator	Frequency	27 MHz	Unlicensed frequency that can be used for practical demonstration and test.
Transmitter Model	Carrier Wave Generator	Amplitude	1 V	Nominal baseline value set. A design of experiments approach was adopted to verify that the absolute number selected was not a significant factor in the results of the simulation.

Model	Simulation Block	Parameter	Value	Rationale for the Value Used
Transmitter Model	Data Signal	Duration	30 seconds	The minimum amount of data required to allow the final navigation result to settle at its final value in all attempted simulations. Note: At the frequencies simulated this duration produced very large data files.
Transmitter Model	Data Signal	Amplitude	0.1 V	Nominally set to 10 % of the carrier wave
Transmitter Model	Magnitude White Noise	3σ Amp	0.01 V	Nominally set to 10 % of the signal. This value was varied significantly during testing as it is a key parameter that affects the accuracy of the results.
Transmitter Model	Magnitude White Noise	-3 dB freq	20 kHz	Noise adjusted with a low pass filter to be within the region of interest on the data signal.
Transmitter Model	Phase Noise	3σ Delay	20 ns	Approx 0.5 x 1/27 MHz chosen to bound the maximum phase noise on the transmission.
Transmitter Model	Phase Noise	Offset	0.1 s	Design of experiments approach taken to prove that the absolute delay is not important. Time chosen to prevent negative delay with noise.
Transmitter Model	Quantization Error	Step Size	0.001 V	Quantization set to 1% of the data signal value.
Physical Interaction Model	Reflection Losses	Absorption Coeff	20	Empirically selected value that is thought to match painted steel surfaces.
Physical Interaction Model	Reflection Losses	Scatter Coeff	15	
Physical Interaction Model	Reflection Losses	Arrival Angle	NA	Angle set by the user in the creation of the environment.
Physical Interaction Model	Reflection Losses	Surface Angle	NA	Angle set by the user in the creation of the environment.
Physical Interaction Model	Refraction Loss	V1	1	Reference Value to reflect the speed of electromagnetic propagation in air.

Model	Simulation Block	Parameter	Value	Rationale for the Value Used
Physical Interaction Model	Refraction Loss	V2	0.9	This is an estimated figure that represents the relative speed of propagation in steel. This parameter was analysed with a design of experiments approach to estimate it's criticality on the final performance of the system. While small changes to this value did affect the final performance in some scenarios, these effects were mitigated where the receiving node was mobile. As the receiving node is mobile is all key examples throughout his thesis, the importance of this parameter is not considered to be critical.
Physical Interaction Model	Refraction Loss	Arrival Angle	NA	Angle set by the user in the creation of the environment.
Physical Interaction Model	Refraction Loss	Surface Angle	NA	Angle set by the user in the creation of the environment.
Physical Interaction Model	Diffraction Losses	Gap Width	NA	Angle set by the user in the creation of the environment.
Physical Interaction Model	Diffraction Losses	Arrival Angle	NA	Angle set by the user in the creation of the environment.
Physical Interaction Model	Direct Path Losses	Power Loss Coeff	28	Recommended in ITU guidance [ITU, 2017]
Physical Interaction Model	Direct Path Losses	Loss Factor	30	Recommended in ITU guidance [ITU, 2017]
Physical Interaction Model	Direct Path Losses	Distance	NA	Angle set by the user in the creation of the environment.
Receiver Model	Quantization Error	Step Size	0.0001 V	Value set to 1 % of the transmitted signal value.
Receiver Model	Phase Noise	3σ Delay	20 ns	Approx 0.5 x 1/27 MHz chosen to bound the maximum phase noise on the transmission.

Model	Simulation Block	Parameter	Value	Rationale for the Value Used
Receiver Model	Phase Noise	Offset	0.1 s	Design of experiments approach taken to prove that the absolute delay is not important. Time chosen to prevent negative delay with noise.

Page left intentionally blank

11. Appendix C – Test Environment Details

11.1 SDR Logger Data Settings

The software used for the testing was SDR#. Please note: When checked in September 2017, the software had been renames AIRSPY, and can be found at http://airspy.com/ [AIRSPY, 2016]. In addition to the settings described in Table 14, the settings used to log the data in the SDR# tool can be seen in Figure 67.

Figure 67 - SDR# (AirSpy) Data Collection Settings

11.2 Example of the collected SDR Data

A screen shot of the playback of the collected I & Q channel file can be seen in Figure 68. The figure shows the data recorded from the 27 MHz amplitude modulated transmitter prior to any processing for filtering with the techniques described in this thesis.

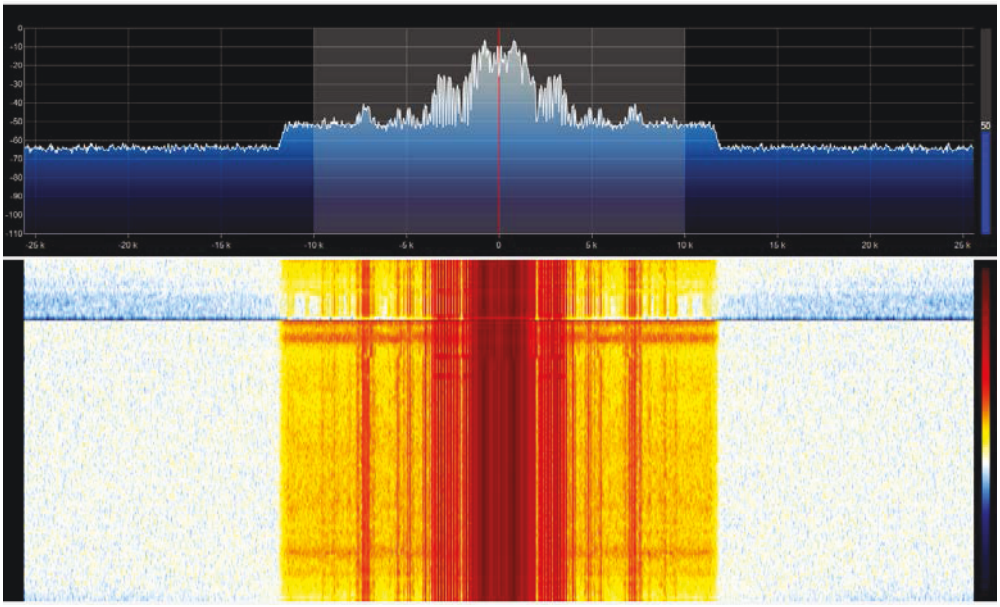

Figure 68 - Playback of the Logged Transmission File

An example of the collected data is also shown in Figure 70. An attempt has been made to correlate the received signal strength with the test case can be seen in Figure 70.

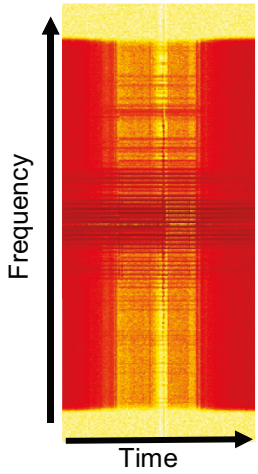

Figure 69 - Waterfall of collected data. Darker colours represent a stronger signal strength.

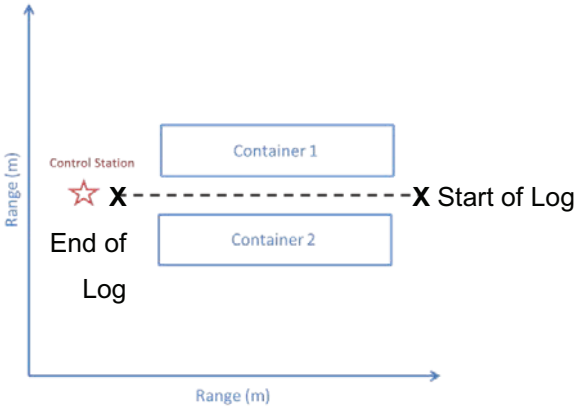

Figure 70 - Path of the receiver throughout the trial.

As the receiver moves towards the transmitter, located at the control station it may be assumes that the received signal strength would either increase, or in the case of a saturated receiver, remain constant. It can be seen however that there is a non-liner signal strength relationship between range and received signal strength. A linear relationship is seen when the experiment is repeated in the open environment with no obstructions.

The presence of a non-linear relationship has been caused by the presence of multi-path. This multipath comes form the interaction of the transmitted signals and the surrounding environment. It is not possible with simple signal strength analysis to determine the range form the transmitter to the receiver in this environment, forming a motivation for carrying out the research in this thesis.

11.3 Example of the collected GNSS Data

An example of the data collected by the GNSS logging tool can be seen in Figure 71. The data is collected in the standard KLM format.

ns1:name	ns1:when3	ns2:coord
Track	2015-10-09T08:22:32.000Z	
Track	2015-10-09T08:22:35.000Z	
Track	2015-10-09T08:22:37.000Z	
Track	2015-10-09T08:22:39.000Z	
Track	2015-10-09T08:22:44.000Z	
Track	2015-10-09T08:22:47.000Z	
Track	2015-10-09T08:22:49.000Z	
Track	2015-10-09T08:22:52.000Z	
Track	2015-10-09T08:22:59.000Z	
Track	2015-10-09T08:23:04.000Z	
Track	2015-10-09T08:23:09.000Z	
Track	2015-10-09T08:23:35.000Z	
Track	2015-10-09T08:23:50.000Z	
Track	2015-10-09T08:23:57.000Z	
Track		-4.1375 50.37636 51.9
Track		-4.13746 50.376507 50.6
Track		-4.1372566 50.37624 49.9
Track		-4.137155 50.37624 49.4
Track		-4.137125 50.37635 48.5
Track		-4.1371417 50.376427 48.2
Track		-4.1371264 50.376373 47.9
Track		-4.1371565 50.37633 48.1
Track		-4.137262 50.37632 47.8
Track		-4.137325 50.376297 47.7
Track		-4.1373916 50.376297 46.9
Track		-4.137252 50.37635 45.7
Track		-4.1371617 50.37631 45.5
Track		-4.137077 50.376343 45.4
Track	2015-10-09T08:29:13.000Z	

Sheet1

Figure 71 - KML Format Data Collected by the GNSS Logging Tool

As additional information, the motivation for this thesis was the poor performance of GNSS in urban environments. For information, an empirical observation of poor GNSS results in urban environments was collected on every test run. The example seen in Figure 66 was typical of the GNSS performance observed an all of the tests in a range of urban environments.

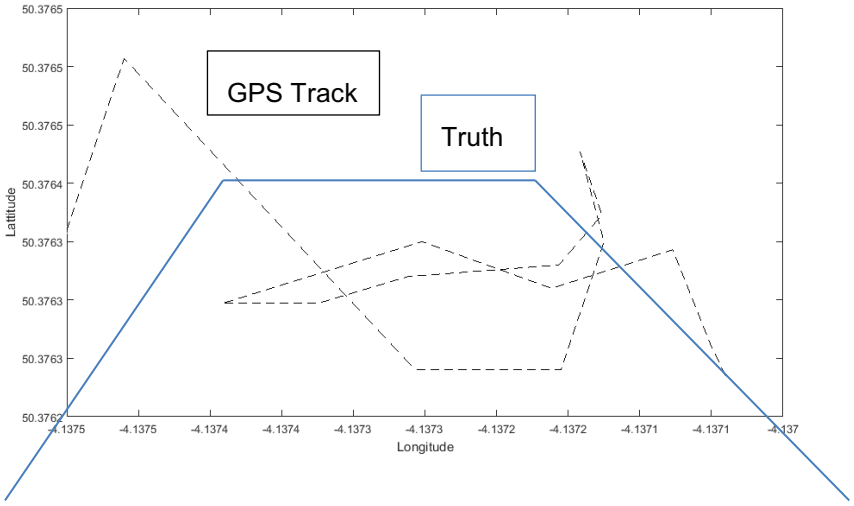

Figure 72 - GPS Obtained Track Data of the Test Environment

Page left intentionally blank

12. Appendix D - System Test Plan

Approach

The initial stage of system testing has provided encouraging results. However, the complex nature of the test environment and flightpath does not allow for individual error drivers to be identified.

This testing will first identify the key error drivers that are likely to be present in the 1st trial. A design of experiments approach will be undertaken to individually identify the key error drivers in as few flight trials as possible.

Highlighted Error Drivers

The potential error drivers in the first trial have been identified by analysis of the environment and are explained in section 3.5 of the thesis. As summary of the key error drivers that are to be stimulated and analysed by hardware test are summarised in Table 27.

Table 27 – Identified Error Drivers

Identified Error Drivers	Error Cause
ToA Errors	Non-normally distributed ToA errors.
Signal Strength Errors	Multipath propagation effects.
Unknown Start Conditions	Poorly weighted confidence values in unknown starting conditions.

To allow a series of test profiles to be determined, a list of controllable variables and observable parameters have been identified. The identified variables and measureable parameters are summarised in Table 28 and Table 29

Table 28 – Environmentsal Variables

Variables
Time from start-up
Range
Velocity
Angle
Multipath (Reflected)
Multipath (Corridor)
Obstacles

Table 29 – Observable Parameters

Parameters
Noise
Range
Velocity
Obstacles Present
Multipath Present
Obstacles
Weighting

The controllable variables are used to develop a series of hardware test scenarios. In each of these test scenarios, all controllable environmental variables will be applied using a controlled design of experiments approach, allowing the performance effects of each environmental variable to be isolated from the combined error measurements and analysed.

The identified variables stimulated in a controlled manner through a set of 5 tests. All tests will allow the monitoring of the parameters shown in Table 29.

Test profiles

The design of experiments approach has identified 5 test profiles are required to identify the effects of the identified variables. Throughout testing a constant altitude and velocity will be maintained unless otherwise stated, isolating the results from these additional variables as far as practicable.

Test 1

This test identifies the effects of range and velocity. The aim of this test is to determine a performance baseline of the system in low multipath areas. The applied flight profile is shown in Figure 73.

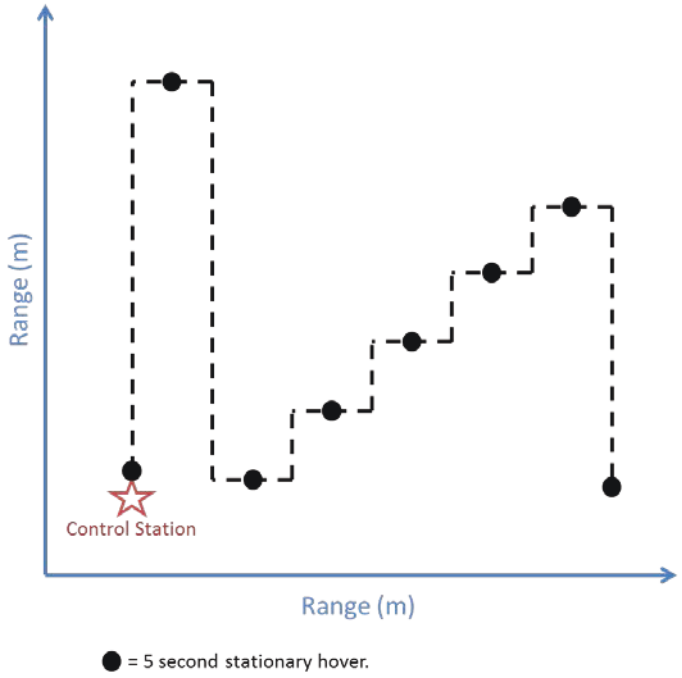

Figure 73 - Test 1 Flight Profile

Test 2

This test identifies the effects of angle. The aim of this test is to determine a performance baseline of the system in low multipath areas. The applied flight profile is shown in Figure 74.

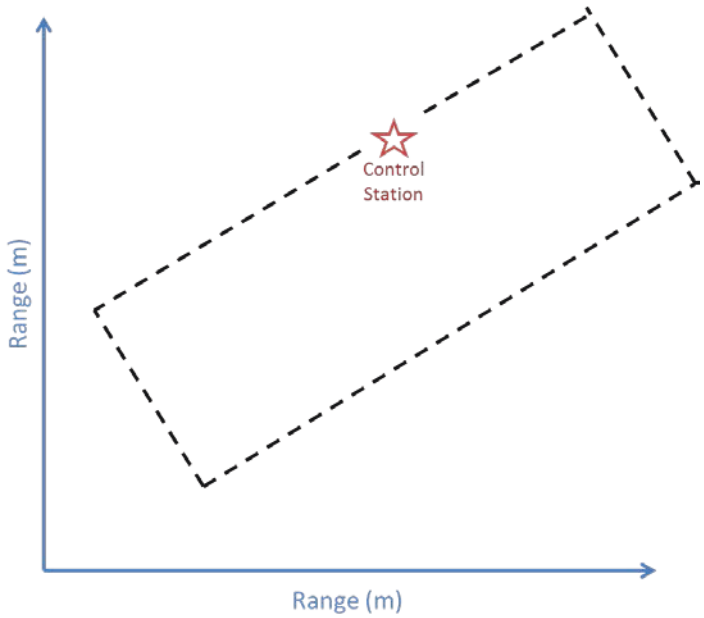

Figure 74 - Test 2 Flight Profile

Test 3

This test identifies the effects of reflected multipath, allowing an analysis of the performance of the designed architecture in areas of non-normally distributed ToA errors. Following the baselining tests described in Test 1 and Test 2, the contribution of multipath as the receiver range from a reflective surface may be determined. This test is required to validate the simulation's ability to recreate the expected effects of multipath error. The test profile to be applied is summarised in Figure 75

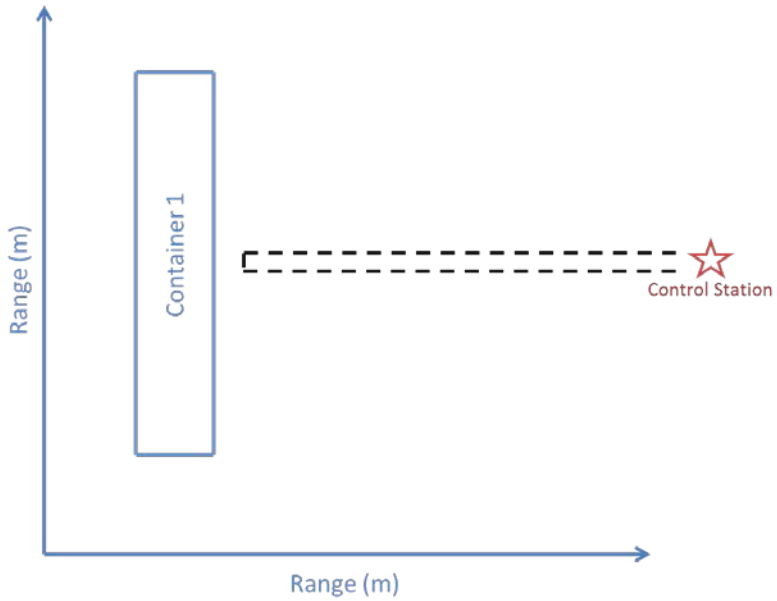

Figure 75 - Test 3 Flight Profile

Test 4

This test identifies the effects of obstacles, allowing an analysis of signal strength variations. The controlled source of signal strength variations will be the obstacle attenuation effects induced by the flight profile. Following analysis of the tests 1 to 3, the additional effects of varying signal strength can be identified and analysed. Additionally, a change in starting position can analysed. The test profile starts the filter in the same multipath environment recorded in part of the test 3 profile which, in conjunction with the baselining tests 1 and 2, allows the effects of multipath on the system start-up to be analysed. The test profile to be applied is shown in Figure 76.

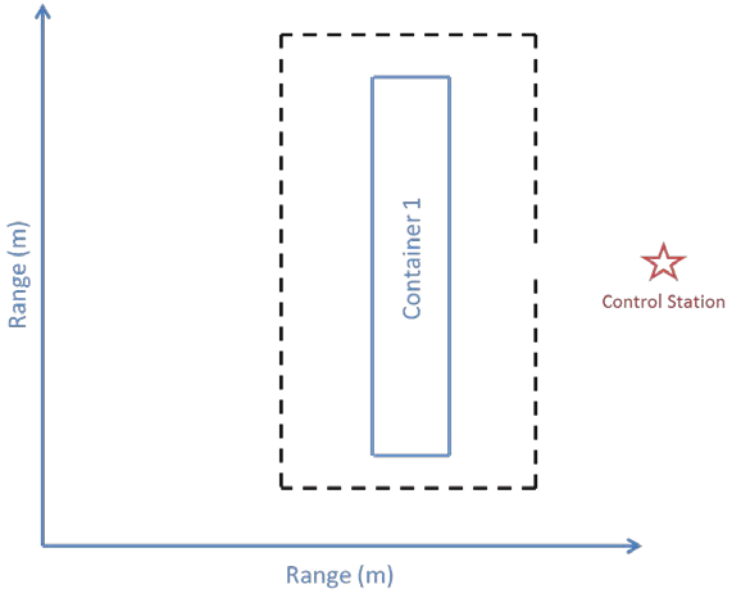

Figure 76 - Test 4 Flight Profile

Test 5

This test identifies the effects of corridor multipath. Following the test and analysis of the designed architecture's performance in environments that create the simulated error sources on an individual basis, a more complex scenario with interacting multipath effects will be applied. This aim of this final test is to verify that, by combining single multipath effects, the simulated environment can represent real world multipath environments. A summary of the test environments is shown in Figure 77.

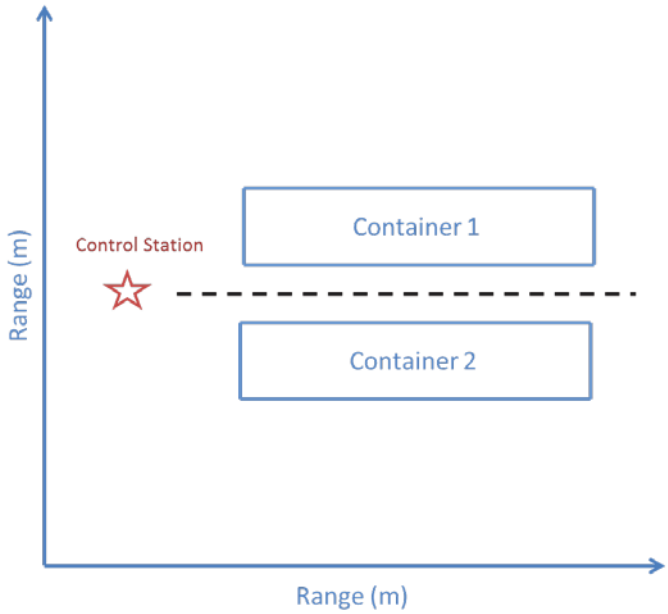

Figure 77 - Test 5 Flight Profile

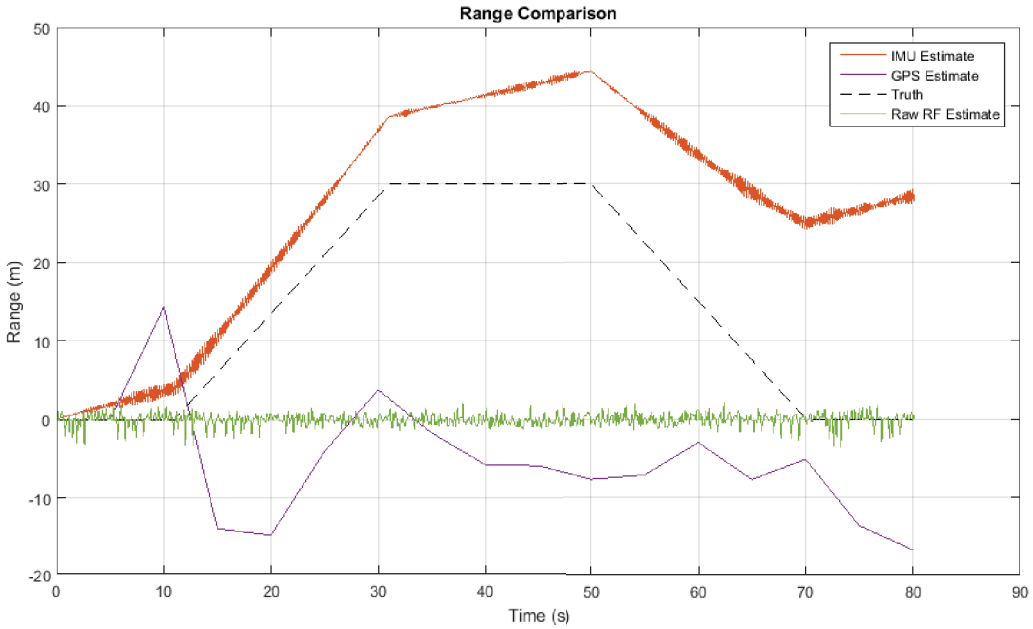

Validation Test

Section 7.2 of this thesis provides the results of validation testing at a range of urban environments. At each of the urban environments, a short flight trail was conducted with a common flight profile. The profile flown is summarised in Figure 78. The flight trial was carried out a fixed altitude of 1.8 m and with a constant ground speed. The flight path is carried out with a 10 second stationary period at the start and end of the profile along with a 20 second stationary period at the maximum range from the control station.

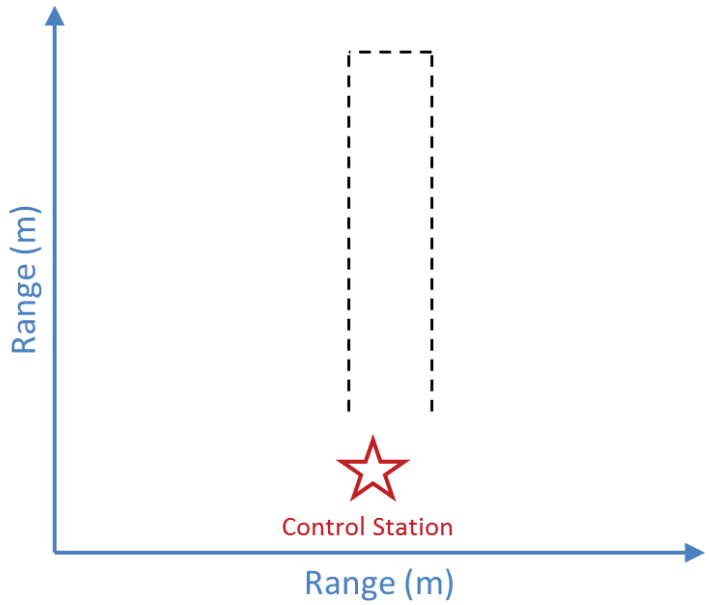

Figure 78 **– Validation Test Flight Profile**

13. References

[A. BROWN, 2003] Alison Brown, “Navigation Using LINK-16 GPS-INS Integration”, (2003). NAVSYS Corporation, ViaSat Inc. 2003.

[AIRSPY, 2016] Airspy, “Airspy Low Cost High Performance SDR”, 2016. http://airspy.com/. Accessed 29th September 2017.

[ALSINDI, 2004] N.A Alsindi, 2004. Performance of TOA Estimation Algorithms in Different Indoor Multipath Conditions. PhD Thesis, Worcester Polytechnic Institute.

[ANWAR et. al. 2013] S. Anwarm Z. Qingjiem N. Qadeer and S.I. Khan, “A Framework for RF- Visual SLAM” (2013). Published in Applied Sciences and Technology (IBCAST), 2013 10th International Bhurban Conference, Islamabad. 15th – 19th January, 2013.

[BAE 2013] BAE Systems, “Navigation via Signals of Opportunity (NAVSOP)”. 2013. http://www.baesystems.com/product/BAES_052848/navigation-via-signals-of-opportunity-navsop. Accessed August 2013.

[BIJ LIPINSKI 2013] Erik van der Bij and Maciej Lipinski. “Network fir European Accurate Time and Frequency Transfer”. November 2012.

[BONNOR 2012] Air Commodore Norman Bonnor. A Brief History of Global Navigation Satellite Systems.. January 2012, Royal Institute of Navigation Journal of Navigation Vol 65.

[BORIO et. al. 2014] D. Borio, C. O’Driscoll and J. Fortuny, “Fast and Flexible Tracking and Mitigatig a Jamming Signal with an Adaptive Notch Filter” (2014). Inside GNSS Journal, March and April 2014. Page 67 – 73.

[BSHARA et. al. 2009] M. Bshara, U. Orguner, L. Van Biesen, “Tracking in WiMAX Networks Using Cell-IDs”. (2009) 2009 IEEE Mobile WiMAX Sympsoium, (2009)

[C STINSON, 2003] Clinton W Stinson, “Internet Protocol over Link-16, Thesis”. (2003). Air Force Institute of Technology, Wright-Patterson Air Force Base, USA. 2003.

[CHEN KOBAYASHI 2002] Y. Chen and H. Kobayashi, “Signal Strength Based Indoor Geolocation” (2002). Department of Electrical Engineering, Princeton University. Published in Communications, 2002, ICC 2002. IEEE International Conference Vol 1.

[CHINA SAT NAV OFFICE 2011] China Satellite Navigation Office BeiDou Navigation Satellite System. Signal in Space Interface Control Document, December 2011.

[COAST GUARD 1994] US Department of Transportation – United States Coast Guard Specification of the Transmitted LORAN-C Signal’. May 18th 1994.

[COAST GUARD 2012] US Coast Guard Navigation Centre, ‘LORAN-C General Information. http://www.navcen.uscg.gov/?pageName=loranMain August 2012. Accessed April 2013.

[DANA 2013] Peter H. Dana, Global Positioning Overview, University of Colorado. http://www.colorado.edu/geography/gcraft/notes/gps/gps_f.html, 5th January 2000. Accessed 9th March 2013.

[DANIELS et. al 2005] T. Daniels, M. Mina, S. F. Russell, “Short Paper: A Signal Fingerprinting Paradigm for General Physical Layer and Sensor Network Security and Assurance” (2005). Department of Electrical and Computer Engineering, Iowa State University. Published in Security and Privacy for Emerging Areas in Communication Networks, 2005.

[DERENICK et. al. 2013] J. Derenick, A. Speranzon and R. Ghrist, “Homological Sensing for Mobile Robot Localisation” (2013). Intelligent Robotics Laboratory, UTC Research Centre, USA and the University of Pensylvania, USA. 2013.

[DIL HAVINGA 2011] B. J. Dil and P. J. M. Havinga, “Stochastic Radio Interferometric Positioning in the 2.4 GHz Range” (2011). Pervasive Systems Group, University of Twente, The Netherlands. Published in SenSys ’11, November 1-4 2011.

[DJURIC at. al. 2003] P. M. Djuric, J. H Kotecha, Z. Jianqui, H. Yufei, T. Ghirmai, M. F. Bugallo and J. Miguez, “Particle Filtering” (2005) Published in Signal Processing Magazine, IEEE (Volume 20 Issue 5) September 2005.

[EBCIN VETH 2007] S. Ebcin and M. Veth “Tightly-Coupled Image-Aided Inertial Navigation Using the Unscented Kalman Filter” (2007). Proceedings of the 20th International Technical Meeting of the Satellite Division of The Institute of Navigation (ION GNSS 2007)*, Fort Worth, TX, September 2007, pp. 1851-1860.*

[FARAGHER 2010] R. Faragher and L. Merry, “Comparison of opportunistic signals for localisation” (2010). Proceedings of the 7th IFAC Symposium on Intelligent Autonomous Vehicles, vol. online, pp. 1-6, 2010 Presented at 7th IFAC Symposium on Intelligent Autonomous Vehicles, Lecce, Italy, 06 Sep. - 08 Sep. 2010.

[FARAGHER et. al. 2010]. R. M. Faragher and P.J Duffett-Smith, ”Measurements of the effects of multipath interference on timing accuracy in a radio positioning system” (2010). IET Radar, Sonar and Navigation, vol. 4, iss. 6, pp. 818-824.

[FARAGHER 2012] R. Faragher, “Understanding the Basics of the Kalman Filter Via a Simple and Intuitive Derivation [Lecture Notes]”, 2012. Advanced Technology Centrem BAE Systems, UK. Published in the Signal Processing Magazine (IEEE) Volume 29, Iuuse 5. September 2005.

[FARAGHER 2013] R. Faragher, “The New Positioning Landscape” (2013). Computing Laboratory , Cambridge University, UK. Cooperative Positioning and M2M Communication for Navigation Conference, Bedfordshire, UK. 25th April 2013.

[FARAGHER et. al., 2014] R. M. Faragher, C. Samo, and M. Newman, “Oppourtunistic Radio SLAM for Indoor Navigation using Smartphone Sensors”, 2014. Sensor Systems, ATC, BAE Systems, UK.

[FAULKNER 2001] N. Faulkner, 1-10426-001-309 – GPS Integration with the LCN. UTC Aerospace Systems. Sept 2001.

[FISHER 2005] K. A. Fisher, “The Navigational Potential of Signals of Opportunity Based Time Difference of Arrival Measurements” (2005). Department of the Air Force, Air Force Institute of Technology, USA. 2005.

[FRIED 1978] W.R. Fried, Hughes Aircraft Company, Principles and Simulation of JTIDS Relative Navigation. January 1978.

[GAI, et. al. 2007] J. Gai, Y. T. Chan, F. Chan, HJ Du, F. A. Dilkes, “Frequency Estimation of Uncooperative Coherent Pulse Radars”. Military Communications Conference, 2007

[GALILEO 2010] European GNSS (Galileo) Open Service, Signal in Space Interface Control Document. Issue 1.1, September 2010.

[GMV 2013] GMV, GLONASS Future and Evolutions, http://www.navipedia.net/index.php/GLONASS_Future_and_Evolutions_2011. Accessed March 2013.

[GOODRICH 2013] Goodrich Corporation, In Focus – Goodrich TERPROM Terrain Reference Navigation to Equip Airbus A400M. http://www.goodrich.com/Goodrich/Enterprise/News/InFocus-Archive/Goodrich-TERPROM%C2%AE-Terrain-Referenced-Navigation-to-Equip-Airbus-A400M 2013. Accessed May 2013.

[GUSTAFSSON 2002] F. Gustafsson, F. Gunnarsson, N. Bergman, U. Forssell, J. Jansson, R. Karlsson and P. J. Nordlund. “Particle Filters for Positionong, Navigation and Tracking”. (2002). IEEE Transactions on Signal Processing, Vol 50 No 2, February 2002.

[HE et. al. 2013] j. He, K. Pahlavan, S. Li and Q. Wnag, “A Testbed for Evaluation of the Effects of Multipath oon Performance of ToA-based Indoor Geolocation”. (2013). University of Science and Technology, Beijing, China. Published in Instrumentation and Measurment, IEEE Transactions, Volume 62, Issue 8. April 2013.

[IEEE 1588] IEEE 1588 ‘Precision Time Protocol (PTP) Version 2 Specification2, March 2008.

[INLOCATION, 2016] InLocation Alliance, “The Opportunity for Indoor Positioning 2016”, 2016. http://inlocationalliance.org/about/the-opportunity-for-indoor-positioning/ Accessed 6th May 2016.

[IOANNIDES, 2016] R. T. Ionnides T. Pany and G. Gibbons, “Known Vulnerabilities of Global Navigation Satellite Systems, Status, and Potential Mitigation Techniques.” (2016). Proceedings of the IEEE (Volume 104, Issue 6). 29th March 2016.

[IRIDIUM 2013] Iridium Communications Inc. The Global Network: Satellite Constellation. http://www.iridium.com/DownloadAttachment.aspx?attachmentID=1197 July 2012. Accessed April 2013.

[ITU, 2017] ITU, “1238 : Propagation data and prediction methods for the planning of indoor radio communication systems and radio local area networks in the frequency range 300 MHz to 100 GHz”. Guidance Recommendations, 20th June 2017.

[J Quistorf, 2006] James Quistorf, “MIDS-LVT Link 16 Introduction” (2006). International Data Link Symposium, Via Sat. 19th Sept 2006.

[KALMAN 1960] R. E. Kalman, “A New Approach to Linear Filtering and Prediction Problems,” (1960). Journal of Basic Engineering, pp. 35-45 (March 1960).

[KONG et. al., 2006] Fantian Kong, Youping Chen, Jingming Xie, GangZhang and Zude Zhou, “Mobile Robot Localization Based on Extended Kalman Filter”, 2006. Proceedings of the 6th IEEE World Congress on Intelligent Control and Automation. Dalan, China. June 21-23, 2006.

[KOUHNE, 2014] Markus Kouhne, Jurgen Sieck, “Location-Based Services with iBeacon Technology” (2014). 2nd International IEEE Conference on Artificial Intelligence, Modelling and Simulation (AIMS), 18-20 Nov 2014, Madrid.

[KUSY et. al. 2007] B. Kusy, J. Sallai, G Balogh, A. Ledeczi, V Protopopescu, J. Tolliver, F. DeNap, M. Parang. “Radio Interferometric Tracking of Mobile Wireless Nodes”. Vanderbilt University, USA, Oak Ridge national Lab, USA and University of Tennessee, USA. 2007.

[K. LAASONEN, 2003] K. Laasonen, “Radio Propagation Modelling”, (2003). Published in Algorithms for Ad Hoc Networking - Seminar talk. 22nd September 2003.

[LATEGAHN et. al. 2011] H. Lategahn, A. Geiger and B. Kitt, “Visual SLAM for Autonomous Ground Vehicles”, (2011). Published in Robotics and Automation (ICRA), 2011 IEE International Conference, Shanghai 9th – 13th May 2011.

[LEE et. al. 2007] B. H. Lee, Y. T. Chan, F. Chan, HJ Du, F. A. Dilkes, “Doppler Frequency Geolocation of Uncooperative Radars”. Military Communications Conference, 2007.

[LIN CHANG 2008] S. Y. Lin and I. C. Chang, "3D Human Motion Tracvking Using Progressive Particle Filter” (2008). Taiwan University and National Dong Hwa University. Advances in Visual Computing, 4th International Symposium, ISVC 2008.

[LOCATA 2013] Locata, “Locata Tech Explained” (2013). Locata Corporation PTY Limited, Locata Commercial Website, http://locata.com/technology/locata-tech-explained/ . Accessed August 2013.

[LORAN 2007] International Loran Association, Enhanced Loran (eLORAN) Definition Document. Version 1.0, 16th October 2007.

[MARKS, 2013] P. Marks, “GPS Loss Kicked Off Fatal Drone Crash” (2012). The New Scientist. http://www.newscientist.com/blogs/onepercent/2012/05/gps-loss-kicked-off-fatal-dron.html. Accessed July 2013.

[MAROTI et. al., 2005] M. Maroti, B Kusy, G Balogh, P Volgyesi, A Nadas, K Molnar, S Dora, A Ledeczi, ‘Radio Interferometric Geolocation’, November 2005. SenSys ’05, November 2-4, 2005 San Diego, USA.

[MENDHAK 2017] Mendhak, “GPSLogger for Andriod; A better efficeinet GPS logging application” (2017). https://code.mendhak.com/gpslogger/ Mendhak, 2017. Accessed September 2017.

[MERRY et. al. 2010] Laura A. Merry, Ramsey M. Farager, Steve Scheding, “Comparison of Opportunistic Signals for Localisation” (2010). Australian Centre for Field Robotics, Sydney and BAE Systems, Filton. 7th IFAC Symposium on Intelligent Autonomous Vehicles, 6th September 2010.

[MILLS 2003] David L Mills, “A Brief History of NTP Time: Confessions of an Internet Timekeeper”, Computer Communications Review 33, http://www.eecis.udel.edu/~mills/database/papers/history.pdf 12th April 2003. Accessed July 2013.

[MILLS 2008] D. L. Mills, “NTP Precision Time Synchronisation”, Slide 6, (2008). University of Deleware. http://www.eecis.udel.edu/~mills/database/brief/precise/precise.pdf . Accessed October 2013.

[MILLS et. al, 2010] D. Mills, U. Delaware, J. Martin, J Burbank, W. Kasch, “Network Time Protocol Version 4: Protocol and Algoruthms Specification”, Internet Engineering Task Force (IETF) RFC 5905. June 2010.

[NATIONAL COORDINATION OFFICE 2013] National Coordination Office for Space-Based Positioning, Navigation and Timing, New Civil Signals. http://www.gps.gov/systems/gps/modernization/civilsignals/#L1C 6th February 2013. Accessed March 2013.

[NAVSTAR 1995] NAVSTAR, Global Positioning System Standard Positioning Service Signal Specification. 2nd Edition, June 2nd 1995.

[NOVATEL 2013] Novatel, GLONASS Overview, http://www.novatel.com/assets/Documents/Papers/GLONASSOverview.pdf.April 2007. Accessed March 2013.

[PARADIGM, 2014] “Skynet 5”, 2014. Paradigm Secure, https://www.paradigmsecure.com/our_services/skynet5. Accessed September 2014.

[POPESCU ROSE, UNKNOWN]. D. C. Popescu, C. Rose, “Emitter Localization in a Multipath Environment Using Extended Kalman Filter” (UNKNOWN). Department id Electrical and Computer Engineering, Rutgers University.

[PULLEN et. al.] Sam Pullen, Todd Walter and Per Enge, System Overview, Recent Developments and Future Outlook for WAAS and LAAS. Department of Aeronautics and Astronautics, Stanford University

[R TURYN, 1974]. R, Turyn, “Four-phase Barker Codes” (1974). IEEE Information Theory, Volume 20, Issue 3, pages 366-371. May 1974.

[R.L RIVEST, 1977]. R. L Rivest, A. Shamir and L. Adleman, “A Method for Obtaining Digital Signatures and Public-Key Cryptosystems” (1977). The Office of Naval Research and Massachusetts institute of technology, USA, 1977.

[RABINOWITZ et. al. 2013] M. Rabinowitz, B.W. Parkinson, J.J. Spilker, Some Capabilities of a Joint GPS-LEO Navigtaion System. September 20, 2000.

[Roxin et. al. 2007] A. Roxin, J. Gaber, M. Wack, A. Nait-Sidi-Moh, “Survey of Wireless Geolocation Techniques” 2007. UTBM, France. IEEE Globecom Workshop 2007.

[S. BASKER, et. al. 2007] S. Basker, et. al. “Enhanced Loran (eLoran) Definition Document”, 2007. International Loran Association, January 2007.

[SAND et. al. 2013] S. Sand, S. Zhang, M. Muhlegg, G. Falconi, C. Zhu, T. Kruger and S. Nowak, “Swarm Exploration and Navigation on Mars” (2013). Published in Localization and GNSS (ICL-GNSS) 2013 International Conference, Turin, 25th – 27th June 2013.

[SCARAMUZZA 2011] Davide Scaramuzza and Friedrich Fraundorfer, “Visual Odometry”, 2011. IEEE Robotics and Automation Magazine, Volume 18: Issue 4 Pages 80-92. December 2004.

[SCIENTIFIC INFO CENTRE 1998] Coordination Scientific Information Center, GLONASS Interface Control Document. 1998.

[SERRAMO 2012] J. Serrano, “Intorduction to WR [White Rabbit] and to the Workshop”. Seventh White Rabbit Workshop, Madrid, Spain. 27-28 November 2012.

[SIMON 2006] D. J. Simon, “Using Nonlinear Kalman Filtering to Estimate Signals” (2006). Cleveland State University. Published in Embedded Systems Design, July 2006.

[SIRTKAYA 2013] Salim Sirtkaya, Burak Seymen, A. Aydin Alatan, “Loosely coupled Kalman filtering for fusion of Visual Odometry and intertian navigation”, 2013. Proceeding of the 16th International Conference on Information Fusion (FUSION), 9-12 July 2013.

[SZILVASI et. al. 2012] S. Szilvasi, P. Volgyesi, J. Sallai, A. Ledeczi and M. Maroti “Interfoerometry in Wireless Sensor Networks” (2012). Institute for Software Integrated Systems, Vanderbilt University, USA and Bolyai Institute, University of Szeged, Hungary. Published in “Interferometry – Research and Applications in Science and Technology” March 2012.

[THOMAS et. al. 2002] N. J. Thomas, D. G. M. Cruickshank and D. I. Laurenson, “A Robust Estimator Architecture with Biased Kalman Filtering of ToA Data for Wireless Systems” (2000). University of Edinburgh. IEEE 6th International Symposium on Spread Spectrum Techniques and Applications, New Jersey. 6th - 8th September 2000.

[TEDALDI et. al. 2014] D. Tedaldi, A. Pretto and E. Menegatti, “A Robust and Easy ro Implement Method for IMU Calibration without External Equipment” (2014). Published in Robotics and Automation (ICRA), IEEE International Conference, June 2014.

[US DoD 2008] United States of America Department of Defense, Global Positioning System Standard Positioning Service Performance Standard. 4th Edition, September 2008.

[VEENEMAN 2013] Dan Veeneman, Iridium – Signals. http://www.decodesystems.com/iridium.html#signals 21st February 2013. Accessed April 2013.

[VOLPE, 2001] J Volpe, “Vulnerability Assessment of the Transportation Infrastructure Relying om the Global Positioning System”, 2001. Office or the Assistant Secretary for Transportation Policy, US Department of Transportation. August 2001.

[WENDLANDT et. al 2005] K. Wendlandt, M. Berhig and P. Robertson, “Indoor localization with probability density functions based on Bluetooth” (2005) .Published in the 16th IEEE International Symposium on Personal, Indoor and Mobile Radio Communications. 11-14 September 2005.

[WILLCOX et. al. 2006] S. Willcox, D. Golberg, J Vaganay and J. Curcio “Multi-Vehicle Cooperative Navigation and Autonomy with the Bluefin Cadre System” (2006) Bluefin Robotics Corporation, USA and Massachusetts Institute of Technology ,USA. International Federation of Automatic Control, 2006.

[WLOSTOWSKI, 2011] Tomasz Wlostowski, “Prescise Time Frequency and Frequency Transfer in a White Rabbit Network”. Warsaw University of Technology, 2011.

[L. PICKERING, 2003] L. Pickering, J. DeRosa, “Refractive Multipdath Model for Line-of-Sight Microwave Relay Links”, 2003. Published in the IEEE Transactions on Communications, 6th January 2003. Pages 1174 to 1182.

[L.J. GREENSTIEN, 1997] L. J. Greenstein, V. Erceg, Y.S. The and M. V. Clark, “A new path-gain/delay-spread propagation model for digital cellular channels”, 1997. Published in the IEEE Transaction on Vehicular Technology, Volume 46, Issue 2, May 1997. Pages 477-485.

Page left intentionally blank

14. Publications

The following publications have been generated during the course of this research project.

Table 30 – A List of the Author's Publications Generated by this Project.

Paper Title	Authors	Conference / Journal	Location	Date
Achieving Improved Network Subscriber Geo-Location	T. Mansfield, B. Ghita and M. Ambroze.	International Networking Conference (INC) 2014.	Plymouth, UK.	Jul 2014.
Improving Signal of Opportunity Localisation Estimates in Multipath Environments	T. Mansfield, B. Ghita and M. Ambroze.	International Conference on Telecommunications and Remote Sensing (ICTRS) 2015	Rhodes, Greece.	Sep 2015.
Integrating Interferometric Measurement Data Into SLAM Systems	T. Mansfield, B. Ghita and M. Ambroze.	IEEE European Navigation Conference (ENC) 2016	Helsinki, Finland.	Jun 2016.
Signals of Opportunity Geo-Location Methods for Urban and Indoor Environments.	T. Mansfield, B. Ghita and M. Ambroze.	Annals of Telecommunications Journal - Wireless and Mobile Sensing Technology for the Future Internet	Journal	Jan 2017.
Data Communication Systems for Navigation	T. Mansfield, B. Ghita and M. Ambroze.	IEEE Transactions on Wireless Communications	Journal	TBC

Achieving Improved Network Subscriber Geo-Location

T.O. Mansfield, B.V. Ghita and M.A. Ambroze.

School of Computing and Mathematics
Plymouth University
Plymouth, United Kingdom
{thomas.mansfield, bogdan.ghita, m.ambroze}@plymouth.ac.uk

Abstract

Future disaster and emergency management requirements are currently under discussion in the US and Europe that will require mobile phone network operators to locate their subscribers to a high level of accuracy within a short time period. Current deployed mobile phone geo-location systems are required to locate the caller to within 125 m. Future systems will require an order of magnitude better accuracy.

This paper proposes a method to achieve improved location accuracy with the addition of carrier phase analysis and accurate time of flight techniques to current systems. The resulting combination of technologies has been analysed using a simplified model to benchmark and compare the subscriber location estimate against existing solutions.

The system described in this paper shows the potential to meet the emerging disaster and emergency management requirements in complex radio frequency environments.

Keywords

Geo-location, SyncE, IEEE1588 PTP, RF navigation, carrier phase analysis.

1. Introduction

Current disaster and emergency management applications require mobile phone network providers to locate the physical position of their subscribers if they contact the emergency services; in the case of US, the enhanced emergency alert (E911) legislation requires the network providers to locate the caller to within 125 m 67 % of the time [3]. Next Generation 911 (NG911) is likely to require more accurate and more reliable position estimation of the user calling the emergency services, likely to be < 10 m up to 95% of the time [7]. This legislation will lead to a requirement for network operators to be able to quickly locate subscribers in many challenging environments.

One of the main challenging environments of operation is likely to be locating users in dense urban environments and urban canyons[1]. These areas typically have very dense subscriber populations and complex radio frequency (RF) environments.

Typical RF problems encountered in dense urban environments include high multipath effects, poor line of sight (Including poor GPS coverage), localised areas of low signal strength and considerable inter-channel interference.

This paper will investigate the viability of combining mature and developing technologies in order to provide a more accurate subscriber location estimate over a wider range of environments than can be obtained from any single technology.

The remainder of this paper is broken into the following sections. Section 2 reviews the current deployed capability for mobile phone geo-location. Section 3 provides a summary of the commonly applied approaches to coupling mature technologies to provide geo-location services. Section 4 provides an overview of a novel system that could be deployed in addition with current geo-location systems to provide an increased level of system accuracy. Method of overcoming the main challenges of this system are described in section 5. Section 6 details the simulation work carried out to verify the described approach. The results obtained from this simulation are provided in and section 7. Sections 8 and 9 provide information on future work and conclusions gained from the paper.

2. Current Deployed Capability

Current E911 compliant geo-location based systems are largely based on time difference of arrival (TDoA) systems. The most accurate and widely deployed system currently used is the AT&T uplink TDoA (U-TDoA) system. [1].

This system relies on sensitive time synchronised location measurement units (LMUs) located at each base station. The LMUs monitor each subscriber's uplink data channel when placing a call. The individual LMUs are time synchronised by GPS and communicate over the inter-base station network to calculate a subscribers position. This system commonly provides geo-location accuracy of around 50 m when the subscriber has a line of sight view of at least 3 network base stations. [True Position, 2011].

3. Current Research Areas

The current state of the art in mobile phone subscriber geo-location can be separated into three main areas: RF based, peripheral device based and hybrid of both systems. Many peripheral and hybrid systems require the use of ancillary sensors within the subscriber's handset. Due to a lack of standardisation in the peripheral devises

[1] Ground level urban areas with very limited direct visibility of the sky/satellites.

available on any mobile phone and the high coverage required to meet the emerging requirements, this review will cover RF based systems which use typical mobile phone RF devices only.

The network based approach relies on using the characteristics of both the mobile phone network and other RF systems, such as Wi-Fi, to provide a geo-location estimate.

Perhaps the most commonly applied technique to provide a geo-location estimate for subscribers within a mobile phone network is to use timing based techniques such as time of arrival (ToA) [11] or time difference of arrival (TDoA) [10]. All time based systems however suffer from several drawbacks. Firstly in areas with poor line of sight from the transmitter to the receiver, the signal cannot take a direct path. This causes significant error at the receiver. Additionally, the reflection of signal produces a multipath environment and associated reading, leading to further measurements errors.

Another approach to network based geo-location is to use an angle of arrival (AoA) approach. This approach commonly requires the calculation of the angle that a signal is received from [12]. If the angle of the subscriber is known from three or more base stations, the users location can be calculated by creating an intersect. Again this approach has several inherent problems, firstly a non-line of sight signal path will cause intersect errors. Secondly, the method of accurately locating the angle of arrival is not trivial and involves the use of sectored, rotation or electronically steerable antennas, all of which have considerable angular measurement errors.

Frequency and carrier phase analysis may also be used to estimate a subscriber's location [14]. Frequency based analysis typically relies on the motion of the subscribers to allow the Doppler shifts in their signals to be tracked. The drawback to this method is the fact that the location of slow moving or stationary subscribers will drift over time. Meanwhile, carrier phase analysis relies on the monitoring of the carrier signal phase of a source RF signal. The drawbacks of this technique are that the signals monitored need an accurate clock to provide reliable phase analysis and that the carrier signal can be affected lowering positional accuracy.

Another RF based approach that can be taken is to monitor certain network properties, from generic signal strength to data recognition, including such as cell IDs or signal fingerprinting [13]. This family of approaches has one main drawback: The subscriber system must have either a pre-determined database of network topology data or have acquired it via a lengthy simultaneous localisation and mapping (SLAM) procedure. Both of these approaches are difficult to implement in practical scenarios where either RF topology changes rapidly without the network operators knowledge or there is no time to build up a complex SLAM calibration scheme.

GPS receivers are currently integrated on many mobile phones. The task of relaying the GPS information over the network to the network operator is trivial. There are however limitations to using GPS in urban environments. To operate successfully,

the receiver needs a clear line of sight view of at least 4 GPS satellites. In most locations, this requires a wide field view of the sky, which is not available in many urban canyon environments. It is worth noting at this point that, although there are many urban areas where there are less than 4 satellites in direct line of sight, many densely populated areas are likely to still allow visibility of 1 or more satellites due to the good constellation spread of existing GPS satellite networks.

Success has been made in combining a single GPS receiver with ToA and carrier phase analysis to determine a geo-location estimation [9]. This approach combines mobile phone network ToA and carrier phase analysis to provide a position estimate in the absence of a full set of GPS satellites. Due to limitations in the measurement accuracy of the phone network component of this system, location estimates only provided an uncertainty of 345 m 95% of the time.

The concept of combining GPS and terrestrial RF systems can be improved selecting a terrestrial signal with better transmission properties than those found in mobile phone networks.

4. Improving U-TDoA Resolution with Short Wave Radio Phase Analysis

The proposed method relies on several layers of techniques with varying accuracy levels that complement each other in a typical urban environment, starting with U-TDoA for coarse acquisition and adding in other techniques to provide added robustness and accuracy.

The system assumes that a U-TDoA system is in operation and can achieve a positional accuracy of < 50 m in good conditions with a clear line of sight to the subscribers. It is also assumed that the area has a good level of coverage from a short wave digital Digital Radio Mondiale (DRM) signal. The DRM radio service is a shortwave radio service that uses a modulated carrier wave frequency of 5-6 MHz [8], providing a wavelength of approximately 50 m. Due to the commercial nature of the DRM service, transmitter location is optimised in urban environments to allow good population coverage.

It is possible in non-multipath environments, with GPS clock accuracy, to carry out phase analysis on the recovered transmission carrier wave with a phase noise of <10 % [4]. This provides a location accuracy of ≈ 5 m if a clear signal is received.

It has been mentioned that the carrier phase technique requires a GPS level clock accuracy of ≈ 100 ns [5]. This only requires visibility of 1 GPS satellite. This external time source may also be provided in indoor environments by a GPS time repeater system.

It can be seen that DRM carrier phase analysis, supported by the GPS clock pulse, can be overlaid onto the existing U-TDoA system and can improve the locational accuracy by an order of magnitude.

The problem still remains that the system would provide poor results in an area of high multipath propagation of the DRM signal.

5. Combatting Multipath

To combat the effects of multipath in the signal, an extra layer of geo-location techniques is required in the system. A typical multipath environment is considered in Figure 2.

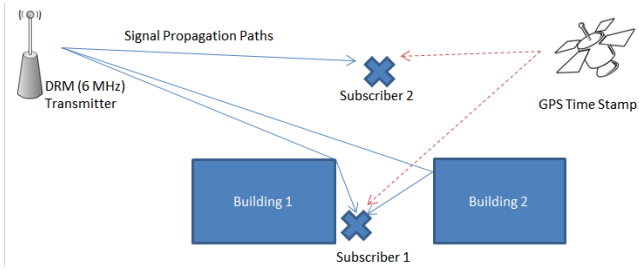

Figure 1: Typical Urban Environment with Multiple Signal Paths

It can be seen in Figure 1 that subscriber 1 does not have a direct line of sight with the DRM transmitter and is receiving both a reflection and a refraction of the transited signal. Receiving both signals, with a slight time delay increases carrier phase noise and makes the position estimation within the DRM signal less accurate.

If the phase analysis is carried out sufficiently frequently (at least 8 samples per sine wave), the subscriber system can calculate the quality of the carrier phase analysis. In the scenario shown in Figure 2, subscriber 2 has a good line of sight with the DRM transmitter, so consequently could easily determine that it has a good Gaussian distributed positional accuracy. Conversely subscriber 1 knows that it has a poorly distributed carrier phase signal and is likely to have a poor positional accuracy distribution.

In this case, subscriber 1 can gain a relative position from subscriber 2. This is possible by using the IEEE 1588 precession time protocol (PTP) in conjunction with ITU Synchronous Ethernet (SyncE) standard. The combination of the PTP time plane and SyncE frequency plane to estimate ToA can provide timing accuracies of ≈ 4.5 ns. [M. Ouellette et. al. 2011] proving a relative positional accuracy of < 2 m between the two users. From this relative navigation solution, it is possible for subscriber 2 to maintain a geo-location with an estimation error of < 10 m, even in an area of high multipath and poor line of sight with any external reference.

6. Simulation Details

The aim of the simulation is to calculate the positional estimation accuracy of subscribers in a system where carrier phase analysis and ToA geo-location are used

simultaneously to determine a user's geo-location in areas of both low and high multipath.

The following major limitations and assumptions have been applied to the simulation model; the subscribers are not moving; During reflections and refractions there is no frequency shift to the affected signal; The received signal strength is suitably high and free from interference, including atmospheric effects, throughout the simulation; Subscriber 1 and 2 are free to share their positional estimate in real time with each other. While these limitations may have minimal impact in certain environments, these limitations are likely to affect the simulation accuracy when compared with most real world environments. The accuracy results derived from the model should be considered a 'best case' example.

The case environment to be simulated is that shown in Figure 2. The simulation will assign typical signal generation errors [8] and free space delays to estimate the positional accuracy and confidence level in a multipath environment. The simulation will be broken into two stages. Stage 1, as shown in Figure 3, will simulate the system relying on DRM phase analysis alone. The second stage of the simulation, as shown in Figure 4, will add the layer of system that relies on relative geo-location between subscriber 1 and 2. This will allow the final positional estimate of subscriber 2 to be calculated after combing the uncertainty of subscriber 1 and the uncertainty of the relative position of subscriber 2 from subscriber 1.

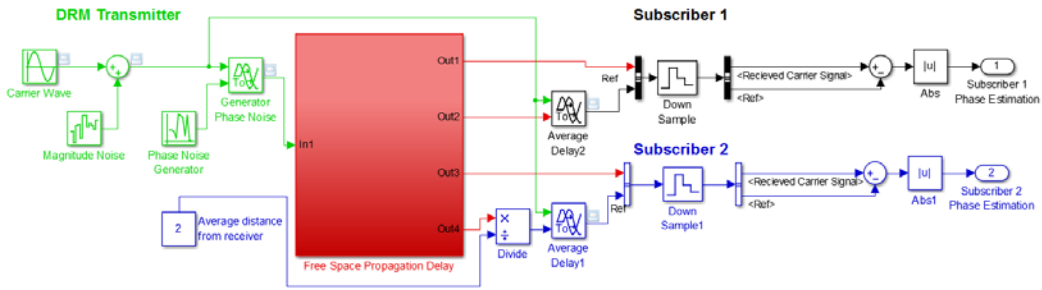

Figure 2 –Simulink Simulation of DRM Phase Analysis System

Figure 4 simulates the maximum likely geo-location accuracy of the DRM based system in an area of good RF line of sight to subscriber 1 and while in an area of high multipath, as seen by subscriber 2. The DRM transmitter, comprising of a carrier wave with amplitude and phase noise added is shown in green. The red blocks calculate typical errors of free space transmission in direct path, reflection and refraction environments. The black and blue blocks simulate the receiving and time stamping errors of subscriber 1 and 2 respectively.

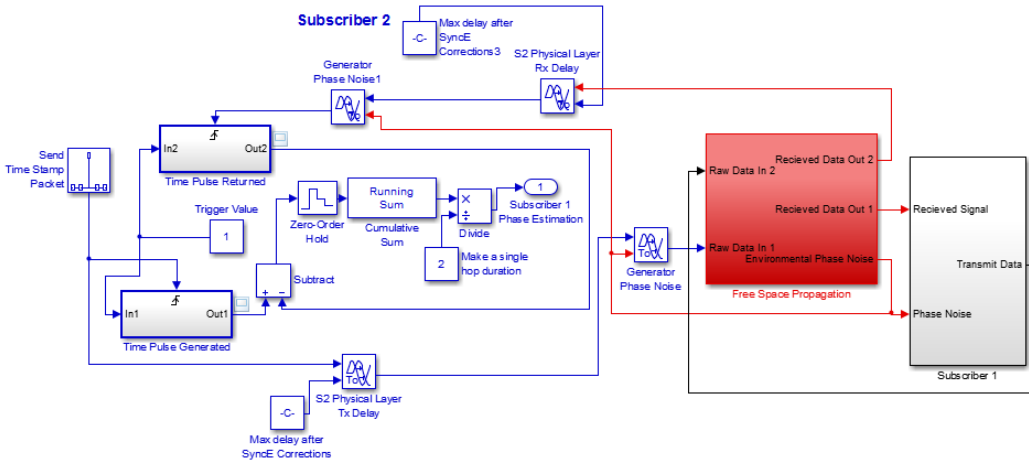

Figure 3 –Simulink Simulation of SyncE and PTP Link

Figure 4 shown the simulation model used to estimate the ToA jitter during relative geolocation via a combination of SyncE and PTP. The red blocks simulate typical errors expected from the free space transmission after the corrections applied by SyncE have been applied. The black blocks attribute the reception, processing and transmission errors expected from the subscriber 1 hardware. Subscriber 2, represented by the blue blocks, simulates the appropriate hardware transmission and reception errors of the system. In addition to this, subscriber 2 also monitors the jitter and delay in the system by comparing the difference in the network layer transmission and reception of a pre-determined packet header.

7. Simulation Results

7.1. DRM Phase Analysis

The simulation shown in Figure 3 was run by Simulink®. The resulting carrier phase analysis noise can be seen in Figure 5.

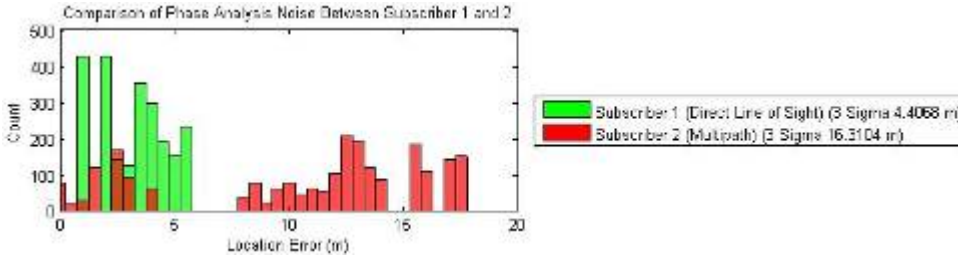

Figure 4 - Comparison of Subscriber 1 and Subscriber 2 with DRM Carrier Phase Geo-Location Only

It can be seen in Figure 5 that subscriber 2, the subscriber that is coping with multipath signals, has a significantly wider spread of signal noise. Analysis of the data revealed that the 3σ estimate of position was 4.41 m for subscriber 1 and 16.31 m for subscriber 2.

7.2. PTP and SyncE

The simulation shown in Figure 4 was run. The resulting ToA jitter, causing positional uncertainty in the relative position of subscriber 2 from subscriber 1, can be seen in Figure 6.

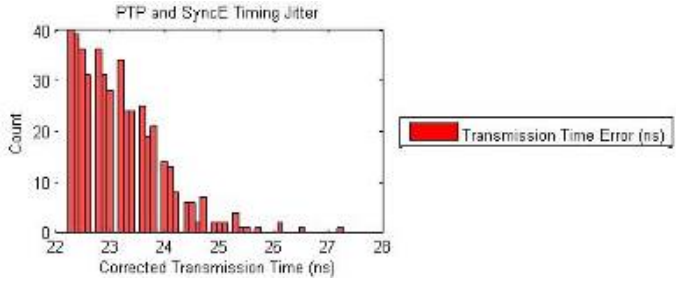

Figure 5 - PTP and SyncE Message Timing Jitter

The PTP and SyncE message jitter has been plotted in Figure 6. The 3σ error of the system between subscriber 1 and 2 is 25.489 ns. This equates to a 3σ relative location error of 7.45 m.

As the absolute positional accuracy of subscriber 2 is a combination of the uncertainty of subscriber 1 and the relative position of subscriber 2, the resulting probability density functions (PDFs) have been multiplied together to produce the distribution shown in Figure 7.

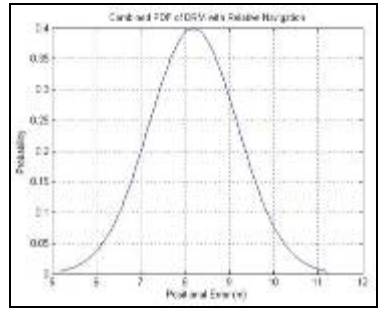

Figure 6 - Subscriber 2 Absolute Positional Accuracy

This provides subscriber 2 with a 3σ geo-location accuracy of 10.52 m.

7.3. Summary

Table 1 - Simulation Results Summary

Subscriber 1 DRM Geolocation Estimate (3σ) (m)	4.4
Subscriber 2 DRM Geolocation Estimate (3σ) (m)	16.3
Subscriber 2 Combined relative and DRM Geolocation Estimate (3σ) (m)	10.5

It can be seen in Table 1 that the DRM phase analysis, in the absence of multipath, can provide an order of magnitude improvement over the existing U-TDoA systems used in current E911 systems and could provide the coverage required by NG911 legislation in the simulated environment. In the multipath environment at subscriber 2, the system alone does improve on the existing U-TDoA systems, but is unlikely to provide accurate enough readings for future NG911systems alone.

With the addition of the PTP and SyncE relative geo-location technology, the positional accuracy of subscriber 2 after combining all system uncertainties provides an absolute uncertainty that is significantly better than that found in existing subscriber geo-location systems and may well provide the coverage required by NG911 legislation

8. Future Work

There is potential for the simulation model to be improved by working to remove some of the significant limitations described in section 6.

9. Conclusion

It has been demonstrated that combining several layers of complimentary geo-location techniques that are either in existence on mature products or emerging from research NG911 geo-location accuracy in dense urban environments could be achieved.

Although each of the technologies used in isolation have significant drawbacks in their ability to provide a geo-location estimate, combining several layers of techniques may allow users to estimate their location in a range of complex environments.

10. References

[1] AT&T, “Legacy Location Based Services FAQ”, 2014. https://developer.att.com/developer/forward.jsp?passedItemId=3100156. Updated 13th December 2013. Accessed December 2013.

[2] True Position Inc, “True Position Guide to Location Technologies”, November 2013. http://www.trueposition.com/resource-center/white-papers/trueposition-guide-to-location-technologies/DownloadSecured Accessed December 2013.

[3] Jeffrey H. Reed, Kevin J. Krizman, Brian D. Woerner, and Theodore S. Rappaport, “An Overview of the Challenges and Progress in Meeting the E-911 Requirement for Location Service”. Virginia Tech, 1998. Published in the IEEE Communications Magazine, April 1998.

[4] Rodrigo Carvajal, Juan C. Aguero, Boris I. Godoy, and Graham C. Goodwin, “On the Accuracy of Phase Noise Bandwidth Estimation in OFDM Systems”. 2011. The University of Newcastle, Australia. Published in the 2011 IEEE 12th International Workshop on Signal Processing Advances in Wireless Communications, 2011.

[5] Peter H Dana, “The Role of GPS in Precise Time and Frequency Dissemination”, 1990. Published in GPSWorld, July August 1990.

[6] Michel Ouellette, Kuiwen Ji, Han Li and Song Liu, “Using IEEE 1588 and Boundary Clock Synchronisation in Telecom Networks”, 2011. Huawei Technologies Inc and China Mobile Research Institute. Published in the IEEE Communications Magazine, Feb 2011.

[7] The US Department of Transportation Research and Innovative Technology Adminsitration, “Research Success Stories Next Generation 9-1-1”. Updated Dec 4th 2013. http://www.its.dot.gov/ng911/index.htm. Updated Dec 4th 2013. Accessed Jan 2014.

[8] 8, “Digital Radio Mondiale (DRM); System Specification” V3.1.1 (2009-08) 2009. European Telecommunications Standards Institute and European Broadcasting Union.

[9]. S. Soliman, P. Agashe, I. Fernandez, A. Vayanos, P. Gaal and M. Oljaca, “gpsOne[tm]: A Hybrid position location system”, 2000. Qualcomm, USA. Spread Spectrum Techniques and Applications, 2000 IEEE Sixth International Symposium on Spread Spectrum Techniques and Applications, Sep 2000.

[10] Locata, “Locata Tech Explained” (2013). Locata Corporation PTY Limited, Locata Commercial Website, http://locata.com/technology/locata-tech-explained/ . Accessed August 2013.

[11] Erik van der Bij and Maciej Lipinski. “Network fir European Accurate Time and Frequency Transfer”. November 2012. Hardware and Timing Section, CERN, 2012.

[12] Dragos Niculescu and Nath, B., “Ad Hoc Positioning System (APS) UsingAoA”, 2003. DATAMAN Lab, Ruters University. INFOCOM 2003.

[13] Mikkel Baun Kjaergaard , “Indoor Positioning with Radio Location Fingerprinting” 2010. PhD Thesis, University of Aarhus, Denmark, 2010.

[14] A. Roxin, J. Gaber, M. Wack, A. Nait-Sidi-Moh, “Survey of Wireless Geolocation Techniques” 2007. UTBM, France. IEEE Globecom Workshop 2007.

Improving Signal of Oppourtunity Localisation Estimates in Multipath Environments

T. O Mansfield, B. V. Ghita and M. A. Ambroze
School of Computing and Mathematics, Plymouth University, Plymouth, UK
{thomas.mansfield, bogdan.ghita, m.ambroze}@plymouth.ac.uk

Keywords: Leading Edge Detection, Time of Arrival Localisation, Indoor Navigation, Signals of Opportunity.

Abstract: Network based geographic localisation has been widely researched in recent years due to the need to locate mobile data communication nodes to a level of accuracy equivalent to that provided by global navigation satellite systems (GNSS) in multipath urban and indoor environments. This paper investigates whether direct sequence spread spectrum (DSSS) signal processing can be applied to narrow-band radio channels to improve the ranging estimates. The DSSS signal processing application is then developed further to provide a method of deriving a measurement confidence indicator, allowing the optimisation of time separated measurements in a dynamic signals of opportunity radio environment. A set of validation tests demonstrates that the proposed method provides a significant improvement in the accuracy and robustness of the ranging estimate compared to simple threshold analysis in multipath environments.

1 INTRODUCTION

Radio positioning systems have achieved common use in a diverse range of systems. The most commonly used radio positioning systems are global navigation satellite systems (GNSS). These systems use signals received from satellite to calculate the position of the user to within 4m during 95% of the time [1]. GNSS systems rely on a line of sight (LoS) view of at least 4 satellites. This requirement cannot however, be guaranteed in urban or indoor environments where 'urban canyons' and roof cover, block sight to much of the surrounding sky. Research has been carried out into using signals of opportunity for localisation in such environments, particular success has been achieved by using time of arrival (ToA) systems to derive a user's location [1], even in urban or indoor environments where multipath propagation is one of the main sources of system error [2]. Constructive and deconstructive interference between the non-line of sight (NLoS) propagating signals can destroy or obscure the LoS signal that is required to derive an accurate ToA estimate.

Ultra wide band (UWB) signal analysis techniques, originally developed for low emission radar [3], have achieved promising results when applied to localisation in wide bandwidth direct sequence spread spectrum (DSSS) networks [4][5]. These techniques rely on the differing multipath properties of the wide spread of frequencies to provide an improved leading edge time of arrival (ToA) estimate and to achieve GNSS levels of accuracy in wide bandwidth multipath environments.

This paper builds on the use of prior art wide bandwidth signal processing techniques and investigates their use in signals of opportunity networks that commonly collect time separated narrow bandwidth measurements such as frequency hopping spread spectrum (FHSS) networks. FHSS networks are typical to military [6] and civilian [7] systems and challenges remain to use them to achieve GNSS levels of location accuracy in multipath environments [8] due to the time separated nature of the received signals.

This paper proposes a method that allows the system to use time separated ToA estimates and, without prior training or additional data collection, generate a low latency and high bandwidth filtered ranging estimate. The benefits of the proposed method are verified through simulation. The accuracy and responsiveness of the ranging estimate shall be analysed in both static and mobile receiver environments.

This paper is organised as follows; Section 2 discusses the prior art. Section 3 proposes a method to use the leading edge detection algorithm to extract the data required to weight the values in a recursive filter. Section 4 provides details of the simulation environment and evaluates the ranging estimate performance. Section 5 concludes and discusses further work.

2 PRIOR ART

2.1 Leading Edge Detection

Basic ToA detection systems commonly use simple threshold based leading edge detection [2], which relies on the assumption that the LoS message will arrive first via the shortest direct path. In many situations however, the LoS component may be heavily attenuated by deconstructive multipath interference providing a leading error driver for indoor or urban ranging system accuracy.

Search-back algorithms improve on the ToA accuracy by analysing the received packet and performing a search-back to determine physical layer properties of the message to determine the time of arrival more robustly [9]. These algorithms require prior knowledge of the multipath environment which cannot be provided in many applications.

The Multiple Signal Classification (MUSIC) algorithm [10] extends the analysis to allow multipath signals to be used as a further information source and has become widely used in research. This algorithm requires a substantial training period to determine the number of multipath signals present to achieve better performance than relying on leading edge detection alone. Again, a training period is not practical in many applications where the device is to be used to navigate around an unknown area.

UWB signal processing techniques utilise the wide frequency range of the received signals to provide an improved ToA estimate. The analysis of the full frequency range available allows the user to determine frequency specific multipath variations and make an improved estimation of the true ToA reading. A widely implemented example of an existing UWB signal processing technique, described in [5], has been selected for further development in this paper. This technique was developed to detect the leading edge of a signal obtained from a wide bandwidth transmission. It has been selected for further development due to the fact that the running filters applied to the raw data may provide additional data to the user following further analysis.

The UWB signal processing technique is applied to any wide band received data as follows: if $h(t)$ represents the received signal in the time domain, it is first passed through a rectified moving average filter as shown in (1).

$$y(t) = \frac{1}{n} \sum_{i=t-n+1}^{t} abs(h([t])) \tag{1}$$

The averaged signal $y[t]$ is then passed through two filters of sizes n_1 and n_2 which return the maximum value from a sliding window, as shown in (2) and (3).

$$\max\_ n_1[t] = \max(y_{t-n_1} \ldots y_t) \tag{2}$$

$$\max\_ n_2[t] = \max(y_{t-n_2} \ldots y_t) \tag{3}$$

A binary indicator of whether a leading edge has been detected can be obtained from (4).

$$r[t] = (\max\_ n_1[t] * 2 > \max\_ n_2[t]) \;\&\; (\max\_ n_2[t] > thresh) \tag{4}$$

The threshold detection level, *thresh*, is typically set to 3σ of inter message in-channel received signal noise.

2.2 Application Considerations for Navigation Filters

Recursive averages are commonly used in navigation systems to produce a low noise and low latency location estimate from a noisy measurement input. In order to provide an efficiently filtered output, the measurement system that populated the recursive filter must provide not only a measurement value, but also a dynamic confidence indicator.

When using a simple threshold detection algorithm to detect the leading edge of a received signal, the only information that can be provided to the navigation filter is the time when a received value is greater than the selected threshold. If this information is available for each FHSS channel, a simple un-weighted recursive filter shown in (5) can be constructed to update the users filtered location based on the its previous position and the latest sensor data where, as commonly used in filter

notation, $\hat{x}$ represents the filter output, $\bar{x}$ represents the previous state and $\tilde{x}$ represents the latest sensor value. The measurement confidence is represented by α.

$$\hat{x} = \alpha\bar{x} + (1-\alpha)\tilde{x} \quad (5)$$

The filter represented in (5) may be tuned by adjusting the value of α by a predetermined value.
A value of $\alpha < 0.5$ reduces the noise of the filter output at the expense of a higher latency if the receivers true location changes. A value of $\alpha > 0.5$ generates a more responsive, lower latency filter output but the filter output noise will be adversely affected. Both of these options are unsuitable for many system applications.

3. PROPOSED METHOD

The leading edge detection algorithm described in section 2.1 has been developed for wide band signal processing and analyses all of the data from the wide frequency range with each measurement.
The receiver system to be developed by this paper makes a ranging estimate upon detection of the leading edge of a received signal using the signal processing technique described in section 2.1. The process of running the n_2 filter (3) to return the maximum value in the longer sliding window continues for the duration of the first message in the current FHSS channel. The data obtained from the maximum value sliding windows is placed into a column vector and a standard deviation taken to determine the presence and magnitude of multipath present throughout the message. This is then correlated to provide a numerical confidence value.
The process is represented in equations (6) and (7). The standard deviation, σ, is first calculated in (6) with n_2 as the filter length, x_i is each iterative filter value and x_a is the current filter average. This standard deviation is then normalised in (7) to produce a dynamic measurement confidence, α.

$$\sigma_{n_2} = \sqrt{\frac{1}{n_2}\sum_{i=1}^{n_2}(x_i - x_a)^2} \quad (6)$$

$$\alpha = (1 - \frac{\sigma_{n_2}}{\mu_{n_2}}) \quad (7)$$

α represents a confidence factor with a weighted value between 0 and 1 for low to high confidence measurements respectively. This confidence measure can then be used to dynamically tune the filter shown in (5) to generate a recursive filter input that benefits from both low noise and low latency. This has been achieved by providing a high weighting value to ranging estimates received with good confidence and a low weighting to estimates with a low confidence, even if there has been true movement by either the transmitter or receiver.
The ability to achieve this from a multipath data source dynamically and without prior knowledge is of a key benefit in higher level navigation systems, as discussed in section 2.2. This confidence weighting has been achieved without the use of any additional information or averages over the ones implemented to allow the improved leading edge detection.

4. SYSTEM VALIDATION

4.1 Simulator Validation

A simulated radio frequency (RF) environment was modelled in Matlab® and Simulink® to evaluate the effectiveness and performance of the techniques discussed in section 3. The simulation uses the standard multipath simulation model [11] shown in (8) where L_p is the number of multipath components, α is the complex attenuation and τ is the propagation delay.

$$h(t) = \sum_{k=0}^{L_p-1} \alpha_k \delta(t - \tau_k) \quad (8)$$

The simulation assumes that an idealised transmitter generates a single frequency modulated pulse; for validation, the FHSS network parameters included 100 20 kHz channels evenly spaced from 3 to 5 GHz. The transmitted pulse is then subjected to empirically derived propagation and receiver distortions to produce a received signal for analysis. The resulting signal includes simulated effects of multipath with the use of separate propagation channels, the number of which can be set by the user. The simulations evaluated throughout this paper will consider a LoS propagation path of 10 m with several multipath reflection paths with an apparent time path from the transmitter to the receiver consistent with 10.1 m to 11.2 m propagation distances.
This simulated environment has been used to ascertain the performance of a simple threshold detection algorithm in a Monte Carlo based simulation of a wide range of FHSS channels in a

fixed geometry. A typical single transmitted message and the received signal patterns in a high multipath environment can be seen in Fig 1.

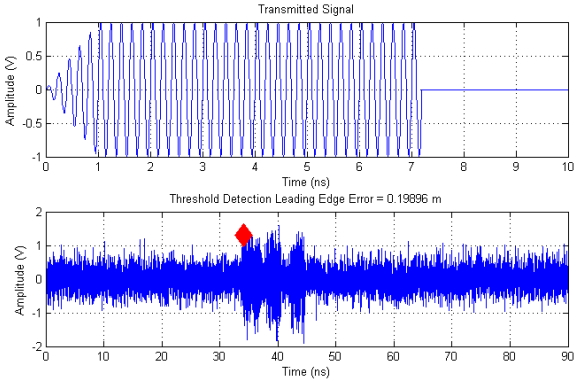

Fig. 1. Transmitted (top) and received (bottom) pulse with the location of the detected leading edge of the pulse marked by the red symbol.

The threshold detection algorithm has been simulated assuming a static receiver and transmitter across a range of FHSS channels to benchmark the simulation. The results can be seen in Fig. 2 and shows properties that are expected in multipath environments, as seen in [1] and [2]. The similarity to data collected by practical test in previous research provides confidence that the simulation is representative.

4.2 Technique Validation

A comparison of edge detection seen by employing UWB signal processing techniques to each narrow bandwidth channel as opposed to simple threshold detection can be seen in Fig. 2.

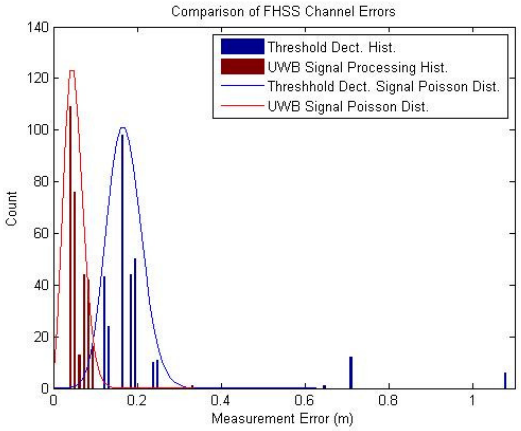

Fig. 2. Comparison of threshold based and UWB signal processing leading edge detection methods.

Analysis shows that the Poisson distribution variance has a λ value of 17 for the threshold detection algorithm and an improved λ value of 5 for the UWB threshold detection. The received estimates across the range of networks not only have less average error but also a greater distribution density than can be obtained from simple threshold detection alone. As well as a significant improvement in the Poisson distribution, the UWB based edge detection algorithm removes the erroneous outliers seen at ≈ 0.7 m and ≈ 1.1 m error in the threshold detection algorithm. This behaviour may account for the high multipath uncertainty seen in [12] where a simple threshold detection algorithm was used to detect the ToA to estimate range.

Detail of the detected trigger timing at the leading edge of a signal with light multipath is shown in Fig. 4.

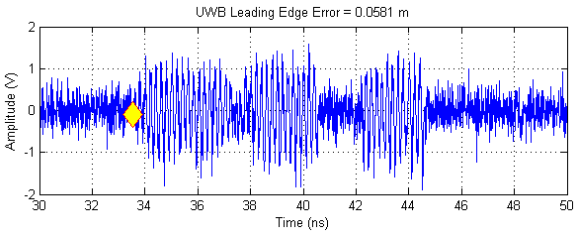

Fig. 3. UWB leading edge detection of pulse in a noisy multipath environment.

Figure 3 is a magnification of the area of interest, related to the transmission pulse as shown in Fig. 2. Areas of constructive and deconstructive multipath effects can be seen throughout the 34 ns to 42 ns region where a non-multipath signal would be expected to produce a stable series of 1 V peaks.

The simulation has shown that the evaluation tests for the UWB algorithms discussed in section 2.1 produce a significant improvement over threshold detection when providing ToA estimation in high multipath FHSS networks when only a single narrow bandwidth channel can analysed at a time.

Further to the improvement shown in ToA estimates in a high multipath environment, the application of the additional data available, described in section 3, to a recursive navigation filter is analysed in the remainder of this section.

The application of threshold analysis data, where no weighting data is available for the new samples, into the simplified recursive filter leads to a noisy and poorly filtered position estimate. Fig 4. compares a plot of the raw measured and filtered ranging estimate obtained from a simulation of a static

system that sweeps through 100 FHSS channels over a 5 second period.

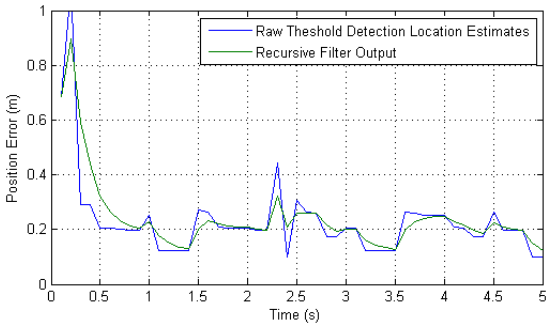

Fig. 4. The raw and filtered output from the threshold detection algorithm with a pre-selected static confidence interval.

The results displayed in Figure 4 verify that the filtered position estimate from an un-weighted recursive filter is comparatively noisy and produces a large filtered error in the event of a multipath $\tilde{x}$ leading edge detection received from the sensor, as seen approximately 0.2 seconds into the simulation.

The application of the position estimates and the relative variance derived using the method described in section 3 has been applied to a weighted navigation filter. The application of this navigation filter in the simulation leads to improved stability to the position estimate which, combined with the improvement in leading edge detection reliability and the absence of outliers, leads to a greatly improved position estimate over the threshold detection algorithm, as shown in Fig. 5.

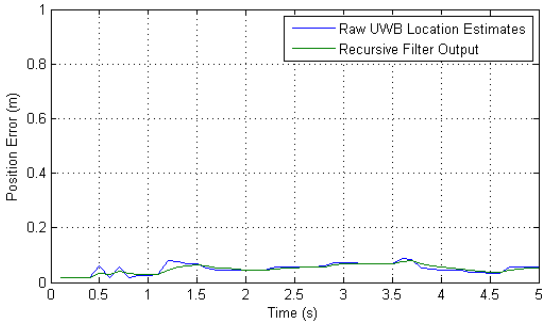

Fig. 5. The raw and filtered output from the navigation filter with UWB leading edge detection and dynamically obtained confidence interval. This should be compared with Fig 6 to see the improvement achieved.

In a physically static system, as simulated in Fig 4 and Fig. 5, where the relative position of the transmitter and receiver does not change, the sensitivity to erroneous data could be mitigated by weighting the raw sensor data by a pre-determined factor of <1 depending on sensor noise. While this will limit the filter error in the event of erroneous multipath readings and produce a more accurate location estimate, it also introduces high latency if the receiver or transmitter truly moves location. The application of a dynamically weighted recursive filter prevents an erroneous multipath ToA reading from causing filter noise. If however, the system truly moves, a new filter input with a new position estimate with a high weighting will be received and the filter output will respond with little latency.

A further simulation was run to evaluate the effect of a true receiver motion on the filter output. To simplify the simulation, a single narrow bandwidth channel with no frequency hopping was used throughout the experiment. After approximately 1.2s into the simulation, the receiver node instantaneously moves 1m within a multipath environment and remains static for the remainder of the simulation.

Fig. 6 shows a comparison of the filter response to the applied motion with both threshold detection and UWB detection inputs.

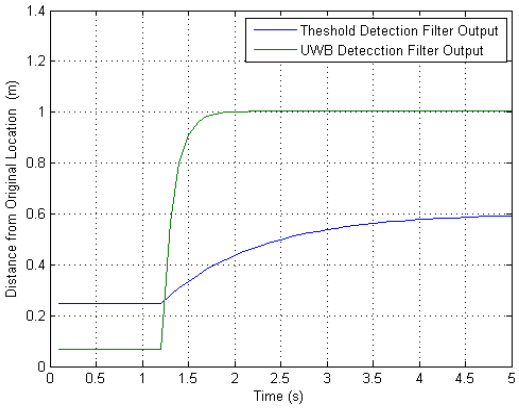

Fig. 6. The response of the filters to an instantaneous 1 m movement of the receiving node.

The threshold detection filter still has a greater error before and after the 1 m move of the receiver node than the UWB filter, as expected. The area of interest highlighted by this simulation is the difference in time taken for the filter output to identify the change in location. The dynamic weighting to $\tilde{x}$ allows the UWB filter to respond with minimal latency in the event of true receiver or transmitter movement. The improvement seen in Fig

6 is due to both the improved UWB ranging estimate, shown in Fig 2 and the ability to weight the measurements. These contributing factors have not been analysed separately due to the fact that the weighted recursive filter may be implemented without any additional data collection and should always be used to provide an optimised solution.

5. CONCLUSIONS AND FURTHER WORK

This paper proposed a set of algorithms and application techniques that improve narrow bandwidth channel ranging estimates in signals of opportunity environments. The novel application and further development of DSSS signal processing techniques to provide not just an improved ranging estimate but, by re-analysing existing data, an additional confidence weighting.

By re-analysing the available data, a filter confidence factor can be obtained that can be calculated dynamically without the need for a training period and without any prior knowledge of the radio system and environment. More specifically, the use of UWB signal processing techniques provided an approximately 4 times improvement in ranging estimation over simple threshold detection even in narrow bandwidth channels, including a better Poisson distribution and higher resilience to false detections.

The main benefit of applying this technique is that a filtered ranging estimate can be obtained that is more accurate, lower noise and lower latency than can be obtained by using simple threshold detection techniques to detect the leading edge of a message.

The analysis of the proposed technique performance throughout this paper has been carried out only in multipath environments. It is anticipated that the benefits of the technique will be significantly less apparent in less hostile environments.

Future work should include the physical test of this system to verify the model. The integration of the algorithm into higher level systems is also required to verify the higher level benefits shown during simulation. The close coupling of this system with higher level navigation systems, in particular Kalman filtering schemes may also allow the development of a significantly improved signal of opportunity based localisation system.

REFERENCES

[1] Air Commodore Norman Bonnor, 2012. *A Brief History of Global Navigation Satellite Systems*, Royal Institute of Navigation Journal of Navigation vol. 65.

[2] R. M Faragher, P.J Duffett-Smith, 2010. *Measurements of the effects of multipath interference on timing accuracy in a radio positioning system*, IET Radar, Sonar and Navigation, vol. 4, iss. 6, pp. 818-824.

[3] R. J. Fontana, 2004. *Recent System Applications of Short-Pulse Ultra-Wideband (UWB) Technology*. Published in IEEE Microwave Theory and Techniques, Vol. 52, Issue 9.

[4] M. R. Mahfouz, et. al, 2008. *Investigation of high accuracy indoor 3-D positioning using UWB technology*, IEEE Trans. Microwave Theory and Technology, pp. 1316-1330.

[5] B.Merkl, 2008. *The future of the operating room: surgical preplanning and navigation using high accuracy ultra wide-band positioning and advanced bone measurement*, Ph.D Dissertation, The University of Tenessee, USA.

[6] Northrop Grumman, 2013. *Understanding Voice and Data Link Networking*, Guidebook, Northrop Grumman, San Diego, USA.

[7] IEEE, 2014. *IEEE 802.22 Working Group – Enabling Broadband Wireless Access Using Cognitive Radio Technology* http://www.ieee802.org/22/ Accessed 14th November 2014.

[8] P. Xu. R.J Palmer and Y Jiang, 2005. *An Analysis of Multipath for Frequency Hopping Spread Spectrum Ranging*. IEEE Conference on Electrical and Computer Engineering.

[9] K. Haneda, 2009. *Performance Evaluation of Theshold Based UWB Ranging Methods – Leading Edge vs, Search Back,* 2rd European Conference on Antennas and Propagation.

[10] R. O. Schmidt. *Multiple Emitter Location and Signal Parameter Estimation*, IEEE Trans. Antennas Propagation, Vol. AP-34 (March 1986), pp.276-280

[11] N.A Alsindi, 2004. *Performance of TOA Estimation Algorithms in Different Indoor Multipath Conditions*. PhD Thesis, Worcester Polytechnic Institute.

[12] R. M. Faragher, 2007. *Effects of Multipath Interference on Radio Positioning Systems*, Ph.D. dissertation, Dept. Physics., University of Cambridge, Cambridge

Integrating Interferometric Measurement Data into SLAM Systems

T.O. Mansfield, B.V. Ghita and M.A. Ambroze.
School of Computing and Mathematics
Plymouth University
Plymouth, United Kingdom
{thomas.mansfield, bogdan.ghita, m.ambroze}@plymouth.ac.uk

Abstract – **Interferometric navigation systems have shown that they can produce accurate geo-location estimates with minimal hardware requirements. They are not however suited to urban and indoor environments where multipath effects corrupt the geo-location estimate. Interferometric systems may however provide an improved data source for simultaneous localisation and mapping techniques, increasing geo-location estimate accuracy while simultaneously reducing hardware requirements and processing load.**

This short paper proposes a method to combine the these existing geo-location techniques, providing an accurate geo-location estimate in urban and indoor environments. Proof of concept is demonstrated via simulation and initial hardware testing.

Keywords — Radio positioning, SLAM, urban and indoor navigation, network geo-location

I. INTRODUCTION

Radio navigation in urban in indoor environments continues to present several challenges to researchers. The ability to use radio frequency (RF) signals to calculate and maintain an accurate geo-location indoors is available today via pre-known RF mapping databases, such as those provided Skyhook [1]. The dependence on a 3rd party database is not desirable in many applications. Instead, many users would prefer to build their own RF mapping data in real time and use this to determine their location. Simultaneous localisation and mapping (SLAM) techniques tailored for low size weight and power (SWAP) devices such as smart phones as presented by Faragher et. al. [2].

Low SWAP hardware has also been used to enable an accurate geo-location estimate for long range localisation, as presented by the radio interferometric positioning system (RIPS) research [3]. This system allows accurate long range localisation in optimal, non-multipath environments, but does not perform well in urban or indoor environments where multipath dominates. The multipath interference measured by the RIPS system in urban environments provides an ideal data source for a SLAM system. An opportunity exists to combine the available RIPS and SLAM systems to improve the accuracy of the geo-location estimate in urban environments while simultaneously reducing hardware requirements. This paper presents methods that will allow the SLAM and RIPS techniques to be combined efficiently to obtain these improvements. The proof of concept is then demonstrated by simulation, using widely accepted simulation techniques.

II. SUMMARY OF PRIOR ART

The combination of two RF geo-location techniques has been proposed. This section will describe the key operation parameters of each system required to allow later integration.

The RIPS system [3] analyses the relative carrier phase for the signal strength at the measured location and uses multiple transmitters to generate a low frequency and long wavelength beat signal. The system has been proven to work well in open environments with few RF propagation variations. In ideal conditions the system has produced location errors as low as 3 cm at a range of greater than 160 m using low SWAP radio hardware. Received signal strength analysis allows the relative location of an unknown transmitter to be calculated using the formula below (1).

$$Phase\ Offset = 2\pi \frac{D_{AD} - D_{BD} + D_{BC} - D_{AC}}{\lambda_{CARRIER}} (\bmod 2\pi) \qquad (1)$$

Experimentation results with the RIPS system does however indicate that the system suffers significant degradation when used in areas that contain multipath. This is caused by the 4 signal paths may suffer difficult to predict apparent phase corruption, degrading the accuracy of the resulting location. This currently limits the potential applications for the RIPS technology due to the fact that it is unsuitable for use in dense urban environments where multipath is common.

One major benefit of this system is that the phase offset, calculated from several high frequency RF signals, produces a low frequency beat frequency measurement, typically at 100

Hz to 400 Hz. The phase of the RSSI offset has been demonstrated to be accurately recorded with low SWAP hardware. In addition, only a single channel has to be monitored by the hardware for the system to operate.

The second RF geo-location to be considered is the low SWAP tailored SLAM technique. This technique uses a modified fingerprint extended Kalman filter (FEKF) to analyse received signal strength indicator (RSSI) 'fingerprints' in an area to produce a real time map of the RF environment. The accuracy achieved by the SLAM technique increases as the signal strength topology becomes increasingly complex as typical in high multipath environments.

The fingerprint extended Kalman filter defines a fingerprint to be a vector of N received signal strength (RSS) measurements from N distinct radio transmitters. The Kalman filter Z matrix is populated with the fingerprint data, shown in (2).

$$z_t = w = [RSS_1, RSS_2 ... RSS_n]^T \tag{2}$$

The predicted value matrix, h, values are drawn from any populated values in the signal strength map, M.

$$h_t = [M_1(x,y), M_2(x,y), ... M_N(x,y)]^T \tag{3}$$

The measurement noise matrix, R, is populated form the variance of the noisy RSS measurements, R, and the variance of the predicted measurements, V , as shown in (4).

$$R = [\sigma_{R_1}^2 + \sigma_{V_1}^2, \sigma_{R_2}^2 + \sigma_{V_2}^2, ... \sigma_{R_N}^2 + \sigma_{V_N}^2]I \tag{4}$$

The measurement matrix, H, is populated from the loop-up coordinates shown in (5), where J related to the Jacobian derivative map.

$$\begin{aligned} H(i,1) &= J_{i,x}(x,y) \\ H(i,2) &= J_{i,y}(x,y) \end{aligned} \tag{5}$$

The advantage of the map is that, as the number of contours in the SLAM map increases, the accuracy of the estimated location and the reliance to unrealistically large geo-location jumps increases.

III. Proposed Technique

The accuracy of the SLAM algorithm is increased as the resolution of the maintained RF map increases. The technique described in this paper uses the inputs from the interferometric signal in a multipath environments as the source of the data for the FEKF SLAM technique.

$$RSS_N = RSS_{BeatSignal} \tag{6}$$

The RIPS interferometric RSS_N values are used as the input to the Kalman filter w matrix (2). In high multipath environments, the phase offset will have many contours due to the varying level of multipath in each of the contributing signals. In multipath environments, the RSSI of the beat signal has many times more contours in that in of a set of separate channel RF transmitters these contours can be monitored at a low frequency, allowing low SWAP hardware to maintain a high resolution topology map of the environment. The remainder of the FEKF matrices are dynamic and will maintain their state efficiently in a range of conditions. No further modifications will be required when transitioning from single channel to interferometric signal strength analysis.

IV. Simulation and Test

A typical SLAM map has been modelled to demonstrate the contour resolution available to the FELF filter for both interfering and non-interfering signal analysis.

The model has been generated in Matlab® using simple signal generation techniques.

The simulation uses the standard multipath simulation model [4] shown in (7) where L_p is the number of multipath components, α is the complex attenuation and τ is the propagation delay.

$$h(t) = \sum_{k=0}^{L_p - 1} \alpha_k \delta(t - \tau_k) \tag{7}$$

The resulting SLAM map available to the FEKF filter in each scenario can be seen in Figure 1 and Figure 2.

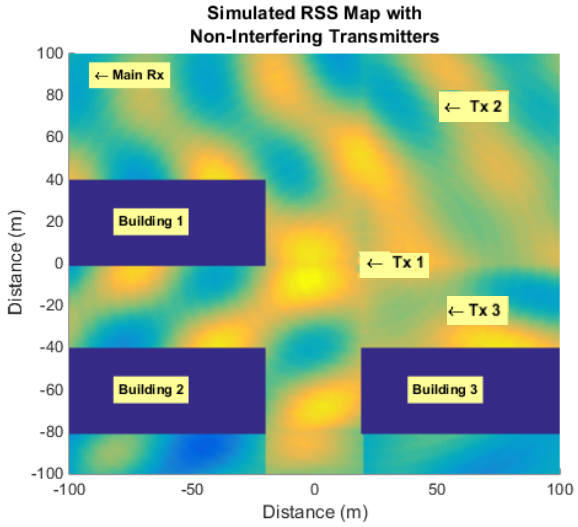

Figure 1 - SLAM Map Simulation with Non-Interfering WiFi Signals as the Measurement Source.

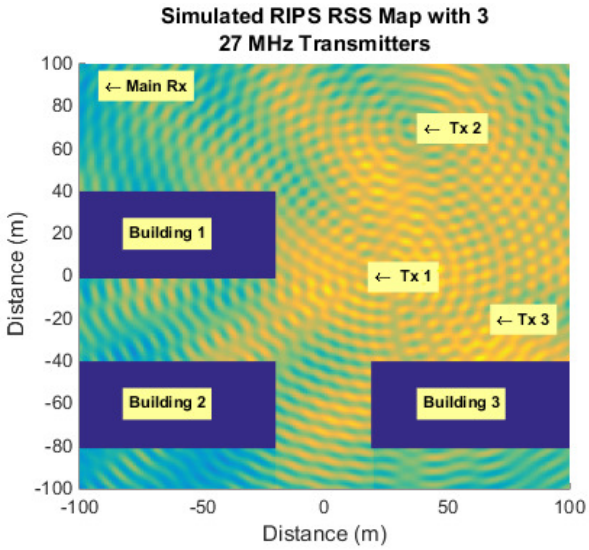

Figure 2 - SLAM Map Simulation with RIPS System as the Measurement Source.

As location accuracy is dominated by the available contour resource, the simulation results shown in Figure 1 provide a contour resolution of around 10 m to 15 m . This is in line with the test results reported from previous FEKF simulations [2][5][6]. The addition of the RIPS system in Figure 2 shows that the potential location accuracy in a multipath environment is likely to be in the region of 1 m to 2 m.

The concept demonstrated by the simulation modelling has been further proved by initial testing with practical hardware. Low SWAP hardware has been used as both the transmitter and receiver. The transmitters used are low bandwidth 27 MHz radio transmitters and the receiver is a modified software defined radio receiver. Both devices are shown in Figure 3.

Figure 3 - Software Defined Radio Receiver and 27 MHz transmitter

The transmitters and receiver have been configured as simulated in Figure 2. Initial testing, aimed at providing a level of confidence in the simulation results, consists of taking spot measurements of the RSS at the simulated locations. A comparison of the RSS spot measurements can be seen in Figure 4.

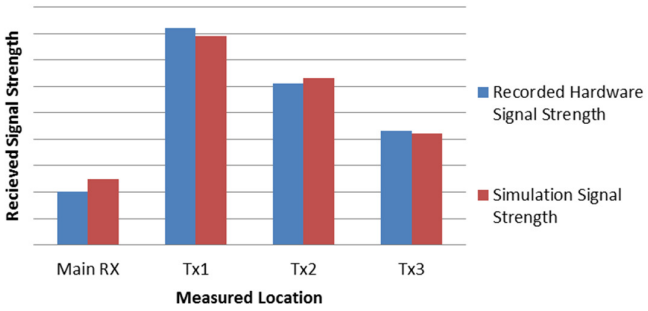

Figure 4 - Normalised RSS Spot Measurements

The comparison of the hardware test and simulation RSS measurements has provided confidence in the simulation environment, adding further weight to the initial proof of concept.

V. Conclusions and Further Work

This short paper has proposed a method to combine two existing urban and in door geo-location techniques to provide an improved geo-location estimate. The dynamic and efficient fingerprint Kalman filtering scheme, designed for use on low SWAP hardware provides a mechanism for efficiently using signal strength data to generate a real-time SLAM map. This system, often limited by a lack of contrast in the signal strength input can be enhanced with the addition of interferometric data. The addition of interferometric data provides a rich resource, providing additional geo-location resolution while simultaneously reducing the required processing load on the target hardware by reducing the number sensing channels.

Initial simulations show good similarity with previous practical test data and with initial hardware testing in a controlled environment. While the simulation has demonstrated the proof of concept, further work is required to conduct more detailed practical testing to provide quantitate results of the combined techniques in a range of indoor and urban environments.

VI. References

[1] Skyhook http://www.skyhookwireless.com/. 2016, Skyhook Wireless Inc. Accessed 4th Feb 2016.

[2] R. M. Faragher, C. Sarno and M. Newman, "Opportunistic Radio SLAM for Indoor Navigation using Smart Phone Sensors", 2012. Advances Technology Centre, BAE Systems, UK. Published in the IEEE Position Location and Navigation Symposium (PLANS), USA, 23-26 April 2012.

[3] B. Kusy, J. Sallai, G. Balogh, V. Protopopescu, J. Tolliver, F. DeNap, M. Parang, "Radio Interfoermetric Tracking of Mobile Wireless Nodes", 2006. Vanderbilt University, Oak Ridge National Lab and University of Tennessee. Published in MobiSys'07, June 11-13, 2007.

[4] N.A Alsindi, 2004. Performance of TOA Estimation Algorithms in Different Indoor Multipath Conditions. PhD Thesis, Worcester Polytechnic Institute.

[5] B. Ferris, D. Hahnel and D Fox, "Gaussian Process for Signal Strength-Based Location Estimation" 2007. Univeristy of Washington, Depatment of Computer Science & Engineering, USA and Intel Research Centre, USA. Published in the Joint Conference on Artificial Intelligence (IJCAI), 2007.

[6] J. Huang, D. Millman, M. Quigley, D. Staven, S Thrun, A. Aggarwal, "Efficient generalized indoor WiFi GraphSLAM" 2011. IEEE International Conference of Robotics and Automation (ICRS) 9-13 May 2011.

Ann. Telecommun. (2017) 72:145–155
DOI 10.1007/s12243-016-0559-y

Signals of opportunity geolocation methods for urban and indoor environments

T. O. Mansfield[1] · **B. V. Ghita**[1] · **M. A. Ambroze**[1]

Received: 8 January 2016 / Accepted: 20 December 2016 / Published online: 4 January 2017

Abstract Motivated by the geolocation requirements of future mobile network applications such as portable internet of things (IoT) devices and automated airborne drone systems, this paper aims to provide techniques for improving device geolocation estimates in urban and indoor locations. In these applications low size, weight and power are vital design constraints. This paper proposes methods for improving the geolocation estimate available to a system in indoor and urban environments without the need for addition sensing or transmitting hardware. This paper proposes novel system application techniques that enable the integration of signals of opportunity, providing a robust geolocation estimate without any additional hardware. The proposed method utilises a sinusoidal Kalman filter architecture to analyse raw radio frequency (RF) signals that surround a system in urban and indoor environments. The introduced techniques efficiently analyse the raw RF data from any signal of opportunity and combine it with higher level geolocation sensors to provide an improved geolocation estimate. The improvements achieved by the system in a range of environments have been simulated, analysed and compared to the results obtained using the prior art. These improvements have been further validated and benchmarked by hardware test. The results obtained provide evidence that the efficient use of signals of opportunity coupled with common navigation sensors can provide a robust and reliable geolocation system in indoor and urban environments.

Keywords Signals of opportunity · Kalman filtering · Radio navigation and geolocation

1 Introduction

Distributed networks of mobile and autonomous devices are likely to become increasingly common as the expected widespread adoption of both internet of things (IoT) and autonomous mobile robotic systems continues. As people spend approximately 90% of their time indoors [1], these systems will be predominantly located in indoor and urban environments. The indoor environment is likely to become crowded with large numbers of portable, low power, small size and wirelessly connected devices. The increasingly busy radio spectrum is expected to be filled with wireless communications from vast numbers of transmitting devices. While this increasingly congested RF spectrum is a concern for many system designers, it does provide a potentially valuable resource for an accurate device geolocation estimate. Geolocation estimates are vital to many system designers for two main reasons; the first is to enable devices to navigate their environment. The second benefit, particularly in IoT applications, is to be able to tag any generated data with a geographical location. This commonly increases the value of the information that can be gained from the vast array of data produced.

Global navigation satellite systems (GNSS) and low cost inertial navigation systems (INS) are commonly used to provide geolocation estimates. While significant work has been carried out to closely couple GPS and INS systems to mitigate their respective error drivers, these coupled systems are unable to provide accurate geolocation estimates in urban and indoor environments where GPS updates may be unavailable for extended periods of time. A review of current research has revealed an opportunity to couple data link RF signal analysis into the INS system, allowing the rich RF resource found in

✉ T. O. Mansfield
thomas.mansfield@plymouth.ac.uk

[1] School of Computing and Mathematics, Plymouth University, Plymouth, UK

urban and indoor environments to maintain geolocation estimates where existing systems encounter their greatest errors.

This paper presents a set of novel techniques aiming to improve the accuracy of geolocation estimates for a wide range of systems. A key principle of the proposed techniques is the ability to monitor the phase estimate of surrounding RF signals to provide a ranging estimate from the transmitter. A sinusoidal Kalman filter is proposed that allows an accurate, low latency and low noise phase estimate to be maintained by the system. The resulting ranging estimation does not drift with time and lends itself to close and ultra-close coupling with INS and other system level geolocation systems, techniques for which are also presented in this paper.

The proposed methods are analysed and compared to existing methods through simulation. The obtained simulation results are further validated with a set of practical tests using data link devices typical to proposed IoT and autonomous mobile systems. The results demonstrate that, with even limited prior knowledge of the wireless data link environment, an accurate geolocation estimate is maintained for prolonged periods in urban environments.

Section 2 discusses existing system capabilities. Section 3 discusses the proposed system implementation. Section 4 presents simulation and test results. Section 5 discusses the key findings, conclusions and further work.

2 Current geolocation solutions

GNSS systems, such as the global positioning system (GPS), are commonplace in cars, mobile phones and a wide range of timing systems. All applications suffer the same significant limitation: current receivers are not sensitive enough and transmissions are not strong enough to operate the system in indoor environments. Even in urban environments such as city centres, GNSS systems frequently provide poor coverage due to the limited line of sight from the satellites to users at ground level when surrounded by tall buildings [2].

An alternative form of geolocation, not requiring an external input, is to use an INS to provide a dead reckoning estimate. INS systems provide information about changes in velocity or angular rate, allowing a user to calculate their position relative to a known starting point. The major drawback of this approach is that the dead reckoning technique integrates errors over time, causing the users calculated position to drift with respect to their actual position. Many grades of INS are available, with differing rates of drift related to the INS's accelerometer and gyro biases during operation. Small, low power systems often have larger biases which cannot be calibrated out for a particular measurement [3].

Coupled IMU and GNSS systems apply the input from both systems into a navigation filter, such as a Kalman filter [4]. Coupled systems have been developed to use the potentially intermittent GNSS system to remove the integration errors accumulated in the continually available IMU data [5]. As detailed in Fig. 1, the provision of an externally generated ranging estimate allows the multiplication of the two probability distributions to provide an improved geolocation estimate.Closer coupling through an extended Kalman filter allows benefits to both the IMU by removing bias errors and the GNSS system by allowing an improved ability to track weak signals [6]. Research has also been carried out to enable extended Kalman filters to carry out feature recognition that, if compared to a known map, allows the Kalman filter to recognise features and objects in a mapped environment. Upon the recognition of a known feature, an external ranging estimate can be calculated. This allows both an improved location estimate and the ability to calculate and remove errors from other system sensors [7, 8].

Recent research has been carried out on the ability to use existing RF signals to provide a feature recognition, with proposed solutions commonly referred to as signals of opportunity systems. System applications use signal strength fingerprinting [9], message content [10] or message flight time [11, 12] to derive geolocation data from the RF signals of opportunity. These systems each have their own limitations; however, the need for prior signal mapping information and poor

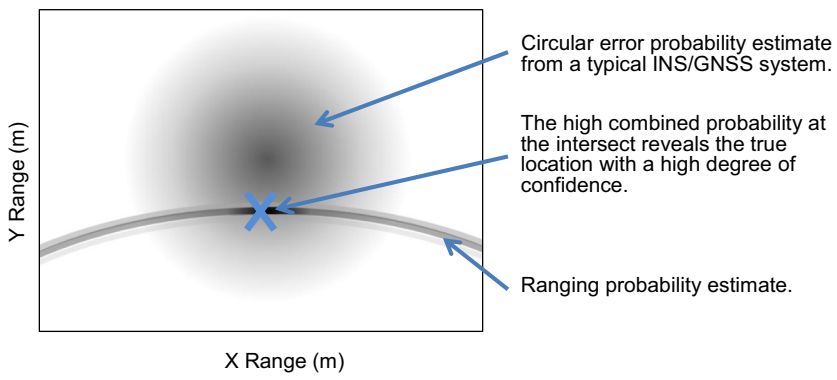

Fig. 1 Geolocation example optimised with the addition of a ranging estimation

Table 1 Estimated geolocation accuracy of existing systems in a dense urban environment

Technique	Typical error (3σ) (m)	Notes
WiFi SLAM [9]	10	Prior knowledge of third party infrastructure required.
Coupled signal of opportunity [13]	20	The most widely adopted technique in current research if no environmental prior knowledge is available.
Phase estimation [16]	30	Single multipath source discussed. A lower level of accuracy is anticipated in urban and indoor environments.
GNSS [1]	40	Not available indoors.
INS [3]	100	Accuracy related to operational time due to integration of error.
ToA estimation [13]	300	Quoted performance is only for 'mid-urban' environments. Dense urban likely to be worse.

performance in multipath environments [13, 14] are limitations in all systems [15].

Estimating the phase in signals of navigation has also been proposed [16]. This technique has produced very encouraging results in low multipath environments with errors of less than 2 m achieved in low latency systems; however, as with other techniques, a vulnerability to multipath interference severely limits its accuracy in indoor and urban environments. While work has been carried out to mitigate this vulnerability with multiple RF channels at separated frequencies [17], no solution has been found that allows the system to operate in multipath while retaining the ability for the system to work on low latency mobile systems.

Following analysis of currently available techniques, geolocation error estimates have been identified for an automated system in a dense urban environment and presented in Table 1.

3 Proposed system development

Current geolocation solutions provide good geolocation accuracy in areas of low multipath interference; this is not possible in areas of multipath such as indoor and urban environments. This paper introduces a novel method for utilising existing RF sources in order to produce a more accurate ranging geolocation estimate in multipath environments.

The proposed technique mitigates the effects of multipath by using a sinusoidal Kalman filter to track the received RF signal. This filter maintains an estimate of the expected signal phase and uses the raw RF data as a measurement input. Using a Kalman filter to maintain the latest measurements, estimates and covariance's provides significant robustness against multipath effects, which tend to be temporary in mobile systems, while still allowing low latency feature recognition.

The filter is designed to update the ranging estimate at each filter iteration. The Kalman filter will be created in two stages, one to predict the phase at the next step and a second to record data and combine it with the estimation. Matrices are created to maintain state within the Kalman filter as well as pass information into and out of the Kalman filter. The proposed implementations of these matrices are described in Eqs. 1 to 6.

The Φ matrix maintains the translation matrix for a sinusoidal system.

$$\Phi = \begin{bmatrix} \cos(\omega\tau) & \frac{\sin(\omega\tau)}{\omega} \\ -\omega\sin(\omega\tau) & \cos(\omega\tau) \end{bmatrix} \tag{1}$$

The P matrix maintains the initial state covariance. As the location of the first reading is unknown, the following P matrix is typically applied.

$$P = \begin{bmatrix} 1e^{6} & 0 \\ 0 & 1e^{6} \end{bmatrix} \tag{2}$$

The measurement noise is represented in the Q matrix.

$$Q = \begin{bmatrix} 1e^{-4} & 1e^{-4} \\ 1e^{-4} & 1e^{-4} \end{bmatrix} \tag{3}$$

The system noise is represented in the R matrix.

$$R = \begin{bmatrix} 1e^{-4} \end{bmatrix} \tag{4}$$

And the measurement matrices are represented by the H and I matrices.

$$H = [1\ 0] \tag{5}$$

$$I = \begin{bmatrix} 1 & 0 \\ 0 & 1 \end{bmatrix} \tag{6}$$

The estimation step is completed by carrying out the Riccatti equations [18] as described below. The estimation step is carried out for each filter iteration:

$$M = \Phi * P * \Phi' + Q \tag{7}$$

$$H_{\text{mtrinv}} = (H * M * H' + R)^{-1} \tag{8}$$

$$K = M * H' * H_{\text{mtrinv}} \tag{9}$$

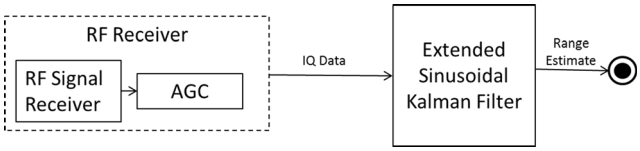

Fig. 2 Basic system configuration

$$K_h = K^*H \tag{10}$$

$$P = I - K_h^*M \tag{11}$$

Following the estimation for the current filter step, the measurement can be made and combined into the estimated location using the maintained Kalman gain, K. Again the measurement stage, shown in Eqs. 12–15, is run at each iteration of the Kalman filter.

$$x_{\text{hold}} = x_h \tag{12}$$

$$r = \frac{Xs - Xh^*cos(\omega\tau) - sin(\omega\tau)^*x_{dh}}{\omega} \tag{13}$$

$$x_h = \frac{\cos(\omega\tau)^*x_h + x_{dh}^*\sin(\omega\tau)}{\omega + K_{(1,1)}^*r} \tag{14}$$

$$x_{dh} = -\omega\sin(\omega\tau)^*x_{\text{hold}} + x_{dh}^*cos(\omega\tau) + K_{(2,1)}^*r \tag{15}$$

This initial Kalman filter provides the coupling from an RF source to the resulting range estimate as shown in Fig. 2.

This initial implementation will provide a ranging estimation from an RF source that is resilient to the signal interference common in indoor and urban environments. The use of a sinusoidal Kalman filter also allows the system to have low latency, resulting in a minimised risk of drift due to phase cycle slip. The lack of estimate drift over time makes the resulting ranging estimate an ideal signal to be coupled to higher level INS based navigation systems. The use of a sinusoidal Kalman filter offers the opportunity for the proposed technique to become the core of a complete navigation system, with any other available navigation systems coupling directly to enhance the accuracy of each subsystem. This paper will continue to present a series of methods for efficiently integrating other navigation sensors into a closely coupled system. Figure 3 shows the three stages of system architecture required for coupled and closely coupled navigation system integration as well as control data link data decoding. The complete system has the sinusoidal Kalman filter at its core, maximising the information that can be obtained from the raw RF data.

The method for integrating the proposed sinusoidal Kalman filter based system consists of three stages. Stage 1 will be the initial close coupling of additional navigation sensors into the sinusoidal Kalman filter, improving the robustness of the RF phase estimation. Stage 2 is the addition of a feedback loop. This allows the ultra-close coupling of the system, improving the performance of surrounding navigation sensors. Stage 3 is the addition of control link data from systems where the motion of the system is controlled via a RF data link.

Stage 1 of the system is an open loop closely coupled system where the sinusoidal Kalman filter measurements come from all available navigation sensors. Although methods exist for closely coupling navigation sensors to provide an improved geolocation estimate, the novel application of a sinusoidal Kalman filter to maintain an estimation of phase allows the additional data to be used to further improve the robustness of the system to multipath and other urban and indoor RF effects.

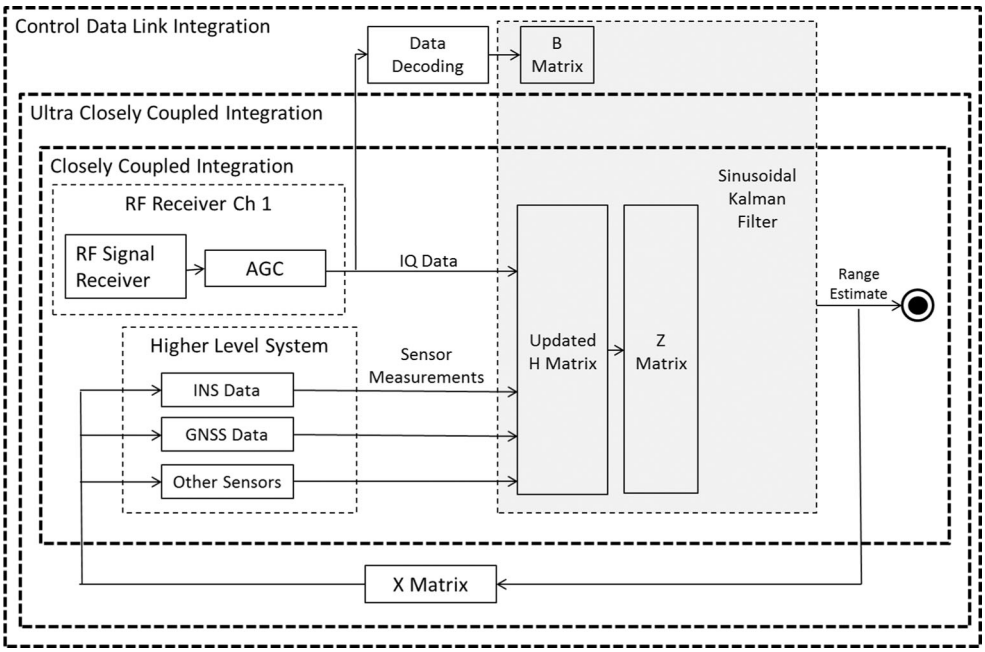

Fig. 3 Three stage system integration with additional higher level navigation sensors. The figure describes the architecture required for closely coupled integration, ultra-closely coupled integration and a method for utilising encoded data in a control data link

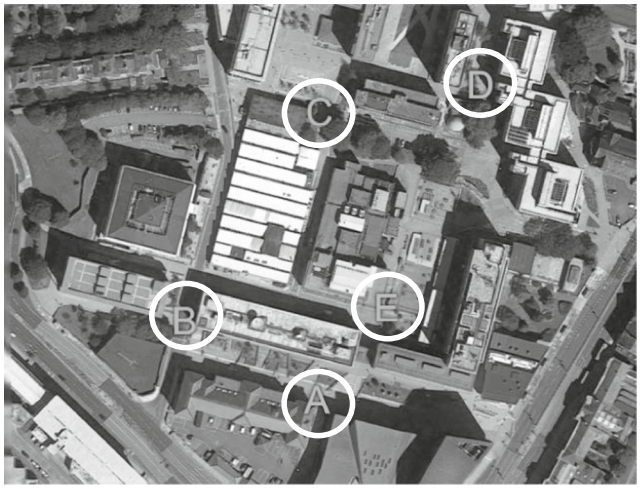

Fig. 4 Urban environment with simulated reception points

The system requires an update to the Kalman filter H matrix and the addition of an F and Z matrix. The updated H matrix relates to the measurements received from each sensor. The F matrix converts the measured sensor reading into a phase estimate based on the calculated range from the transmitter. An example updated H and F matrix for a typical data stream with RF and GNSS data can be seen below.

$$H = \begin{bmatrix} 1 & 0 \\ 1 & 0 \end{bmatrix} \tag{16}$$

$$F = \begin{bmatrix} 1 & \sqrt{x^2 + y^2} * \sin(\omega\tau) \end{bmatrix} \tag{17}$$

Upon each time separation iteration of the Kalman filter the H matrix is multiplied by the corresponding F and then Z matrix.

$$Z = [\text{a b}] \tag{18}$$

The Z matrix is updated at each iteration, depending upon what fresh measurement data is available from the system. In the below example, if a raw RF data measurement is available, $a = 1$ and $b = 0$. If a GNSS measurement is available, $a = 0$ and $b = 1$.

This implementation allows the Kalman filter to be updated with all available data. The covariance of the H matrix is maintained by Kalman filter, providing additional robustness to multipath effects. Erroneous RF signals are identified by a lowering in the covariance values in the Kalman filters P matrix and will have limited effect on the maintained phase estimate.

Following the integration of the additional navigation sensors, an additional stage of ultra-close coupling is possible using conventional methods of using an X matrix to convert the range update back into a known position estimate for each sensor. The advantage of this technique for the proposed system is that further robustness to indoor and urban RF effects is provided, allowing a highly robust phase estimate to be maintained by the Kalman filter due to accurately maintained measurement covariance's in the P matrix.

The system architecture described so far is applicable to any signals of opportunity source, where the location of the transmitter is either known in advance or can be calculated using simultaneous localisation and mapping techniques. The system uses only the RF carrier signal, so it can be used without knowledge of any of the data on the link. Even encrypted data links can be used to provide a ranging estimate.

The movement of many robotic systems is controlled by an RF data-link. This datalink is likely to provide an ideal RF data source from a known transmitter location and could be utilised in many systems. In systems that use the control datalink as the RF input to the system, the data contained within the datalink can be decoded, providing the commanded

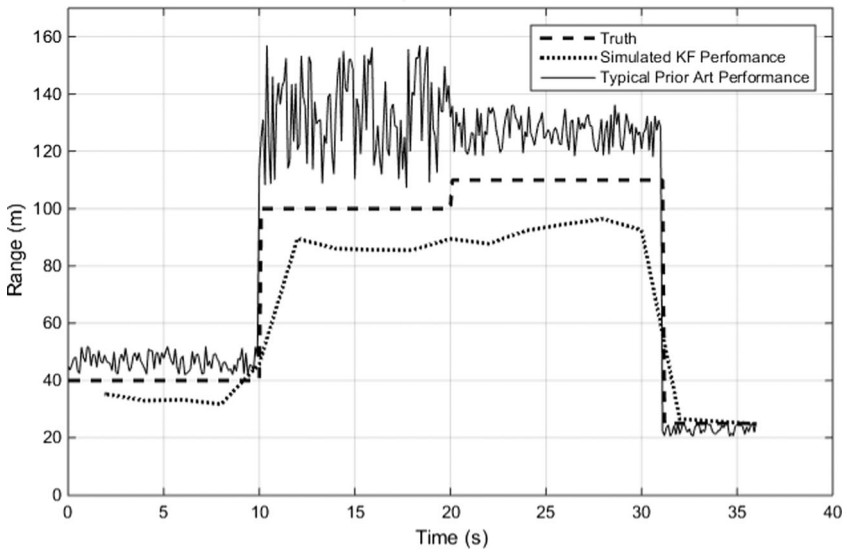

Fig. 5 Simulated range estimate provided at points B to E with respect to point A for two ranging methods

Table 2 Tabulated range estimate averages

Reception point	Reception environment		True range (*m*)	Average error (m)		Improvement (%)
	Range	Building density		Prior art method	Proposed method	
B	Near	High	40	6.7	5.8	13
C	Long	Low	100	33.2	10.8	67
D	Long	High	110	17.3	15.3	12
E	Near	Low	25	2.0	0.7	65

system motion. This commanded motion can be, via a control matrix (B), used to update the prediction estimate made by the Kalman filter. The B matrix is multiplied with the Φ matrix, allowing the prediction part of the Kalman filter to account for the motion expected by the system. The B matrix must have a prior knowledge of the system dynamics that will apply following any commanded motion input. Once again, the addition of an improved prediction estimate within the Kalman filter will provide additional robustness to measurement uncertainty. The ability for the system to command data in this way is a unique benefit that comes from using signal of opportunity inputs into a sinusoidal Kalman filter architecture.

4 Simulation and experiment

4.1 Simulation

The performance of the proposed sinusoidal Kalman filter based system will be simulated in a typical urban environment. The aim of the simulation is to allow an analysis of the proposed approach alongside that of the most widely adopted prior art [13], enabling a comparison of performance to be made. The simulation has created a radio fingerprint of the dense urban environment shown in Fig. 4 with signals generated from point A.

Reception points B to E have been selected to allow performance analysis at both near and long range and, to simulate performance in areas of high and low multipath, areas of high and low building density. The results are show in Fig. 5 and Table 2.

While the greatest improvements have been made in areas of relatively low multipath, greater ranging accuracy has been achieved at all reception points with the average error reducing from 14.8 m with the prior art to 8.2 m with the proposed method.

4.2 Hardware benchmarking

To validate and benchmark the system improvements obtained, the proposed method has been tested with hardware at the point shown in simulation to be the most challenging, reception point D. The system has been tested in the incremental stages outlined in Section 4. Each stage has been tested to validate the proposed technique and to provide evidence that the anticipated performance has been achieved. All testing has been carried out with a drone, modified to be controlled with a 27 MHz amplitude modulated transmitter. The flying drone contains a microelectromechanical system (MEMS) IMU with three accelerometers and three gyros. The Single RF channel has been recorded using a low power software defined radio (SDR) receiver attached to the drone The test apparatus can be seen in the photographs below. A smart phone GPS receiver has been added to the drone to provide comparative GNSS geolocation data (Figs. 6, 7 and 8).

The test area was in a densely populated urban city centre location with tall buildings surrounding the trial. A clear view of the sky above the trial was present, although sight was limited by tall buildings on all sides. The test consists of a 60 s drone flight at a constant altitude of 6 ft. The flight profile consisted of the 4 steps shown in Fig. 9.

All data has been collected in separate files for post processing. Post processing has been carried out on the data recorded by each of the trial sensors. Raw IMU and GPS data has been collected. These raw data sources, available to

Fig. 6 Drone system

Fig. 7 SDR receiver

Fig. 8 27 MHz transmitter

typical automated robotic systems, have been plotted throughout the test trial in Fig. 10.

The data presented in Fig. 10 shows the challenges faced by many systems navigating in an urban environment. The first challenge is the poor fidelity of the GPS location provided in a dense urban environment; it is hard to determine any component of the flight during the trial. The poor performance of the GPS is typical when receiving signals in urban environments. The inertial data presented by the INS system shows that the stages of the flight can be determined; however, the significant drift of approximately 30 m at the end of an 80 s flight presents the second challenge of error integration. The inertial drift will continue to accumulate for the entirety for the mission without the aid of an external data source. Whilst this paper aims to use the RF signal present in the systems control datalink to provide an external source of navigation data, it is hard to see how this data source could provide information when the time domain RF amplitude data is plotted. Due to the limited flight range and the fact that the datalink contains an automated gain control loop, the amplitude of the raw RF data does not appear to provide any useful ranging information. The raw data obtained from the flight appears to show that accurate, low drift navigation for a drone system, using only the existing hardware will be a very challenging task The techniques proposed by this paper shall now be applied in stages to show the contribution of each technique in building an accurate drift-free navigation solution.

As described in Section 4, the raw RF data will be fed though the Kalman filter to create a low noise sinusoid of the raw RF carrier signal. The phase of this low noise sinusoid is analysed and shifts in the maintained phase estimate have been be used to estimate a change in range from the transmitter to the recording receiver mounted on the drone. Analysing the data's phase shift with a sinusoidal Kalman filter provides the ranging estimate shown in Fig. 11.

It can be seen that by comparing the estimates from the low noise sinusoidal Kalman filter, a low drift range estimate can be seen throughout the 80 s flight. This low drift ranging estimate was able to track the range changes with low latency throughout the flight, resulting in a good localisation estimate throughout the flight. As predicted, errors in the recordings throughout the flight do not integrate together and the estimate tends towards the true location at the stationary points in the data. The limitation of the processed RF data is that there is that range estimation errors of up to 12 m present for periods of several seconds. This may have been caused by multipath effects in the RF data due to the test being carried out at low altitude in a dense urban environment. The cause of this deviation will be determined in later testing but, even with this deviation, the observed performance is significantly better than existing navigation systems, providing evidence that using the sinusoidal Kalman filter at the core of the system provides a significant benefit.

The next analysis proposed by this paper is designed to remove these short-term errors by ultra-closely coupling the RF data with that of a low noise, but high drift INS system. This technique has been carried out and is presented in Fig. 12.

It can be seen in the data provided that ultra-closely coupling the Kalman filter and IMU system has had an effect. The largest effect can be seen in the IMU drift. The integrated error at the end of the flight has reduced from 28 m in the uncoupled

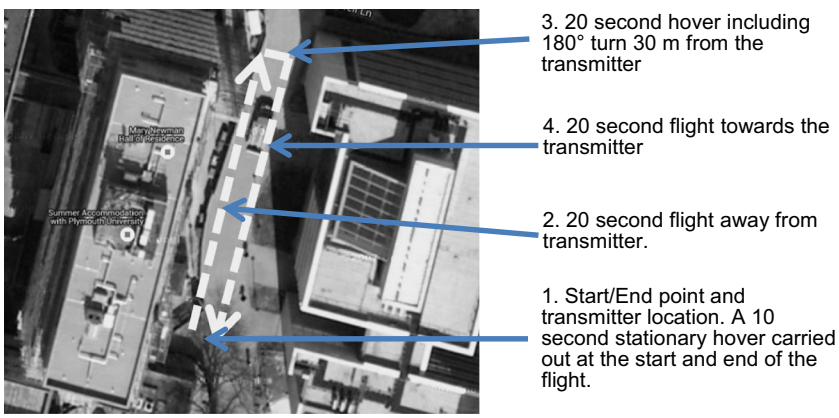

Fig. 9 Test flight map

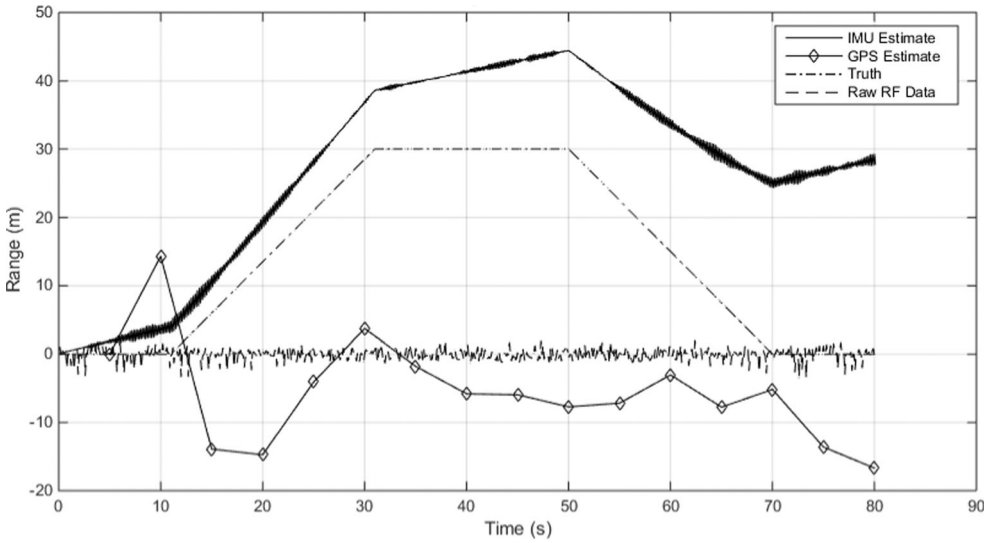

Fig. 10 Ranging estimate from the raw data sources

trial to 17 m in the coupled trial. The magnitude of the IMU following coupling is strongly linked to the Kalman filter estimate in the stationary period in the first 10 s of the trial where the Kalman filter P matrix experiences a period of convergence on the present system errors. Another key observation is that the output from the Kalman filter has changed very little, and the deviations of up to 12 m remain. This suggests that the deviations are not in fact caused by multipath and another unknown error source is dominating the Kalman filter errors. Although the identification of this error source is proposed as further work, the systems resilience to multipath is likely to have been proven.

For many systems where the RF signal recorded by the drone mounted equipment is not controlled by the system operator, as found in many signal of opportunity systems where third party RF networks are used as the data source, no further navigation data is available from the techniques proposed in this paper. The results presented in Fig. 12 will be the final performance of the system. When this performance is compared with the GPS ranging estimate shown in Fig. 10, a drastic performance improvement has been achieved. Even if the GPS data were to be combined with the INS data also shown in Fig. 10, no accurate ranging estimate during the flight would have been provided; The GPS signal obtained in an urban environment was of such poor quality that the INS estimate could not have been improved by coupling it with the GPS signal with existing techniques. Coupling the INS data to the output of the proposed system has reduced the error at the end of the 80 s flight considerably.

Further to this already considerable improvement in performance over existing INS coupling systems, the drone system under test is controlled by a frequency modulated command signal which is operated by the system designer. This command signal is used to provide the stop, forward, backwards,

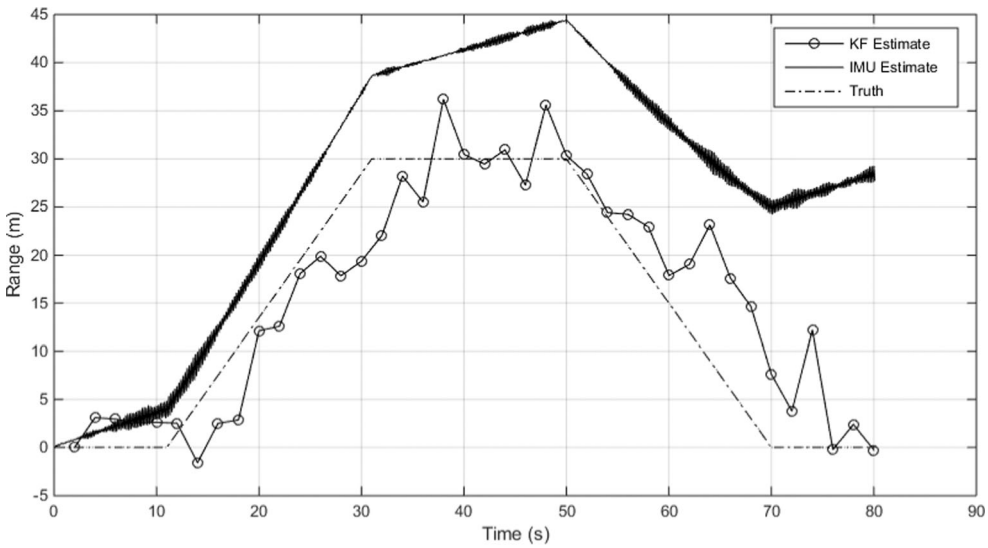

Fig. 11 Ranging estimate from the RF post sinusoidal Kalman filter processing

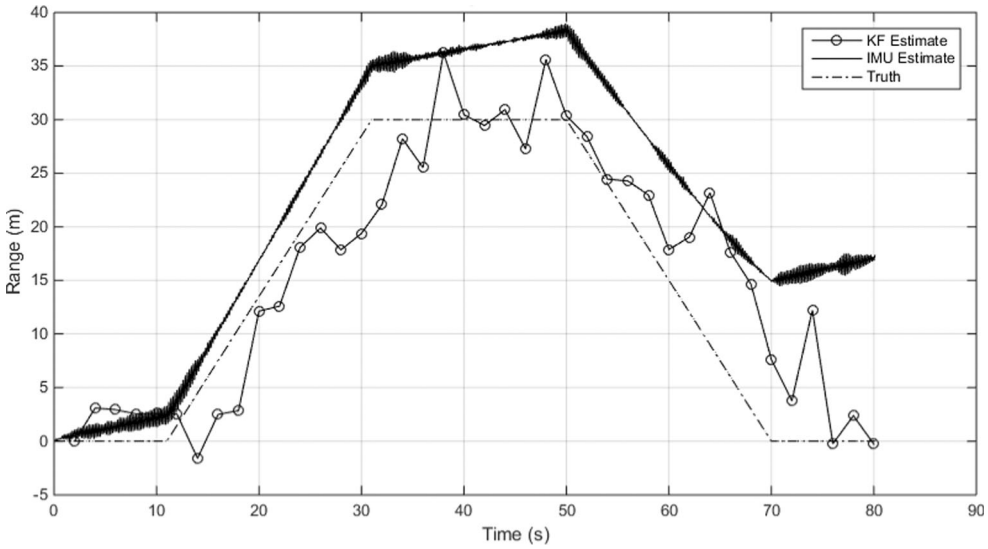

Fig. 12 Ranging estimate from the processed RF and ultra-closely coupled IMU data

turn left and turn right commands to the drone and is decoded by the on-board RF receiver. This data can be made available to the filter along with a basic kinematic model representation of the drone. The following information about the kinematic model is known and is captured in the trial *B* matrix:

Forward motion is typically 5 m/s
Turn rate is typically 90 °/s.

The resulting ranging estimate from using this data as described in Section 4 is presented in Fig. 13.

The addition of the encoded data reveals further detail about the system behaviour. The first thing to note is the fact that the assumed kinematic model appears to be incorrect. The system appears to have not correctly measured the 180° yaw command at the turning point half way through the trial. Despite this, the Kalman filters estimated range remains accurate. The benefit of adding the decoded command data is seen in the first 10 s of the trial where the *P* matrix is converging. The addition of the stop command information has allowed the Kalman filter to better remove the IMU biases. This has reduced the integrated IMU drift at the end of the trial from 17 to 5 m. This will again further increase the systems resilience to multipath and other urban and indoor RF effects.

The Kalman filter errors throughout the hardware test has been analysed. The average error between truth and the Kalman filter estimate was recorded to be 3.3 m with a 3σ error prediction of 12 m. The performance of the proposed technique, compared against existing methods in a similar environments, as described in Section 3, can be seen in Table 3.

Hardware test of the geolocation techniques researched in this paper have provided a reduction in geolocation error indoor and urban environments over existing techniques. While the system has proven resilient to the presence of an erroneous kinematic model in the test, further optimisation of this

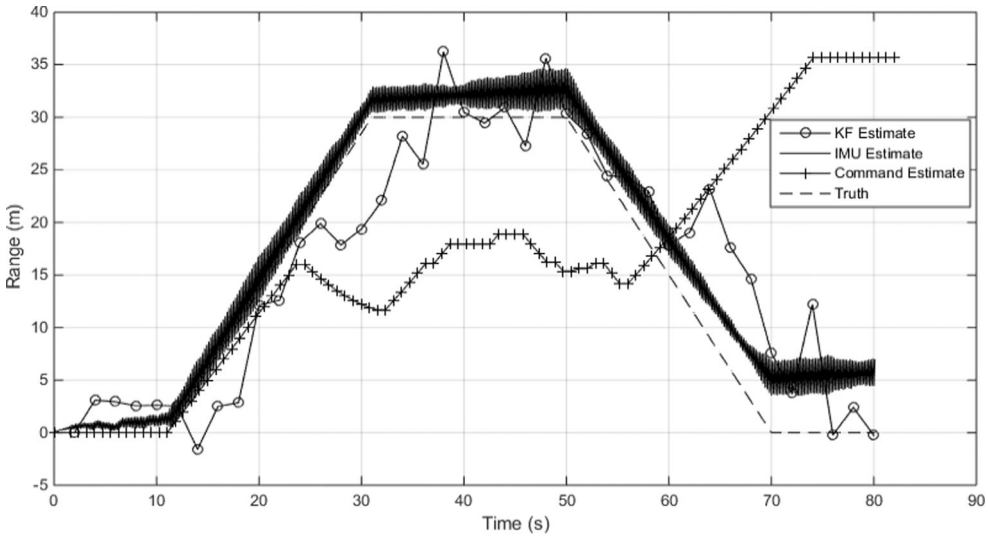

Fig. 13 Ranging including data obtained from the encoded data

Table 3 Estimated geolocation accuracy comparison in a dense urban environment

Technique	Typical error (*m*)	Notes
Proposed technique	12	12 m (3σ) error achieved with hardware test. No prior knowledge of a third party system required.
WiFi SLAM [9]	10	Prior knowledge of third party infrastructure required.
Coupled signal of opportunity [13]	20	The most widely adopted technique in current research if no environmental prior knowledge is available.

parameter is likely to allow the achieved performance to match that of systems that can utilise prior knowledge of the environment, overcoming a common system application constraint.

5 Conclusions

Mature systems exist that closely couple INS and GNSS data to enable an improved geolocation estimate. Initial testing in a typical urban environment has showed that, as predicted, GNSS performance is limited by a combination of poor line of sight view of the sky, multipath effects and poor performance of low size, power and weight GNSS receivers common to many small robotic and IoT systems produce considerable geolocation errors. GNSS does not provide a suitable external coupling partner for INS systems in these systems. Research has also been carried out into using signals of opportunity to provide a ranging estimate. These systems are adversely affected by multipath in urban environments or require prior knowledge of third party datalinks to provide a ranging estimate.

This paper has presented novel techniques for using a single RF data source to maintain a ranging estimate by comparing the predicted output of a sinusoidal Kalman filter with a noisy recorded RF signal. This comparison allows a low latency ranging estimate to be produced that provides resilience to the adverse effects of multipath. Testing has shown that in a typical urban environment this ranging estimate can be coupled to the output of an INS to produce a high fidelity and robust ranging estimate. Further, an addition to the basic technique allows for closer coupling of the signals of opportunity system, and the existing INS system can be made if the contents of the datalink message can be decoded by the target system.

This paper has presented a significant improvement on the resilience and robustness of signals of opportunity systems and allows them to provide a reliable external source of information for ranging systems without the need for any additional system hardware. Further, this technique effectively removes a common design constraint that previously limited geolocation performance in many applications. This will enable system designers to gain more information from their mobile robotic and IoT data, enabling the next generation of advanced urban information networks.

The testing carried out in this paper is extremely encouraging but limited to a single 80 s flight in an urban environment. Further work is required to characterise the performance of the system in a range of environments and test scenarios.

References

1. Klepeis NE et al. (2001), The National Human Activity Pattern Survey (NHAPS): a resource for assessing exposure to environmental pollutants. US National Library of Medicine
2. Air Commodore Norman Bonnor (2012) *A brief history of global navigation satellite systems*," Royal Institute of Navigation Journal of Navigation vol. 65
3. Novatel, IMU Errors and Their Effects 2014. Novatel bulletin, 21st February 2015. http://www.novatel.com/assets/Documents/Bulletins/APN064.pdf. Accessed 17th December 2015
4. Kalman R (1960) A new approach to linear filtering and prediction problems. Transactions of the ASME Journal of Basic Engineering 82:35–45
5. Salmon DC, Bevly DM (2014) An exploration of low-cost sensor and vehicle model Solutions for ground vehicle navigation Published in IEEE PLANS 2014, 5–8 May 2014
6. Li T et al. 2010 Ultra-tight Coupled GPS/Vehicle Sensor Integration for Land Vehicle Navigation. University of Calgary. Navigation 57, 4:248–259
7. Negenborn R (2003) Robot Localization and Kalman Filters–On finding your position in an noisy world. Thesis, Utrecht University, 1st September 2003
8. Kong F, Chen Y, Xie J and Zhang G (2006) Mobile robot localization based on extended Kalman filter 2006. 2006 6th World Congress in Intelligent Control and Automation (Volume 2)
9. Papapostolou A and Chaouchi H (2011) Scene analysis indoor positioning enhancements. Ann. Telecommun. 2011
10. Roxin A, Gaber J, Wack M, Nait-Sidi-Moh A (2007) Survey of wireless geolocation techniques 2007. UTBM, France. IEEE Globecom Workshop
11. N. A Alsindi Performance of TOA estimation algorithms in different indoor multipath conditions PhD Thesis, Worcester Polytechnic Institute, April 2004
12. Selmi I and Samama N (2014) Indoor positioning with GPS and GLONASS-like signals use of new codes and a repealite-based infrastructure in a typical museum building Ann. Telecommun. 2014
13. Faragher RM, Duffett-Smith PJ (2010) Measurements of the effects of multipath interference on timing accuracy in a radio positioning system. IET Radar, Sonar and Navigation 4(6):818–824

14. Faragher RM (2007) Effects of multipath interference on radio positioning systems Ph.D. dissertation, Dept. Physics., University of Cambridge, Cambridge, UK
15. Reed JH, Krizman KJ, Woerner BD, and Rappaport TS (1998) An overview of the challenges and progress in meeting the E-911 requirement for location service. Virginia Tech, 1998. Published in the IEEE Communications Magazine
16. Arnitz D, Witrisal K and Muehlmann U (2009) Multifrequency continuous-wave radar approach to ranging in passive UHF RFID. IEEE transactions on microwave theory and techniques Vol. 57 No 5
17. Pelka M, Bollmeyer C and Hellbruck H (2014) Accurate radio distance estimation by phase measurements with multipole frequencies. International Conference on Indoor Positioning and Indoor Navigations, 27th October 2014
18. Arnold WF, Laub AJ (1984) Generalized Eigenproblem algorithms and software for algebraic Riccati equations. Proc IEEE 72:1746–1754